Numerical Study of Error Propagation in Monte Carlo Depletion Simulations

A Thesis
Presented to
The Academic Faculty

by

Timothy Joseph Wyant

In Partial Fulfillment
of the Requirements for the Degree
Master of Science in Nuclear Engineering in the
School of Mechanical Engineering

Georgia Institute of Technology
August 2012

Numerical Study of Error Propagation in Monte Carlo Depletion Calculations

Approved by:

Dr. Bojan Petrovic, Advisor
School of Mechanical Engineering
Georgia Institute of Technology

Dr. Glenn Sjoden
School of Mechanical Engineering
Georgia Institute of Technology

Dr. Dingkang Zhang
School of Mechanical Engineering
Georgia Institute of Technology

Date Approved: 13 JUNE 2012

Acknowledgements

I wish to thank Dr. Bojan Petrovic, my academic advisor, whose guidance, mentorship, and knowledge have been essential to my completion of this research work. I would also like to thank Dr. Sjoden and Dr. Zhang for serving on my thesis committee.

The developer of the SERPENT lattice physics code, Dr. Jaakko Leppanen, was also critical in answering all of my questions about how to install and use the code and interpret its results. His willingness and timeliness in assisting me is greatly appreciated.

Kevin Manalo, a Ph.D. student studying under Dr. Glenn Sjoden at Georgia Institute of Technology, offered a tremendous amount of assistance in compiling and running the SERPENT code in parallel, which was necessary to complete the full core calculations.

Finally, I wish to thank my wife Le and son Phong, who have endured my continued absence the last year so that I can commit the time and energy needed to complete this work. Your love and support have been a constant source of comfort to me.

TABLE OF CONTENTS

LIST OF TABLES

LIST OF FIGURES

LIST OF SYMBOLS AND ABBREVIATIONS

BC	Boundary Condition
BOC	Beginning Of Cycle
BU	Burnup
CPU	Central Processing Unit
CRAM	Chebyshev Rational Approximation Method
DR	Dominance Ratio
FA	Fuel Assembly
GT	Guide Tube
HM	Heavy Metal
IFBA	Integral Fuel Burnable Absorber
IRIS	Innovative Reactor Innovative and Secure
LLN	Law of Large Numbers
LWR	Light Water Reactor
MA	Minor Actinide
MC	Monte Carlo
MCNP	Monte Carlo N-Particle
NND	Nuclide Number Density
NPP	Nuclear Power Plant
ODE	Ordinary Differential Equation
ORNL	Oak Ridge National Laboratory
pcm	percent mille
PWR	Pressurized Water Reactor
RAM	Random Access Memory

TP	Test Problem
TRISO	Tri-ISOtopic
UO_2	Uranium Dioxide
316SS	316 Stainless Steel

SUMMARY

This thesis is the culmination of a numerical study of the error propagation in Monte Carlo depletion calculations. In Monte Carlo reactor physics codes, the statistical uncertainty of one step is combined with errors propagating through the calculation from previous steps. Over time, these errors accumulate, though to which degree these errors are amplified and/or dampened has previously been unclear. The objective of this work was to investigate this error propagation and identify some common regularities in the behavior of uncertainty in several key parameters of some common types of depletion calculations.

All Monte Carlo test problems were done using SERPENT: a Continuous-Energy Monte Carlo Reactor Physics Burnup Calculation Code developed at VTT Technical Research Center of Finland. Four test problems were developed for analysis, with three problems consisting of different arrangements of four 17 x 17 fuel assemblies, and the fourth problem being a full core model of the International Reactor Innovative and Secure (IRIS). By changing the code's initial random number seed, the data produced by a series of 19 identical "replica" runs was used to investigate the variance in k-eff, pin powers, and number densities of several isotopes. The average uncertainty produced by the code for each parameter at each burnstep is compared to the observed uncertainty in the parameters produced by the 19 replica runs. Results show how well the code estimates the true uncertainty and how these uncertainty measures evolve as a simulation progresses.

CHAPTER 1

INTRODUCTION

Since computers have made it possible for researchers to develop numerical solutions to the neutron transport equation, a number of solution methods have been developed to model the working of a nuclear reactor. One of these techniques, the Monte Carlo (MC) method, has the ability to accurately model the extreme heterogeneity of the nuclear reactor environment. Another powerful advantage of the MC method is the ability to treat neutron energy dependence correctly with essentially no approximations, quite unlike deterministic codes that must create arbitrary "splits" in the energy range in order to create multigroup cross sections.[1] The continued and dramatic improvement in processing speed of today's computers, as well as the ability to parallelize many aspects of the MC calculation, make this technique increasingly more attractive.

In his paper "Challenges and Prospects for Whole Core Monte Carlo Analysis," Martin discusses six challenges in the use of the MC method for full-core reactor analysis. They are:

1) Prohibitive computational time for acceptable statistics
2) Excessive demand on computer memory
3) Slow convergence of the fission source
4) Apparent vs. true variance
5) Accounting for multiphysics feedback
6) Adapting to future computer architecture

This paper sets out to specifically investigate the fourth of these challenges, the relationship between the true and apparent variance in key reactor simulation parameters. Along the way, several of the other issues will be discussed, and data collected during the course of this research effort will be presented that demonstrates the degree to which these other challenges were present in the test problems developed for this study.

Any exercise to understand the behavior of uncertainty must begin by taking a closer look at how the uncertainty arises. In any stochastic process, there will always be a legitimate statistical uncertainty. In a MC depletion simulation, a random process simulates the transport of neutrons and based on those results, the nuclear fuel is depleted using a series of equations that model the creation and destruction of each isotope. In order to improve results, especially if the depletion is occurring over a large time span, the problem is divided into a series of depletion steps ("burnsteps"). Even assuming that we know perfectly the starting conditions of the fuel and its cross section, a statistical error in step n introduces some error in the starting conditions of step n+1. When the calculation is repeated for step n+1, the error from step n is combined with new errors that over time will propagate and/or combine with a varying degree of amplification and/or dampening.

But to understand how significant a challenge the measurement of uncertainty is in MC simulations, a method must be developed to compare the true and the apparent (or code reported) uncertainty estimates. In order to estimate the true variance in MC parameters, a system was developed to run a test problem multiple times changing nothing except the seed number of the pseudo-random number generator that provides the foundation of the MC method (and will be discussed further in Chapter 2). The multiple "replica" runs of each test problem will produce a set of numbers for each parameter that will have an observed uncertainty. The observed uncertainty can be compared to the average estimate of the code's uncertainty prediction to determine whether there is a difference in the true vs. apparent uncertainty.

The following chapters present the work performed. Chapter 2 provides a literature review showing the state-of-the-art in Monte Carlo techniques and an understanding of error propagation. Chapter 3 provides an overview of the SERPENT Monte Carlo depletion code and the code settings used for this study. Chapter 4 describes the development of three fuel assembly domain, 2-dimensional test problems while Chapter 5 presents the assembly domain test results. Chapter 6 describes the development of a full core, 2-dimensional test problem based on the IRIS project and Chapter 7 presents the core domain results. Chapter 8 describes the uncertainty

observed in the isotopic evolution of several nuclides of importance in the reactor environment. Chapter 9 summarizes the work and proposes areas for future investigation.

CHAPTER 2

MONTE CARLO THEORY AND APPLICATION

2.1 The Monte Carlo Method as a Numerical Solution Tool

The transport of neutrons, the particles that maintain the fission chain reaction in a nuclear reactor, are described by the transport equation. The movement of neutrons is a function of seven independent variables: x, y, z; E; Ω(θ, ϕ); and t. The neutron transport equation is

$$\frac{1}{v}\frac{\partial \Psi}{\partial t} + \hat{\Omega} \cdot \nabla \Psi + \sum_t \Psi(\vec{r},\, E, \hat{\Omega}, t) = \int d\hat{\Omega}'\, \int_0^\infty dE' \Sigma_s(E' \to E, \hat{\Omega}' \to \hat{\Omega})\, \Psi(\vec{r}\, E, \hat{\Omega}, t) +$$

$$\chi(E) \int d\hat{\Omega}'\, \int_0^\infty dE' \nu \sum_f (E', \hat{\Omega}' \to \hat{\Omega})\, \Psi(\vec{r}\, E, \hat{\Omega}, t)$$

Where $\Psi(\vec{r}\, E, \hat{\Omega}, t)$ is the angular flux and the other terms include the time derivative of the flux, net streaming, scattering, and the neutron source term which could be a fixed source similar to a shielding calculation, or an eigenvalue problem where the source can change depending on a multitude of reactor conditions. [2]

In an effort to develop highly accurate and timely solutions to the transport equation, researchers have developed reactor codes that use deterministic and stochastic methods. In deterministic codes, the defined geometry is divided into mesh spaces and algebraic equations are applied to each mesh for discretized values such as energy, angle, et. The NEWT (New ESC-based Transport Code) functional module in SCALE (Standardized Computer Analysis for Licensing Evaluation) is one example of a deterministic numerical method which uses the discrete ordinates method. [3] Another technique developed for solving fixed source and eigenvalue problems is the Monte Carlo method. As Shreider discussed in "The Monte Carlo Method," MC techniques can be used when a problem can be modeled by means of constructing a random process with the parameters of the process equal to the parameters of the initial problem. Because the process being observed is random, the Law of Large Numbers (LLN) dictates that by observing the random process over a large number of cases, a computation of the

random processes' statistics can be made, which will be an approximation of the answer to the problem.[4]

Instead of the discretization techniques of deterministic methods, Monte Carlo codes use a finite number of neutron histories to sample the processes within the region(s) being studied. As stated by Forrest Brown at Los Alamos National Laboratory (LANL), the key to MC methods is the notion of "random sampling," which involves the use of a pseudo random number generator for sampling probabilities of neutrons from their birth until it is either absorbed or boundary conditions are applied.[5] The outcomes of each neutron history are tracked and after a sufficient number of histories are completed, averages of the parameters in question are calculated. This process is repeated for a defined (by the user) number of generations. In eigenvalue calculations such as the ones presented in this study, the source (both in magnitude and spatial distribution) is unknown at the beginning of the simulation, so a guess is made. After the first generation of neutron histories, the tallies are used to refine the initial guess of the source distribution for the second generation. The first few generations will clearly have poor statistics because the code has not accumulated enough neutron historical data to develop a precise source distribution. Therefore, in Eigenvalue calculations the first few generation are used for source convergence only. The number of generations "skipped" is determined by the user and is based on their experience and the complexity of the problem. The user also defines the number of "active" generations that will be used to develop the statistical bounds of the parameters of interest. Obviously, the more skipped and active generations run would yield better results, but this comes at the cost of longer runtimes and larger memory requirements. Therefore, the user must balance the need to assuring source convergence and statistical accuracy with the time and computer system available to them.

At the end of all active generations, the average and the associated uncertainty are established by calculating the standard deviation of the parameter values from each sampled generation.[2] In a depletion calculation, the time period over which the simulation is conducted is divided into N burnsteps. For each burnstep one through N, the Monte Carlo process of

producing neutron history samples, parameter and uncertainty calculations, and depletion is repeated until the Nth step is complete.

Forrest Brown noted that the steady increase in computing power has caused an evolution in the use of MC methods for reactor analysis problems over the years. In the 1960's, the principal use of MC methods was for k_{eff} calculations. The 1970's saw a move into more detailed assembly power calculations, while the 1980's moved toward more detailed 2D whole-core problems. The 1990's expanded their use to 3D whole-core applications, and today 3D whole-core problems can be tied into detailed depletion and reactor design examinations.[6]

There are many Monte Carlo codes currently in use in the nuclear industry, but several stand out for their capabilities and the strong record of validation when benchmark problems have been compared with the results from deterministic codes. The Monte Carlo N-Particle (MCNP) code developed by Los Alamos National Laboratory commonly serves as the reference for validation of many other MC and deterministic codes. KENO is a MC subroutine that as part of the SCALE package can operate as a stand-alone program or within a sequence of other SCALE subroutines such as TRITON6 (for depletion) or CSAS5 (for criticality). MC21 is a relatively new MC transport code under joint development at Knolls Atomic Power Laboratory and the Bettis Atomic Power Laboratory. MC21 has been validated against MCNP and has several features that its developers hope will push the MC method into a more dominant role in reactor analysis.[7] The SERPENT code, developed in Finland and also well published and validated, was the principal code used in this research effort and will be more specifically covered in Chapter 3.

2.2 The Normal Distribution: Established Bounds of Uncertainty

The random sampling at the heart of the MC method described previously typically involves a large number of repeated trials. When these trials are independent, the population of the calculated parameters will form a normal distribution, one of the most important continuous

probability distributions in mathematics.[8] The mean value of the distribution will fall in the middle of the probability distribution, and is calculated by

$$\boldsymbol{m = \frac{1}{N}\sum_{i=1}^{N} m_i}$$

The variance of the sample, which is the measure of how much spread there is in a set of numbers, is found by

$$\boldsymbol{\sigma^2 = \frac{\sum_{i=1}^{N}(X_i - m)^2}{N-1}}$$

where N is the number of random tests and m is the mean average from N tests.[8] The standard deviation (σ), which is always positive, is the square root of the variance and has several key applications. One of the properties of the standard deviation is that 68.27% of the population in the normal distribution will fall within one standard deviation of the mean. Therefore, it is common to represent a value derived from a normal distribution as a pair of numbers; the first being the mean and the second being the $\pm$ standard deviation. Typically, approximately 95% of the normal distribution population will fall within two standard deviations of the mean. Finally, 99.7% of the population will fall within three standard deviations of the mean. This property of the normal distribution is critical in helping scientists and engineers establish a level of confidence in their results.[8]

2.3 Is Monte Carlo's Randomness Really Random?

Now equipped with an understanding of the perceived confidence level of MC calculations, it is important to understand the computational challenges that make an accurate solution either difficult or expensive (in terms of effort and computational resources). Two of the six issues mentioned by Martin and also cited as concerns by Brown are the convergence of

the source distribution and the under-prediction bias in confidence intervals. As Brown points out, conventional MC methods use power iteration to converge on a source distribution across the problem geometry. During this process, the starting locations for the neutron histories for step n are determined by the fission sites from step n-1. This problem creates an inter-cycle correlation, meaning that the random events discussed above that are used to form our normal distribution are no longer completely independent. While this effect does not change the calculated parameter values, it does effect the variance of these values. And due to the correlation being positive, the result will be an under-estimation of the variance, meaning the perceived variance will be smaller than the actual variance in the parameter. The degree to which this effect has an impact on results depends on the geometry of the problem and on the steps that MC user takes to account for it.

2.3.1 Problem Geometry: Because Size Does Matter

Dumonteil and Courau outline the issue facing the use of MC techniques for large scale simulations because of their unique difficulty in correct source convergence.[9] A simplified version of the Boltzman transport equation described previously can be iterated using an eigenvalue such that:

$$\Psi = \frac{1}{k_{eff}} F\Psi$$

Where Ψ is again the angular flux, k_{eff} the eigenvalue to be iterated, and F the leakage, collision, scattering, and fission operators. With power iteration an initial guess at the angular flux is made (Ψ^n) and the eigenvalue is calculated. This eigenvalue is then used to calculate the next value of angular flux and the next eigenvalue using:

$$\Psi^{n+1} = \frac{1}{k_{eff}} * F\Psi^n$$

$$k^{n+1} = k^n * \frac{\int dVM\Psi^{n+1}}{\int dVM\Psi^n}$$

Because the operator F has a series of solutions, the eigenvalues can be ordered by magnitude such that:

$$k_0 = k_{eff} > k_1 > k_2 > \cdots$$

The Dominance Ratio (DR) is defined as the ratio between this first and second eigenvalue and is given by:

$$DR = \frac{k_1}{k_0} \leq 1$$

The DR is important in eigenvalue problems because it helps to determine the speed with which the fission source will converge. In a problem with a small geometry, where the mean free path of a neutron is such that neutrons can stream from one side to another, the two sides of the geometry can "communicate" with one another and are thus the behavior in one area is closely coupled to the other. Conversely, large geometries are typically more loosely coupled, and the convergence of k_{eff} and even more so the flux distribution may be very slow, which can have an adverse effect on the statistics of the MC calculation.

Problems with a small DR may require only a few cycles to converge, but problems with DR's approaching unity may require hundreds or thousands of cycles. Determining the number of inactive cycles necessary for proper source convergence is critical to achieving an accurate solution, but will come at the cost of a more expensive computation.

2.4 Understanding True Variance and Why it Matters

In a 2011 paper, Hoogenboom, Martin, and Petrovic proposed a 3D MC benchmark problem for detailed power density calculation in a full-size PWR reactor core.[10] While the purpose of the benchmark was to track the progress of MC code developers in increasing the performance of their systems, the benchmark set the bar for the acceptable standard deviation in

each power region to be <1%. The authors specifically note that this level of statistical uncertainty is important because it is the typical objective for current design calculations of a nuclear reactor core while also noting that in requiring the standard deviation in each region be <1%, the real standard deviation in the regions may be higher. Therefore, if MC were to be used as the primary means of design verification by approval authorities such as the Nuclear Regulatory Commission (NRC), gaining more insight into the magnitude of the difference between the reported and true variances is essential.

CHAPTER 3

THE MONTE CARLO SERPENT CODE

This section describes the SERPENT code that was selected for use in this numerical study and describes several of the code settings that were used.

3.1 SERPENT Code Description for Reactor Physics Calculations

SERPENT is a Continuous-Energy Monte Carlo reactor physics burnup calculation code developed by the VTT Technical Research Centre of Finland. The code uses a universe based geometry model that allows for the highly accurate modeling of virtually any two or three dimensional environment including fuel lattices, microscopic TRISO (TRi-ISOtopic) fuel particles, and pebble bed fuel designs.[11]

Cross section data is reconstructed on a unionized energy grid used for all reaction modes and for all nuclides. The advantage of the technique is a significant speed up of the calculation because it minimizes the amount of grid iteration required. The drawback of the approach is that the grid size may become extremely large due to the significant number of actinide and fission products that are tracked, and the cross section data oftentimes requires gigabytes of computer memory.[12] In order to minimize the memory needed for the grid, a fractional reconstruction tolerance is used to combine data points with little relative difference. The default value of 5E-5 was used in all test problems, well under a tolerance of 1E-3 that has shown to be the cutoff where the accuracy of the results begin to be significantly affected. [13]

SERPENT reads neutron interaction data from ACE format cross section library files. While any ACE data may be downloaded and used in a calculation, default cross section libraries included with the code are ENDF/B-VI.8 and ENDF/B-VII. All numerical studies conducted as part of this research effort used the ENDF/B-VII library.

As discussed previously, all neutrons are tracked in a Monte Carlo simulation until the neutron is either absorbed or it leaves the defined environment, at which point the boundary condition (BC) is applied. The three options are:

1) Black- the neutron is killed
2) Reflective- the neutron is reflected back into the geometry (mirror reflection)
3) Periodic- the neutron is moved to the opposite side of the geometry

Reflective and Periodic boundary conditions can be used to create an infinite and semi-infinite lattice arrangements, but they can only be applied to square or hexagonal lattices. All test problems in this research study used reflective BC's except the full core model, which used black.

In order to set the reaction rate for the burnup calculation, SERPENT provides seven options. The options are source, fission, loss, absorption rate, flux, power, and power density. Power density (kW/g of Heavy Metal (HM)) was the option used for all test problems in this study.

Like many deterministic and stochastic reactor physics codes, SERPENT offers symmetry settings to simplify problems and reduce statistical error. Symmetry options were intentionally not used in any test problems in order to determine any statistical bias in the calculation.

3.2 Burnup Calculations in SERPENT

At the start, the composition of fuel is known from user inputs of the isotopes and their atomic densities. In the case of the Uranium Dioxide (UO_2) fuel used in these simulations, the material was modeled as a mixture of three isotopes of Uranium (^{234}U, ^{235}U, and ^{238}U with atom densities varying with enrichment) and three isotopes of Oxygen (^{16}O, ^{17}O, and ^{18}O at their natural abundance). From this initial composition, the code will calculate and track the evolution of 100's of isotopes produced from fission, neutron absorption, or radioactive decay. The

isotopic evolution of fuel in nuclear reactors is modeled using the Bateman equations, which are a series of differential equations to model abundance at any time *t* based on the initial abundance, reactor flux, and isotope cross section. Using the two digit superscript convention, the Bateman equations for the Plutonium isotopes ^{239}Pu, ^{240}Pu, and ^{241}Pu are:

$$\frac{\partial n^{49}}{\partial t} = \lambda^{39} n^{39} - \sigma_a^{49} \phi n^{49} + \sigma_\gamma^{48} \phi n^{48}$$

$$\frac{\partial n^{40}}{\partial t} = \sigma_\gamma^{49} \phi n^{49} - \sigma_a^{40} \phi n^{40} + \sigma_\gamma^{29} \phi n^{29} + \sigma_\gamma^{39} \phi n^{39}$$

$$\frac{\partial n^{41}}{\partial t} = \sigma_\gamma^{40} \phi n^{40} - (\lambda^{41} + \sigma_a^{41} \phi) n^{41}$$

In this example, the rate of change of the isotopic density of ^{239}Pu is a function of the beta decay of ^{239}Np, production from the neutron absorption of ^{238}Pu, and the destruction of ^{239}Pu due to neutron absorption (including fission). The rate of change in the isotopic density of ^{240}Pu is a function of the neutron capture of ^{239}Pu, the absorption and subsequent beta decay of ^{239}Np, the absorption and subsequent beta decay (twice) of ^{239}U, and the destruction of ^{240}Pu due to neutron absorption (including fission). [14]

In the SERPENT code, Transmutation Trajectory Analysis (TTA) and the Chebyshev Rational Approximation Method (CRAM) are two techniques used to solve the coupled differential equations for each isotope. The CRAM method is an advanced matrix exponential solution that has been shown to significantly speed up depletion calculations while producing results that have been validated against the popular CASMO-4E deterministic depletion code. [12] The CRAM method was used for all tests conducted as part of this research study.

3.3 SERPENT Code Uncertainty Estimation

SERPENT uses a consistent method to calculate the uncertainty of each output parameter. During each neutron source cycle the code sums the collisions, fissions, and other events that occur in that cycle. After all of the active cycles are complete, the code takes these cycle-specific values and determines the statistical mean and associated standard deviation.

Because the uncertainty estimate in SERPENT is based on the assumption of independent events, the code does not contain an algorithm that propagates the uncertainties from one burn-step to the next; instead, the estimate is based only on each separate step by itself. The code's estimate of the uncertainty typically increases with Burnup (BU) due to the increased diversity and amount of fission products and minor actinides in the system.

CHAPTER 4

ERROR PROPAGATION IN THE ASSEMBLY DOMAIN

This section describes the development of three test problems designed to investigate the propagation of errors at the fuel assembly (FA) level. All three test problems are based on the 2004 NEA Depletion Calculation Benchmark Devoted to Fuel Cycle Issues.[15] The geometric layout, material composition, and code settings for each test problem are described.

4.1 NEA Phase I Benchmark Fuel Assembly Problem

The NEA Fuel Cycle Benchmark was developed to provide a basis for comparing depletion calculations obtained with various codes and data libraries in a variety of fuel cycle configurations. The 17 x 17 fuel assembly described by the benchmark is a 2-D model that allows direct comparison of theoretical simulation results with experimental data obtained from TAKAHAMA-3, a Japanese Light Water Reactor (LWR).

The fuel assembly design, shown in Figure 4.1, features 264 fuel pins and 25 water filled Zircaloy-4 Guide Tubes (GT) that in practical applications would be used for the insertion of control rods or essential reactor instrumentation.

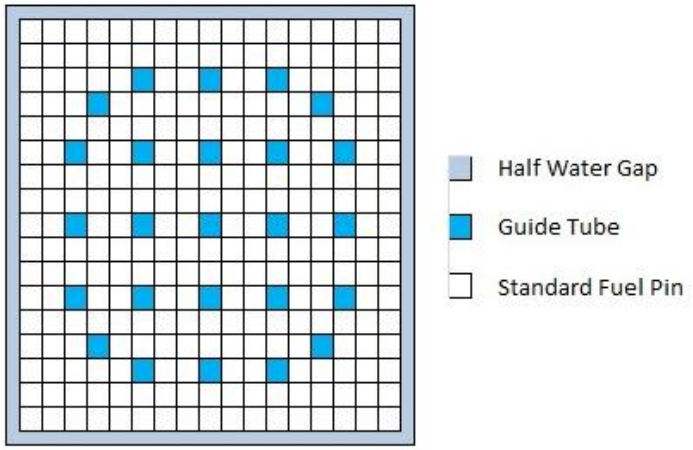

Figure 4.1 Layout of NEA benchmark fuel assembly

Each fuel pin is a Zircaloy tube filled with pellets of UO_2 fuel. The cross section of each fuel pin is shown in Figure 4.2 with the dimensions described in Table 4.1. It should be noted that the fuel pin does not feature a gap that is typically present in pin designs to allow for thermal and radiation induced swelling of the UO_2 fuel pellets.

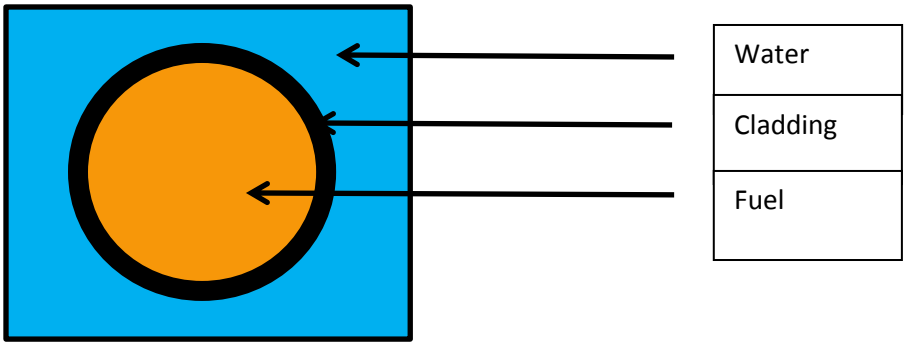

Figure 4.2: Cross Section of Fuel Pin

Table 4.1: Fuel Pin and GT Dimensions

Component	Dimension (cm)
Fuel Pellet Radius	0.4025
Fuel Pin Radius	0.475
Clad Thickness	0.0725
Pin Pitch	1.265
GT Inner Radius	0.573
GT Thickness	0.04

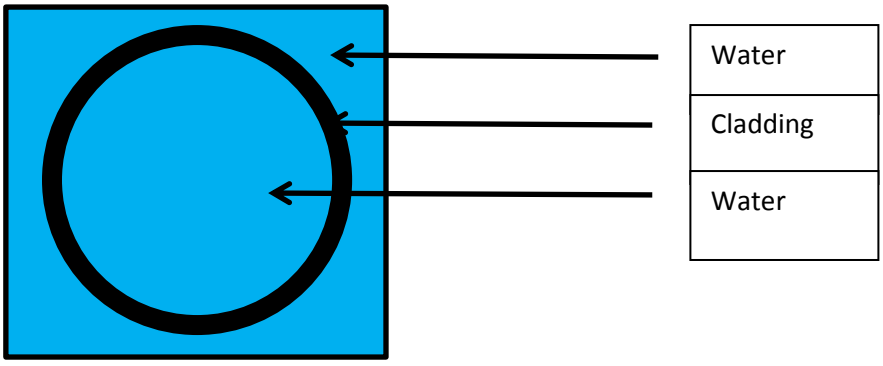

Figure 4.3: Cross Section of Guide Tube

Material compositions for the fuel pins, cladding, and moderator are in Table 4.2. It is important to note that each fuel pin was modeled and tracked as a separate fuel mixture. While each pin had the same initial composition as that found in Table 4.1, the separation in tracking each pin eliminated the averaging of flux across an assembly that would occur if any symmetry was incorporated into the model. Thus, each 17 x 17 fuel assembly had 264 individually modeled fuel pins and 25 guide tubes.

Table 4.2: Material Composition

	Density	Isotope	Weight Fraction
UO_2	10.412 g/cm^3	^{234}U	0.022%
		^{235}U	4.10%
		^{238}U	95.878%
Zirc-4	6.44 g/cm^3	^{nat}Zr	98.38%
		^{nat}Sn	1.30%
		^{nat}Fe	0.22%
		^{nat}Cr	0.10%
H_2O	0.7295 g/cm^3		

4.2 Development of the 2 x 2 "Quad"

In order to develop a model that would provide insight into error propagation at the fuel assembly level, yet still provide a problem complex enough to "challenge" the code, the fuel assembly described previously was placed in a 2 x 2 arrangement called a "Quad." Again, in an effort to avoid any symmetry or flux averaging across the test space, the pins of each assembly were modeled separately from one another, thus yielding a test problem with 1056 individually tracked fuel mixtures. A half water gap of 0.0538cm was modeled around each assembly to allow for the thermal expansion of the assembly that would occur at operating temperatures inside a reactor. Figure 4.4, produced by the reaction rate plotter within the SERPENT code,

shows the geometry of the Quad assembly. The half water gap surrounds the quad assembly and the full water gap bisects the model on the x and y axis and is visible upon close inspection.

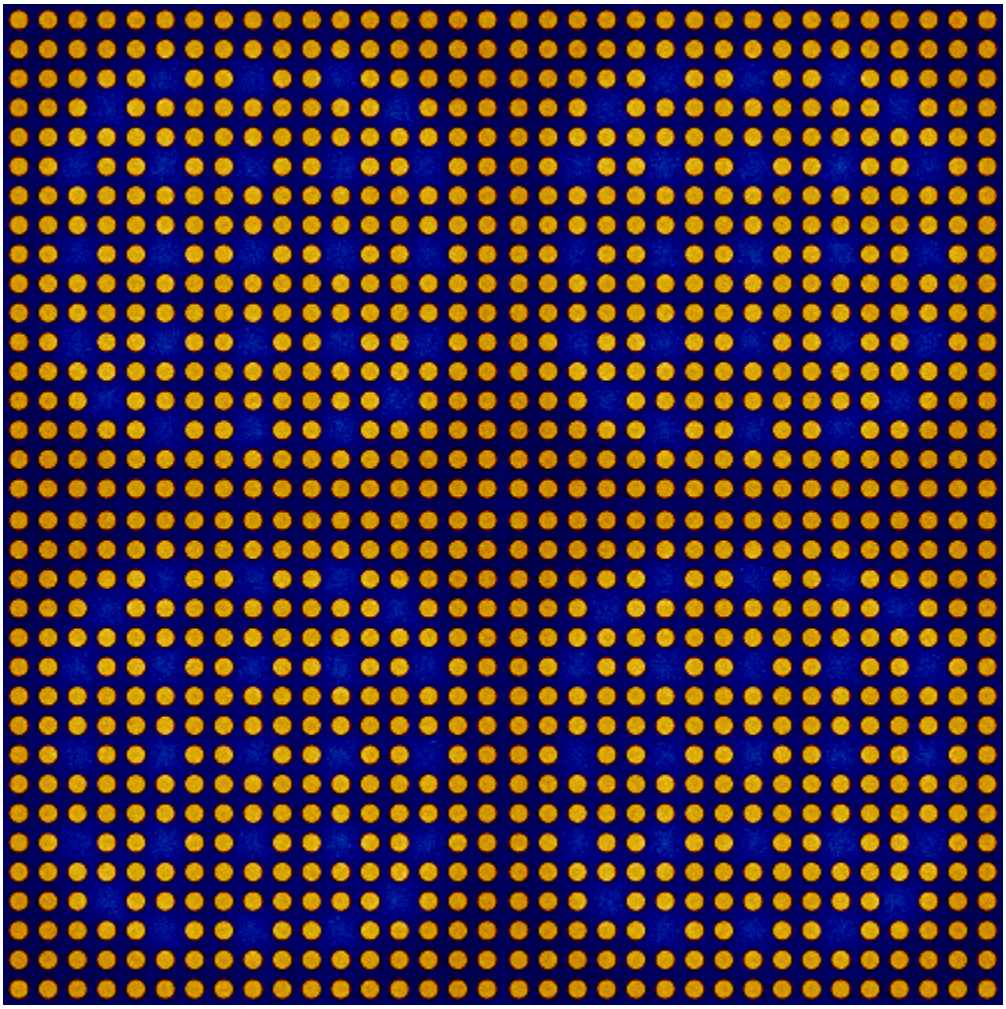

Figure 4.4: Geometry of the 2 x 2 “Quad” Fuel Assembly Model

4.3 Integration of Burnable Absorber

Nuclear reactors, by design, exist because they can maintain a chain reaction from one generation to the next whereby the neutron population remains constant. In order for this chain reaction to remain possible over long periods of time, excess reactivity is initially built into the system. This excess reactivity must be suppressed initially to prevent the reactor from spiraling out of control. While this can be done with the use of control rods or soluble boron, the most

economical method has been to use a burnable absorber that is integrated into the fuel pin at the time of its construction to control the majority of the excess reactivity, and use control rods and soluble boron only for minor adjustments. The idea is to place a strong absorbing material that will control this excess reactivity at low BU but will be consumed at higher BU. Traditionally, strong absorbers like Gadolinium or Europium were mixed with UO_2, although the strong self-shielding characteristics of these materials meant that they had to be incorporated with fuel of lower enrichment and could shorten the cycle length if they were consumed too slowly. Westinghouse has developed an innovative technology called Integral Fuel Burnable Absorber (IFBA) whereby ZrB_2 is sputtered onto the surface of the fuel pellets. The strong absorption cross section of the Boron helps reduce the excess reactivity, but it is consumed quickly and does not require a lower fuel enrichment.[16]

In order to significantly change the shape of the k_{eff} curve a sputtered layer of 2.25 mg ^{10}B/in. was modeled by subtracting the IFBA coating thickness from the thickness of the cladding. The geometry of the IFBA pins is given in Table 4.3

Table 4.3: Fuel Pin and GT Dimensions with IFBA

Component	Dimension (cm)
Fuel Pellet Radius	0.4025
IFBA Coating Radius	0.4041
Fuel Pin Radius	0.475
Clad Thickness	0.0709
Pin Pitch	1.265
GT Inner Radius	0.573
GT Thickness	0.04

Pins equipped with an IFBA coating can be arranged in varying patterns depending on the amount of burnable absorber needed for adequate reactivity suppression. For the fuel

assembly test problems a 156 pin loading pattern described by the Oak Ridge National Laboratory (ORNL) was selected.[17] This pattern is shown in Figure 4.5

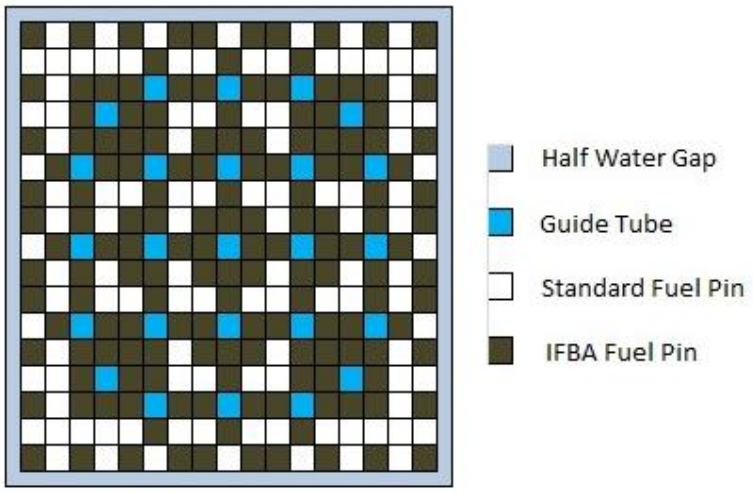

Figure 4.5: 156 Pin IFBA Loading Pattern

4.4 Quad Arrangement

In a nuclear reactor fuel assemblies are often shuffled so that fresh assemblies are interspersed with once, twice, or even thrice burned fuel depending on the fuel reloading pattern the reactor uses. In addition to maximizing the burnup of the nuclear fuel, this shuffling system also flattens the flux and helps control power peaking. In order to understand how this shuffling of high and low reactivity fuel could affect MC simulation results, three quads were designed with fresh fuel and IFBA equipped fuel in varying arrangements. Test problem one was a quad consisting of entirely fresh fuel assemblies. Test problem two was a quad consisting of entirely IFBA equipped fuel assemblies. Test problem three, a pattern that would be most likely to be found within an operating nuclear reactor, was a quad with two fresh fuel assemblies and two IFBA assemblies, with the IFBA assemblies found on the anti-diagonal. The arrangement of the three quads can be found in Figure 4.6.

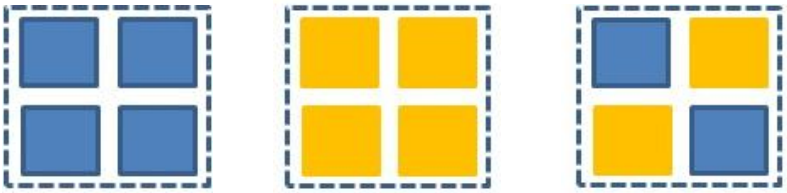

Figure 4.6: Quad Layouts for Test Problems 1-3, Respectively

4.5 Neutron Histories, Burnsteps, and Other Settings

If the statistical uncertainty of a simulation is large, the uncertainty bounds can mask effects that may be present. Put another way, it is possible to hide a 747 under a camouflage net if the net is big enough. But once the net is up, it is impossible to determine if there is a 747 underneath, or just a jeep and two guys with lawn chairs. In order for our tests to yield noteworthy results, it was determined that uncertainties should be kept low. To this end, several steps were taken to reduce uncertainty including the use of the Predictor-Corrector method (which repeated the neutron histories at the end of each cycle to average the flux for the depletion step), and keeping the length of the burnsteps as small as was practical. But the best way to insure good statistics was to run as many neutrons and generations as possible. Running 40,000 neutrons/generation with 500 active cycles 100 inactive or "skipped" cycles used for source convergence yielded a good blend of small statistical uncertainty and practical calculation runtime. Thirty-seven total burnsteps were run, with shorter burnsteps in the beginning and longer ones (never exceeding fifty days in length) on the back end. A complete listing of all simulation parameters can be found in Appendix A.

CHAPTER 5

ASSEMBLY DOMAIN ERROR PROPAGATION RESULTS

This section describes the results obtained from the simulation of the three test problems described in Chapter 4. Each test problem was run 19 times by changing the initial seed number. The observed uncertainty obtained from the 19 identical simulations is compared to the uncertainty estimated by the code. A detailed analysis of this comparison follows.

5.1 Calculation Time and System Resources Required

All test problems were run on a Linux cluster, in serial mode, using one core of a Quad-Core AMD Opteron processor (2.3GHz). The required runtime and memory demands of each test problem can be found in Table 5.1.

Table 5.1: Wall-clock Calculation Time and Memory Requirements

Test Problem	Memory Req. (GB RAM)	Ave. Runtime	
		Hours	Days
One	30.1	174	7.2
Two	30.4	184	7.7
Three	30.4	191	8

SERPENT is very memory intensive for several reasons. As discussed in Chapter 3, the continuous energy grid speeds up calculation but is very memory intensive unless thinning techniques are used (which can introduce unwanted error into the system). Additionally, the larger the neutron population used for the transport calculation, the more memory will be required. According to the code's developer, a calculation using ENDF/B-VII cross sections, the default settings on the energy grid, all available fission product cross sections, and a single burnable material required 4.4 GB RAM, with each additional depletion zone adding 0.03GB to

the required memory.[18] Considering the large number of source neutrons and the 1056 fuel mixtures in the test problems, it is easy to see why the test problems required so much memory.

5.2 Uncertainty in K_{eff}

Each of the three test problems consisted of 37 burnsteps, which can be found in Appendix A, At each of these 37 burnsteps, the SERPENT code produces a keff and uncertainty value in the form

$$(\boldsymbol{K_{eff}}, \boldsymbol{\sigma})$$

The 19 values of k_{eff} and their uncertainty at each burnstep were averaged. The average value of the uncertainty is referred to as σ(reported).

$$\overline{\boldsymbol{K_{eff}}} = \frac{1}{N}\sum_{n=1}^{N} k_{eff_n}$$

$$\overline{\boldsymbol{\sigma}} = \frac{1}{N}\sum_{n=1}^{N} \sigma_n$$

The set of 19 k_{eff} values also produced a standard deviation. The standard deviation of the set is referred to as σ(observed). Thus a ratio of the two values takes the form

$$\boldsymbol{R} = \frac{\boldsymbol{\sigma(observed)}}{\boldsymbol{\sigma(reported)}} = \frac{\boldsymbol{\sigma}}{\overline{\boldsymbol{\sigma}}}$$

5.2.1 Behavior of K_{eff}

The mean average values of k_{eff} derived from the 19 runs were plotted with burnup and can be found in Figure 5.1. Test problem one, consisting of the four fresh fuel assemblies, obviously has the highest initial k_{eff}, while test problem two, which features four IFBA assemblies, had the lowest initial k_{eff}. It is also interesting to note that of the three test problems, test problem two had the highest final k_{eff} (0.93145$\pm$0.00029) while test problem one had the

lowest final k_{eff} (0.92719±0.00029). The final k_{eff} for test problem three fell in between the others (0.92941±0.00029).

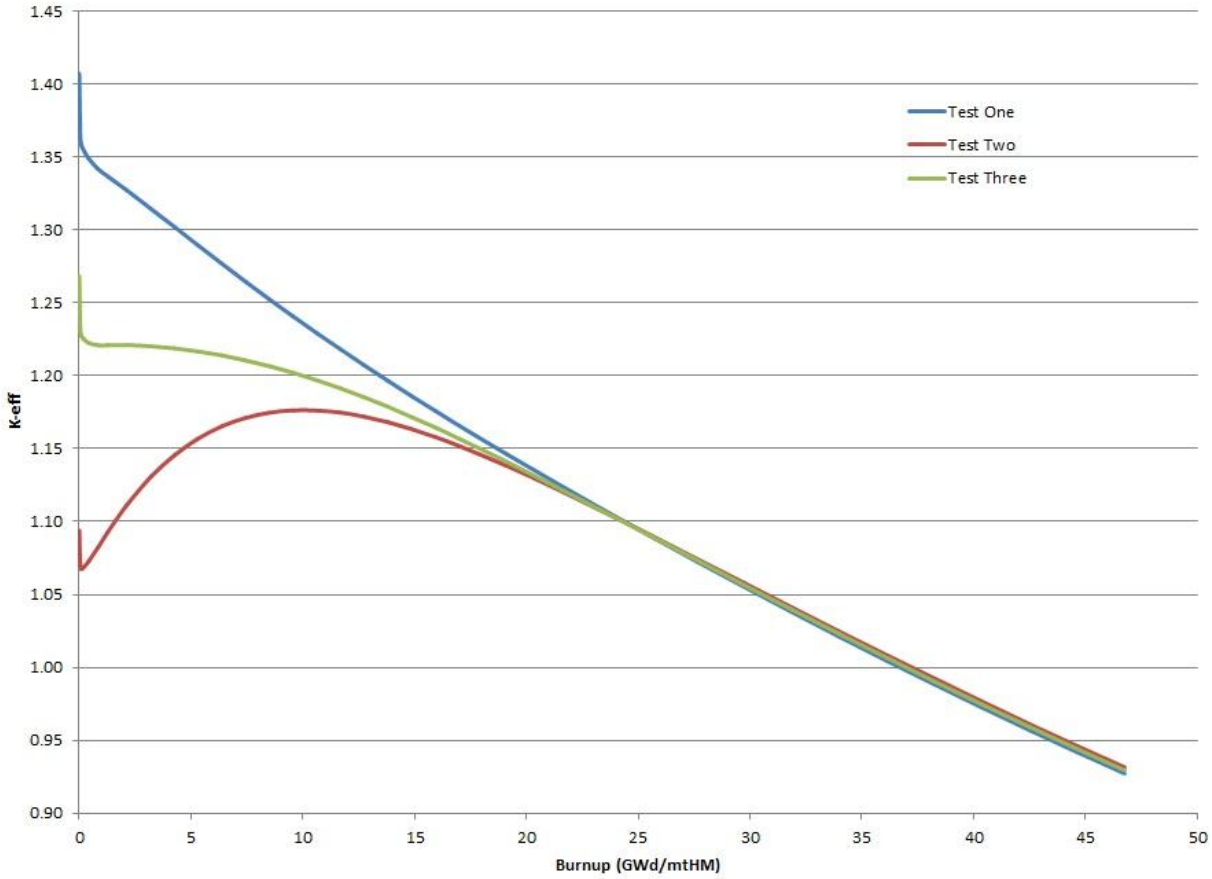

Figure 5.1: Keff vs. BU for Test Problems 1-3

5.2.2 Behavior of Observed and Reported Uncertainties TP One

The plots of the observed and reported uncertainties in test problem one, found in Figure 5.2 and Figure 5.3, show that for BU less than 20GWd, the code's reported uncertainty in k_{eff} is less than the true uncertainty of the parameter. At BU greater than 20GWd, the observed uncertainty of k_{eff} tends to oscillate between exceeding and being less than the reported uncertainty. While there is obvious statistical noise in the data, it is interesting to note that the addition of a trendline shows that the true uncertainty is nearly constant. The proximity of the

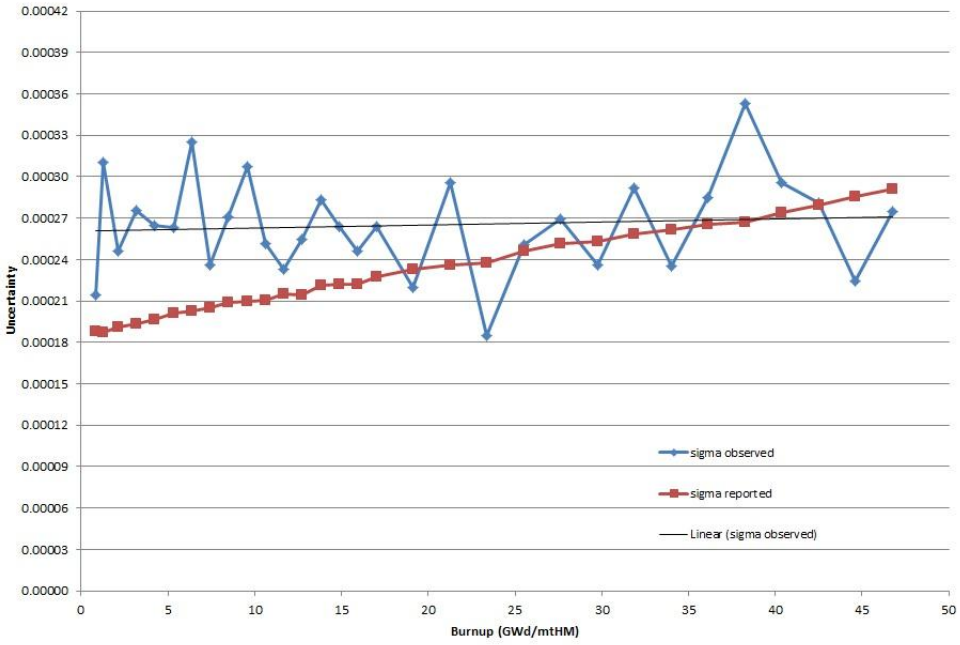

Figure 5.2: Observed and Reported Uncertainty vs. BU, TP 1

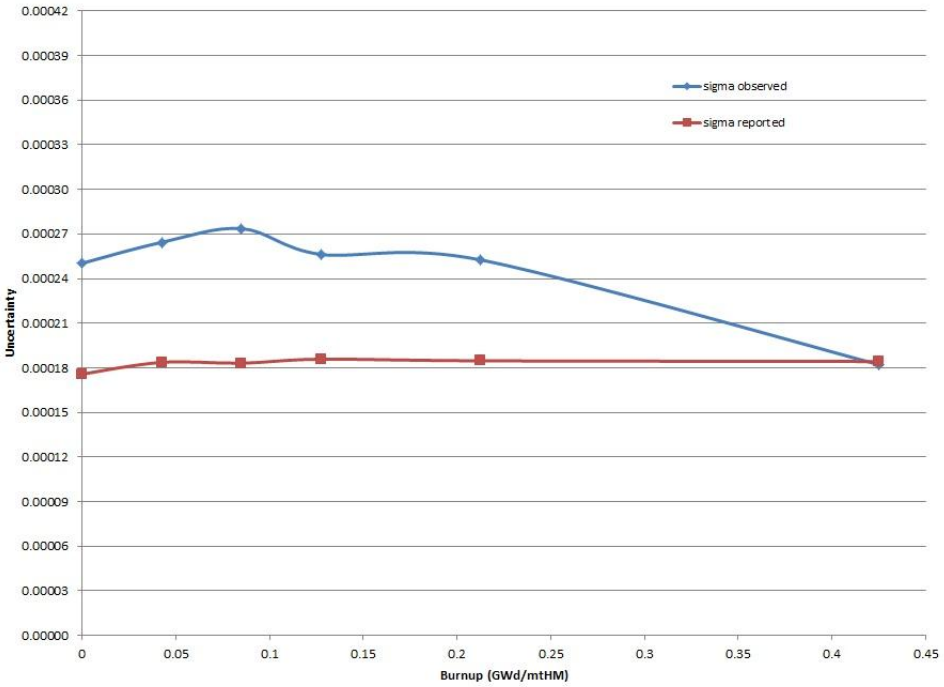

Figure 5.3: Observed and Reported Uncertainty at BOC vs. BU, TP 1

trendline and the observed uncertainty shows little variance. Across all 37 depletion steps, the mean observed uncertainty in test problem one was 26 percent mille (pcm). The mean reported uncertainty was 22pcm.

5.2.3 Behavior of Observed and Reported Uncertainties TP Two

The plots of the observed and reported uncertainties in test problem two, found in Figure 5.4 and Figure 5.5, show that for BU less than 20GWd, the observed uncertainty tends to oscillate above and below the reported uncertainty. At BU greater than 20GWd, the observed uncertainty is either very close to the reported uncertainty or falls below the reported uncertainty. While a trendline again shows that the true uncertainty is nearly constant, the variance in the observed uncertainty was 26% lower in test problem one than in test problem two. Across all 37 depletion steps, the mean observed uncertainty in test problem two was 25pcm, while the mean reported uncertainty in test problem two was 24pcm.

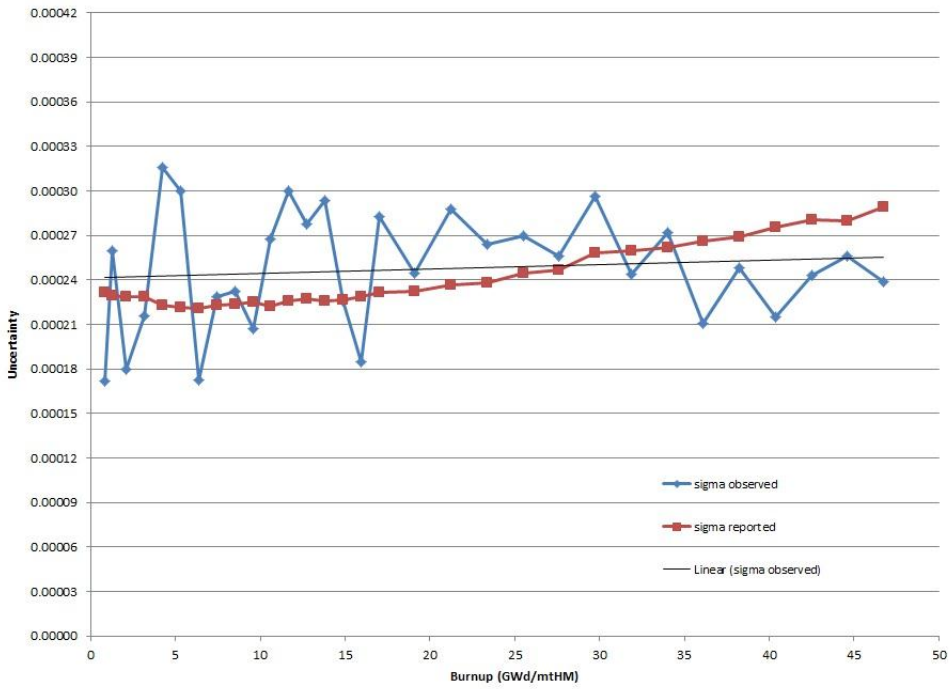

Figure 5.4: Observed and Reported Uncertainty vs. BU, TP 2

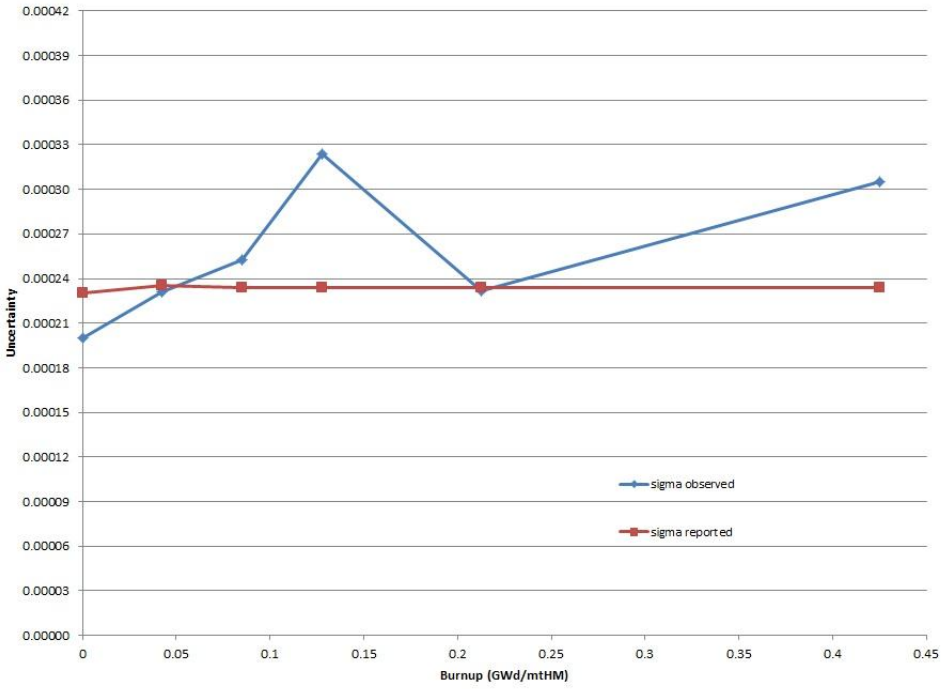

Figure 5.5: Observed and Reported Uncertainty at BOC vs. BU, TP 2

5.2.4 Behavior of Observed and Reported Uncertainties TP Three

The plots of the observed and reported uncertainties in test problem three, found in Figure 5.6 and Figure 5.7, show that for BU less than 30GWd, the observed uncertainty was nearly always higher than the reported uncertainty. At higher BU, the observed uncertainty still tended to be higher than the reported, but the difference between reported and observed uncertainties was much less than at lower BU. While a trendline again shows that the true uncertainty is generally constant, the variance in the observed uncertainty was an incredible 65% lower in test problem one than in test problem three. Across all 37 depletion steps, the mean observed uncertainty in test problem two was 27pcm, while the mean reported uncertainty in test problem three is 23pcm. Table 5.2 summarizes the average reported and observed uncertainties in k_{eff} for all three test problems.

Table 5.2: Average Reported and Observed Uncertainty in k_{eff}, TP1-3

Test Problem	Rep (pcm)	Obs (pcm)
TP1	22	26
TP2	24	25
TP3	23	27

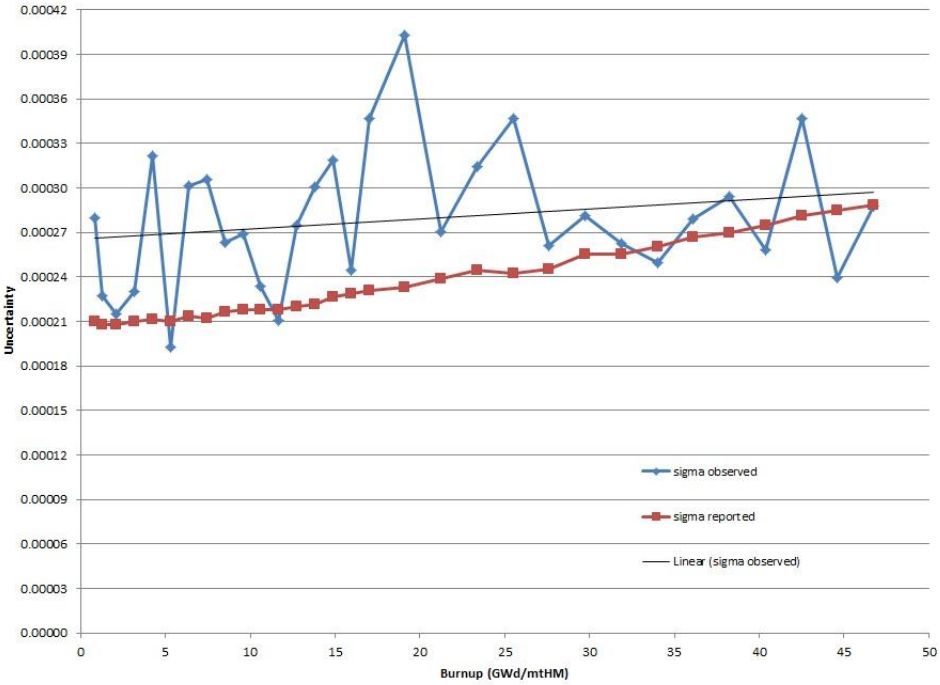

Figure 5.6: Observed and Reported Uncertainty vs. BU, TP 3

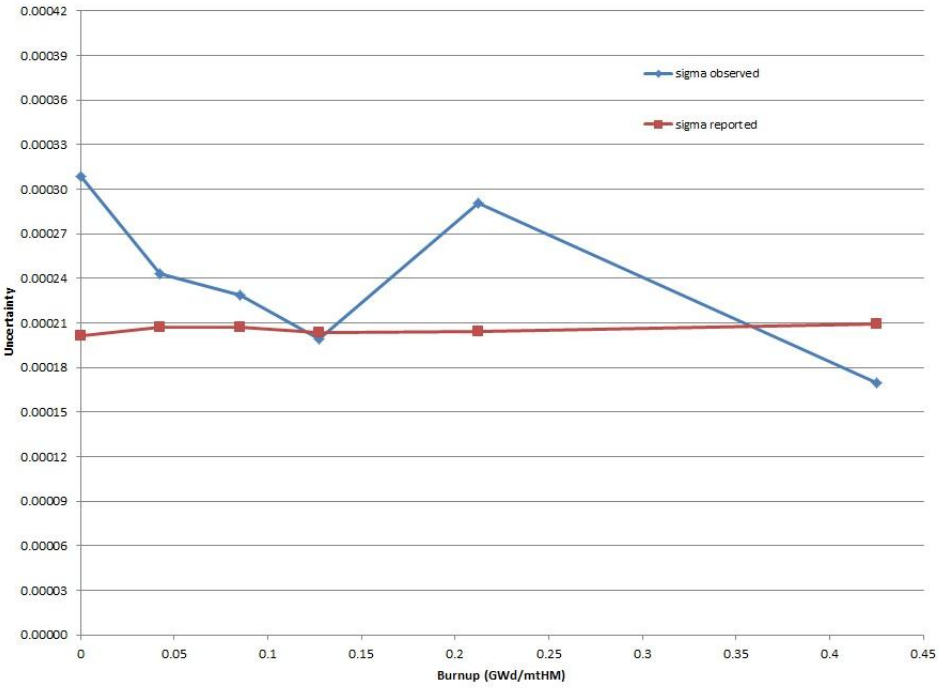

Figure 5.7: Observed and Reported Uncertainty at BOC vs. BU, TP 3

5.3 Uncertainty in Pin Powers

At each of the 37 burnsteps in each test problem, the SERPENT code produces a pin power edit with the pin power and its relative uncertainty for each lattice in the domain. This parameter takes the form

$$(\boldsymbol{P}, \frac{\boldsymbol{\sigma}}{\boldsymbol{P}})$$

The 19 pin powers and their relative uncertainty at each burnstep were averaged. The average value of the relative uncertainty is referred to as σ(reported).

$$\overline{\boldsymbol{P}} = \frac{1}{N}\sum_{1}^{N} P_n$$

$$\sigma(reported) = \overline{\left(\frac{\boldsymbol{\sigma}}{\boldsymbol{P}}\right)} = \frac{1}{N}\sum_{1}^{N}\left(\frac{\sigma}{P}\right)_n$$

The set of 19 pin powers produced a standard deviation, σ, which was divided by the average pin power and is referred to as σ(observed). Thus a ratio of the two values takes the form

$$\boldsymbol{R = \frac{\sigma(observed)}{\sigma(reported)} = \frac{\frac{\sigma}{\overline{P}}}{\left(\frac{\sigma}{\overline{P}}\right)}}$$

When the R value for each pin location is calculated, a measure of the accuracy (or rather, deviation from accuracy) with which the code predicts uncertainty, as well as the spatial distribution of these values, was easily observable.

At this point, it is also useful to introduce a numbering convention for each of the four assemblies in the Quad for easier reference. Figure 5.8 illustrates the reference numbers 1-4 and how they shall be applied to the geometric orientation of each assembly in the three test problems.

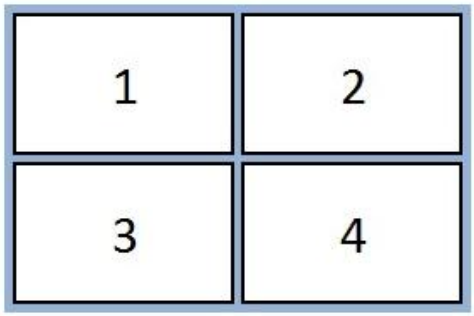

Figure 5.8: Numbering Convention of Fuel Assemblies within the Quad

5.3.1 Pin Power Observed and Reported Uncertainties TP One

A plot of the R values for each pin was made for each burnstep. In order to pictorially demonstrate the magnitude of the differences in observed and reported uncertainty for each pin, a color coding was applied to the R value for each pin location. Figure 5.8, a ratio map at startup, clearly shows a dramatic underestimation of uncertainty by the code.

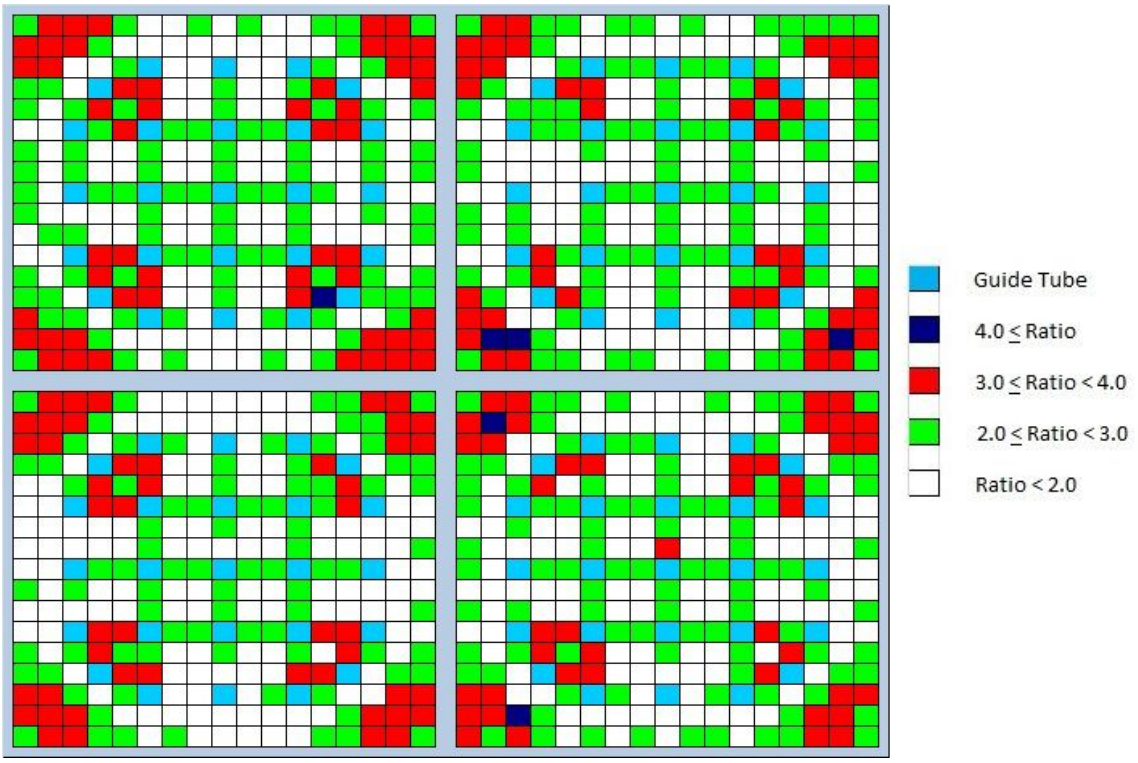

Figure 5.9: Observed-to-Reported Uncertainty Ratio, Startup, TP 1

The ratio map above clearly shows that the highest ratios of observed-to-reported uncertainty occur in the corners and around the cluster of guide tubes of each FA. At startup, the peak uncertainty in assemblies 1-4 was 4.11, 4.04, 3.99, and 4.10 respectively. Applying the Normal Distribution to the pins would suggest that 68.3% of pins in each assembly should fall within 1σ, 95.5% within 2σ, and 99.7% within 3σ. However, at startup we find that in FA 1, only 9.8% of all pins are within 1σ, 44.7% within 2σ, and only 79.9% within 3σ. Table 5.3 shows the percentage of pins in each assembly that fall within the sigma bounds for all 37 burnsteps. All the pins fell within 4σ except for a small number of burnsteps, when 2-4 pins exceeded the 4σ range. Clearly the true uncertainty of the pin powers is much higher than the uncertainty values estimated by the code.

As BU increased, the relative locations of the highest magnitude of uncertainty remained consistent, although the magnitude of the uncertainty ratios decreased. In contrast to the peak

uncertainty ratios at startup, the peak uncertainty ratios for FA's 1-4 at 900 days core residence time was 2.51, 2.67, 2.73, and 2.59 respectively. From Table 5.3, we can see that 14.4% of all pins are within 1σ, 93.9% are within 2σ, and 100% are within 3σ. These results indicate that the code still underestimates the true uncertainty of the vast majority of the pin powers, but that the magnitude of the underestimation largely diminishes over time. The ratio map at 900 days can be seen in Figure 5.9.

It is also important to note that there appears to be a bias in the reporting, which is clearly born out in Table 5.3. While the statistics do improve as residence time increases, it is interesting to note that FA 1 has much better statistics than any of the other three. In fact, from 750 days onward, over 90% of the pins in FA1 fall within 2σ, while FA's 2-4 rarely ever exceed even 80%. The uncertainty ratio maps for BU steps every 100 days can be found in Appendix B.

Table 5.3: Percentage of pins in each FA within given Standard Deviations, TP 1

Day	Assembly One			Assembly Two			Assembly Three			Assembly Four		
	3σ	2σ	1σ	3σ	2σ	1σ	3σ	2σ	1σ	3σ	2σ	1σ
0	79.9%	44.7%	9.8%	83.3%	47.3%	8.0%	82.2%	50.4%	7.2%	83.0%	47.0%	5.7%
1	82.6%	44.3%	7.2%	80.3%	43.2%	8.0%	81.1%	46.6%	6.1%	81.8%	47.0%	5.7%
2	79.2%	46.6%	9.1%	82.2%	43.9%	7.2%	81.4%	45.5%	8.0%	82.6%	46.2%	6.4%
3	81.4%	44.3%	8.3%	79.9%	43.6%	8.3%	82.6%	47.3%	4.9%	82.6%	48.1%	4.2%
5	82.2%	45.8%	9.5%	82.6%	44.3%	7.2%	81.8%	49.2%	7.2%	80.7%	48.5%	6.4%
10	81.1%	43.6%	9.5%	83.0%	47.3%	8.0%	81.8%	47.3%	5.3%	83.0%	45.8%	7.2%
20	80.7%	45.8%	9.8%	81.4%	45.1%	6.4%	83.0%	49.6%	7.6%	83.0%	46.6%	5.3%
30	80.7%	46.2%	8.0%	81.4%	43.9%	8.3%	82.6%	45.5%	6.4%	82.2%	45.8%	5.7%
50	81.8%	45.8%	9.1%	84.1%	45.8%	7.6%	83.3%	47.3%	5.3%	83.0%	48.1%	5.7%
75	83.3%	46.2%	8.7%	82.6%	46.6%	9.1%	81.8%	48.1%	6.8%	82.2%	49.2%	4.2%
100	86.0%	48.1%	7.2%	84.8%	50.8%	8.7%	84.8%	50.0%	6.8%	82.6%	48.9%	4.9%
125	86.4%	50.0%	10.6%	85.2%	50.0%	6.4%	84.5%	50.8%	7.6%	86.0%	50.0%	3.8%
150	89.0%	50.8%	9.1%	85.2%	51.1%	9.1%	87.9%	51.9%	5.3%	86.0%	51.5%	6.8%
175	88.6%	51.9%	8.3%	88.6%	51.9%	7.6%	87.1%	50.4%	8.0%	85.2%	52.7%	4.9%
200	93.2%	54.9%	7.2%	87.9%	51.9%	8.3%	89.0%	56.1%	6.4%	86.4%	54.2%	6.1%
225	90.9%	54.9%	10.2%	89.4%	54.5%	6.8%	89.0%	56.1%	7.6%	87.1%	56.8%	6.8%
250	94.3%	58.7%	10.2%	90.9%	54.9%	7.6%	90.5%	56.4%	5.7%	91.3%	54.2%	5.7%
275	94.7%	56.8%	11.4%	91.3%	58.7%	8.7%	91.3%	56.1%	6.8%	91.3%	56.4%	6.1%
300	95.8%	62.5%	8.7%	93.2%	58.0%	7.2%	92.8%	60.6%	7.6%	92.8%	57.6%	3.8%
325	97.0%	62.1%	8.7%	93.6%	60.2%	7.2%	95.1%	60.6%	8.3%	93.2%	61.0%	3.4%
350	96.2%	65.5%	9.8%	95.5%	62.9%	6.1%	95.8%	63.3%	8.0%	95.1%	61.4%	6.1%
375	98.1%	65.9%	11.0%	95.5%	67.4%	11.0%	95.5%	62.9%	8.0%	95.5%	63.6%	4.9%
400	98.9%	68.6%	7.6%	97.3%	67.4%	8.0%	96.2%	65.5%	7.6%	97.0%	64.0%	5.7%
450	99.6%	70.1%	8.3%	98.9%	70.8%	10.6%	97.7%	67.4%	4.5%	97.7%	68.6%	6.8%
500	100.0%	73.5%	7.2%	99.2%	73.1%	8.3%	99.6%	70.8%	9.5%	98.9%	73.5%	8.7%
550	100.0%	79.5%	10.2%	99.6%	73.1%	9.1%	99.2%	73.5%	8.7%	100.0%	73.9%	6.4%
600	100.0%	79.5%	10.6%	100.0%	76.5%	10.6%	100.0%	75.4%	8.7%	100.0%	75.0%	9.5%
650	100.0%	83.7%	12.5%	100.0%	76.1%	8.7%	100.0%	77.7%	6.1%	100.0%	77.3%	8.3%
700	100.0%	89.8%	11.4%	100.0%	78.0%	9.5%	100.0%	78.4%	8.0%	100.0%	79.5%	7.6%
750	100.0%	90.9%	10.6%	100.0%	79.5%	9.5%	100.0%	79.9%	8.7%	100.0%	79.9%	5.3%
800	100.0%	92.4%	11.0%	100.0%	79.5%	11.0%	100.0%	79.9%	9.1%	100.0%	81.4%	6.8%
850	100.0%	95.5%	14.4%	100.0%	79.9%	9.5%	100.0%	80.7%	8.0%	100.0%	80.3%	8.7%
900	100.0%	93.9%	14.4%	100.0%	79.5%	10.2%	100.0%	79.2%	6.1%	100.0%	79.2%	8.7%
950	100.0%	95.1%	12.5%	100.0%	78.4%	12.1%	100.0%	78.0%	10.2%	100.0%	79.2%	9.5%
1000	100.0%	93.6%	12.5%	100.0%	79.2%	9.8%	100.0%	79.2%	9.5%	100.0%	76.5%	8.0%
1050	100.0%	93.2%	14.0%	100.0%	76.9%	10.6%	100.0%	75.8%	8.0%	100.0%	76.5%	7.6%
1100	100.0%	93.6%	12.9%	100.0%	76.1%	9.5%	100.0%	74.6%	8.3%	100.0%	76.9%	9.5%

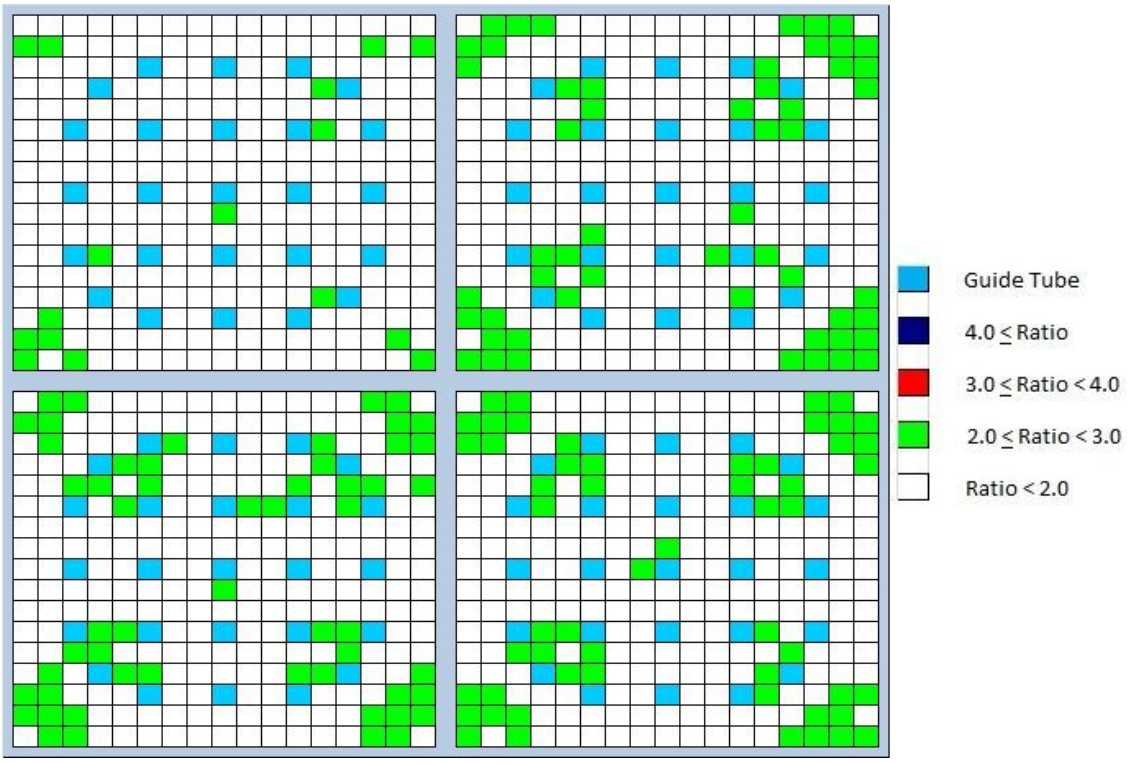

Figure 5.10: Observed-to-Reported Uncertainty Ratio, 900 Days, TP 1

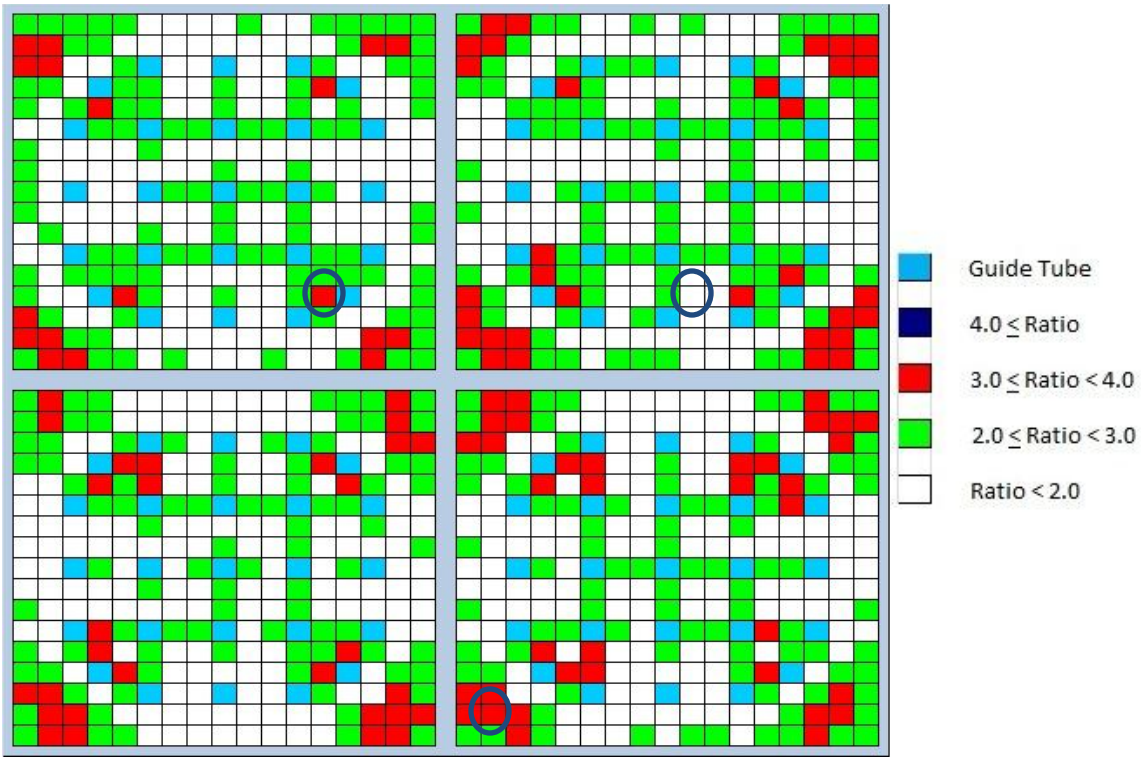

Figure 5.11: High and Low Uncertainty Ratio Pins, 200 Days, TP 1

Figure 5.11 is the pin power ratio map at 200 days. The highlighted pins in assemblies 1, 2, and 4 correspond to uncertainty ratios of 3.54, 0.98, and 3.88 respectively. A plot of the pin powers in these three FA's for each of the 19 runs was made with the uncertainty shown as error bars, and is shown in Figure 5.12 and 5.13. Figure 5.12, the pin with an uncertainty ratio less than 1, shows little variance in the pin powers. Figure 5.13, a plot of the pins in FA's 1 and 4 with high uncertainty ratios, shows a much higher variance in the pin powers. Also of note is the behavior of the pin powers in relation to each other. When the pin in FA1 is burning higher than its mean average, the pin in FA4 is burning lower than its mean. Conversely, a below average burn power in FA1 relates to an above average burn power in FA4. Since the distribution of power in a reactor must exhibit a zero-sum property (unless the power of the entire reactor is changes), this relationship is not unexpected, but it is worth noting.

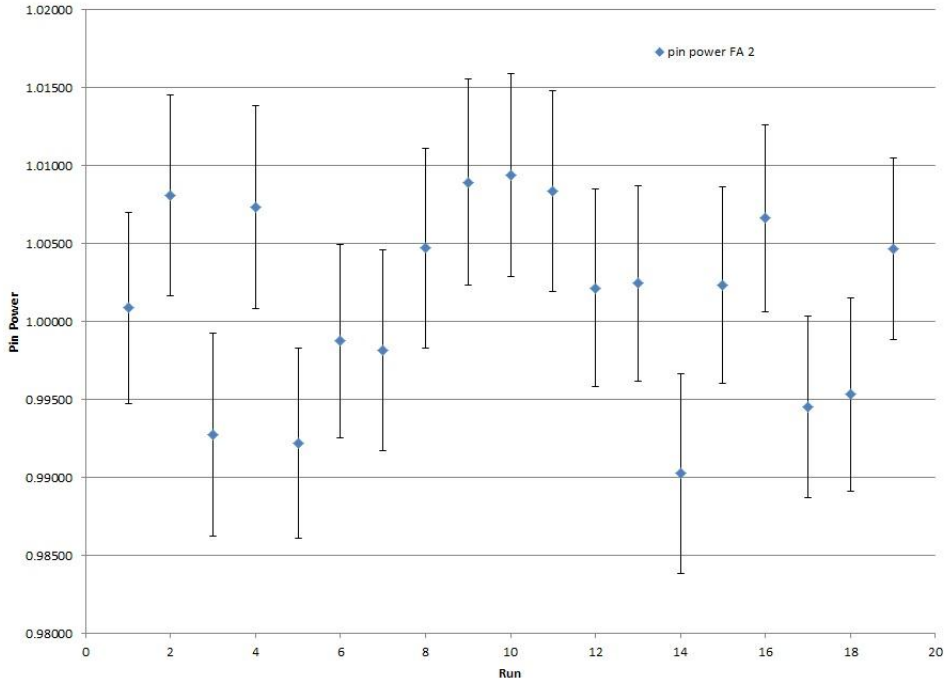

Figure 5.12: Pin Power with Absolute Uncertainty Ratio, FA 2, 200 Days, TP 1

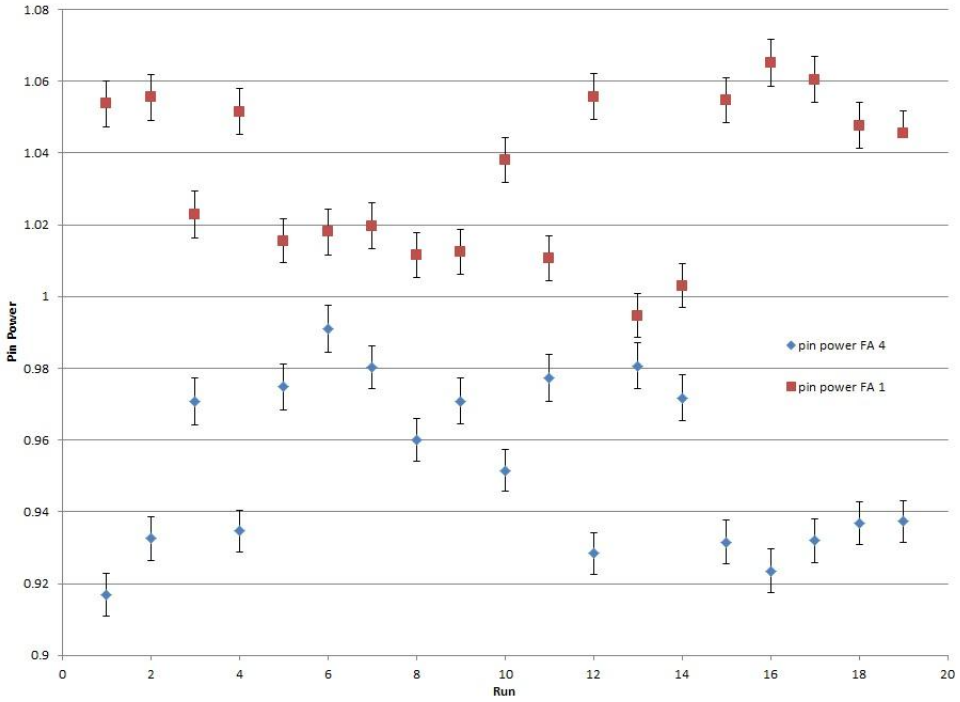

Figure 5.13: Pin Powers with Absolute Uncertainty Ratio, FA 1 & 4, 200 Days, TP 1

5.3.2 Pin Power Observed and Reported Uncertainties TP Two

The same process of uncertainty ratio comparison was applied to test problem two. Figure 5.14 shows the uncertainty ratio map at startup (please note the change in the color coding scale). The ratio map clearly shows that the distribution of ratios above and below unity are scattered randomly across the FA's. At startup, the peak uncertainty in assemblies 1-4 was 1.78, 1.59, 1.55, and 1.39 respectively. At startup we find that in FA 1, 51.1% of all pins are within 1σ, 99.2% within 1.5σ, and 100% within 2σ. Table 5.4 shows the percentage of pins in each assembly that fall within the sigma bounds for all 37 burnsteps. The true uncertainty for the majority of pins is clearly higher than the code's estimation, although the significance of the difference in the true and reported uncertainties is much less than in test problem one.

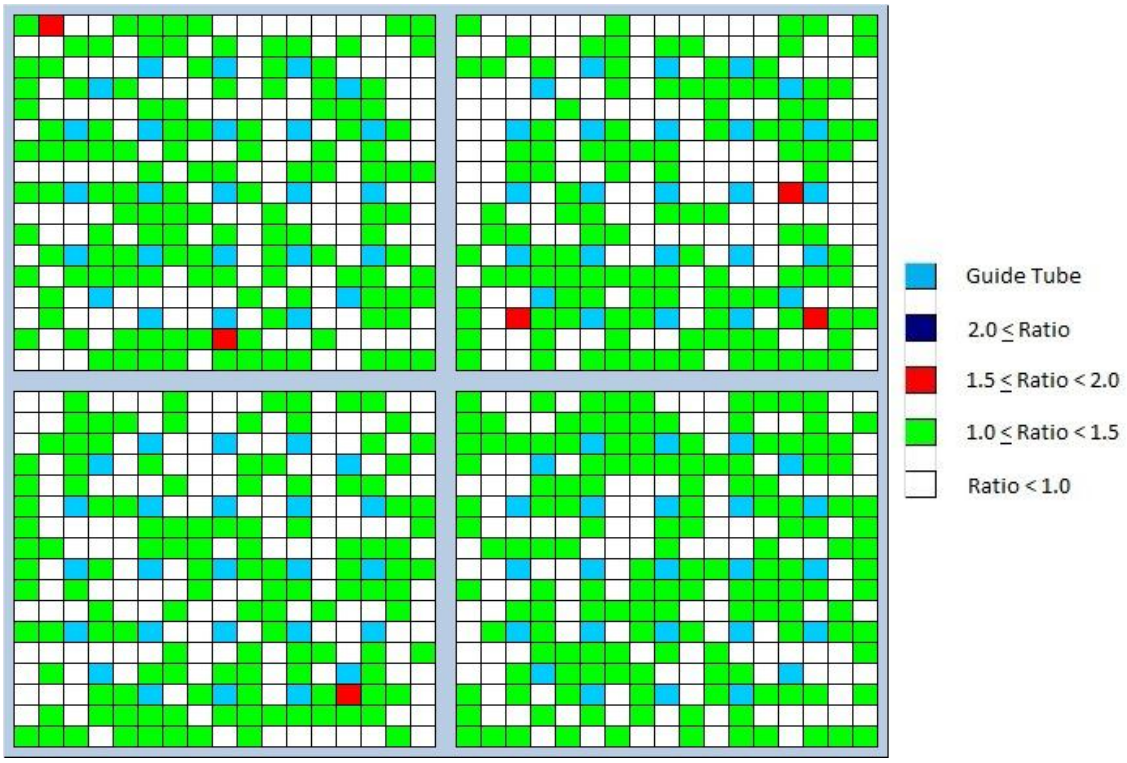

Figure 5.14: Observed-to-Reported Uncertainty Ratio, Startup, Test Problem 2

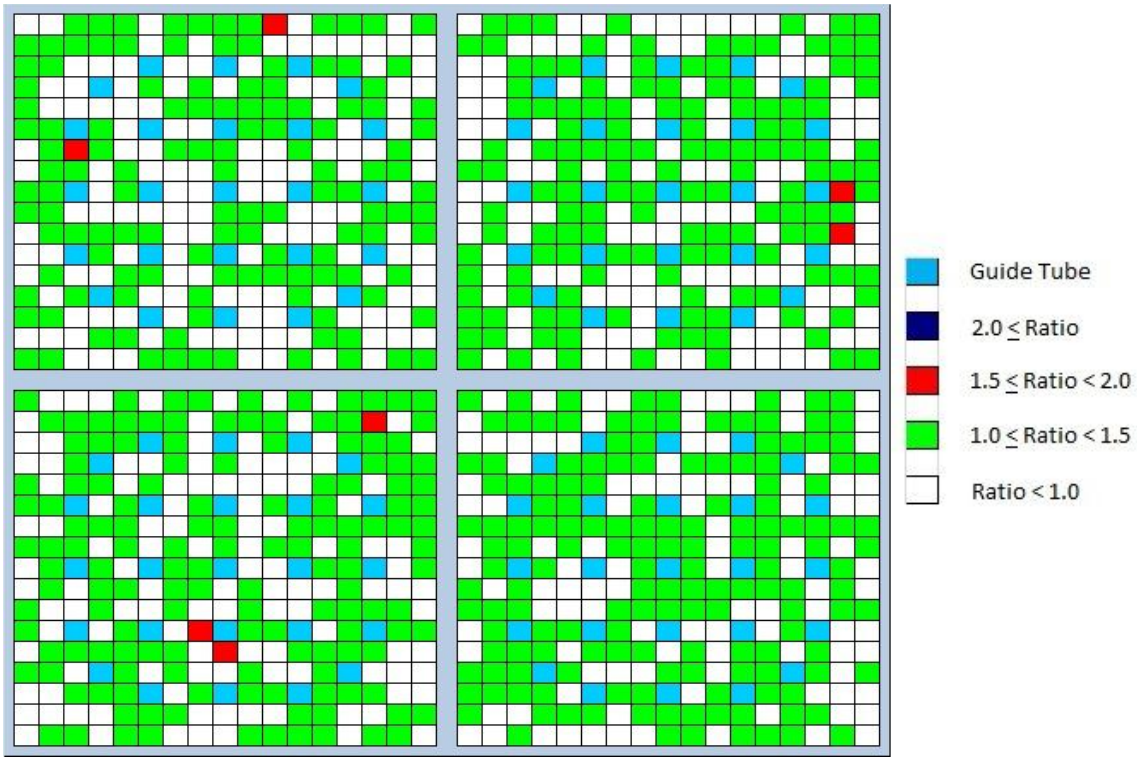

Figure 5.15: Observed-to-Reported Uncertainty Ratio, 900 Days, Test Problem 2

Table 5.4: Percentage of pins in each FA within given Standard Deviations, TP 2

Day	Assembly One			Assembly Two			Assembly Three			Assembly Four		
	2σ	1.5σ	1σ	2σ	1.5σ	1σ	2σ	1.5σ	1σ	2σ	1.5σ	1σ
0	100.0%	99.2%	51.1%	100.0%	98.9%	54.2%	100.0%	99.6%	53.8%	100.0%	100.0%	45.5%
1	100.0%	99.6%	53.0%	100.0%	100.0%	52.3%	100.0%	98.5%	53.4%	100.0%	98.9%	52.3%
2	100.0%	99.2%	45.1%	100.0%	99.6%	53.0%	100.0%	99.6%	56.1%	100.0%	100.0%	58.7%
3	100.0%	99.6%	52.3%	100.0%	99.6%	51.9%	100.0%	100.0%	52.3%	100.0%	100.0%	48.5%
5	100.0%	99.6%	54.5%	100.0%	100.0%	52.3%	100.0%	100.0%	51.5%	100.0%	99.2%	52.7%
10	100.0%	99.6%	49.2%	100.0%	99.2%	53.4%	100.0%	100.0%	51.1%	100.0%	98.1%	48.1%
20	100.0%	99.6%	48.5%	100.0%	98.1%	47.7%	100.0%	100.0%	50.0%	100.0%	100.0%	49.2%
30	100.0%	99.2%	48.5%	100.0%	99.6%	52.7%	100.0%	99.2%	46.6%	100.0%	99.6%	50.0%
50	100.0%	100.0%	52.3%	100.0%	99.2%	53.0%	100.0%	99.6%	56.4%	100.0%	99.6%	53.0%
75	100.0%	98.9%	53.8%	100.0%	98.9%	52.3%	100.0%	100.0%	50.4%	100.0%	99.6%	52.7%
100	100.0%	100.0%	51.9%	100.0%	99.6%	53.8%	100.0%	98.9%	57.2%	100.0%	100.0%	48.1%
125	100.0%	100.0%	51.5%	100.0%	99.6%	54.9%	100.0%	99.6%	56.1%	100.0%	100.0%	50.0%
150	100.0%	99.6%	50.4%	100.0%	100.0%	50.8%	100.0%	99.6%	50.8%	100.0%	100.0%	49.2%
175	100.0%	99.6%	50.4%	100.0%	99.2%	56.1%	100.0%	99.6%	51.1%	100.0%	99.6%	48.1%
200	100.0%	99.2%	47.3%	100.0%	99.6%	56.4%	100.0%	100.0%	50.4%	100.0%	99.6%	51.5%
225	100.0%	100.0%	50.8%	100.0%	99.6%	46.6%	100.0%	100.0%	50.0%	100.0%	99.6%	50.4%
250	100.0%	99.6%	52.7%	100.0%	99.2%	48.5%	100.0%	100.0%	45.8%	100.0%	99.6%	47.7%
275	100.0%	98.9%	50.4%	100.0%	99.6%	50.8%	100.0%	99.2%	50.4%	100.0%	99.6%	53.4%
300	100.0%	99.2%	49.2%	100.0%	99.6%	41.7%	100.0%	100.0%	50.4%	100.0%	99.2%	52.3%
325	100.0%	100.0%	47.7%	100.0%	99.6%	43.6%	100.0%	99.6%	51.5%	100.0%	100.0%	51.1%
350	100.0%	100.0%	48.1%	100.0%	100.0%	53.4%	100.0%	100.0%	47.7%	100.0%	99.2%	47.3%
375	100.0%	99.6%	57.2%	100.0%	99.6%	48.9%	100.0%	99.2%	49.2%	100.0%	99.6%	51.5%
400	100.0%	99.6%	45.8%	100.0%	99.6%	47.7%	100.0%	98.9%	45.8%	100.0%	100.0%	47.3%
450	100.0%	100.0%	46.2%	100.0%	99.2%	54.9%	100.0%	98.9%	48.9%	100.0%	99.2%	51.9%
500	100.0%	100.0%	48.5%	100.0%	98.9%	51.1%	100.0%	99.6%	47.0%	100.0%	98.9%	48.1%
550	100.0%	99.2%	46.6%	100.0%	100.0%	47.7%	100.0%	99.6%	49.2%	100.0%	99.6%	50.4%
600	100.0%	99.6%	48.9%	100.0%	99.2%	45.5%	100.0%	99.6%	51.1%	100.0%	98.9%	48.9%
650	100.0%	98.9%	47.3%	100.0%	99.6%	49.2%	100.0%	98.1%	40.5%	100.0%	99.6%	45.1%
700	100.0%	100.0%	45.8%	100.0%	99.2%	46.6%	100.0%	99.2%	43.6%	100.0%	99.6%	47.0%
750	100.0%	99.6%	40.2%	100.0%	98.9%	42.4%	100.0%	100.0%	51.1%	100.0%	99.6%	48.9%
800	100.0%	99.6%	50.0%	100.0%	100.0%	47.7%	100.0%	100.0%	48.1%	100.0%	100.0%	48.1%
850	100.0%	99.6%	53.0%	100.0%	99.2%	48.9%	100.0%	99.6%	48.5%	100.0%	100.0%	43.9%
900	100.0%	99.2%	51.5%	100.0%	99.2%	45.5%	100.0%	98.9%	44.3%	100.0%	100.0%	40.9%
950	100.0%	100.0%	46.6%	100.0%	98.9%	43.2%	100.0%	99.6%	45.5%	100.0%	99.6%	43.9%
1000	100.0%	99.2%	42.8%	100.0%	99.2%	44.3%	100.0%	99.2%	43.9%	100.0%	100.0%	42.8%
1050	100.0%	100.0%	46.2%	100.0%	99.2%	41.7%	100.0%	98.9%	42.4%	100.0%	98.9%	43.6%
1100	100.0%	99.2%	47.3%	100.0%	98.9%	42.8%	100.0%	100.0%	48.1%	100.0%	99.2%	38.3%

The behavior of the uncertainty ratios over time was significantly different in test problem 2 than in test problem one. In test problem one, peak ratios were extremely high at startup and significantly decreased over time. In test problem two, the magnitude of peak uncertainties at 900 days in FA's 1-4 was 1.58, 1.83, 1.55, and 1.49 respectively. At 900 days

we find that in FA 1, 51.5% of all pins are within 1σ, 99.2% within 1.5σ, and 100% within 2σ. Clearly the uncertainty ratios did not fall within the bounds of the normal distribution. The correlation introduced from generation to generation by refining the source distribution likely leads to the under-estimation of the true uncertainty in the pin power. Another interesting observation is that unlike test problem one, which showed obvious areas where high uncertainty ratios were consistently present, test problem two did not demonstrate a similar tendency. Pins tend to oscillate between ratios above and below unity as BU increases.

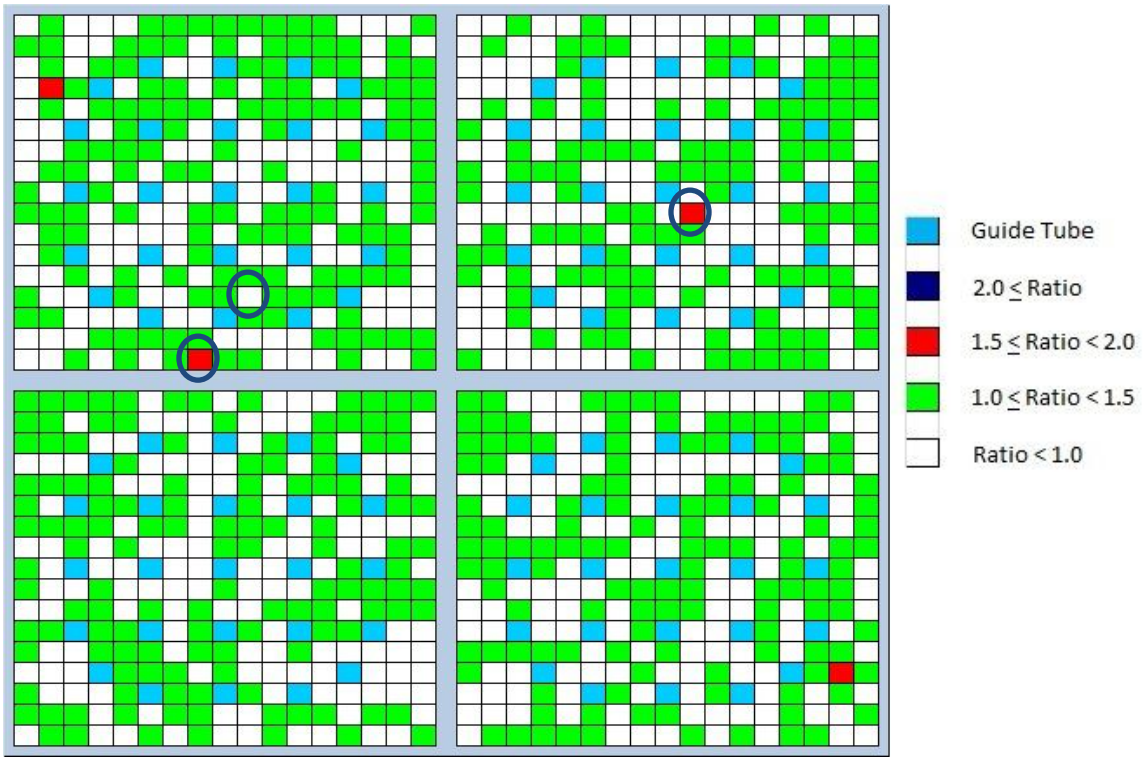

Figure 5.16: High and Low Uncertainty Ratio Pins, 200 Days, TP 2

Figure 5.16 is the pin power ratio map at 200 days. The highlighted pins (from left to right) in assemblies 1 and 2 correspond to uncertainty ratios of 1.67, 0.63, and 1.53 respectively. A plot of the pin powers in these three FA's for each of the 19 runs was made with the uncertainty shown as error bars, and is shown in Figure 5.17 and 5.18. Figure 5.17, the pin with

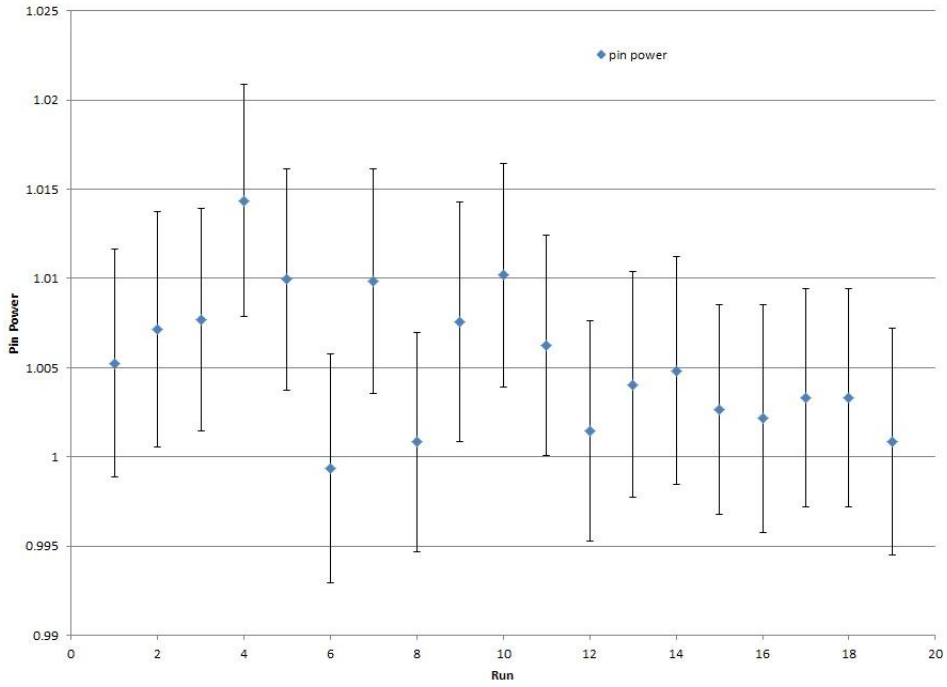

Figure 5.17: Pin Power with .63 Absolute Uncertainty Ratio, FA 1, 200 Days, TP 2

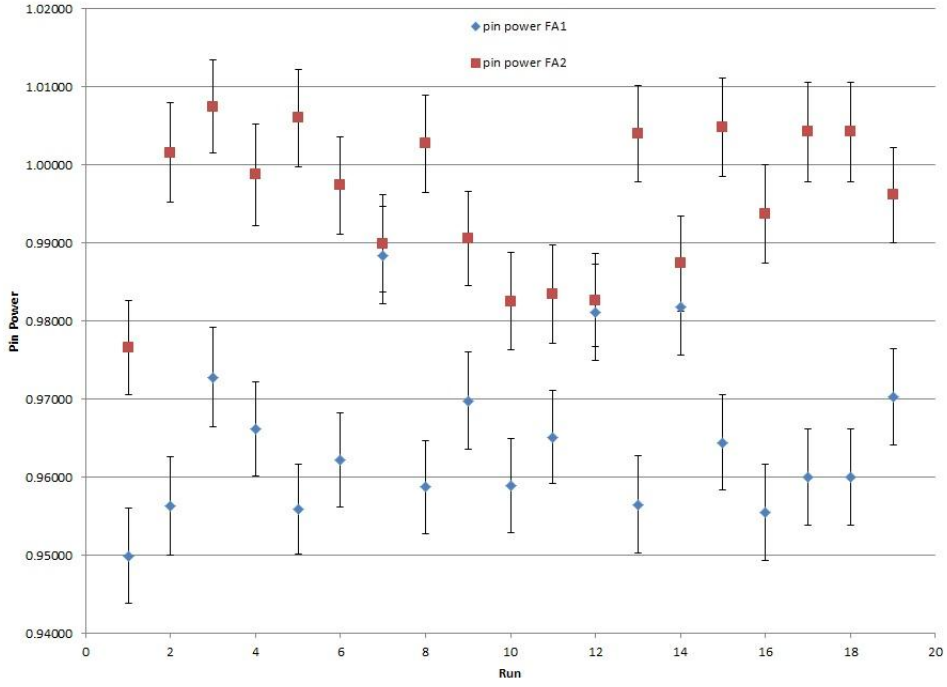

Figure 5.18: Pin Power with Absolute Uncertainty Ratio, FA 1 & 2, 200 Days, TP 2

an uncertainty ratio of 0.63, shows little variance in the pin powers. Figure 5.18, a plot of the pins in FA's 1 and 2 with high uncertainty ratios, shows a larger variance in the pin powers. Again, the behavior of the pin powers in relation to each other appears to be tied, but not for all runs. When a pin burns at a power lower than its average, other pins must burn at a higher rate in relation to their mean to make up the difference. The zero-sum property is still in effect, but the smaller differences in the pin powers is likely spread across any of the remaining pins in the test problem, not just two pins being compared in this plot.

5.3.3 Pin Power Observed and Reported Uncertainties TP Three

Figure 5.19 shows the uncertainty ratio map of test problem three at startup. The ratio map clearly shows that the distribution of ratios above and below unity are scattered randomly across the FA's. At startup, the peak uncertainty in assemblies 1-4 was 1.55, 1.48, 1.56, and 1.58 respectively.

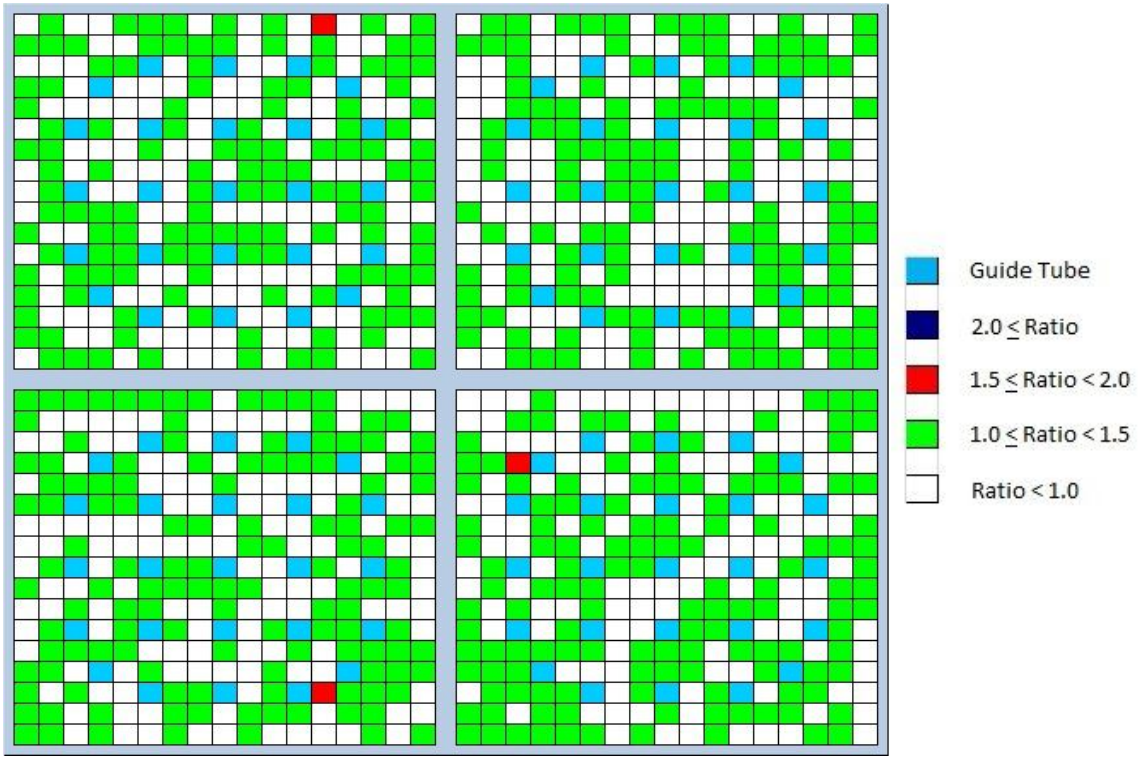

Figure 5.19: Observed-to-Reported Uncertainty Ratio, Startup, Test Problem 3

At startup we find that in FA 1, 50.8% of all pins are within 1σ, 99.6% within 1.5σ, and 100% within 2σ.

Table 5.5 shows the percentage of pins in each assembly that fall within the sigma bounds for all 37 burnsteps. Once again, the true uncertainty is underestimated for the majority of the pins, but nearly all of the pins fall within 2σ.

Table 5.5: Percentage of pins in each FA within given Standard Deviations, TP 3

Day	Assembly One			Assembly Two			Assembly Three			Assembly One		
	2σ	1.5σ	1σ	2σ	1.5σ	1σ	2σ	1.5σ	1σ	2σ	1.5σ	1σ
0	100.0%	99.6%	50.8%	100.0%	100.0%	52.3%	100.0%	99.6%	50.8%	100.0%	99.6%	49.6%
1	100.0%	100.0%	50.4%	100.0%	100.0%	56.1%	100.0%	100.0%	49.6%	100.0%	100.0%	50.8%
2	100.0%	100.0%	51.5%	100.0%	100.0%	56.1%	100.0%	100.0%	47.0%	100.0%	100.0%	47.3%
3	100.0%	99.6%	49.2%	100.0%	99.2%	54.5%	100.0%	100.0%	47.3%	100.0%	99.6%	48.5%
5	100.0%	99.2%	56.1%	100.0%	99.2%	45.5%	100.0%	99.6%	50.0%	100.0%	100.0%	57.6%
10	100.0%	99.6%	48.1%	100.0%	100.0%	45.8%	100.0%	99.6%	50.8%	100.0%	98.9%	48.5%
20	100.0%	99.6%	50.8%	100.0%	100.0%	51.5%	100.0%	99.6%	52.3%	100.0%	100.0%	56.4%
30	100.0%	100.0%	52.3%	100.0%	100.0%	53.4%	100.0%	99.6%	51.1%	100.0%	99.6%	45.1%
50	100.0%	100.0%	51.1%	100.0%	99.6%	48.1%	100.0%	100.0%	47.7%	100.0%	99.6%	49.2%
75	100.0%	99.6%	51.9%	100.0%	100.0%	55.3%	100.0%	99.6%	49.2%	100.0%	100.0%	50.8%
100	100.0%	99.6%	51.9%	100.0%	100.0%	47.3%	100.0%	99.2%	48.9%	100.0%	99.2%	50.0%
125	100.0%	99.2%	56.1%	100.0%	100.0%	50.4%	100.0%	100.0%	53.8%	100.0%	100.0%	50.8%
150	100.0%	98.9%	47.7%	100.0%	99.2%	48.5%	100.0%	99.6%	49.6%	100.0%	99.6%	52.7%
175	100.0%	100.0%	43.9%	100.0%	99.6%	51.1%	100.0%	99.6%	51.5%	100.0%	100.0%	47.7%
200	100.0%	99.2%	44.7%	100.0%	99.6%	48.5%	100.0%	100.0%	50.4%	100.0%	99.6%	44.7%
225	100.0%	99.2%	48.5%	100.0%	100.0%	51.1%	100.0%	100.0%	46.6%	100.0%	99.2%	51.5%
250	100.0%	100.0%	51.9%	100.0%	99.6%	56.4%	100.0%	99.2%	45.8%	100.0%	100.0%	46.6%
275	100.0%	99.6%	46.6%	100.0%	99.2%	53.0%	100.0%	99.6%	46.2%	100.0%	99.6%	47.0%
300	100.0%	99.6%	50.4%	100.0%	99.6%	45.5%	100.0%	99.6%	43.9%	100.0%	99.2%	50.0%
325	100.0%	100.0%	49.2%	100.0%	100.0%	51.9%	100.0%	100.0%	50.4%	100.0%	99.6%	51.1%
350	100.0%	100.0%	43.2%	100.0%	99.6%	48.9%	100.0%	100.0%	53.0%	100.0%	99.2%	50.0%
375	100.0%	100.0%	50.0%	100.0%	99.6%	51.1%	100.0%	99.6%	45.8%	100.0%	100.0%	52.3%
400	100.0%	100.0%	45.8%	100.0%	98.5%	50.8%	100.0%	100.0%	48.5%	100.0%	99.6%	48.1%
450	100.0%	99.2%	49.2%	100.0%	99.6%	47.0%	100.0%	99.6%	48.9%	100.0%	100.0%	50.4%
500	100.0%	99.6%	39.8%	100.0%	99.6%	46.6%	100.0%	99.2%	48.1%	100.0%	99.6%	48.5%
550	100.0%	100.0%	49.2%	100.0%	100.0%	48.5%	100.0%	100.0%	49.2%	100.0%	99.6%	47.3%
600	100.0%	100.0%	49.6%	100.0%	99.2%	46.2%	100.0%	100.0%	50.0%	100.0%	99.6%	48.9%
650	100.0%	99.6%	41.7%	100.0%	99.6%	46.6%	100.0%	100.0%	39.4%	100.0%	100.0%	50.0%
700	100.0%	99.2%	45.8%	100.0%	98.9%	43.2%	100.0%	99.2%	47.0%	100.0%	97.7%	49.6%
750	100.0%	100.0%	51.9%	100.0%	99.6%	42.8%	100.0%	98.9%	47.0%	100.0%	99.6%	47.0%
800	100.0%	98.9%	45.5%	100.0%	99.2%	48.1%	100.0%	99.6%	41.7%	100.0%	99.6%	51.5%
850	100.0%	99.6%	47.3%	100.0%	100.0%	42.8%	100.0%	100.0%	49.2%	100.0%	98.5%	46.6%
900	100.0%	100.0%	47.0%	100.0%	100.0%	49.6%	100.0%	99.6%	43.2%	100.0%	99.6%	43.6%
950	100.0%	99.6%	47.0%	100.0%	99.6%	39.0%	100.0%	98.9%	45.8%	100.0%	99.6%	47.0%
1000	100.0%	99.2%	48.5%	100.0%	99.6%	39.8%	100.0%	99.6%	39.0%	100.0%	98.9%	42.4%
1050	100.0%	99.2%	45.1%	100.0%	99.6%	40.5%	100.0%	99.2%	40.2%	100.0%	98.5%	44.3%
1100	100.0%	99.2%	39.4%	100.0%	99.6%	41.3%	100.0%	99.2%	48.9%	100.0%	99.6%	49.6%

The behavior of the uncertainty ratios over time in test problem three was similar to the behavior of test problem 2. In test problem 3, the magnitude of peak uncertainties at 900 days in FA's 1-4 was 1.48, 1.46, 1.50, and 1.59 respectively. At 900 days we find that in FA 1, 47.0% of all pins are within 1σ and 100% within 1.5σ. Figure 5.20 shows the ratio map at 900 days.

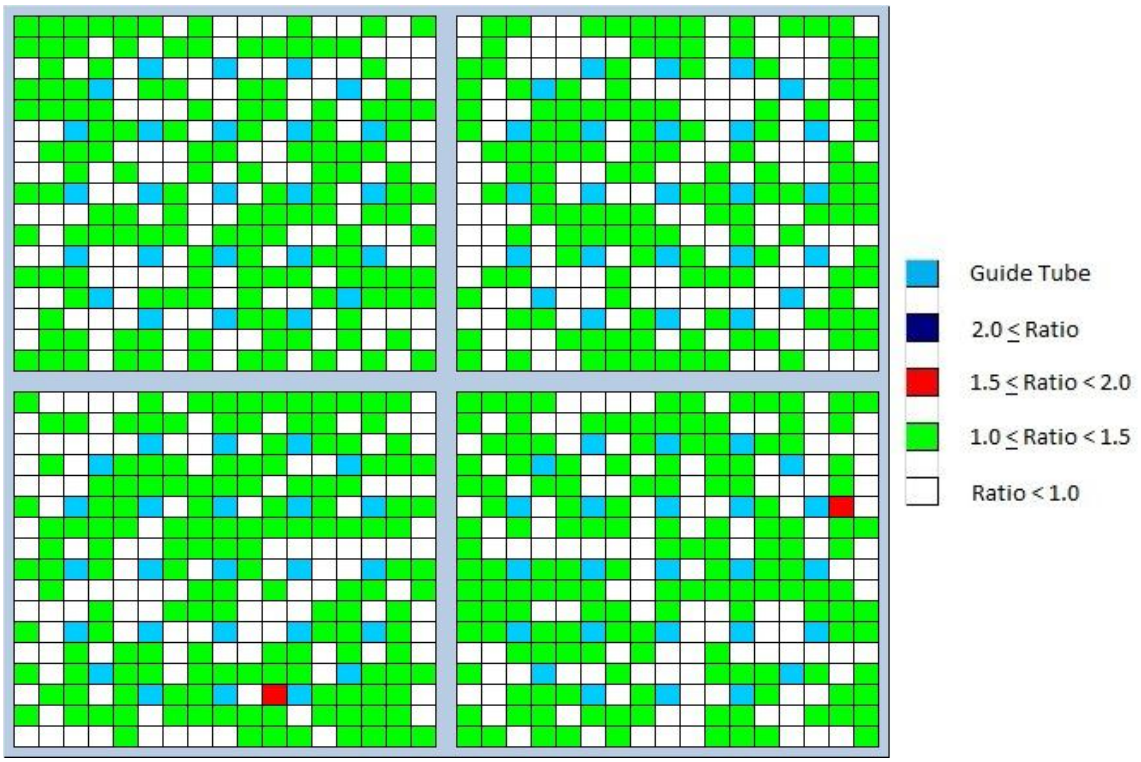

Figure 5.20: Observed-to-Reported Uncertainty Ratio, 900 Days, Test Problem 3

Figure 5.21 is the pin power ratio map at 200 days. The highlighted pins in assemblies 1 and 2 correspond to uncertainty ratios of 0.47 and 1.67 respectively. A plot of the pin powers in these three FA's for each of the 19 runs was made with the uncertainty shown as error bars, and is shown in Figure 5.22 and 5.23. Figure 5.22, the pin with an uncertainty ratio of 0.47, shows little variance in the pin powers. Figure 5.23, a plot of the pin in FA 2 with a high uncertainty ratio, shows a larger variance in the pin powers.

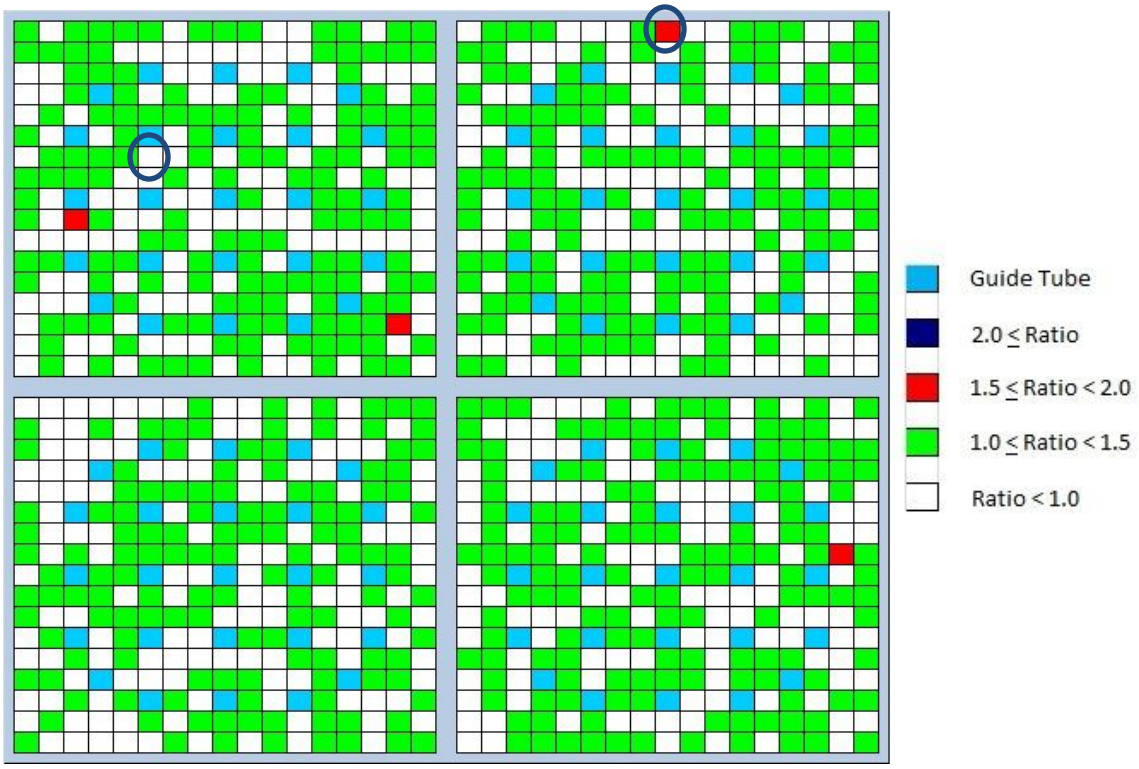

Figure 5.21: High and Low Uncertainty Ratio Pins, 200 Days, TP 3

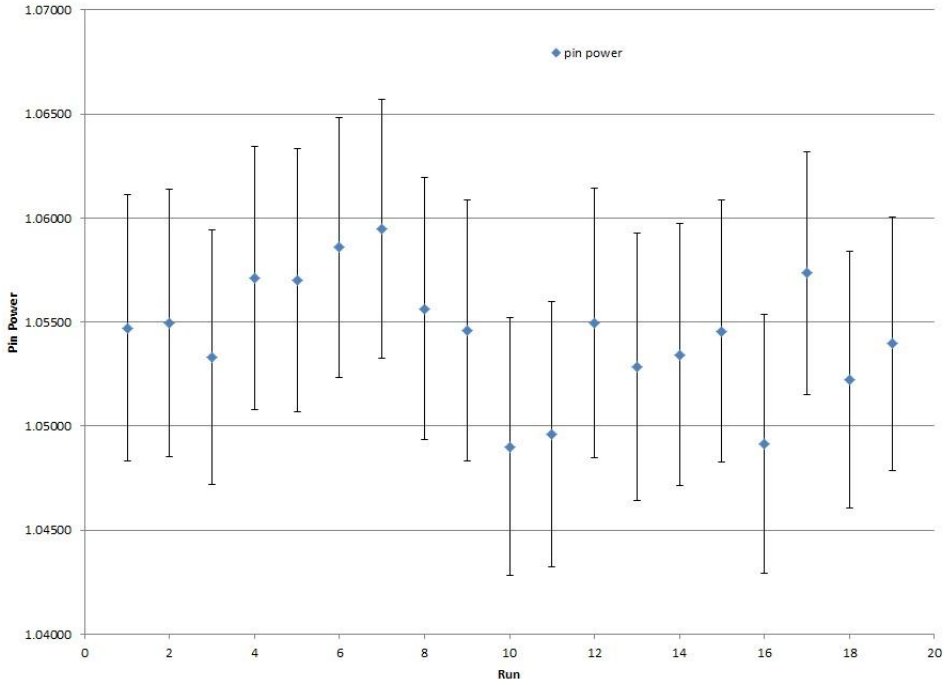

Figure 5.22: Pin Power with .47 Absolute Uncertainty Ratio, FA 1, 200 Days, TP 3

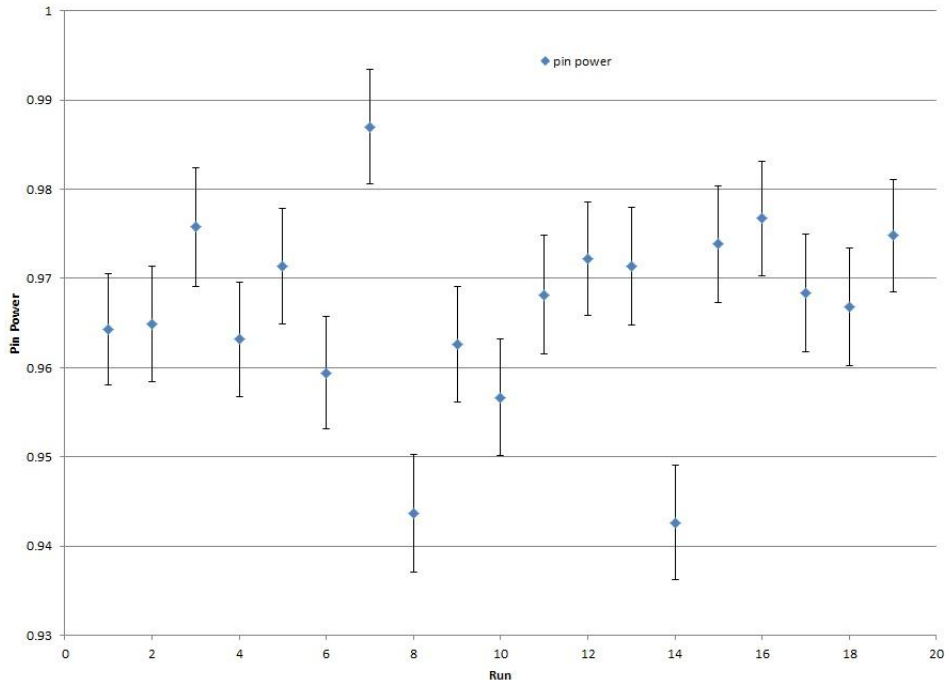

Figure 5.23: Pin Power with 1.67 Absolute Uncertainty Ratio, FA 2, 200 Days, TP 3

CHAPTER 6

ERROR PROPAGATION IN THE CORE DOMAIN

After thoroughly studying the error propagation in the assembly domain, this chapter presents a similar analysis at the core level, noting that SERPENT has already been validated in full-core calculations.[19] The 2-D core domain model was designed with a reflective boundary condition on the top and bottom. The geometric layout, material composition, and code settings for the core domain test problem are described.

6.1 The IRIS Reactor

The IRIS project had the objective of developing a novel type of water cooled reactor with integral primary circuit to address the Generation IV design goals of 1) fuel cycle sustainability 2) enhanced reliability and safety and 3) improved economics.[20, 21] The 1000 MegaWatt thermal (MWt) core design was intentionally selected to be smaller than most other reactors in development so that it can be manufactured in a modular fashion and more easily built and financed by smaller utilities and less developed nation-states.

6.1.1 The IRIS Fuel Assembly

Similarly to the NEA Benchmark fuel assembly, the IRIS design uses a 17 x 17 assembly with integrated Zirc-4 guide tubes for control rod and instrumentation insertion. Figure 6.1 shows the assembly layout.

Also similarly to the previous problems, each fuel pin uses the same UO_2 fuel enclosed in the same Zircaloy cladding material, although the fuel is enriched to different levels in the IRIS design. However, there are some important differences in the two designs. For starters, each fuel pin in the IRIS design makes use of a gas gap that is filled with inert helium gas under

pressure. This gas gap prevents thermal and radiation induced expansion of the fuel pellet from cracking or swelling the cladding in addition to preventing the high pressure of the moderator from collapsing the cladding material. Figure 6.2 shows the cross sectional view of the fuel pin.

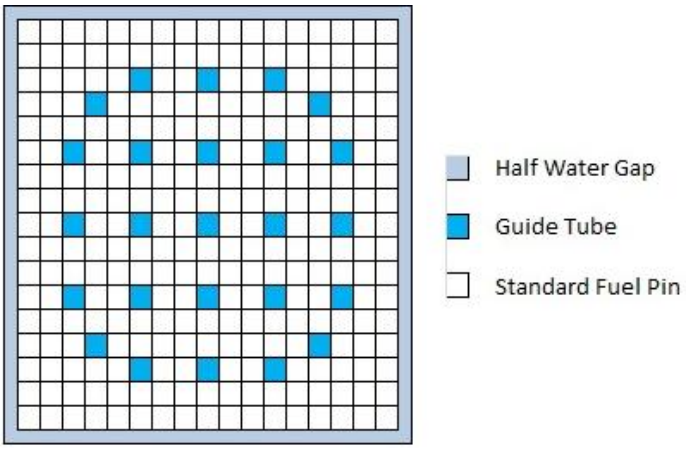

Figure 6.1: Layout of IRIS Fuel Assembly

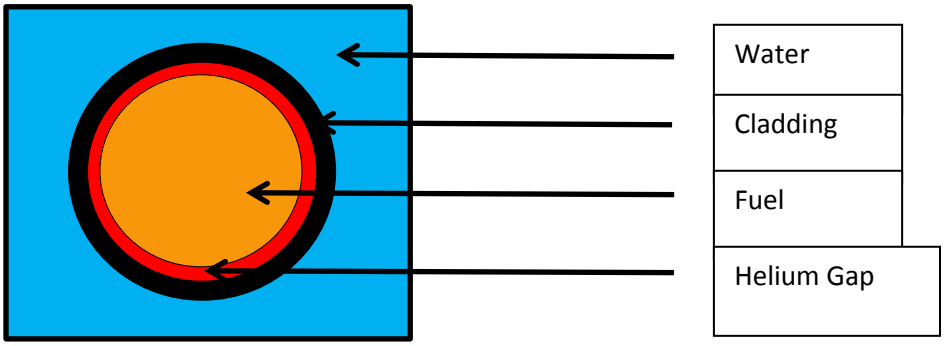

Figure 6.2: Cross Section of Fuel Pin

The dimensions of the fuel pins and its assembly are also different. Table 6.1 describes the dimensions of assembly components. Some pins were coated with the IFBA coating as discussed previously, with the ZrB_2 layer sputtered onto the outside of the fuel pellet in the amount of 2.25mg ^{10}B/in. A discussion of how many and where these IFBA pins were located will occur later.

Material compositions for the fuel pins, cladding, and moderator are in Table 6.2. It is important to note the two different enrichments of UO_2 listed. Commonly, reactor operators will employ a multiple batch reloading scheme that increases the amount of energy that can be extracted from each fuel assembly before discharge. While the reactor is shut down more often for a partial reloading, the effect of extending the time a fuel assembly spends in the reactor is to increase its discharge BU. In order to run the reactor most economically and to get the core in an equilibrium as quickly as possible, the core at startup is loaded with a mixture of assemblies at the maximum 4.95% enrichment and assemblies at 2.6%, which would be similar to the remaining enrichment if fresh assemblies were burned for one fuel cycle.

Table 6.1: IRIS Fuel Pin and GT Dimensions

Component	Dimension (cm)
Fuel Pellet Radius	0.4096
IFBA Coating Radius	0.4112
Gas Gap Radius	0.4217
Fuel Pin Radius	0.475
Clad Thickness	0.0533
Pin Pitch	1.3284
GT Inner Radius	0.5922
GT Thickness	0.053

Table 6.2: Material Composition

	Density	Isotope	Weight Fraction	
			High	Low
UO_2	10.412 g/cm^3	^{234}U	0.022%	0.022%
		^{235}U	4.95%	2.60%
		^{238}U	95.878%	97.378%
Zirc-4	6.44 g/cm^3	^{nat}Zr	98.38%	
		^{nat}Sn	1.30%	
		^{nat}Fe	0.22%	
		^{nat}Cr	0.10%	
H_2O	0.7295 g/cm^3			

The most significant difference in the assembly and core domain calculations was the way the fuel pins were modeled and tracked. The previous problems tracked each pin separately, which worked well enough when only four assemblies were used. But if that same technique were used in the IRIS core, 23,496 separate fuel pins would have to be modeled, tracked, and reported, requiring far too much time and computer system resources. Instead of tracking each pin, each fuel assembly was divided into four fuel mixtures. To do this, a 9 x 9 lattice was built and then the pins in the 9^{th} row and the 9^{th} column were severed in half. This process was repeated thrice more and the four partially severed lattices were placed together to form one 17 x 17 fuel assembly containing four separate fuel mixtures.

6.1.2 The IRIS Core

Because IRIS is specifically designed to be smaller and more modular than most reactor designs, the core layout is very compact. The IRIS core consists of 89 fuel assemblies arrayed in the pattern shown in Figure 6.3. At four fuel mixtures in each assembly, the entire core has 356 fuel mixtures separately tracked and reported. The core is surrounded by a stainless steel reflector, which is in turn surrounded by a large downcomer region of water. The downcomer is the region through which cold water is pumped to the bottom of the reactor vessel, and then forced to pass up through the core and carry heat from the fuel pins to the heat exchanger.

Another important design feature of the IRIS core is the use of IFBA pin coatings to provide an economical control of excess reactivity. Since the fuel assemblies with the highest initial fuel enrichment will have the highest excess reactivity, using IFBA coatings on those same fuel assemblies will flatten the flux profile across the reactor core and reduce peaking factors that could exceed thermal margins. Figure 6.4 shows the arrangement of the 44 4.95% enriched IFBA equipped fresh fuel assemblies and the 45 2.6% enriched fresh fuel assemblies.

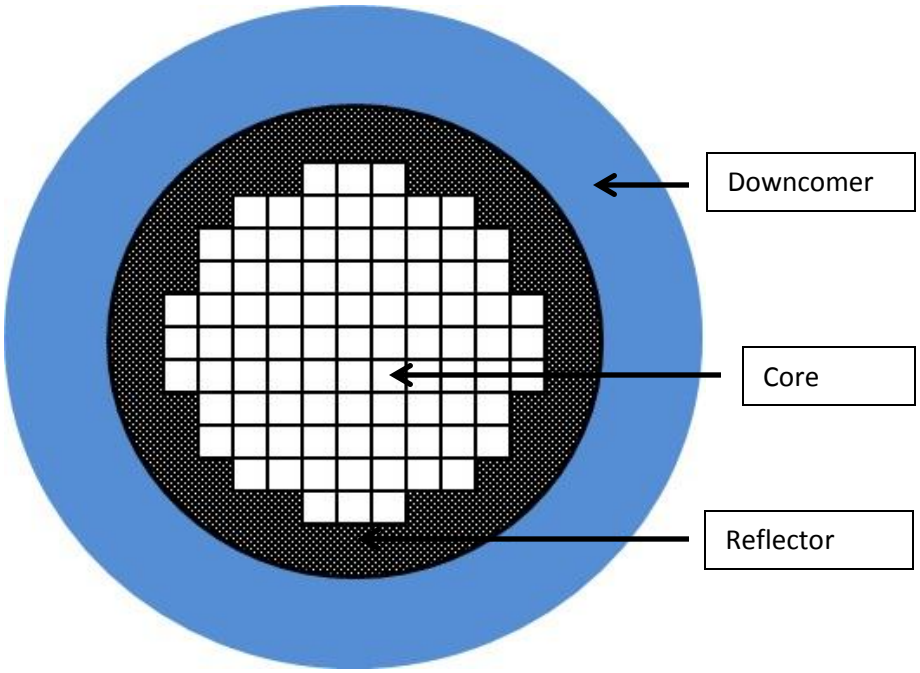

Figure 6.3: IRIS Core Layout

			2.6% No IFBA	2.6% No IFBA	2.6% No IFBA					
		2.6% No IFBA	4.95% 32 IFBA	4.95% 128 IFBA	4.95% 80 IFBA	4.95% 128 IFBA	4.95% 32 IFBA	2.6% No IFBA		
	2.6% No IFBA	2.6% No IFBA	4.95% 128 IFBA	2.6% No IFBA	4.95% 128 IFBA	2.6% No IFBA	4.95% 128 IFBA	2.6% No IFBA	2.6% No IFBA	
	4.95% 32 IFBA	4.95% 128 IFBA	2.6% No IFBA	4.95% 156 IFBA	2.6% No IFBA	4.95% 156 IFBA	2.6% No IFBA	4.95% 128 IFBA	4.95% 32 IFBA	
2.6% No IFBA	4.95% 128 IFBA	2.6% No IFBA	4.95% 156 IFBA	2.6% No IFBA	4.95% 156 IFBA	2.6% No IFBA	4.95% 156 IFBA	2.6% No IFBA	4.95% 128 IFBA	2.6% No IFBA
2.6% No IFBA	4.95% 80 IFBA	4.95% 128 IFBA	2.6% No IFBA	4.95% 156 IFBA	2.6% No IFBA	4.95% 156 IFBA	2.6% No IFBA	4.95% 128 IFBA	4.95% 80 IFBA	2.6% No IFBA
2.6% No IFBA	4.95% 128 IFBA	2.6% No IFBA	4.95% 156 IFBA	2.6% No IFBA	4.95% 156 IFBA	2.6% No IFBA	4.95% 156 IFBA	2.6% No IFBA	4.95% 128 IFBA	2.6% No IFBA
	4.95% 32 IFBA	4.95% 128 IFBA	2.6% No IFBA	4.95% 156 IFBA	2.6% No IFBA	4.95% 156 IFBA	2.6% No IFBA	4.95% 128 IFBA	4.95% 32 IFBA	
	2.6% No IFBA	2.6% No IFBA	4.95% 128 IFBA	2.6% No IFBA	4.95% 128 IFBA	2.6% No IFBA	4.95% 128 IFBA	2.6% No IFBA	2.6% No IFBA	
		2.6% No IFBA	4.95% 32 IFBA	4.95% 128 IFBA	4.95% 80 IFBA	4.95% 128 IFBA	4.95% 32 IFBA	2.6% No IFBA		
			2.6% No IFBA	2.6% No IFBA	2.6% No IFBA					

Figure 6.4: Enrichment and IFBA Loading Pattern, IRIS Core[22]

Unlike previous test problems which used only one IFBA pattern, the IRIS core makes use of four separate patterns of varying number of IFBA pins, with assemblies containing more IFBA pins located in more central core positions with fewer IFBA pins located at the periphery. The four IFBA patterns used in test problem 4 have IFBA pin concentrations of 32, 80, 128, and 156. The patterns employed can be found in Figure 6.5.[17, 23]

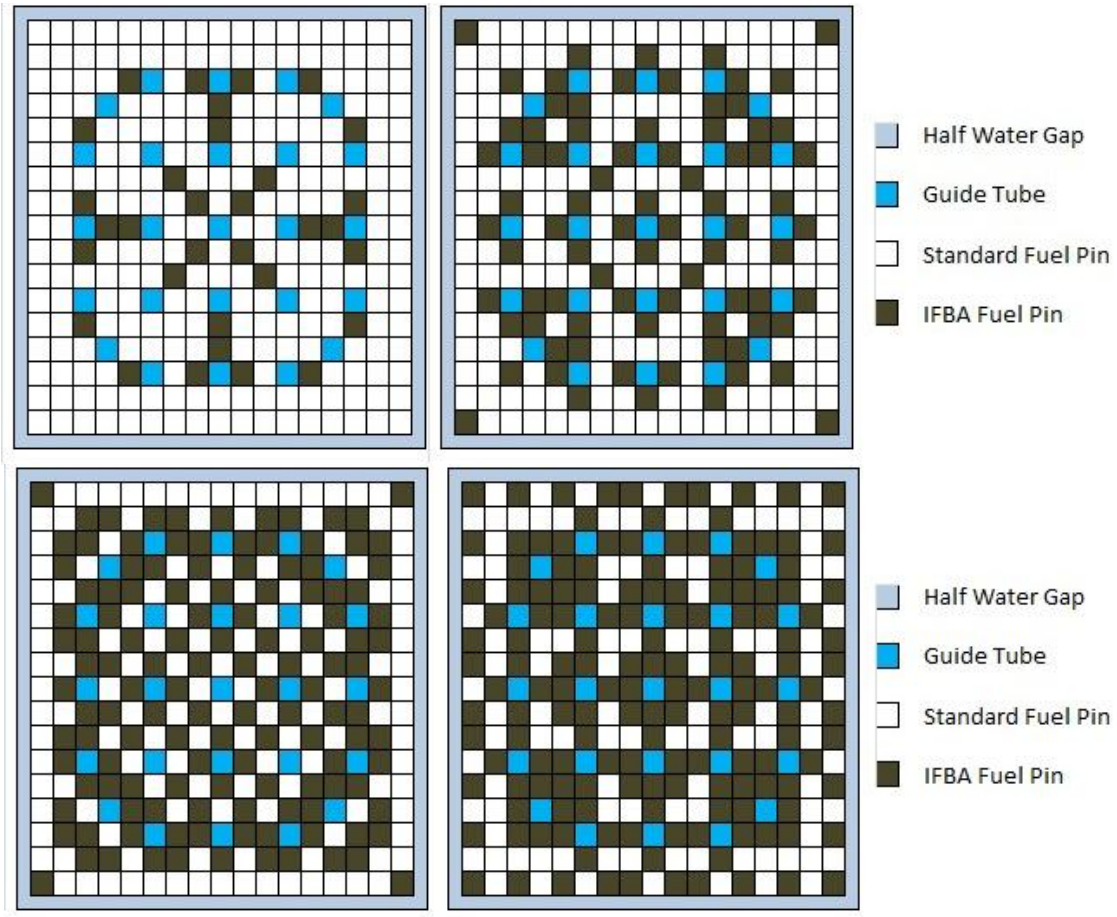

Figure 6.5: IFBA Arrangements in FA's with 32, 80, 128, and 156 IFBA Pins

6.1.3 The IRIS Reflector and Downcomer Region

The IRIS Reactor is surrounded by a 316 Stainless Steel (316SS) reflector that helps to scatter neutrons that leave the core back into the core and prevent their loss. The radius of the reflector is 140.5cm but because the outside edge of the fuel assemblies is not a consistent

distance from the center of the core, the reflector varies in thickness. The reflector was modeled as a solid region of material. The material composition of the 316SS was taken from the SCALE Standard Composition Library and is shown if Table 6.3.[24]

Table 6.3: Material Composition of the 316SS Reflector

	Density	Composition	Weight Fraction
SS316	8.03 g/cm^3	^{nat}C	0.08%
		^{nat}Si	1.0%
		^{nat}P	0.045%
		^{nat}Cr	17.0%
		^{55}Mn	2.0%
		^{nat}Fe	65.375%
		^{nat}Ni	12.0%
		^{nat}Mo	2.5%

Outside of the reflector is a downcomer region of water. In order to save modeling and computational effort on tracking neutrons that enter the downcomer region but are unlikely to reenter the core (due to their distance from the core space, a test case was undertaken to determine the size of downcomer that could adequately be modeled without affecting the results.

Table 6.4: Downcomer Region Thickness Test Results

Reflector Thickness (cm)	K-eff	uncertainty
40	1.19013	0.00011
70	1.18993	0.00011
100	1.19022	0.00011

A full-core criticality test was conducted with 90,000,000 neutron histories using three downcomer sizes (40, 70, and 100cm thicknesses). The results, shown in Table 6.4, show that the 40cm thickness was adequate for effectively modeling the reactor core because the k_{eff} from the 40cm test is within the uncertainty bounds of the 100cm test. Therefore, a 40cm thick downcomer region was modeled.

6.2 Neutron Histories, Burnsteps, and Other Settings

As with the previous test problems, it was of critical importance to run simulations that kept uncertainty estimates as small as was reasonable possible. To this end, 200,000 neutrons/generation with 750 total cycles (300 skipped for source convergence) yielded a good blend of small statistical uncertainty and acceptable calculation runtime. Forty-three total burnsteps were run, going out to a total of 1400 burn days (28.8GWd/mtHM), and once again the longest burnstep not being longer than 50 days. Also as before, the Predictor-Corrector method was used. A complete listing of all simulation parameters can be found in Appendix A.

CHAPTER 7

CORE DOMAIN ERROR PROPAGATION RESULTS

This section describes the results obtained from the simulation of the core domain test problem described in Chapter 6. The test problem modeling the IRIS reactor was run 19 times by changing the initial seed number. The observed uncertainty obtained from the 19 identical simulations is compared to the uncertainty estimated by the code. A detailed analysis of this comparison follows.

7.1 Calculation Time and System Resources Required

All test problems were run on a Linux cluster, on a Quad-Core AMD Opteron processor (2.3GHz). Eight runs were run in serial mode while eleven runs were performed in parallel across five CPU's using one core per CPU. The runtime and memory demands of the serial and parallel runs can be found in Table 7.1.

Table 7.1: Wall-clock Calculation Time and Memory Requirements

Simulation Type	Runs Conducted	CPU's/Run	Memory Req. (GB RAM)	Ave. Runtime	
				Hours	Days
Serial	8	1	17.739	1099	45.7
Parallel	11	5	17.723	280	11.7

Because the core domain problem had only 356 depletion zones (in comparison to the 1056 depletion zones in TP 1-3, the core domain required far less memory in spite of the fact that the core domain required nearly 4x as many neutron histories. Nodes of 16GB, 32GB, and 64GB were available on the cluster, but the memory requirements meant that the 16GB nodes were unusable and runs on the 32GB nodes had to be executed such that only one core could be used on each node. Only the large 64GB nodes allowed for multiple cores to be used on one node. These large nodes also had the fastest average wall-clock time of all the runs executed.

It is also notable that running in parallel sped up the overall calculation time on average by 3.92x or roughly 80% parallel efficiency. Running in parallel speeds up the transport calculation of the simulation because neutron histories are easily parallelizable, but there is no speedup in the depletion step and some gains are lost due to the need for the multiple CPU's and nodes to constantly communicate with one another.

7.2 Uncertainty in K_{eff}

The core domain problem consisted of 43 burnsteps, which can be found in Appendix A, The same process outlined in Chapter 5 was applied to the k_{eff} data produced by the core domain test and a comparison of the observed and reported uncertainty in k_{eff} was made.

7.2.1 Behavior of K_{eff}

Using the data produced from the 19 replica runs, the mean keff for each of the 43 burnsteps was calculated and plotted in Figure 7.1. The plot shows the customary sharp drop in keff upon startup due to the buildup of ^{135}Xe. Upon reaching its equilibrium value, the k_{eff} remains relatively steady due to the simultaneous depletion of ^{235}U and the ^{10}B in the IFBA coated fuel pins. Eventually, the IFBA coating is sufficiently consumed and k_{eff} begins to decrease again. At 1400 days, when the calculation was terminated, k_{eff} was 1.01540 $\pm$ 0.00014. Using this and the keff average at 1350 days (1.02455 $\pm$ 0.00013), the k-values are converted into reactivity values using the equation

$$\boldsymbol{\rho = \frac{(k_{eff} - 1)}{k_{eff}}}$$

The two reactivity, daystep pairs are used to linearly interpolate the point when the core's reactivity would reach 0 and the chain reaction would cease.

$$y = 1350 + (1400 - 1350)\frac{(0 - .02396)}{(.01517 - .02396)} = 1486\ days$$

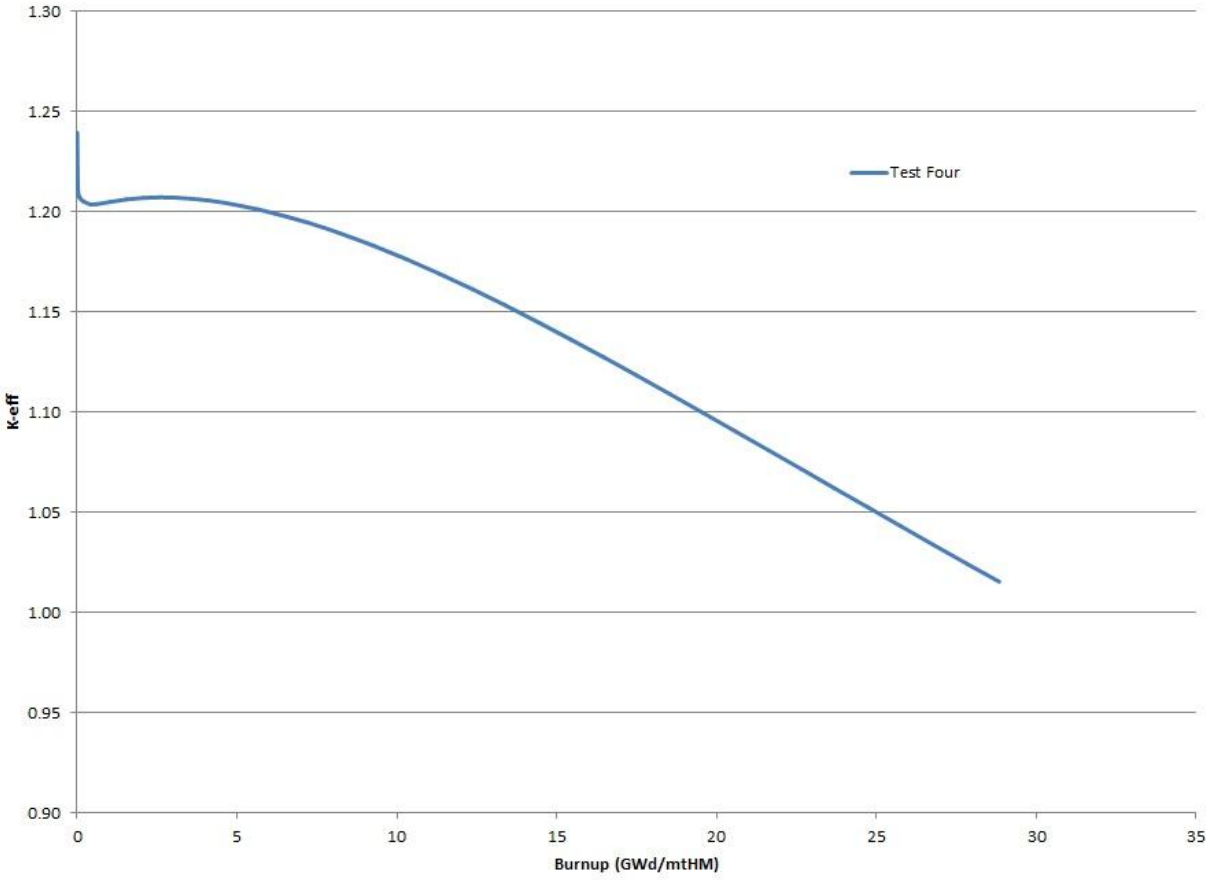

Figure 7.1: Keff vs. BU, TP 4

7.2.2 Behavior of Observed and Reported Uncertainties

The plots of the observed and reported k_{eff} uncertainties in test problem four, found in Figure 7.2 and Figure 7.3, show that for the vast majority of burnsteps, the observed uncertainty in k_{eff} is slightly higher than the code's reported uncertainty. Just as in the previous test problems, there is some statistical noise in the data. But it is also important to note that the addition of a trendline shows that the true uncertainty in nearly constant, a finding also identical to the previous test problems. Across all 43 depletion steps, the mean observed uncertainty in test problem four was 14pcm. The mean reported uncertainty was 12pcm.

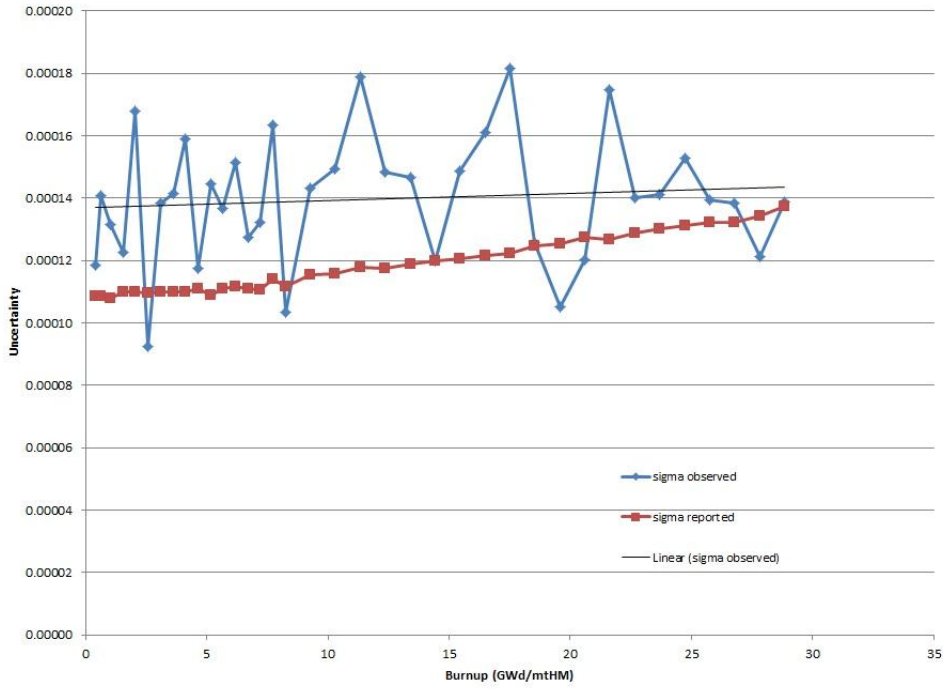

Figure 7.2: Observed and Reported Uncertainty vs. BU, TP 4

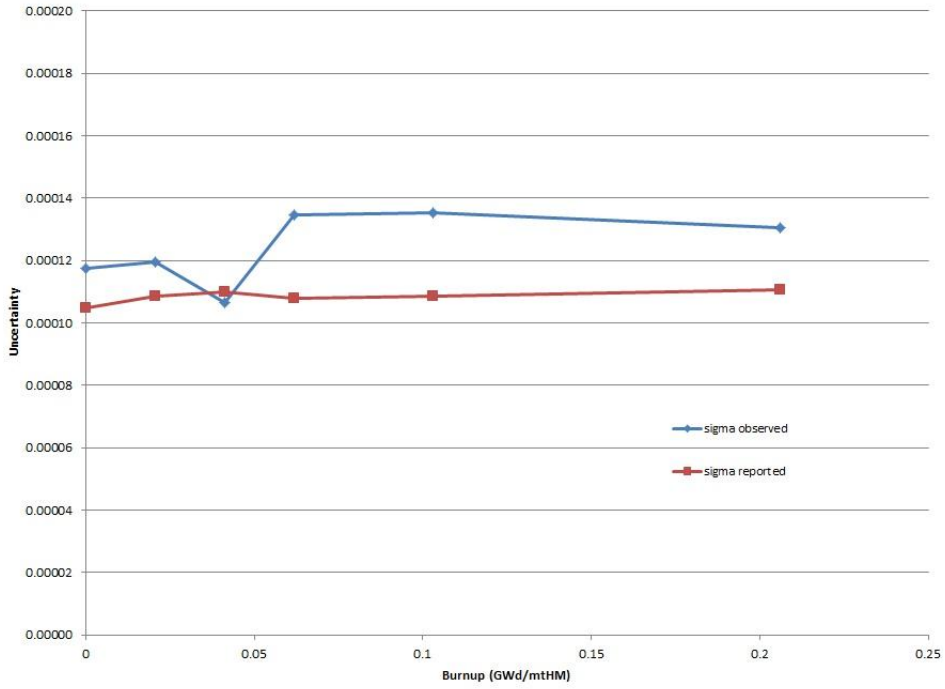

Figure 7.3: Observed and Reported Uncertainty at BOC vs. BU, TP 4

7.3 Uncertainty in Pin Powers

For each of the 43 burnsteps in test problem four, the same process outlined in Chapter 5 was applied to the pin power and uncertainty maps produced by SERPENT. The ratio of observed-to-reported uncertainty for each pin location was calculated. A plot of these values provides a measure of the accuracy (or rather, deviation from accuracy) with which the code predicts uncertainty, as well as the spatial distribution of these values.

7.3.1 Pin Power Observed and Reported Uncertainties

A plot of the R values for each pin was made for each burnstep. In order to pictorially demonstrate the magnitude of the differences in observed and reported uncertainty for each pin, a

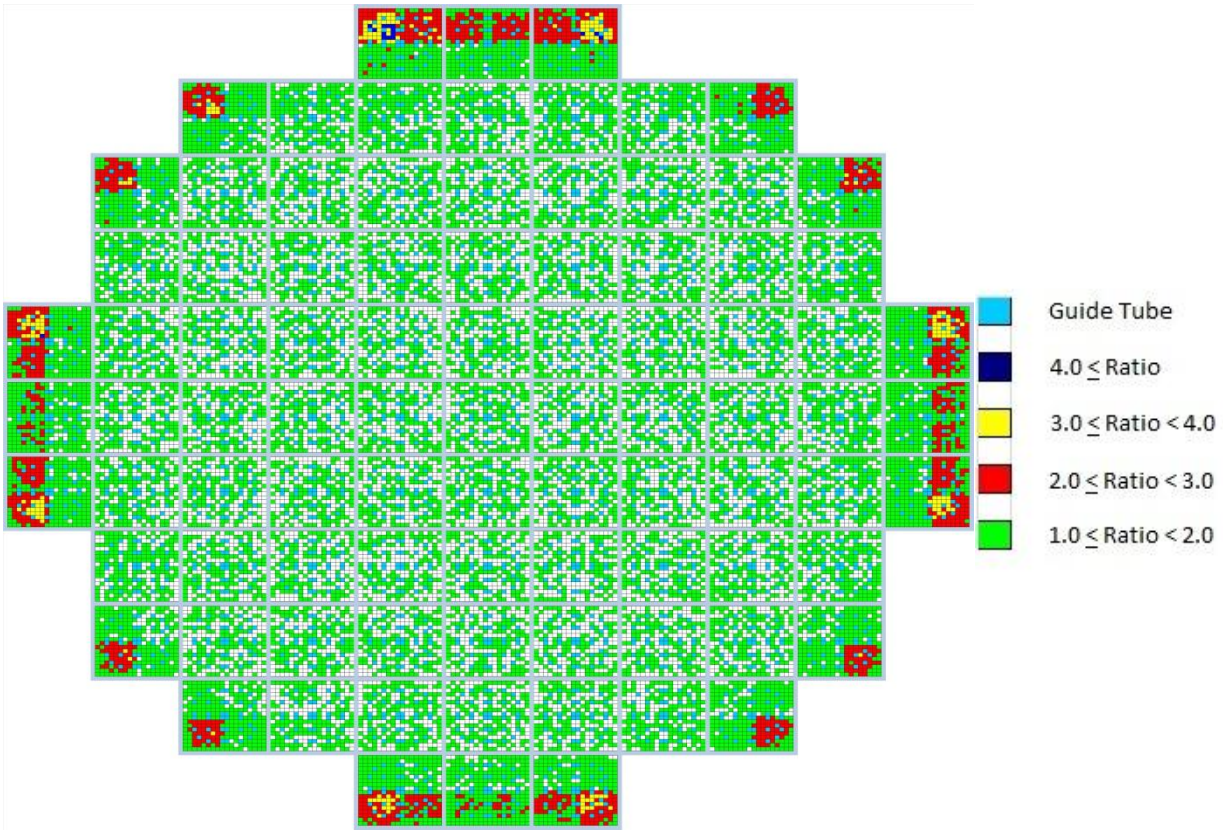

Figure 7.4: Observed-to-Reported Uncertainty Ratio, Startup, TP 4

color code was applied to the R value for each pin location. Figure 7.4, a ratio map at startup, shows the distribution of uncertainty by the code. The figure clearly shows that the highest ratios of observed to reported uncertainty occur on the edges of the core. The Normal Distibution would suggest that 68.3% of pins in each assembly should fall within 1σ, 95.5% within 2σ, and 99.7% within 3σ. However, at startup we find that across the core, only 39.8% of all pins are within 1σ, but 94.8% were within 2σ, and 99.4% within 3σ. Table 7.2 shows the percentage of pins in the core that fall within the sigma bounds for all 43 burnsteps.

Table 7.2: Percentage of Pins in Core within given Standard Deviations, TP 4

Day	Core				Day	Core			
	4σ	3σ	2σ	1σ		4σ	3σ	2σ	1σ
0	99.9%	99.1%	94.2%	39.4%	750	100.0%	99.7%	96.5%	41.3%
50	100.0%	99.4%	94.8%	39.8%	800	100.0%	99.8%	96.8%	41.7%
100	100.0%	99.3%	94.9%	39.4%	850	100.0%	99.8%	96.9%	41.5%
150	100.0%	99.2%	94.8%	40.2%	900	100.0%	99.9%	97.1%	41.5%
200	100.0%	99.3%	94.8%	40.0%	950	100.0%	99.9%	97.1%	41.5%
250	100.0%	99.3%	95.1%	39.8%	1000	100.0%	100.0%	97.4%	42.1%
300	100.0%	99.4%	95.4%	41.6%	1050	100.0%	100.0%	97.6%	41.5%
350	100.0%	99.3%	95.3%	40.7%	1100	100.0%	100.0%	97.7%	41.8%
400	100.0%	99.3%	95.5%	40.8%	1150	100.0%	100.0%	97.9%	41.9%
450	100.0%	99.4%	95.5%	40.3%	1200	100.0%	100.0%	98.2%	42.3%
500	99.9%	99.3%	95.8%	40.6%	1250	100.0%	100.0%	98.2%	41.7%
550	100.0%	99.5%	95.8%	40.8%	1300	100.0%	100.0%	98.3%	42.2%
600	100.0%	99.5%	96.0%	40.7%	1350	100.0%	100.0%	98.6%	42.7%
650	100.0%	99.6%	96.2%	40.9%	1400	99.9%	99.9%	98.5%	42.6%
700	100.0%	99.7%	96.2%	41.1%					

As BU increased, the relative locations of the highest magnitude of uncertainty remained consistent, although the magnitude of the uncertainty ratios decreased, a pattern of behavior that was also seen in test problem one. Figure 7.5 shows the observed-to-reported uncertainty ratio map at 1000 days. The ratio map and the data in Table 7.2 show that while the areas of highest uncertainty ratios remain on the core edges, a greater percentage of pins fall within 1σ and 2σ than did at startup. Clearly the true uncertainty of the majority of the pin powers is higher than the uncertainty predicted by the code.

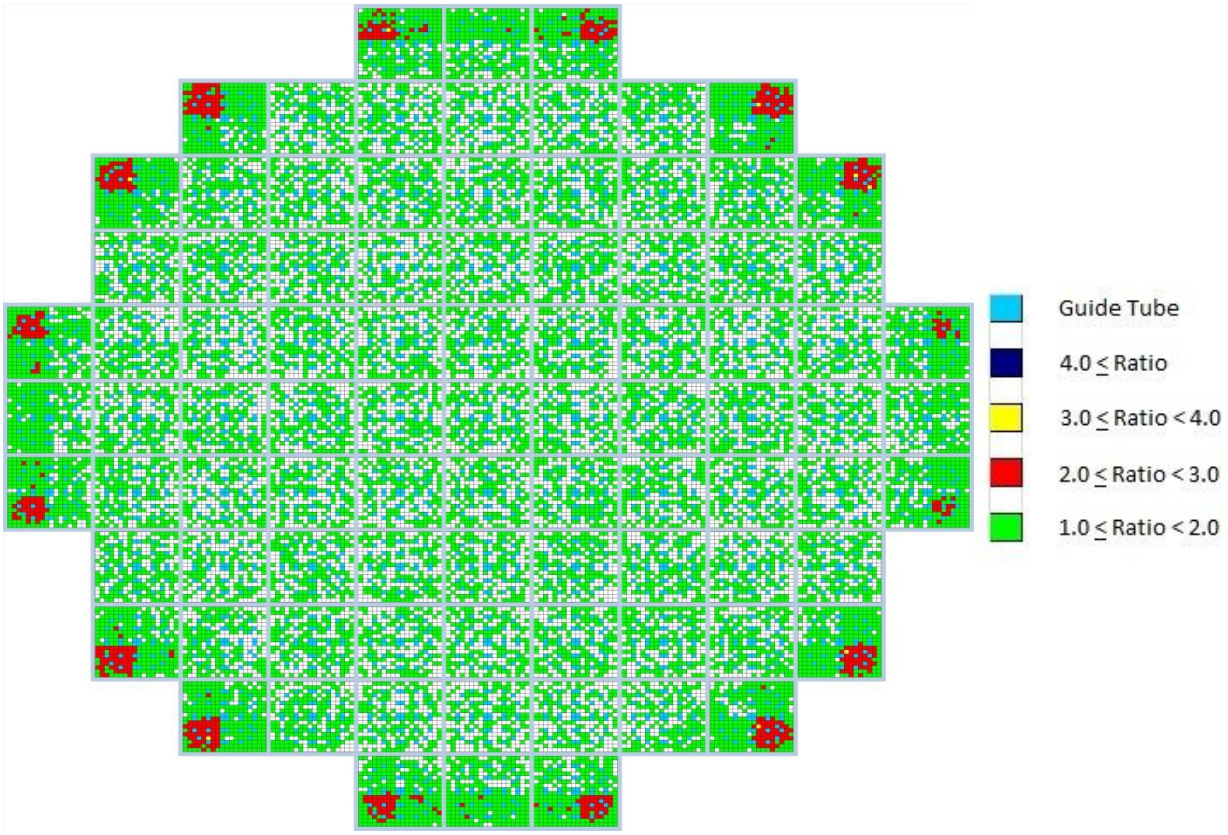

Figure 7.5: Observed-to-Reported Uncertainty Ratio, 1000 Days, TP 4

Figure 7.4 and 7.5, as well as the remaining uncertainty ratio maps found in Appendix E, indicate that the core can be divided into three regions based on the behavior of the uncertainty ratios of the fuel pins. It is obvious that the fuel assemblies on the edge of the core have the highest uncertainty ratios, and that these ratios remain elevated throughout the simulation. Just as obvious is the behavior of the uncertainty in the assemblies in the central region of the core, which show a behavior in their uncertainty very similar to the behavior of test problems two and three. It was also noticed that just inside of the edge assemblies is a ring of 12 assemblies that appear to be transitional; the diagonal half of the assembly closest to the center behaves like that of assemblies in the interior of the core, while the diagonal half closest to the core's edge tends to have a higher concentration of pins that show an uncertainty underestimation. Therefore, the core was broken into three regions according to Figure 7.6 and statistics were analyzed.

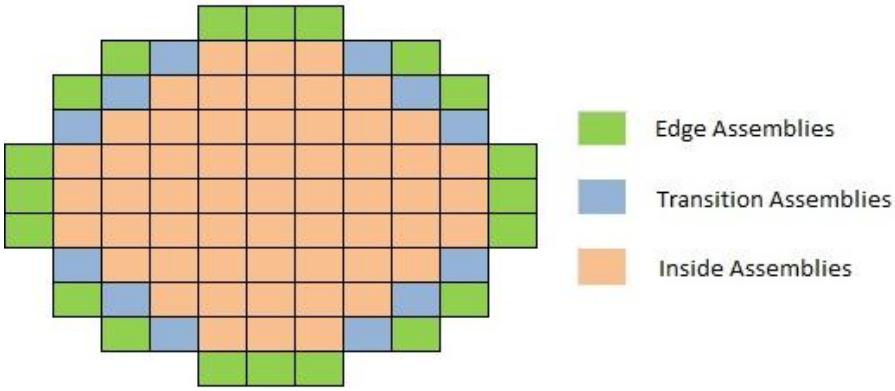

Figure 7.6: Core Region Designation

Table 7.3: Percentage of Region-Wise Pins Within Given Standard Deviations, TP 4

Day	Edge Assemblies				Transition Assemblies				Inside Assemblies			
	4σ	3σ	2σ	1σ	4σ	3σ	2σ	1σ	4σ	3σ	2σ	1σ
0	99.7%	96.1%	74.0%	8.2%	100.0%	100.0%	100.0%	41.6%	100.0%	100.0%	100.0%	49.8%
50	100.0%	97.2%	77.0%	8.9%	100.0%	100.0%	100.0%	42.7%	100.0%	100.0%	100.0%	49.9%
100	100.0%	96.8%	77.1%	9.1%	100.0%	100.0%	100.0%	42.8%	100.0%	100.0%	100.0%	49.2%
150	100.0%	96.6%	76.9%	9.0%	100.0%	100.0%	100.0%	41.8%	100.0%	100.0%	100.0%	50.7%
200	100.0%	96.7%	78.0%	10.0%	100.0%	100.0%	100.0%	41.2%	100.0%	100.0%	100.0%	50.2%
250	100.0%	96.7%	77.9%	9.6%	100.0%	100.0%	100.0%	42.1%	100.0%	100.0%	100.0%	49.9%
300	100.0%	97.3%	79.3%	11.6%	100.0%	100.0%	100.0%	43.7%	100.0%	100.0%	100.0%	51.7%
350	100.0%	96.9%	78.8%	10.5%	100.0%	100.0%	100.0%	41.5%	100.0%	100.0%	100.0%	51.1%
400	100.0%	97.0%	79.1%	10.4%	100.0%	100.0%	100.0%	41.1%	100.0%	100.0%	100.0%	51.4%
450	100.0%	97.2%	80.1%	10.7%	100.0%	100.0%	100.0%	42.3%	100.0%	100.0%	100.0%	50.2%
500	99.7%	97.0%	80.2%	11.3%	100.0%	100.0%	100.0%	42.2%	100.0%	100.0%	100.0%	50.5%
550	100.0%	97.6%	81.3%	11.5%	100.0%	100.0%	100.0%	41.8%	100.0%	100.0%	100.0%	50.8%
600	100.0%	97.9%	82.0%	11.9%	100.0%	100.0%	100.0%	42.8%	100.0%	100.0%	100.0%	50.4%
650	100.0%	98.2%	83.0%	13.2%	100.0%	100.0%	100.0%	42.8%	100.0%	100.0%	100.0%	50.2%
700	100.0%	98.5%	83.2%	12.5%	100.0%	100.0%	100.0%	44.5%	100.0%	100.0%	100.0%	50.4%
750	100.0%	98.6%	84.5%	13.5%	100.0%	100.0%	100.0%	44.5%	100.0%	100.0%	100.0%	50.4%
800	100.0%	99.0%	85.6%	13.5%	100.0%	100.0%	100.0%	45.3%	100.0%	100.0%	100.0%	50.8%
850	100.0%	99.3%	86.2%	13.9%	100.0%	100.0%	100.0%	44.9%	100.0%	100.0%	100.0%	50.4%
900	100.0%	99.4%	86.9%	14.6%	100.0%	100.0%	100.0%	45.2%	100.0%	100.0%	100.0%	50.1%
950	100.0%	99.5%	87.1%	15.1%	100.0%	100.0%	100.0%	45.0%	100.0%	100.0%	100.0%	50.0%
1000	100.0%	99.9%	88.2%	16.1%	100.0%	100.0%	100.0%	45.4%	100.0%	100.0%	100.0%	50.5%
1050	100.0%	99.8%	89.5%	15.6%	100.0%	100.0%	100.0%	45.3%	100.0%	100.0%	100.0%	49.8%
1100	100.0%	99.9%	89.5%	16.3%	100.0%	100.0%	100.0%	44.6%	100.0%	100.0%	100.0%	50.1%
1150	100.0%	99.9%	90.4%	16.7%	100.0%	100.0%	100.0%	46.5%	100.0%	100.0%	100.0%	49.7%
1200	100.0%	99.9%	91.8%	17.7%	100.0%	100.0%	100.0%	45.2%	100.0%	100.0%	100.0%	50.2%
1250	100.0%	100.0%	92.1%	18.1%	100.0%	100.0%	100.0%	46.7%	100.0%	100.0%	100.0%	48.9%
1300	100.0%	100.0%	92.6%	18.5%	100.0%	100.0%	100.0%	45.9%	100.0%	100.0%	100.0%	49.7%
1350	100.0%	100.0%	93.6%	18.2%	100.0%	100.0%	100.0%	46.5%	100.0%	100.0%	100.0%	50.5%
1400	99.7%	99.6%	93.1%	18.9%	100.0%	100.0%	100.0%	46.6%	100.0%	100.0%	100.0%	50.1%

Table 7.3 shows the percentage of pins that fall within the given standard deviations for pins in each of the three regions described above. The inside assemblies are remarkably consistent; the number of pins within the code's 1σ estimation of uncertainty never dropped below 48.9% and never exceeded 51.7%. Additionally, the code never had a single pin with an uncertainty exceeding 2σ. Within the transition assemblies, the number of pins within the code's 1σ estimation of uncertainty increased slightly with BU, although the percentage of pins with uncertainty estimated less than 1σ was never higher than 46.6%. Much like the inside assemblies, the code never had a single pin with an uncertainty exceeding 2σ. The edge assemblies clearly had the worst statistics of the three regions. Inside the edge region, the number of pins within the code's 1σ estimation of uncertainty fell between 8.2% and 18.9%. Similarly, the number of pins within the code's 2σ estimation of uncertainty fell between 74.0% and 93.6%. While the percentage of pins within 2σ is very low at low BU, it is obvious that the statistics improve dramatically as BU increases, eventually approaching the values expected within a normal distribution.

CHAPTER 8

UNCERTAINTY IN FUEL COMPOSITION (NUCLIDE NUMBER DENSITY)

8.1 Sources of Error

The current depletion algorithm in SERPENT takes the tallies from the MC neutron histories and using the source profile at the end of the transport calculations, solves the Bateman equations for the evolution of isotopic number densities. At startup, the nuclear fuel consists of only a select number of isotopes (Uranium and Oxygen), but as the calculation progresses, the isotopic composition at the start of each cycle may consist of hundreds of fission products, minor actinides, and isotopes that have evolved during previous steps.

Estimating the uncertainty in the atomic density of a nuclide in a burnup calculation is extremely difficult because the uncertainty of the factors used to calculate the atomic number density arises from many sources. There are statistical and propagated uncertainties in the evaluation of source distribution as well as uncertainties in the microscopic cross section data.[25]

In previous chapters, the methodology of using a normal distribution of random and independent events to establish bounds for uncertainty was discussed. This method was used by SERPENT to determine the uncertainty bounds for parameters such as k_{eff} and pin power. Because depletion calculations do not use a series of random tests but instead solve a system of linear Ordinary Differential Equations (ODE's) using starting conditions from the user or the previous burnstep along with the source distribution from the transport calculation, SERPENT

does not give an estimate of the uncertainty in the Nuclide Number Density (NND). Therefore, in order to gain some insight into the uncertainties in NND, the uncertainty in observed NND from the 19 replica runs was examined in selected fuel mixtures. No attempt to separate the statistical, propagated or cross section errors observed in the NND was made, but the goal was rather to understand the magnitudes and behavior of the total uncertainty. The observed uncertainty in ^{235}U, ^{239}Pu, ^{241}Pu, ^{237}Np, and ^{243}Am was examined.

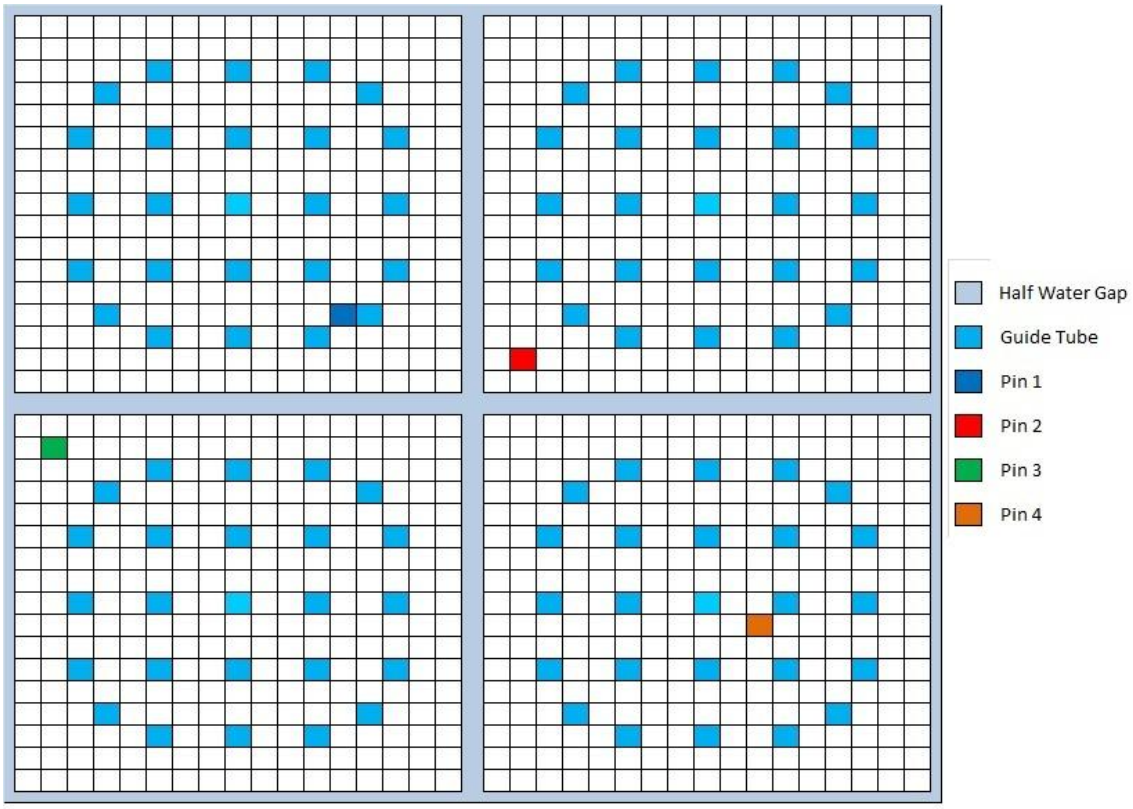

Figure 8.1: Location of Pins for NND Uncertainty Evaluation, TP 1

8.2 Uncertainty in Nuclide Number Density, Test Problem 1

Because 1056 individual fuel mixtures were modeled and tracked in the Quad developed for the three assembly domain test problems, fuel pins from each assembly were selected based on the uncertainty ratios of their pin powers with a total of four fuel pins being analyzed. Figure 8.1 shows the location of the four pins analyzed. Pins 1, 2, and 3 were selected because of the 37

total burnsteps, these pins were the location of the highest uncertainty ratio in their assembly 27, 12, and 5 times respectively. Pin 4, which was in a location that often had an uncertainty ratio less than unity, was selected for comparison. The mean NND of the isotopes of interest in each

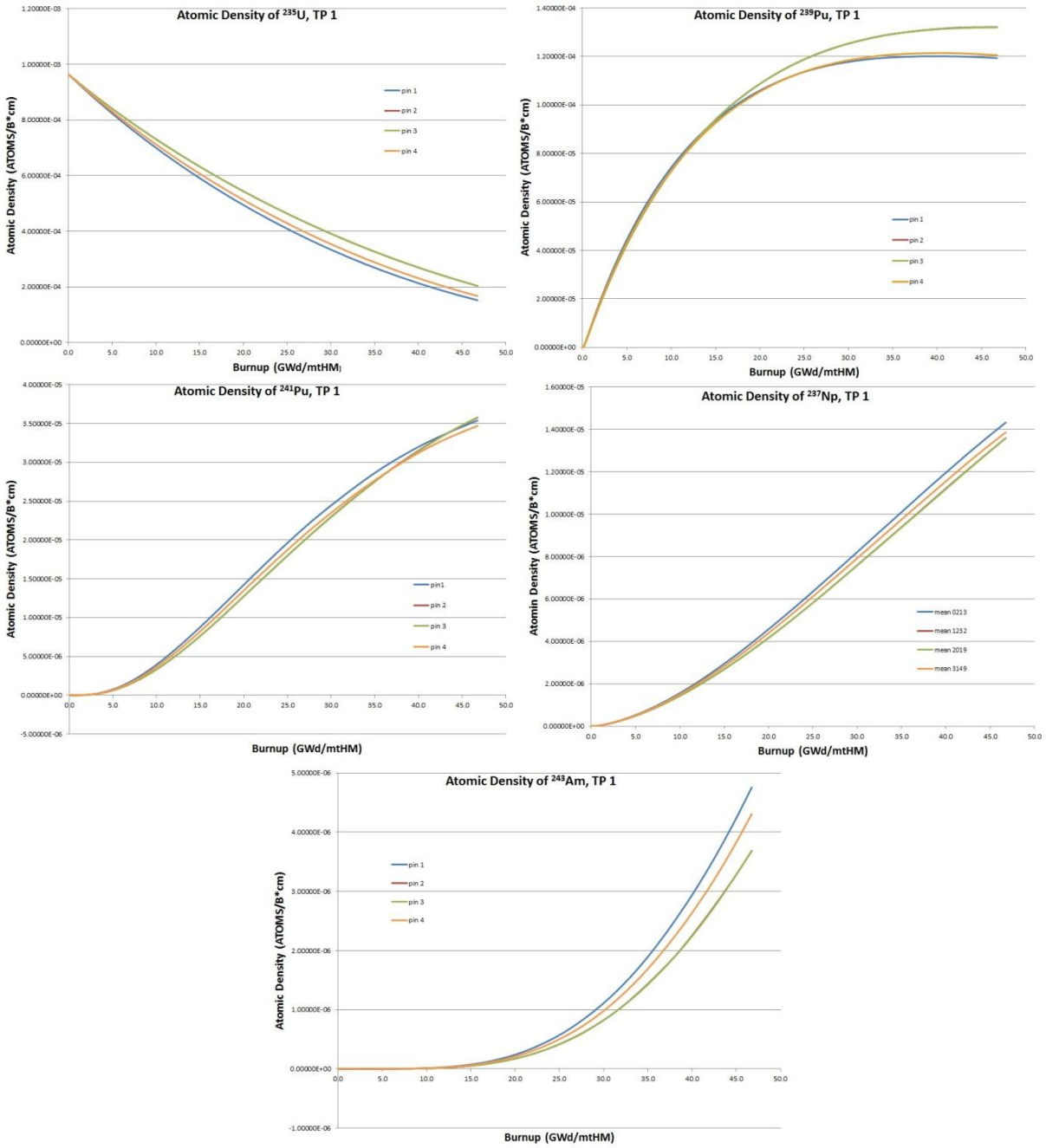

Figure 8.2: Mean Nuclide Number Densities, TP1

pin are shown in Figure 8.2. It should be noted that the plot of pin 2 is oftentimes not visible because it tracks nearly identically the NND of pin 3 and thus is masked by the line of pin 3.

The fact that the NND of ^{235}U and ^{239}Pu, both of which have large thermal neutron cross sections, is lower in pin 1 (particularly at higher BU) than in the other pins indicates that it is in a region of higher flux and burns at a higher power, a conclusion that is validated by the pin power edits that show pin 1 burns hotter on average than the other three pins. This conclusion also explains why the concentration of ^{237}Np and ^{241}Am is higher in pin 1, since these isotopes, which are referred to as minor actinides because of their location on the periodic table, are caused by neutron capture in ^{238}U and transitions into a series of precursor isotopes. Additionally, the fact that the mass densities of all of the tracked isotopes are nearly identical in pins 2 and 3 throughout the calculation indicate that the flux in these regions is also nearly identical.

The observed standard deviation of the NND of the isotopes of interest in each pin is shown in Figure 8.3. The first item of note is that the standard deviation of the NND in ^{235}U increases from zero more quickly than any other isotope because at startup, ^{235}U is the only isotope present in the fuel. Because ^{239}Pu is formed rather quickly, its uncertainty increases rapidly as well. The uncertainty of ^{243}Am, on the other hand, never reaches an appreciable amount until the BU of the fuel nears 20GWd. This is because the creation pathways for ^{243}Am involve multiple neutron captures and nuclide decays.

While the absolute uncertainty in the NND is useful as one measure of understanding the differences in nuclide evolution between replica runs, another metric is the relative uncertainty, which relates the uncertainty of the measurement and the average concentration of the nuclide. Table 8.1 gives an accounting of the mean concentration of each nuclide and its relative

uncertainty in pin 1 for each of the 43 burnsteps. The relative uncertainty of ^{235}U increases with BU because it is being depleted, settling around 0.20% at discharge. The uncertainty of ^{239}Pu is

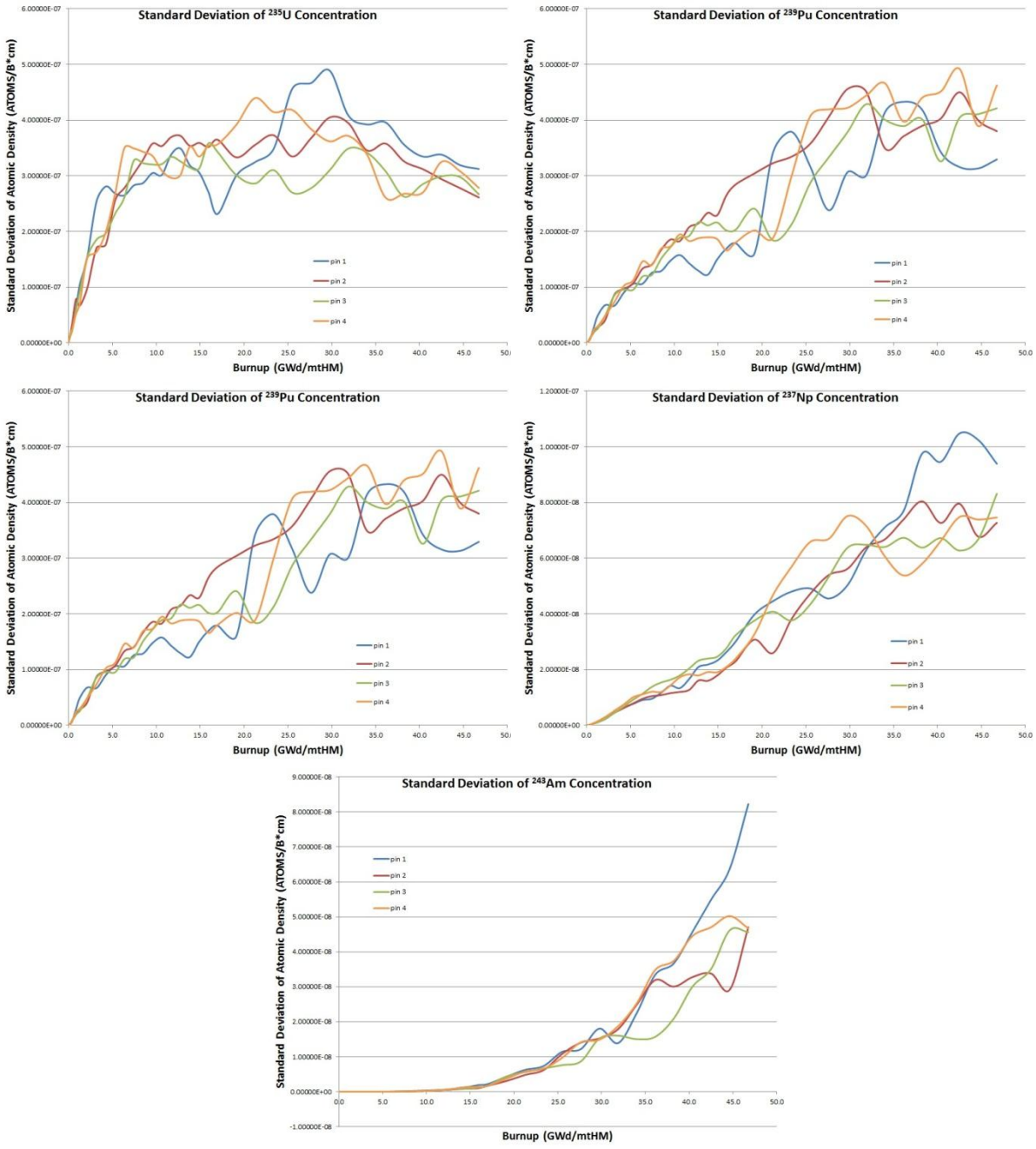

Figure 8.3: Absolute Standard Deviations of Nuclide Number Densities, TP1

Table 8.1: Mean and Relative Standard Deviations of NND, Pin 1, TP1

Day	Pin One									
	^{235}U		^{239}Pu		^{241}Pu		^{237}Np		^{243}Am	
	mean	1σ (%)	mean	1σ (%)	mean	1σ (%)	mean	1σ (%)	mean	1σ (%)
0	9.642E-04	0.00%	0.000E+00	0.00%	0.000E+00	0.00%	0.000E+00	0.00%	0.000E+00	0.00%
1	9.629E-04	0.00%	6.092E-08	0.55%	1.819E-13	3.39%	1.235E-10	3.82%	2.222E-21	5.27%
2	9.617E-04	0.00%	2.280E-07	0.39%	1.891E-12	2.67%	4.838E-10	3.05%	1.465E-19	4.55%
3	9.604E-04	0.00%	4.745E-07	0.30%	7.484E-12	2.77%	1.065E-09	2.62%	1.587E-18	3.76%
5	9.578E-04	0.00%	1.129E-06	0.23%	4.208E-11	2.86%	2.826E-09	2.26%	2.894E-17	3.87%
10	9.515E-04	0.00%	3.208E-06	0.24%	4.327E-10	1.65%	1.016E-08	2.28%	1.399E-15	3.57%
20	9.388E-04	0.01%	7.747E-06	0.37%	4.145E-09	2.48%	3.361E-08	2.06%	6.129E-14	4.03%
30	9.264E-04	0.01%	1.219E-05	0.40%	1.489E-08	2.42%	6.477E-08	1.72%	5.203E-13	3.36%
50	9.019E-04	0.02%	2.057E-05	0.33%	6.963E-08	3.11%	1.428E-07	1.55%	7.133E-12	5.29%
75	8.722E-04	0.03%	3.017E-05	0.22%	2.230E-07	1.96%	2.658E-07	1.70%	5.553E-11	3.72%
100	8.433E-04	0.03%	3.887E-05	0.23%	4.893E-07	1.67%	4.135E-07	1.56%	2.300E-10	4.10%
125	8.153E-04	0.03%	4.677E-05	0.23%	8.811E-07	1.06%	5.828E-07	1.31%	6.788E-10	3.29%
150	7.880E-04	0.03%	5.400E-05	0.20%	1.389E-06	0.85%	7.743E-07	1.17%	1.624E-09	3.63%
175	7.614E-04	0.04%	6.058E-05	0.21%	2.019E-06	0.80%	9.861E-07	0.96%	3.290E-09	2.95%
200	7.355E-04	0.04%	6.659E-05	0.19%	2.754E-06	1.07%	1.215E-06	0.96%	6.055E-09	3.50%
225	7.103E-04	0.04%	7.209E-05	0.20%	3.575E-06	0.79%	1.460E-06	0.97%	1.032E-08	2.92%
250	6.858E-04	0.04%	7.712E-05	0.20%	4.482E-06	1.13%	1.722E-06	0.77%	1.663E-08	2.29%
275	6.618E-04	0.05%	8.171E-05	0.17%	5.457E-06	1.00%	1.997E-06	0.83%	2.539E-08	2.04%
300	6.385E-04	0.05%	8.590E-05	0.15%	6.481E-06	0.84%	2.290E-06	0.91%	3.719E-08	1.64%
325	6.157E-04	0.05%	8.973E-05	0.14%	7.554E-06	0.87%	2.597E-06	0.84%	5.246E-08	2.14%
350	5.936E-04	0.05%	9.320E-05	0.16%	8.655E-06	0.63%	2.913E-06	0.80%	7.179E-08	1.98%
375	5.720E-04	0.05%	9.636E-05	0.18%	9.785E-06	0.55%	3.238E-06	0.81%	9.557E-08	2.00%
400	5.509E-04	0.04%	9.926E-05	0.18%	1.094E-05	0.37%	3.572E-06	0.84%	1.246E-07	1.76%
450	5.103E-04	0.06%	1.042E-04	0.15%	1.327E-05	0.64%	4.277E-06	0.93%	2.001E-07	2.14%
500	4.718E-04	0.07%	1.082E-04	0.32%	1.562E-05	0.63%	5.008E-06	0.89%	3.057E-07	2.04%
550	4.354E-04	0.08%	1.116E-04	0.34%	1.792E-05	0.67%	5.759E-06	0.83%	4.446E-07	1.65%
600	4.009E-04	0.11%	1.142E-04	0.28%	2.016E-05	0.68%	6.536E-06	0.75%	6.142E-07	1.86%
650	3.682E-04	0.13%	1.162E-04	0.20%	2.228E-05	0.59%	7.323E-06	0.62%	8.282E-07	1.47%
700	3.373E-04	0.14%	1.176E-04	0.26%	2.424E-05	0.47%	8.119E-06	0.62%	1.079E-06	1.67%
750	3.083E-04	0.13%	1.187E-04	0.25%	2.610E-05	0.50%	8.923E-06	0.71%	1.373E-06	1.01%
800	2.810E-04	0.14%	1.194E-04	0.35%	2.786E-05	0.39%	9.717E-06	0.73%	1.715E-06	1.31%
850	2.555E-04	0.15%	1.198E-04	0.36%	2.948E-05	0.43%	1.052E-05	0.73%	2.108E-06	1.59%
900	2.317E-04	0.15%	1.200E-04	0.35%	3.091E-05	0.39%	1.132E-05	0.86%	2.548E-06	1.44%
950	2.094E-04	0.16%	1.201E-04	0.28%	3.223E-05	0.38%	1.209E-05	0.78%	3.026E-06	1.51%
1000	1.888E-04	0.18%	1.200E-04	0.26%	3.337E-05	0.56%	1.286E-05	0.82%	3.554E-06	1.55%
1050	1.696E-04	0.19%	1.197E-04	0.26%	3.442E-05	0.48%	1.360E-05	0.75%	4.132E-06	1.54%
1100	1.520E-04	0.21%	1.193E-04	0.28%	3.538E-05	0.36%	1.432E-05	0.66%	4.757E-06	1.73%

between 0.25%-0.35% once the ^{239}Pu concentration approaches its equilibrium and between 0.40%-0.50% for ^{241}Pu. The relative uncertainty of ^{237}Np is 0.70%-0.80% and 1.5%-1.7% for

^{243}Am at discharge. A similar table for all four of the pins analyzed in TP1 can be found in Appendix F.

8.3 Uncertainty in Nuclide Number Density, Test Problem 2

Figure 8.4 shows the location of the four pins analyzed. Pins 1, 2, and 4 were selected because they were IFBA pins. Pin 3, which did not have an IFBA coating, was selected for comparison. The mean NND of the isotopes of interest in each pin are shown in Figure 8.5.

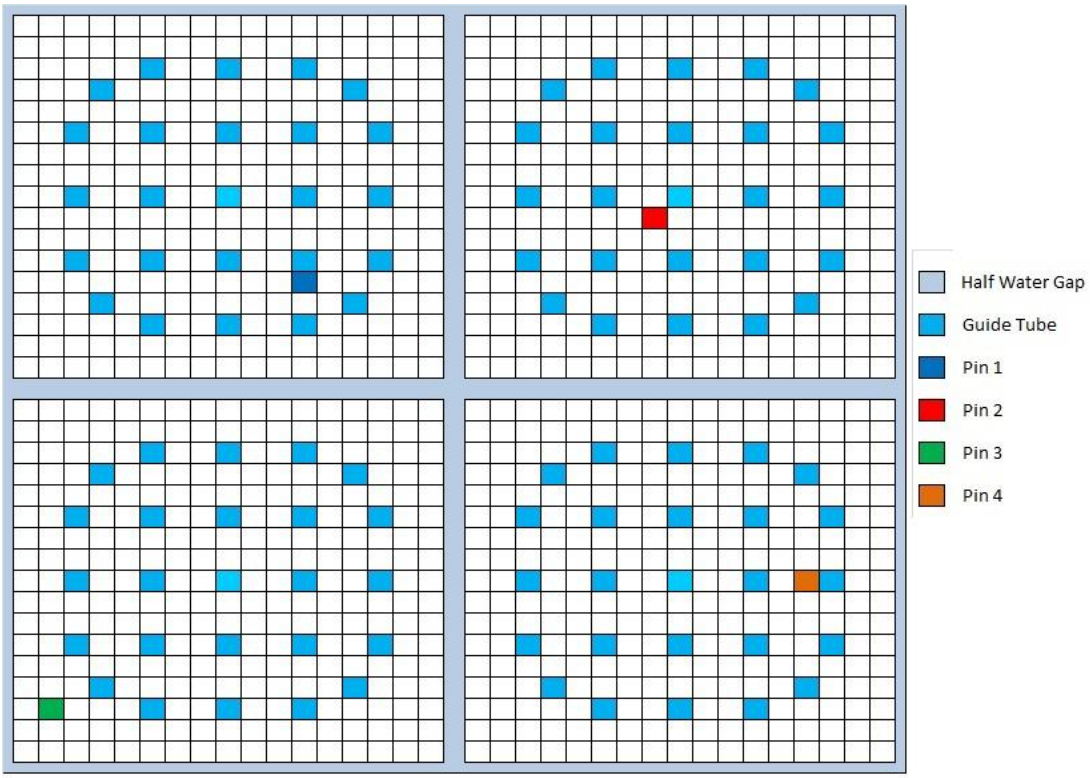

Figure 8.4: Location of Pins for NND Uncertainty Evaluation, TP 2

The mean concentration graphs of ^{235}U and ^{239}Pu indicate that the flux spectrum for the IFBA pins are fairly consistent with one another, while the non IFBA pin is depleted slightly slower in a region of lower flux. A check of the mean pin powers of pin 3 in the first couple burnsteps shows that pin 3 does initially burn hotter than the others, but the speed with which the IFBA coating is depleted exposes the fresher, less depleted fuel of those pins.

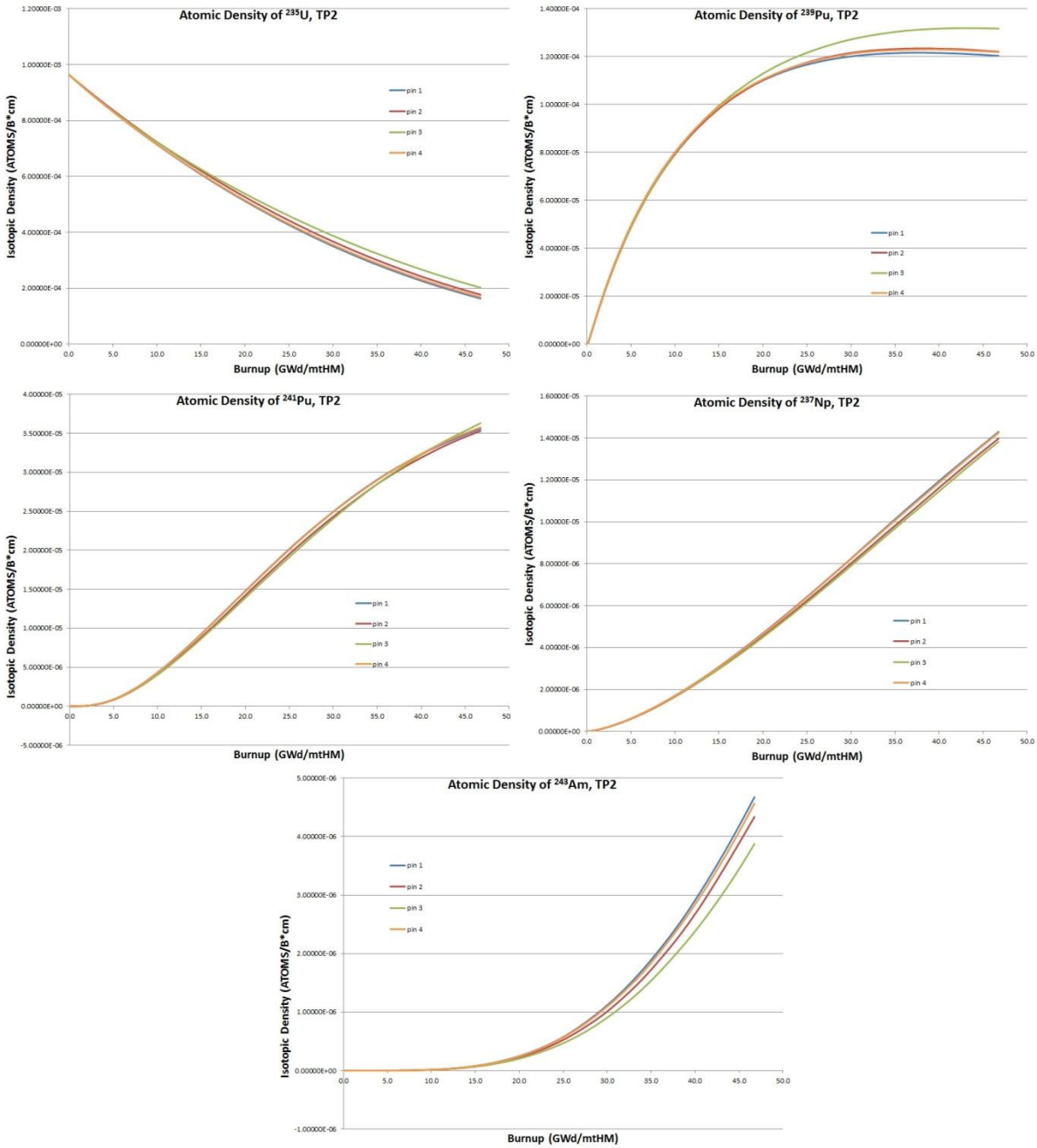

Figure 8.5: Mean Nuclide Number Densities, TP2

The plots of the absolute uncertainty of the pins can be found in Figure 8.6. Overall, both the magnitude and the behavior of the uncertainties for each isotope in TP2 are similar to the uncertainties in TP1 with one exception. At 30GWd, the mean absolute uncertainty of ^{237}Np

was ~6.0E-07 in TP1, but was ~5.0E-07 in TP2. This is notable because the concentration of ^{237}Np at 30GWd does not appear to be different in the two test problems. Again, Table 8.2 gives

Figure 8.6: Absolute Standard Deviations of Nuclide Number Densities, TP2

Table 8.2: Mean and Relative Standard Deviations of NND, Pin 1, TP2

Day	Pin One									
	^{235}U		^{239}Pu		^{241}Pu		^{237}Np		^{243}Am	
	mean	1σ (%)	mean	1σ (%)	mean	1σ (%)	mean	1σ (%)	mean	1σ (%)
0	9.642E-04	0.00%	0.000E+00	0.00%	0.000E+00	0.00%	0.000E+00	0.00%	0.000E+00	0.00%
1	9.630E-04	0.00%	7.034E-08	0.75%	2.627E-13	3.77%	1.549E-10	3.22%	3.657E-21	5.23%
2	9.619E-04	0.00%	2.636E-07	0.56%	2.680E-12	2.78%	6.074E-10	2.61%	2.363E-19	5.12%
3	9.607E-04	0.00%	5.488E-07	0.50%	1.044E-11	2.62%	1.339E-09	2.39%	2.532E-18	4.44%
5	9.583E-04	0.00%	1.305E-06	0.36%	5.691E-11	2.43%	3.567E-09	2.06%	4.541E-17	4.54%
10	9.524E-04	0.00%	3.698E-06	0.31%	5.759E-10	2.95%	1.271E-08	1.74%	2.081E-15	4.49%
20	9.406E-04	0.01%	8.891E-06	0.26%	5.355E-09	2.06%	4.127E-08	1.92%	8.835E-14	4.52%
30	9.291E-04	0.01%	1.393E-05	0.28%	1.897E-08	2.16%	7.867E-08	1.81%	7.304E-13	3.25%
50	9.063E-04	0.01%	2.332E-05	0.34%	8.683E-08	3.39%	1.707E-07	1.98%	9.892E-12	5.10%
75	8.784E-04	0.02%	3.391E-05	0.32%	2.699E-07	1.87%	3.104E-07	2.25%	7.499E-11	3.57%
100	8.512E-04	0.02%	4.335E-05	0.28%	5.811E-07	1.24%	4.750E-07	2.06%	2.962E-10	3.63%
125	8.245E-04	0.03%	5.181E-05	0.29%	1.027E-06	1.12%	6.631E-07	1.69%	8.355E-10	3.36%
150	7.985E-04	0.04%	5.938E-05	0.26%	1.596E-06	1.07%	8.684E-07	1.35%	1.947E-09	2.96%
175	7.731E-04	0.04%	6.619E-05	0.24%	2.279E-06	0.87%	1.092E-06	1.00%	3.890E-09	2.01%
200	7.483E-04	0.04%	7.233E-05	0.24%	3.068E-06	1.15%	1.333E-06	0.89%	7.048E-09	2.68%
225	7.240E-04	0.04%	7.784E-05	0.26%	3.945E-06	0.98%	1.589E-06	0.75%	1.187E-08	2.37%
250	7.002E-04	0.04%	8.284E-05	0.24%	4.889E-06	0.85%	1.858E-06	0.57%	1.873E-08	2.53%
275	6.768E-04	0.04%	8.733E-05	0.20%	5.895E-06	0.54%	2.139E-06	0.55%	2.806E-08	2.22%
300	6.540E-04	0.04%	9.138E-05	0.18%	6.945E-06	0.45%	2.429E-06	0.57%	4.051E-08	1.82%
325	6.317E-04	0.05%	9.502E-05	0.16%	8.040E-06	0.55%	2.733E-06	0.62%	5.636E-08	2.07%
350	6.099E-04	0.05%	9.831E-05	0.14%	9.167E-06	0.61%	3.050E-06	0.69%	7.655E-08	2.00%
375	5.886E-04	0.06%	1.012E-04	0.12%	1.032E-05	0.50%	3.374E-06	0.73%	1.012E-07	1.73%
400	5.678E-04	0.06%	1.039E-04	0.13%	1.149E-05	0.38%	3.706E-06	0.74%	1.312E-07	1.87%
450	5.276E-04	0.06%	1.085E-04	0.16%	1.384E-05	0.44%	4.393E-06	0.71%	2.091E-07	1.91%
500	4.892E-04	0.08%	1.121E-04	0.22%	1.617E-05	0.44%	5.107E-06	0.76%	3.130E-07	1.56%
550	4.528E-04	0.08%	1.150E-04	0.22%	1.847E-05	0.56%	5.846E-06	0.89%	4.472E-07	1.51%
600	4.180E-04	0.09%	1.171E-04	0.22%	2.069E-05	0.44%	6.603E-06	0.78%	6.194E-07	1.28%
650	3.850E-04	0.09%	1.188E-04	0.24%	2.277E-05	0.51%	7.371E-06	0.71%	8.342E-07	2.11%
700	3.538E-04	0.08%	1.200E-04	0.26%	2.473E-05	0.41%	8.153E-06	0.68%	1.085E-06	2.01%
750	3.243E-04	0.09%	1.208E-04	0.27%	2.660E-05	0.47%	8.956E-06	0.65%	1.378E-06	1.77%
800	2.965E-04	0.09%	1.213E-04	0.19%	2.830E-05	0.53%	9.754E-06	0.54%	1.718E-06	1.92%
850	2.703E-04	0.08%	1.216E-04	0.20%	2.987E-05	0.40%	1.054E-05	0.48%	2.101E-06	1.65%
900	2.457E-04	0.10%	1.216E-04	0.24%	3.124E-05	0.44%	1.131E-05	0.57%	2.523E-06	1.95%
950	2.227E-04	0.10%	1.215E-04	0.30%	3.252E-05	0.35%	1.208E-05	0.71%	2.999E-06	1.83%
1000	2.013E-04	0.07%	1.212E-04	0.38%	3.365E-05	0.56%	1.283E-05	0.76%	3.520E-06	1.81%
1050	1.814E-04	0.08%	1.208E-04	0.37%	3.467E-05	0.59%	1.356E-05	0.67%	4.078E-06	1.65%
1100	1.630E-04	0.10%	1.203E-04	0.25%	3.557E-05	0.54%	1.429E-05	0.58%	4.673E-06	1.42%

an accounting of the mean concentration of each nuclide and its relative uncertainty in pin 1, and a similar table for all four pins can be found in Appendix F.

8.4 Uncertainty in Nuclide Number Density, Test Problem 3

Figure 8.7 shows the location of the four pins analyzed. Pins 2 and3 were selected because they were IFBA pins. Pins 1 and 4, which did not have an IFBA coating, was selected for comparison. The mean NND of the isotopes of interest in each pin are shown in Figure 8.8.

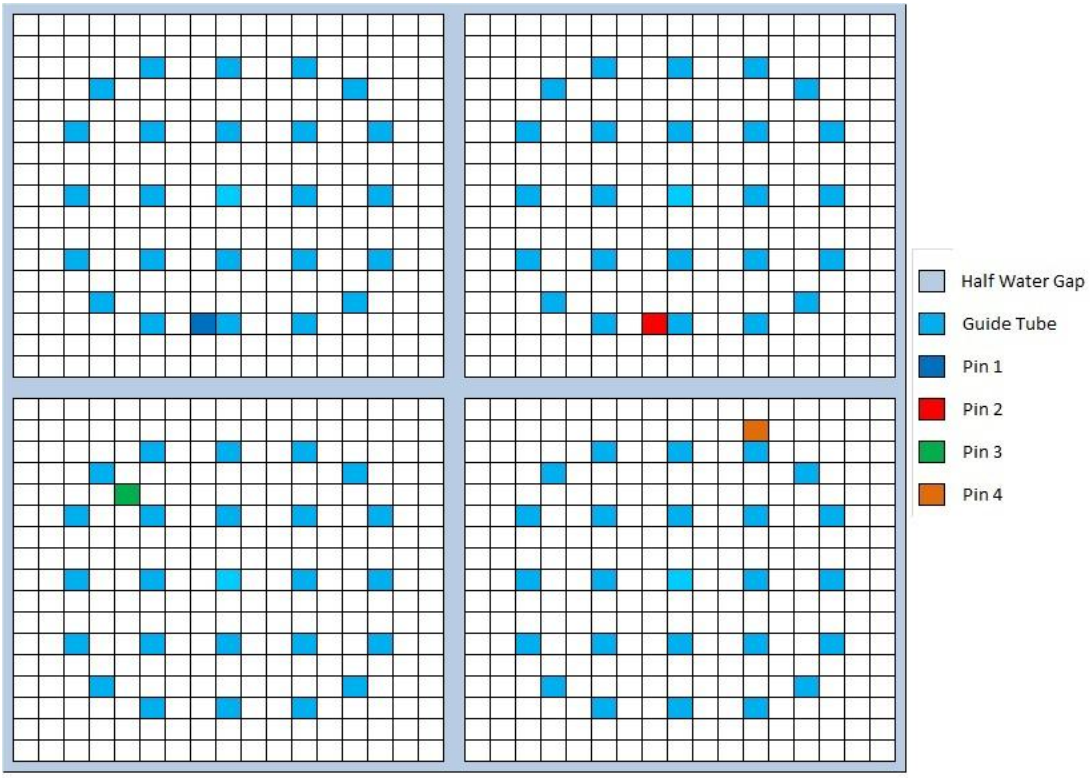

Figure 8.7: Location of Pins for NND Uncertainty Evaluation, TP 3

From Figure 8.8, the fact that pins 2 and 3 are IFBA pins can be clearly seen due to the slower depletion of ^{235}U and the slower buildup of ^{239}Pu, ^{237}Np, and ^{243}Am. It is also interesting to note that the rate of consumption of ^{235}U in the IFBA pins is higher toward the end of cycle, since their isotopic composition contains a slightly larger amount of the fissile Uranium material.

The plots of the absolute uncertainty of the pins can be found in Figure 8.9. Overall, both the magnitude and the behavior of the uncertainties for each isotope in TP3 are similar to the uncertainties in TP2. No clear distinction can be made in the uncertainties seen in IFBA and

non-IFBA pins, but this may be simply due to the small sample size . Table 8.3 gives an accounting of the mean concentration of each nuclide and its relative uncertainty in pin 1 for all 37 burnsteps, and a similar table for all four pins can be found in Appendix F.

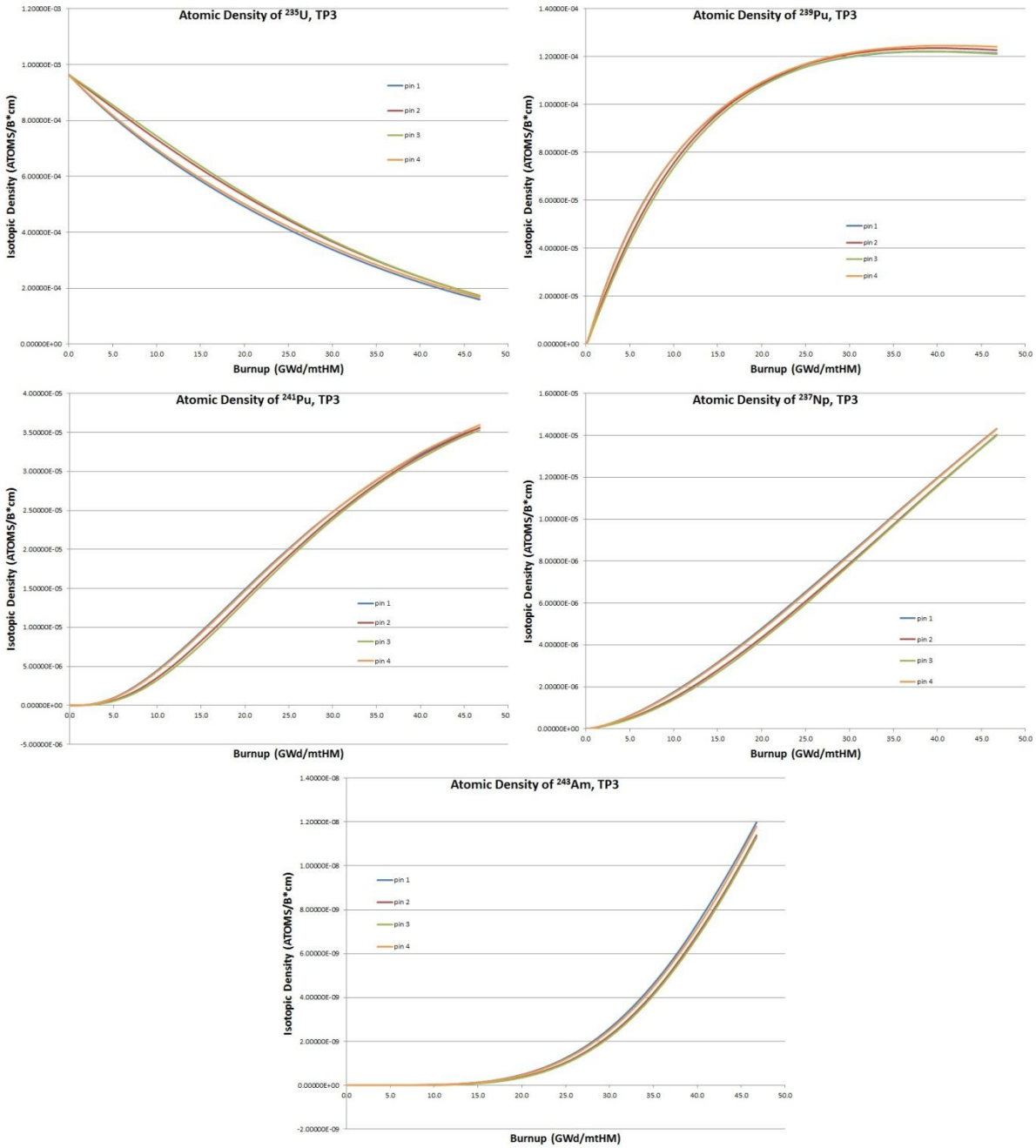

Figure 8.8: Mean Nuclide Number Densities, TP3

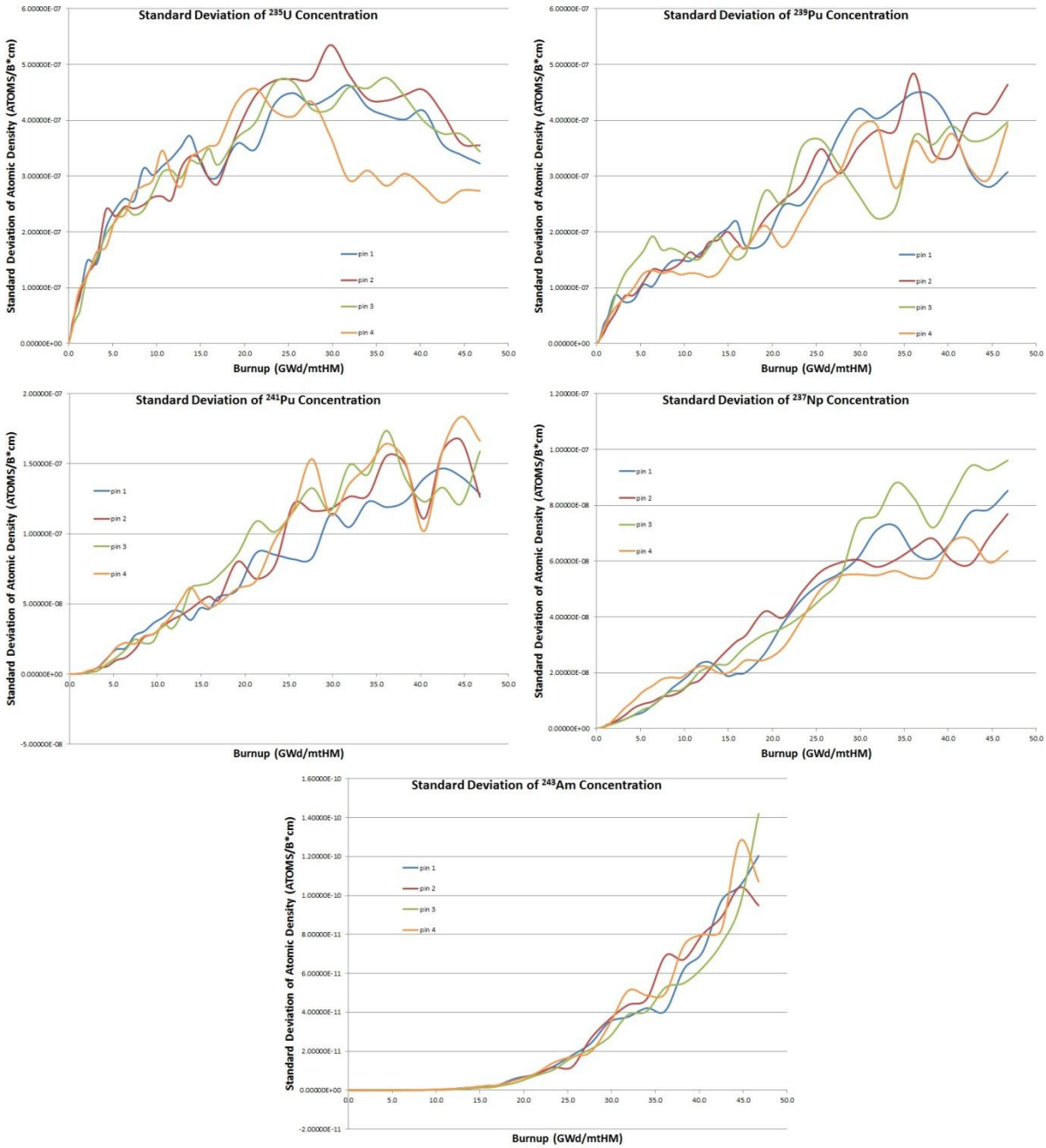

Figure 8.9: Absolute Standard Deviations of Nuclide Number Densities, TP3

Table 8.3: Mean and Relative Standard Deviations of NND, Pin 1, TP3

Day	Pin One									
	^{235}U		^{239}Pu		^{241}Pu		^{237}Np		^{243}Am	
	mean	1σ (%)	mean	1σ (%)	mean	1σ (%)	mean	1σ (%)	mean	1σ (%)
0	9.642E-04	0.00%	0.000E+00	0.00%	0.000E+00	0.00%	0.000E+00	0.00%	0.000E+00	0.00%
1	9.628E-04	0.00%	6.969E-08	0.43%	2.670E-13	3.73%	1.513E-10	3.78%	7.511E-27	4.67%
2	9.614E-04	0.00%	2.609E-07	0.35%	2.821E-12	2.57%	5.924E-10	2.55%	1.201E-24	3.99%
3	9.600E-04	0.00%	5.428E-07	0.26%	1.100E-11	2.50%	1.305E-09	2.15%	2.202E-23	3.06%
5	9.571E-04	0.00%	1.290E-06	0.19%	6.209E-11	2.81%	3.441E-09	1.70%	7.981E-22	3.12%
10	9.501E-04	0.00%	3.658E-06	0.32%	6.271E-10	2.61%	1.226E-08	1.68%	9.434E-20	2.89%
20	9.362E-04	0.01%	8.782E-06	0.40%	5.970E-09	2.06%	4.030E-08	1.54%	9.181E-18	2.96%
30	9.226E-04	0.01%	1.374E-05	0.34%	2.100E-08	1.74%	7.747E-08	1.63%	1.232E-16	2.50%
50	8.962E-04	0.02%	2.294E-05	0.38%	9.622E-08	1.94%	1.696E-07	1.32%	2.908E-15	2.13%
75	8.646E-04	0.02%	3.326E-05	0.22%	2.972E-07	1.55%	3.138E-07	1.04%	3.317E-14	3.05%
100	8.345E-04	0.02%	4.246E-05	0.19%	6.354E-07	1.76%	4.856E-07	0.98%	1.728E-13	3.23%
125	8.055E-04	0.03%	5.068E-05	0.21%	1.110E-06	1.58%	6.798E-07	0.86%	6.073E-13	2.41%
150	7.778E-04	0.03%	5.805E-05	0.18%	1.707E-06	1.08%	8.923E-07	0.93%	1.650E-12	2.07%
175	7.511E-04	0.03%	6.466E-05	0.20%	2.415E-06	1.14%	1.125E-06	0.97%	3.786E-12	2.18%
200	7.253E-04	0.04%	7.065E-05	0.21%	3.224E-06	0.95%	1.374E-06	1.03%	7.655E-12	1.35%
225	7.004E-04	0.04%	7.601E-05	0.20%	4.105E-06	0.88%	1.637E-06	1.02%	1.398E-11	1.39%
250	6.763E-04	0.05%	8.091E-05	0.18%	5.057E-06	0.80%	1.914E-06	1.02%	2.391E-11	1.85%
275	6.530E-04	0.05%	8.537E-05	0.19%	6.062E-06	0.74%	2.201E-06	1.05%	3.837E-11	1.52%
300	6.304E-04	0.06%	8.943E-05	0.20%	7.116E-06	0.62%	2.498E-06	0.96%	5.862E-11	1.69%
325	6.084E-04	0.06%	9.305E-05	0.21%	8.199E-06	0.47%	2.806E-06	0.77%	8.615E-11	1.51%
350	5.871E-04	0.06%	9.634E-05	0.21%	9.324E-06	0.50%	3.126E-06	0.60%	1.222E-10	1.29%
375	5.663E-04	0.05%	9.937E-05	0.22%	1.046E-05	0.45%	3.453E-06	0.57%	1.695E-10	1.38%
400	5.461E-04	0.05%	1.021E-04	0.17%	1.160E-05	0.48%	3.790E-06	0.53%	2.286E-10	1.11%
450	5.073E-04	0.07%	1.068E-04	0.17%	1.393E-05	0.43%	4.485E-06	0.60%	3.919E-10	1.57%
500	4.705E-04	0.07%	1.106E-04	0.22%	1.622E-05	0.53%	5.208E-06	0.73%	6.242E-10	1.29%
550	4.356E-04	0.10%	1.138E-04	0.22%	1.847E-05	0.46%	5.948E-06	0.78%	9.379E-10	1.30%
600	4.024E-04	0.11%	1.163E-04	0.26%	2.060E-05	0.40%	6.709E-06	0.77%	1.350E-09	1.33%
650	3.711E-04	0.12%	1.182E-04	0.32%	2.268E-05	0.37%	7.476E-06	0.74%	1.864E-09	1.29%
700	3.414E-04	0.13%	1.197E-04	0.35%	2.459E-05	0.46%	8.247E-06	0.74%	2.509E-09	1.40%
750	3.133E-04	0.15%	1.208E-04	0.33%	2.641E-05	0.40%	9.018E-06	0.79%	3.268E-09	1.15%
800	2.868E-04	0.15%	1.215E-04	0.35%	2.809E-05	0.44%	9.804E-06	0.74%	4.155E-09	1.01%
850	2.619E-04	0.16%	1.220E-04	0.37%	2.971E-05	0.40%	1.059E-05	0.59%	5.166E-09	0.79%
900	2.385E-04	0.17%	1.221E-04	0.36%	3.114E-05	0.40%	1.135E-05	0.54%	6.312E-09	0.99%
950	2.166E-04	0.19%	1.221E-04	0.32%	3.242E-05	0.43%	1.211E-05	0.55%	7.594E-09	0.94%
1000	1.961E-04	0.18%	1.220E-04	0.25%	3.360E-05	0.44%	1.286E-05	0.60%	8.978E-09	1.08%
1050	1.771E-04	0.19%	1.217E-04	0.23%	3.469E-05	0.41%	1.360E-05	0.58%	1.043E-08	1.01%
1100	1.595E-04	0.20%	1.214E-04	0.25%	3.560E-05	0.36%	1.432E-05	0.60%	1.199E-08	1.00%

8.5 Uncertainty in Nuclide Number Density, Test Problem 4

Figure 8.10 shows the location of the four fuel regions analyzed. Fuel region 1 is an edge assembly, enriched to 2.6% and has no IFBA pins. Fuel region 2 is a middle assembly, enriched to 4.95%, and has 156 IFBA pins. Fuel region 3 is also enriched to 4.95% but has only 32 IFBA pins. Fuel region 4 is enriched to 2.6% and does not have any IFBA pins. Regions 3 and 4 are both transition assemblies. The mean NND of the isotopes of interest in each fuel region are shown in Figure 8.11.

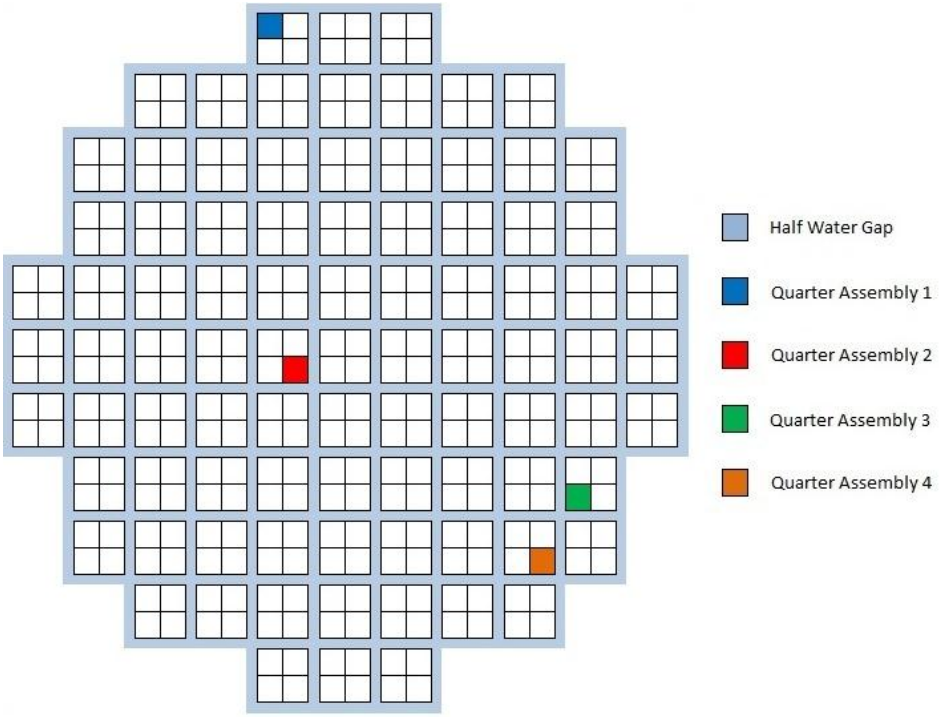

Figure 8.10: Location of Fuel Regions for NND Uncertainty Evaluation, TP 4

Figure 8.11 clearly shows a large difference in the power produced by each fuel region. Region 2 in the center of the core is depleted rapidly, as evidenced by the steep depletion slope of ^{235}U and the speed with which ^{239}Pu inventories are built up. It is also interesting to note the extreme differences in the power of regions 3 and 4 despite their very close proximity. This demonstrates that the enrichment of the fuel makes a large difference in flux that region will see

unless a local strong absorber is added to suppress the reactivity. The higher flux in region 4 also led to the higher concentrations of actinides in those regions, especially at higher BU.

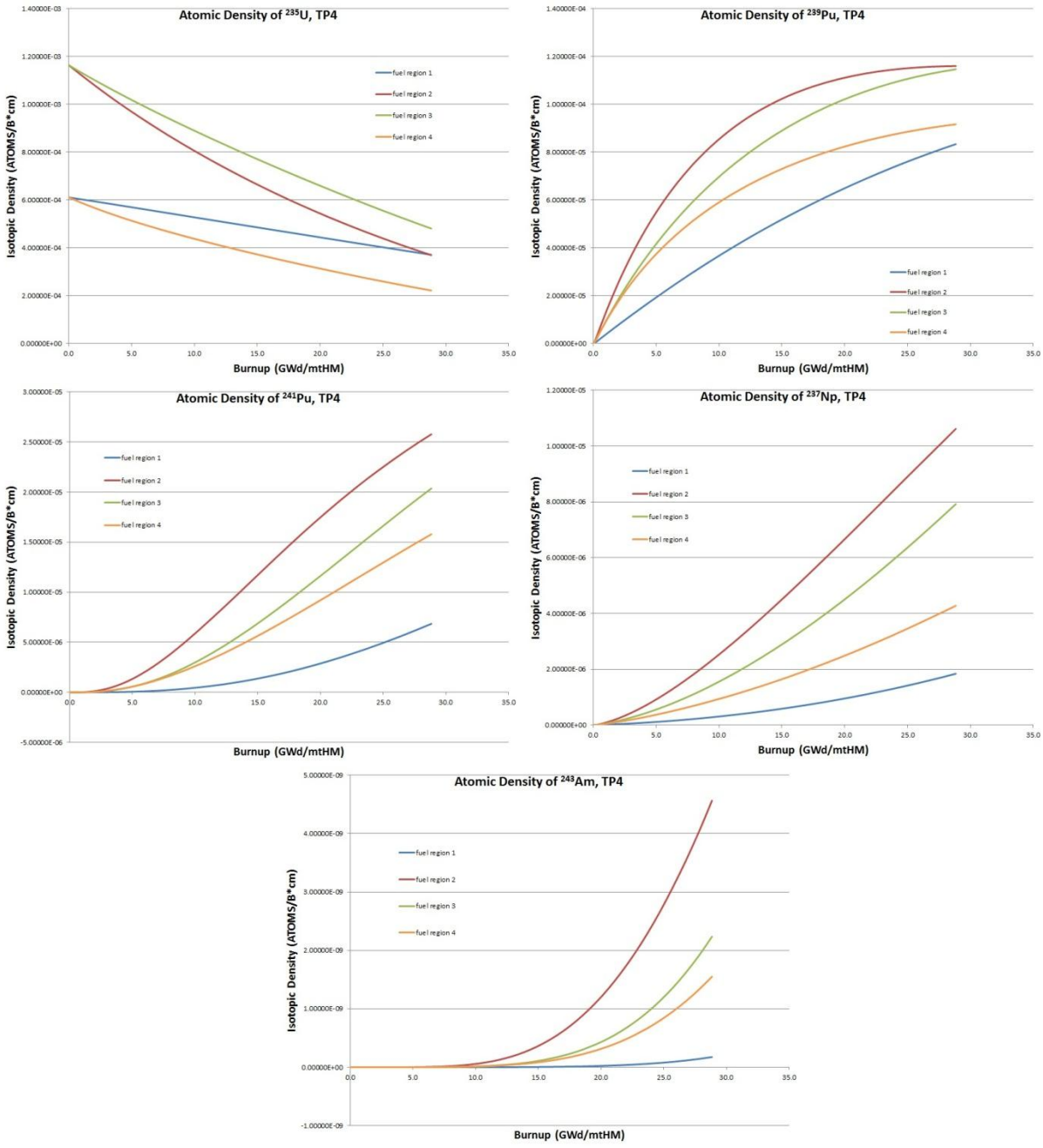

Figure 8.11: Mean Nuclide Number Densities, TP4

Figure 8.12: Absolute Standard Deviations of Nuclide Number Densities, TP4

Table 8.4: Mean and Relative Standard Deviations of NND, Fuel Region 1, TP4

Day	Fuel Region One									
	^{235}U		^{239}Pu		^{241}Pu		^{237}Np		^{243}Am	
	mean	1σ (%)	mean	1σ (%)	mean	1σ (%)	mean	1σ (%)	mean	1σ (%)
0	6.114E-04	0.00%	0.000E+00	0.00%	0.000E+00	0.00%	0.000E+00	0.00%	0.000E+00	0.00%
1	6.112E-04	0.00%	1.047E-08	0.86%	9.387E-16	2.36%	1.610E-11	2.99%	6.544E-31	3.39%
2	6.110E-04	0.00%	3.956E-08	0.56%	1.043E-14	1.69%	6.311E-11	1.85%	1.139E-28	1.82%
3	6.109E-04	0.00%	8.294E-08	0.39%	4.208E-14	1.32%	1.387E-10	1.47%	2.133E-27	2.09%
5	6.105E-04	0.00%	1.991E-07	0.24%	2.444E-13	1.88%	3.654E-10	1.52%	8.138E-26	2.23%
10	6.097E-04	0.00%	5.747E-07	0.31%	2.596E-12	2.13%	1.285E-09	1.33%	1.011E-23	2.35%
20	6.080E-04	0.00%	1.416E-06	0.44%	2.639E-11	1.78%	4.028E-09	1.38%	1.066E-21	2.73%
30	6.062E-04	0.00%	2.266E-06	0.38%	9.794E-11	1.44%	7.352E-09	1.20%	1.518E-20	2.29%
50	6.028E-04	0.01%	3.947E-06	0.37%	4.933E-10	1.44%	1.475E-08	0.96%	3.932E-19	2.51%
75	5.986E-04	0.01%	6.014E-06	0.35%	1.719E-09	1.75%	2.472E-08	1.20%	4.953E-18	2.31%
100	5.944E-04	0.01%	8.050E-06	0.28%	4.143E-09	1.22%	3.540E-08	1.06%	2.922E-17	2.09%
125	5.901E-04	0.01%	1.007E-05	0.26%	8.166E-09	1.11%	4.689E-08	0.84%	1.147E-16	2.25%
150	5.858E-04	0.01%	1.206E-05	0.26%	1.413E-08	0.79%	5.922E-08	0.89%	3.479E-16	1.61%
175	5.815E-04	0.01%	1.404E-05	0.22%	2.247E-08	0.84%	7.235E-08	0.91%	8.910E-16	1.52%
200	5.773E-04	0.01%	1.599E-05	0.23%	3.360E-08	0.86%	8.623E-08	0.89%	2.012E-15	1.54%
225	5.730E-04	0.02%	1.792E-05	0.21%	4.772E-08	0.83%	1.010E-07	0.80%	4.096E-15	1.35%
250	5.687E-04	0.02%	1.983E-05	0.23%	6.532E-08	0.90%	1.164E-07	0.75%	7.739E-15	1.52%
275	5.643E-04	0.02%	2.171E-05	0.21%	8.686E-08	0.91%	1.327E-07	0.71%	1.376E-14	1.30%
300	5.600E-04	0.02%	2.359E-05	0.20%	1.125E-07	0.81%	1.501E-07	0.65%	2.323E-14	1.35%
325	5.556E-04	0.02%	2.544E-05	0.18%	1.426E-07	0.64%	1.683E-07	0.59%	3.765E-14	1.24%
350	5.513E-04	0.02%	2.725E-05	0.16%	1.770E-07	0.59%	1.873E-07	0.55%	5.866E-14	1.16%
375	5.470E-04	0.02%	2.905E-05	0.16%	2.165E-07	0.70%	2.072E-07	0.52%	8.870E-14	1.28%
400	5.426E-04	0.02%	3.082E-05	0.14%	2.610E-07	0.68%	2.280E-07	0.51%	1.303E-13	1.04%
450	5.339E-04	0.02%	3.431E-05	0.15%	3.656E-07	0.62%	2.726E-07	0.48%	2.621E-13	1.13%
500	5.253E-04	0.03%	3.768E-05	0.14%	4.920E-07	0.66%	3.203E-07	0.44%	4.877E-13	1.18%
550	5.166E-04	0.03%	4.096E-05	0.12%	6.414E-07	0.45%	3.717E-07	0.50%	8.572E-13	1.08%
600	5.079E-04	0.03%	4.414E-05	0.08%	8.142E-07	0.59%	4.267E-07	0.57%	1.428E-12	1.08%
650	4.993E-04	0.03%	4.723E-05	0.09%	1.012E-06	0.68%	4.854E-07	0.43%	2.271E-12	0.90%
700	4.906E-04	0.03%	5.022E-05	0.11%	1.235E-06	0.64%	5.478E-07	0.38%	3.491E-12	0.83%
750	4.820E-04	0.03%	5.312E-05	0.11%	1.485E-06	0.59%	6.139E-07	0.36%	5.192E-12	0.85%
800	4.734E-04	0.03%	5.593E-05	0.11%	1.757E-06	0.52%	6.837E-07	0.36%	7.510E-12	0.78%
850	4.648E-04	0.03%	5.866E-05	0.12%	2.055E-06	0.40%	7.573E-07	0.37%	1.062E-11	0.72%
900	4.562E-04	0.03%	6.131E-05	0.11%	2.379E-06	0.38%	8.348E-07	0.41%	1.472E-11	0.83%
950	4.476E-04	0.04%	6.389E-05	0.11%	2.729E-06	0.31%	9.165E-07	0.38%	2.001E-11	0.80%
1000	4.390E-04	0.04%	6.638E-05	0.11%	3.102E-06	0.37%	1.003E-06	0.41%	2.677E-11	0.81%
1050	4.304E-04	0.04%	6.877E-05	0.10%	3.494E-06	0.41%	1.092E-06	0.39%	3.527E-11	0.89%
1100	4.218E-04	0.04%	7.109E-05	0.10%	3.914E-06	0.35%	1.187E-06	0.35%	4.587E-11	0.72%
1150	4.133E-04	0.04%	7.334E-05	0.10%	4.353E-06	0.31%	1.284E-06	0.32%	5.880E-11	0.69%
1200	4.048E-04	0.04%	7.551E-05	0.10%	4.813E-06	0.30%	1.386E-06	0.33%	7.452E-11	0.61%
1250	3.963E-04	0.04%	7.758E-05	0.10%	5.291E-06	0.24%	1.492E-06	0.30%	9.334E-11	0.45%
1300	3.879E-04	0.04%	7.958E-05	0.10%	5.790E-06	0.33%	1.604E-06	0.29%	1.159E-10	0.43%
1350	3.795E-04	0.05%	8.151E-05	0.10%	6.310E-06	0.31%	1.719E-06	0.30%	1.427E-10	0.44%
1400	3.710E-04	0.06%	8.337E-05	0.10%	6.845E-06	0.33%	1.839E-06	0.29%	1.742E-10	0.61%

Table 8.4 clearly shows that the relative uncertainties in TP4 are much lower than the uncertainties at discharge in the previous test problems. However, it should be noted that the discharge BU of the fuel in TP1-3 was ~46GWd, while the discharge BU in TP4 was 28.8GWd. Because of the drastically lower BU, the inventory or remaining ^{235}U was higher in TP4 and the inventories of minor actinides was 1-3 orders of magnitude lower in TP4. This would indicate that BU and isotope inventory are key components to determining uncertainty in NND.

Another factor impacting the difference between the higher observed variance in NND in TP1-3 and the lower variance in TP4 is the fact that the variance in early test problems was taken from a single pin, while TP4 is the average of the quarter fuel assembly. The averaging of flux across the FA, which is done before NND is calculated, certainly helps to reduce the variance in NND.

CHAPTER 9

CONCLUSIONS AND FUTURE WORK

9.1 Conclusions

A numerical study of the error propagation in Monte Carlo depletion simulations was undertaken in order to gain insight into the magnitude and behavior or statistical errors and uncertainties in several common depletion problems. Four test problems were developed, three incorporated a fuel assembly "Quad" of varying enrichments and material compositions and the fourth was a full-core test problem modeled on the IRIS reactor. Using the SERPENT Continuous Energy MC Code developed by the VTT Technical Research Centre of Finland, each test problem was simulated 19 times by changing the code's initial seed number. The observed variance of several key parameters produced by the 19 replica runs was compared with the average reported variance.

9.1.1 Calculation Time and System Resources Required

The three assembly domain problems required on average 7-8 days to complete 37 burnsteps on a 2.3GHz Opteron processor. These runs required just over 30GB RAM. The core domain simulation required on average 46 days when run in serial and 12 days when run in parallel on 5 processors, each run requiring over 17.7GB RAM in either mode. The extreme time and memory demands of these simulations support the assertion discussed in Chapter 1 that time and computer resource requirements hold back more widespread use of MC methods for full-core calculations.[1]

9.1.2 Uncertainty in K_{eff}

The study of error propagation in the calculation of k_{eff} yielded very similar results in all four test problems. The observed uncertainty in k_{eff} tends to be slightly higher than the reported uncertainty, sometimes by up to 50%. The ratio of the observed-to-reported uncertainty is usually above 1, but will oscillate about unity especially at higher BU. The trendline of observed uncertainty is relatively constant, with only a slight increase in conjunction with BU.

9.1.3 Uncertainty in Pin Powers

Uncertainty is generally underestimated in the pin power estimated produced by the code. Errors are particularly egregious when there is no heavy absorber present in the defined geometry (like fresh fuel assemblies at BOC) or when the pins are close to boundaries. Observed uncertainty does appear to diminish slightly with BU, likely the result of the decreased reactivity and increasing absorption cross section of fission products and Minor Actinide accumulation. In most cases, the true uncertainty is higher for a majority of pins than the uncertainty reported by the code, although true uncertainty tends to be within 2σ more often than a normal distribution would predict.

9.1.4 Uncertainty in Nuclide Number Density

The difference of the variance of ^{235}U, ^{239}Pu, ^{241}Pu, ^{237}Np, and ^{243}Am showed that variance is tied to the amount of fuel and the size of the region across which flux is averaged. The BU of the fuel is also critical to determining the variance in NND, especially in isotopes like 243Am that are only formed in meaningful amounts at higher BU because of the complexity of their creation chains. While the work presented here does provide a snapshot of uncertainty behavior, the small sample size prevents to development of more concrete conclusions.

9.2 Future Work

One important observation of this research effort has been the importance of source convergence on accurate uncertainty prediction. Source convergence may be particularly difficult in cases like the full-core simulations because few neutron histories will be recorded in the edge regions, since the neutron history population is determined from the source distribution of previous cycles. Understanding how to insure source convergence is an ongoing research effort, and could be looked at further in conjunction with this research study.

One other area of interest is in gaining a greater insight into the errors, both statistical and propagated, in the nuclide number densities in MC BU. A method of predicting the variance in MC depletion was proposed by Tojjoh et al. in a 2006 paper.[26] Using only 10 replicas, they saw favorable results with their methodology. It may be possible to use the data from the 19 replica runs here to investigate the validity of their conclusions.

APPENDIX A

ASSEMBLY, CORE, AND SIMULATION PARAMETERS

Table A.1: Test 1-4 Assembly Parameters

Assembly Parameters	Test Problem 1	Test Problem 2	Test Problem 3	Test Problem 4
fuel pellet rad (cm)	0.4025	0.4025	0.4025	0.4096
IFBA rad (cm)	N/A	0.4041	0.4041	0.4112
Air gap rad (cm)	N/A	N/A	N/A	0.4217
Cladding rad (cm)	0.4750	0.4750	0.4750	0.4750
Fuel rod pitch (cm)	1.265	1.265	1.265	1.3284
Guide tube inner rad (cm)	0.5730	0.5730	0.5730	0.5922
Guide tube thickness (cm)	0.0400	0.0400	0.0400	0.0530
Assembly type	17 x 17	17 x 17	17 x 17	17 x 17
Assembly pitch (cm)	21.6126	21.6126	21.6126	22.6644

Table A.2: Test 1-4 Material Parameters

Material Parameters	Test Problem 1	Test Problem 2	Test Problem 3	Test Problem 4
Fuel enrichment (wt %)	4.7	4.7	4.7	2.6 & 4.95
Fuel density (g/cm^3)	10.412	10.412	10.412	10.412
IFBA coating (mg/in ^{10}B)	N/A	2.25	2.25	2.25
Air gap material	N/A	N/A	N/A	He
Gas density (g/cm^3)	N/A	N/A	N/A	2.65152E-05
Clad/Guide tube composition (wt %)	^{nat}Zr=98.38, ^{nat}Sn=1.30, ^{nat}Fe=0.22, ^{nat}Cr=0.10	^{nat}Zr=98.38, ^{nat}Sn=1.30, ^{nat}Fe=0.22, ^{nat}Cr=0.10	^{nat}Zr=98.38, ^{nat}Sn=1.30, ^{nat}Fe=0.22, ^{nat}Cr=0.10	^{nat}Zr=98.38, ^{nat}Sn=1.30, ^{nat}Fe=0.22, ^{nat}Cr=0.10
Clad/Guide tube density (g/cm^3)	6.44	6.44	6.44	6.44

Table A.3: Core Parameters

Core Parameters	Test Problem 1	Test Problem 2	Test Problem 3	Test Problem 4
Assemblies	4	4	4	89
Reflector material	N/A	N/A	N/A	SS316
Water density (g/cm^3)	0.7291	0.7291	0.7291	0.7291
Reflector rad (cm)	N/A	N/A	N/A	140.5
Downcomer rad (cm)	N/A	N/A	N/A	180.5
Power density (W/kgU)	4.25E-02	4.25E-02	4.25E-02	2.06E-02
Boundary condition	reflective	reflective	reflective	vacuum
Neutrons/generation	40,000	40,000	40,000	200,000
Skipped generations	100	100	100	300
Active generations	600	600	600	450

Table A.4: SERPENT Code Parameters

Calculation code	SERPENT: The Continuous-energy Monte Carlo Depletion Code 1.1.16
XS Library	ENDF/B-VII
Energy Grid Parameters	5E-5 Fractional reconstruction tolerance
	15.0 (MeV) Maximum energy in the grid
	1.0E-9 (MeV) Minimum energy in the grid
Burnup Points (Tests 1-3) (days)	0, 1, 2, 3, 5, 10, 20, 30, 50, 75, 100, 125, 150, 175. 200, 225, 250, 275, 300, 325
	350, 375, 400, 450, 500, 550, 600, 650, 700, 750, 800, 850, 900, 950, 1000, 1050
	1100
Burnup Points (Tests 1-3) (MWd)	0, 42.5, 85, 127.5, 212.5, 425, 850, 1275, 2125, 3187.5, 4250, 5312.5, 6375,
	7437.5, 8500, 9562.5, 10625, 11687.5, 12750, 13812.5, 14875, 15937.5, 17000
	19125, 21250, 23375, 25500, 27625, 29750, 31875, 34000, 36125, 38250,
	40375, 42500, 44625, 46750
Burnup Points (Tests 4) (days)	0, 1, 2, 3, 5, 10, 20, 30, 50, 75, 100, 125, 150, 175. 200, 225, 250, 275, 300, 325
	350, 375, 400, 450, 500, 550, 600, 650, 700, 750, 800, 850, 900, 950, 1000, 1050
	1100, 1150, 1200, 1250, 1300, 1350, 1400
Burnup Points (Test 4) (MWd)	0, 20.6, 41.2, 61.8, 103, 206, 412, 618, 1030, 1545, 2060, 2575, 3090, 3605
	4120, 4635, 5150, 5665, 6180, 12750, 6695, 7210, 7725, 8240, 9270, 10300
	11330, 12360, 13390, 14420, 15450, 16480, , 17510, 18540, 19570, 20600
	21630, 22660, 23690, 24720, 25750, 26780, 27810, 28840
Burnup Options	The "predictor-corrector" was activated for all calculation points

APPENDIX B

PIN POWER EDITS FOR TEST PROBLEM ONE

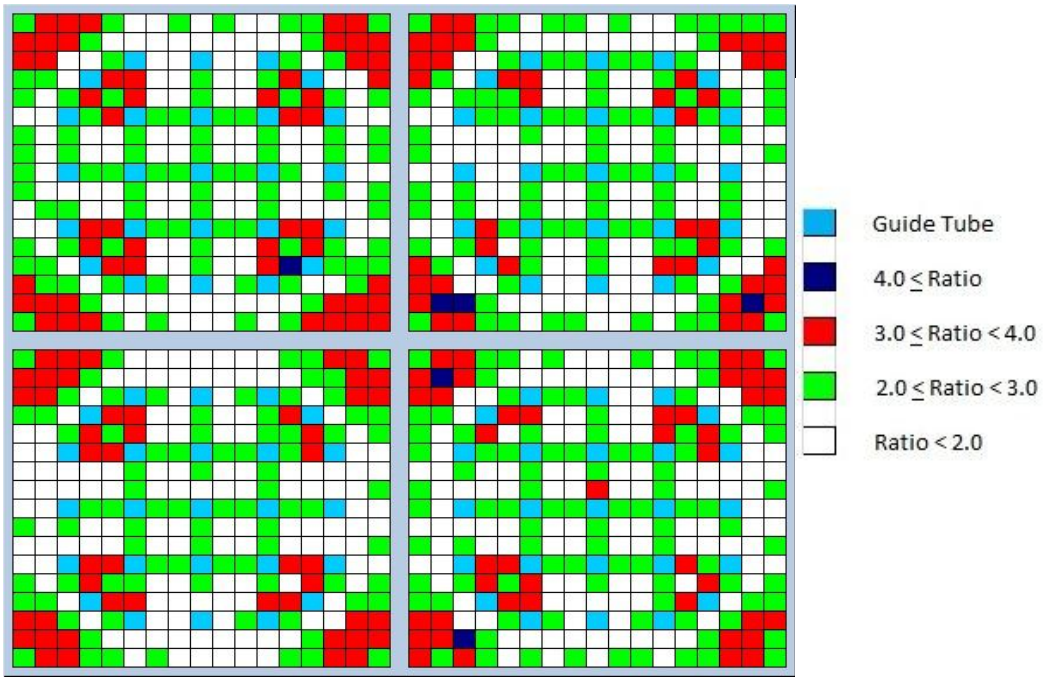

Figure B.1: Uncertainty Ratio: Startup

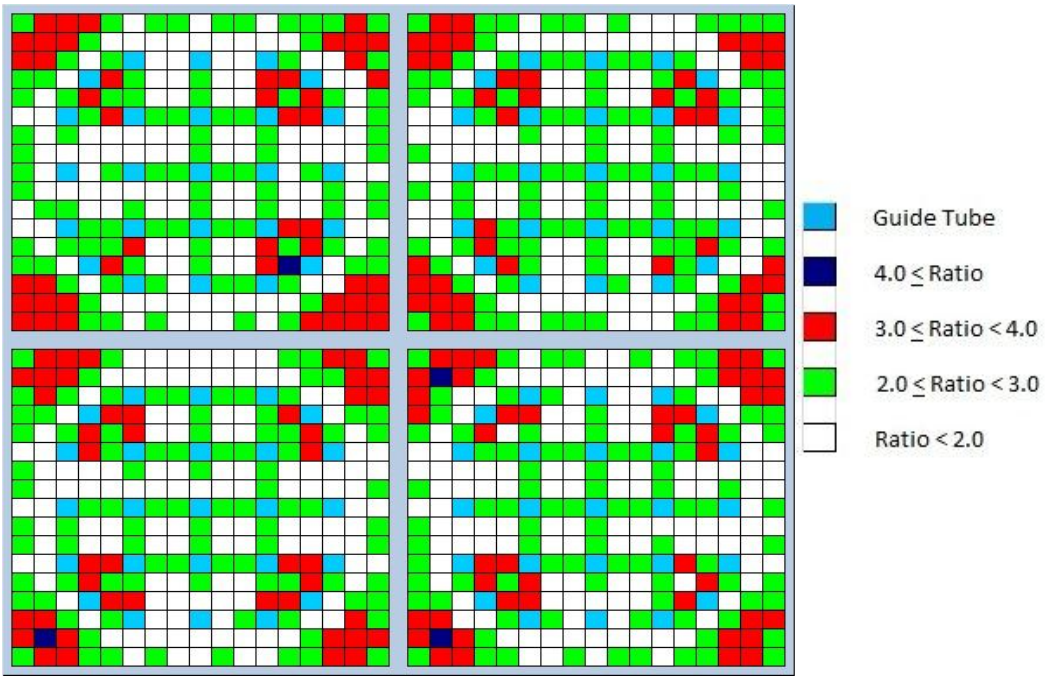

Figure B.2: Uncertainty Ratio 50 Days

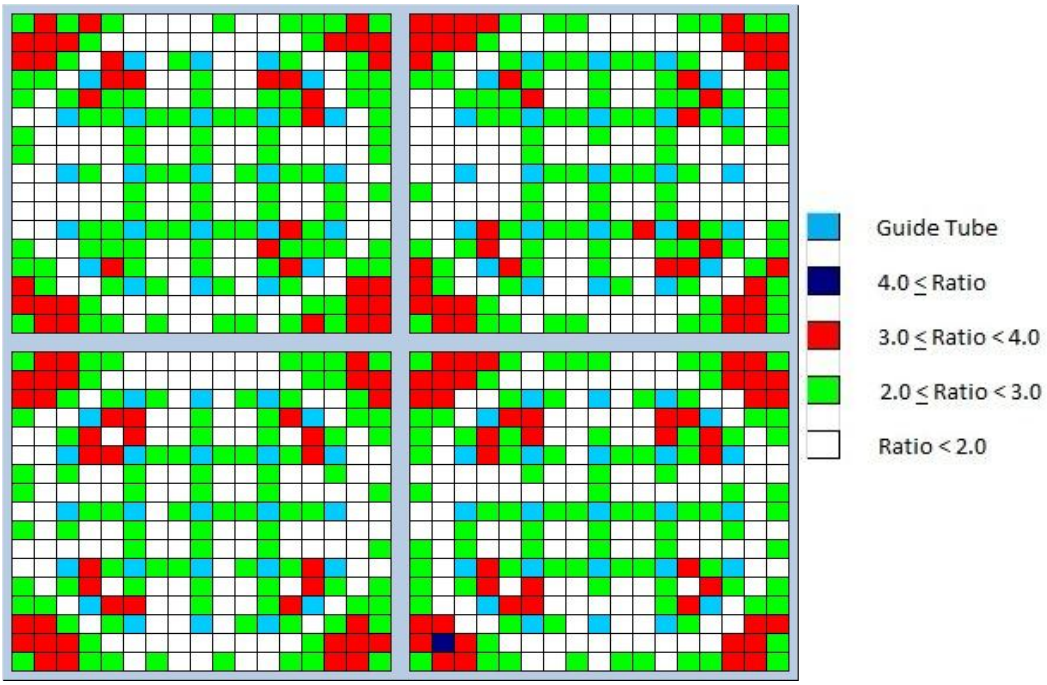

Figure B.3: Uncertainty Ratio 100 Days

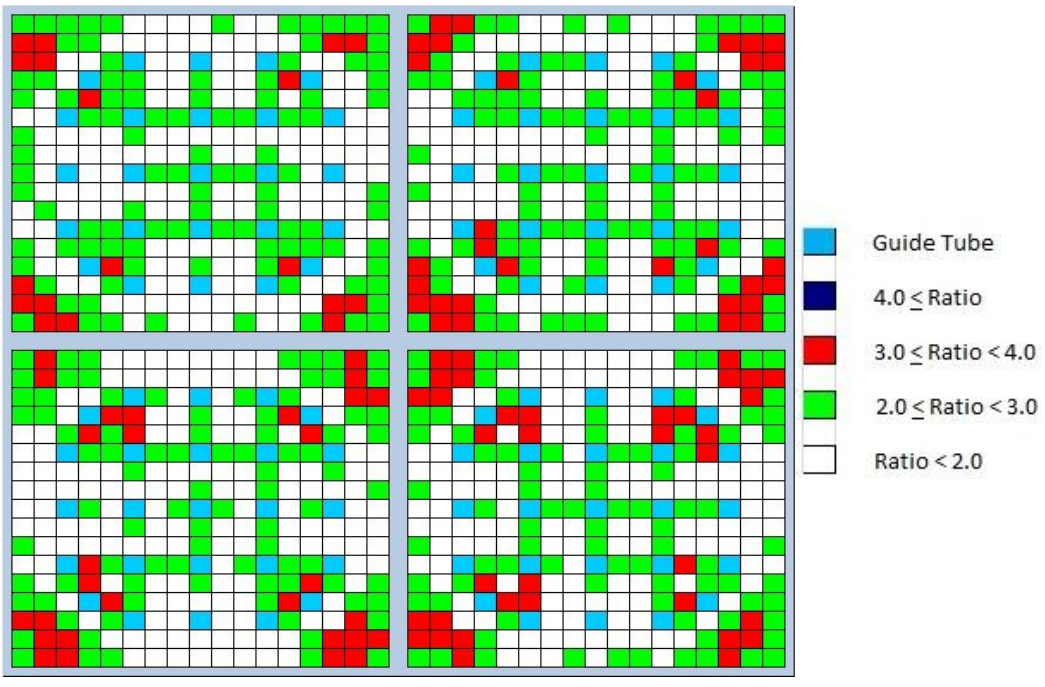

Figure B.4: Uncertainty Ratio 200 Days

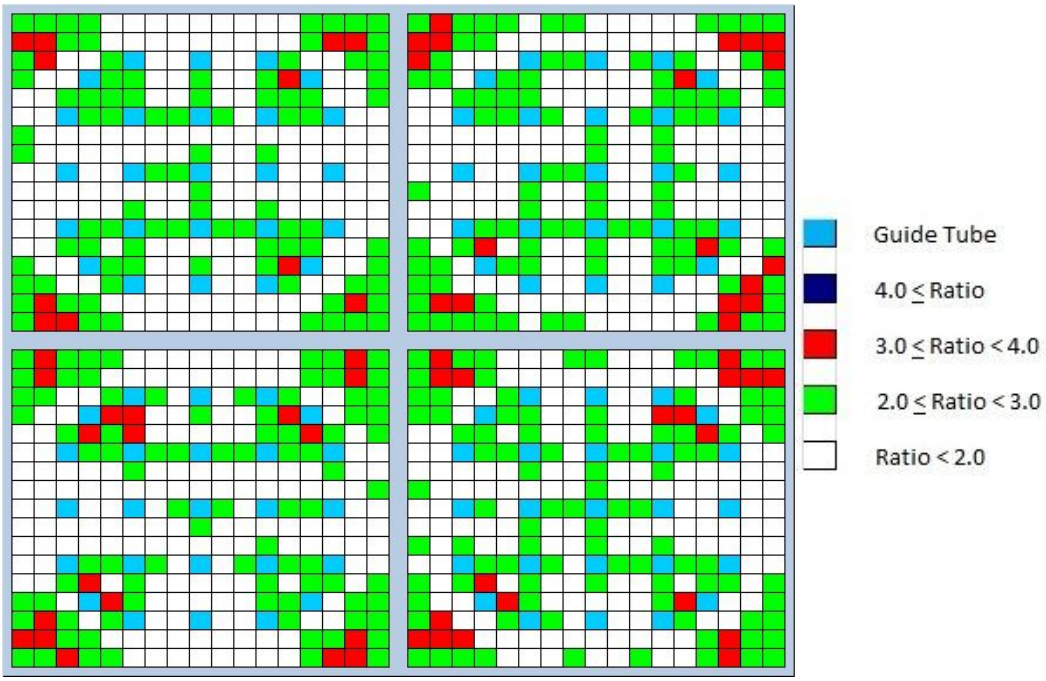

Figure B.5: Uncertainty Ratio 300 Days

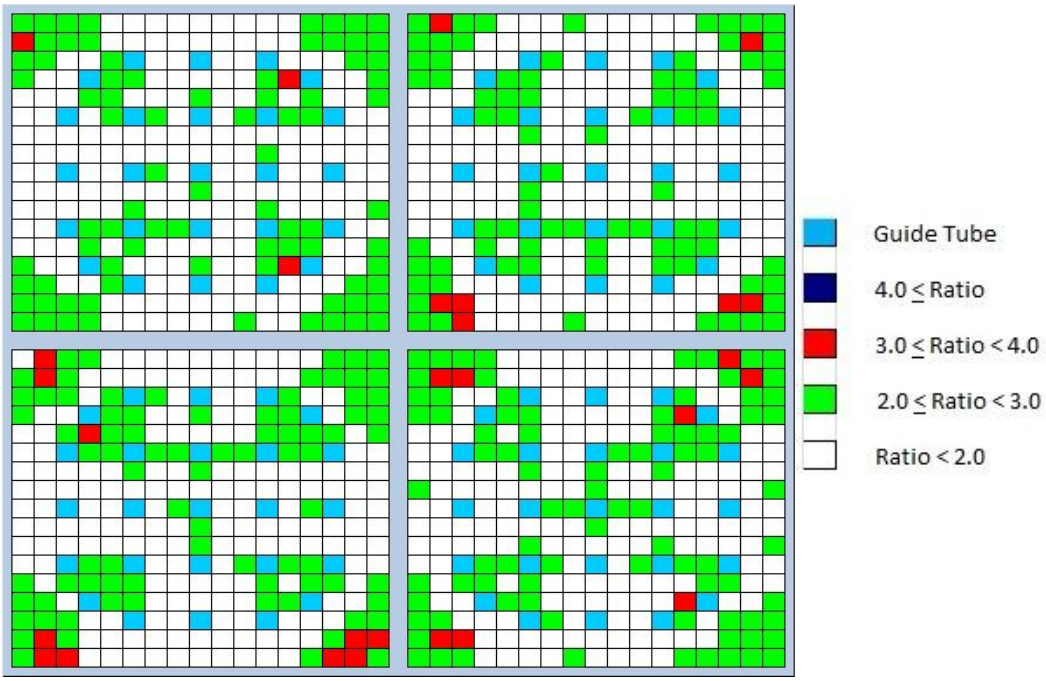

Figure B.6: Uncertainty Ratio 400 Days

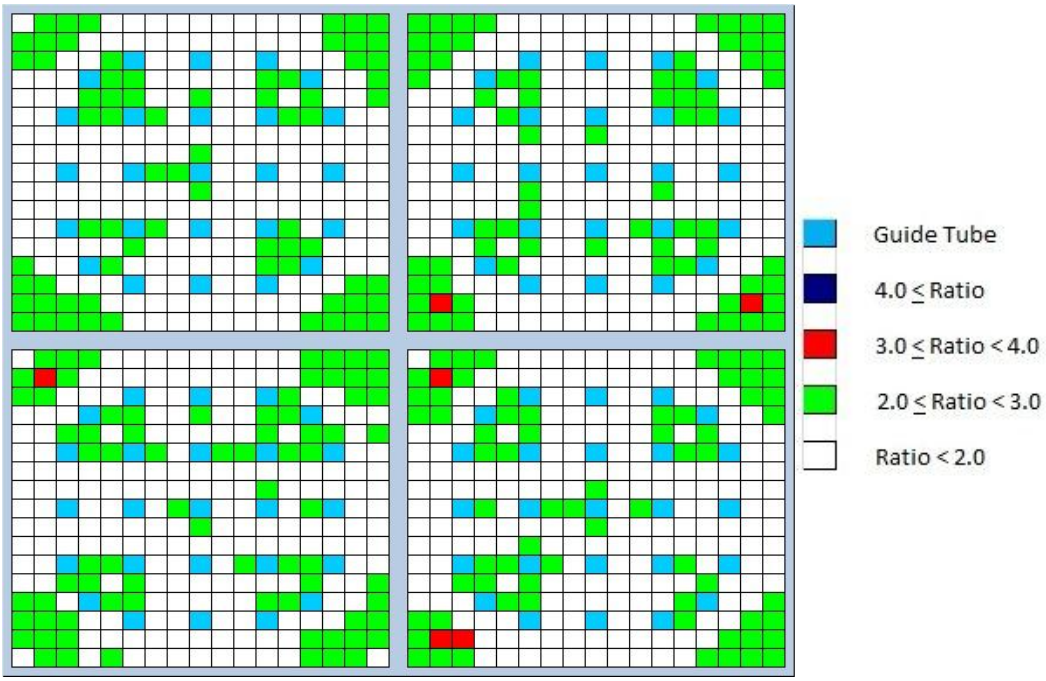

Figure B.7: Uncertainty Ratio 500 Days

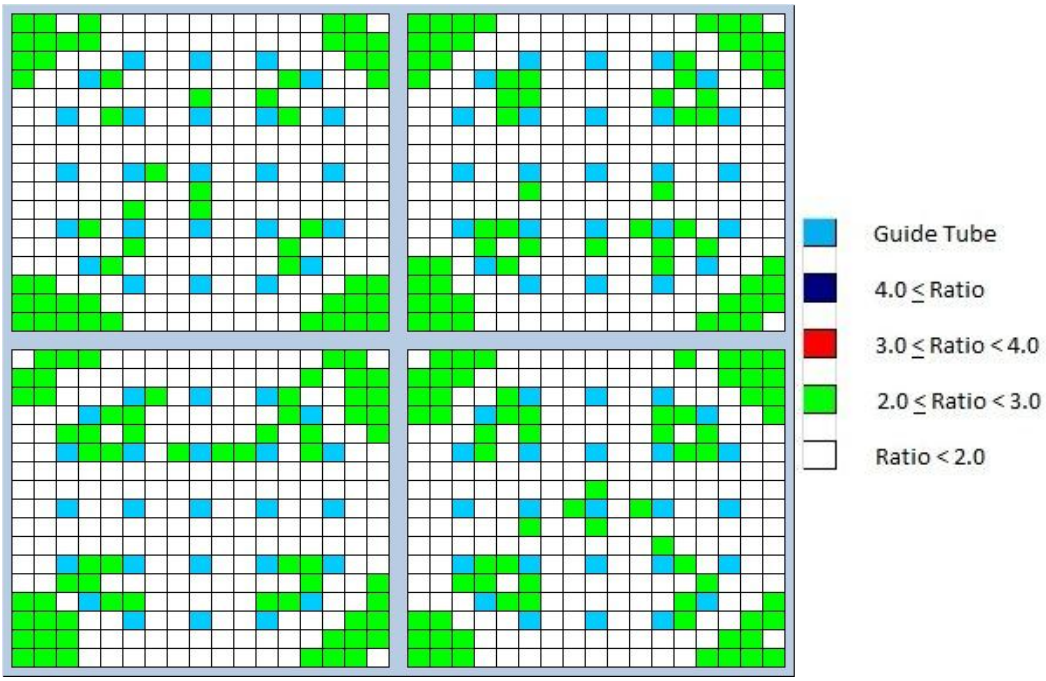

Figure B.8: Uncertainty Ratio 600 Days

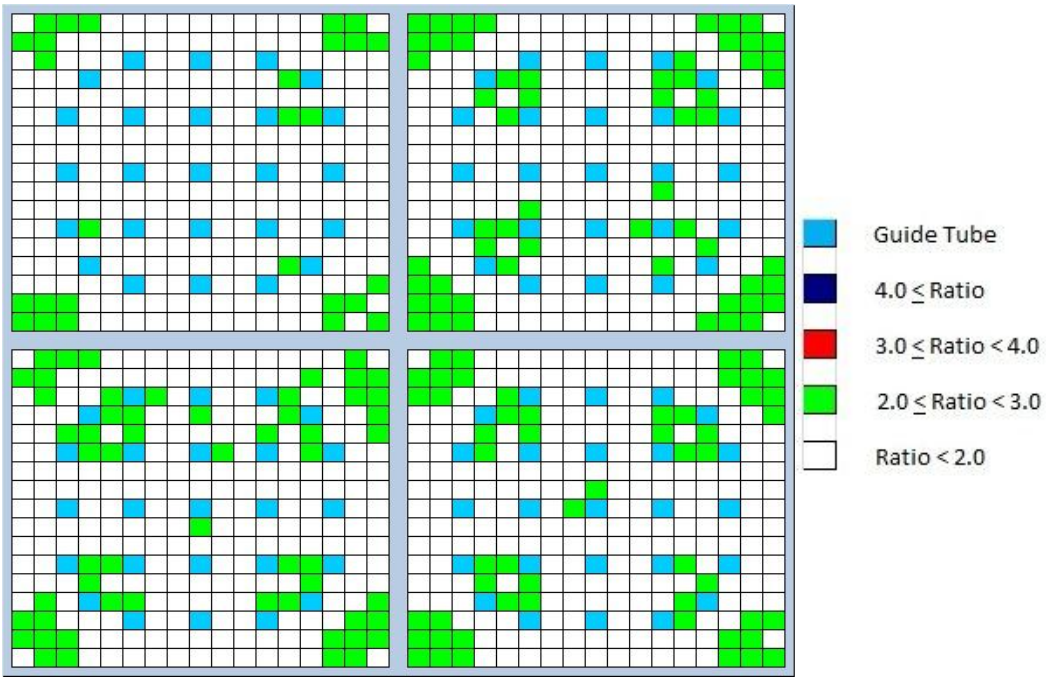

Figure B.9: Uncertainty Ratio 700 Days

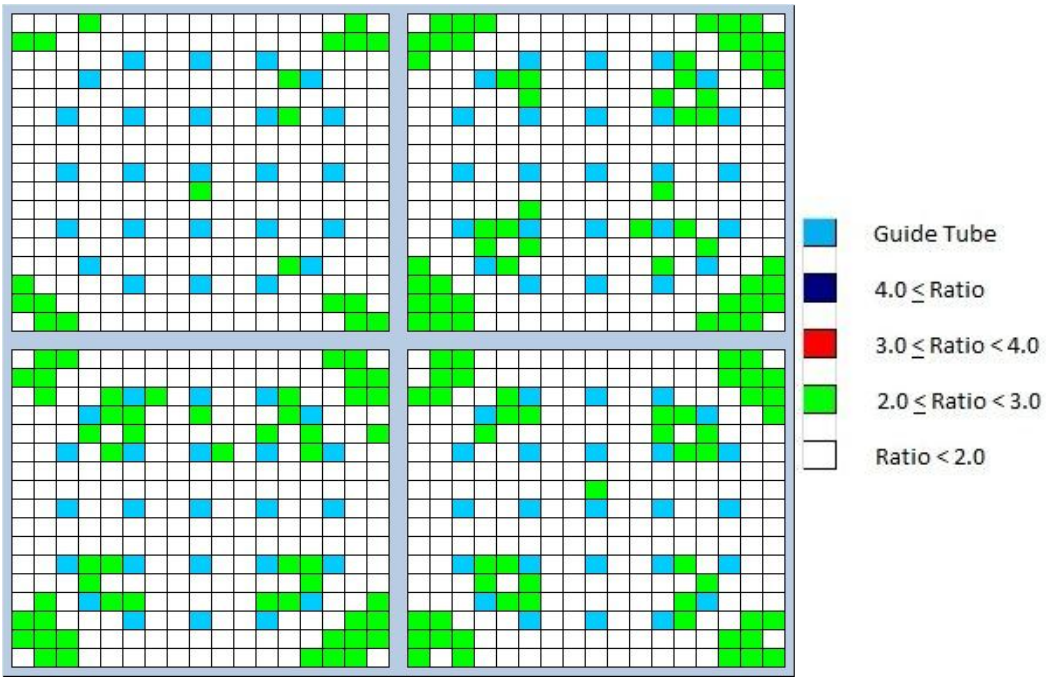

Figure B.10: Uncertainty Ratio 800 Days

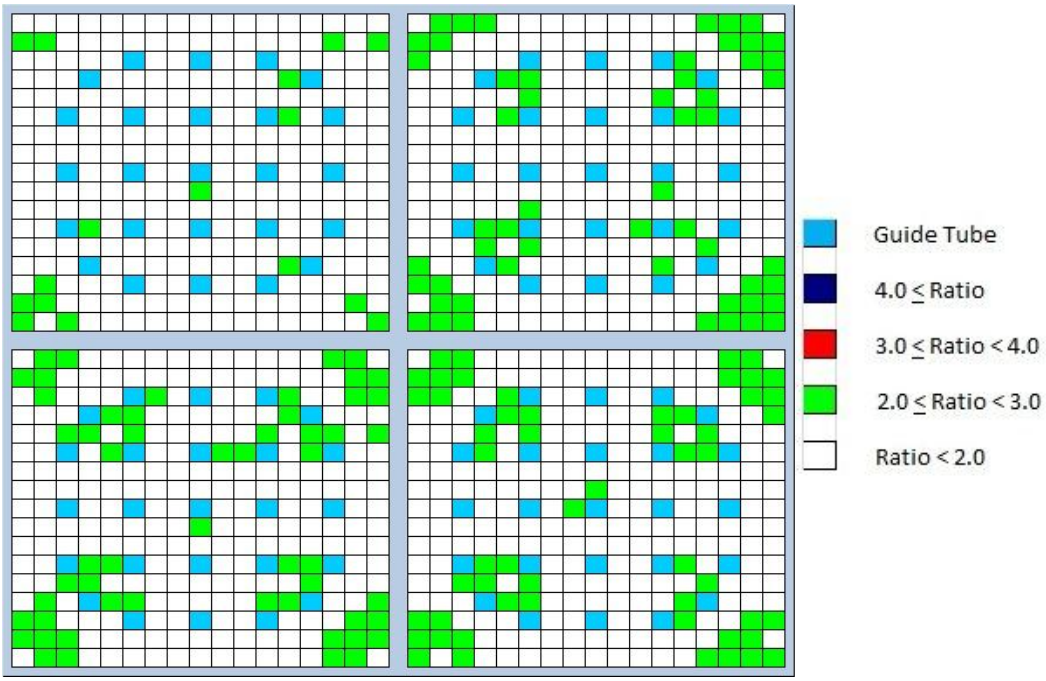

Figure B.11: Uncertainty Ratio 900 Days

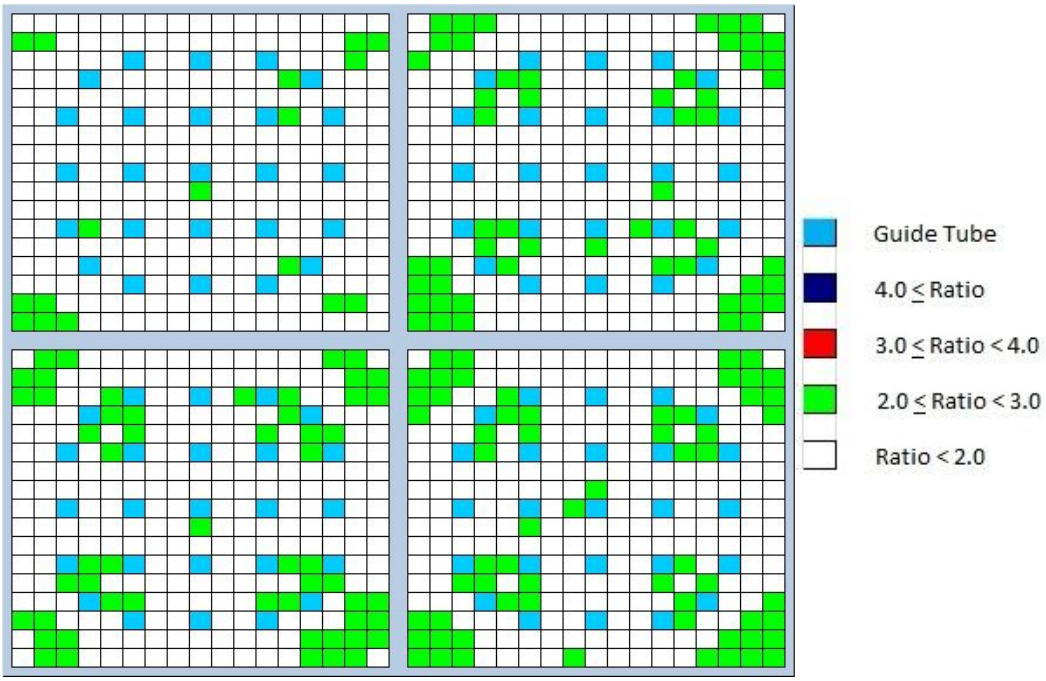

Figure B.12: Uncertainty Ratio 1000 Days

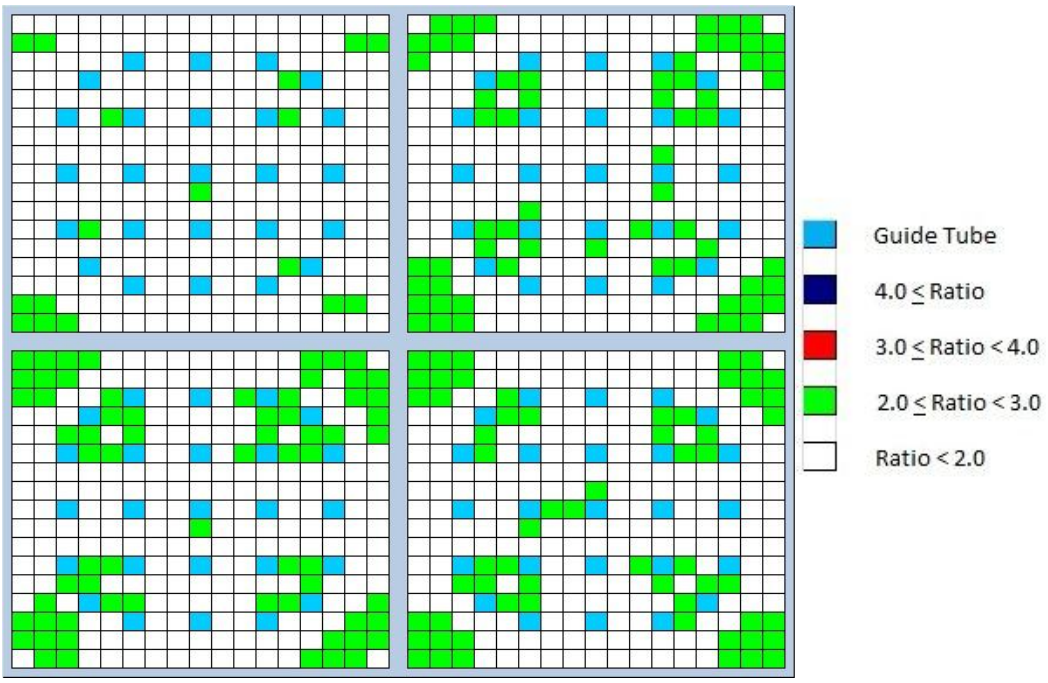

Figure B.13: Uncertainty Ratio 1100 Days

APPENDIX C

PIN POWER EDITS FOR TEST PROBLEM TWO

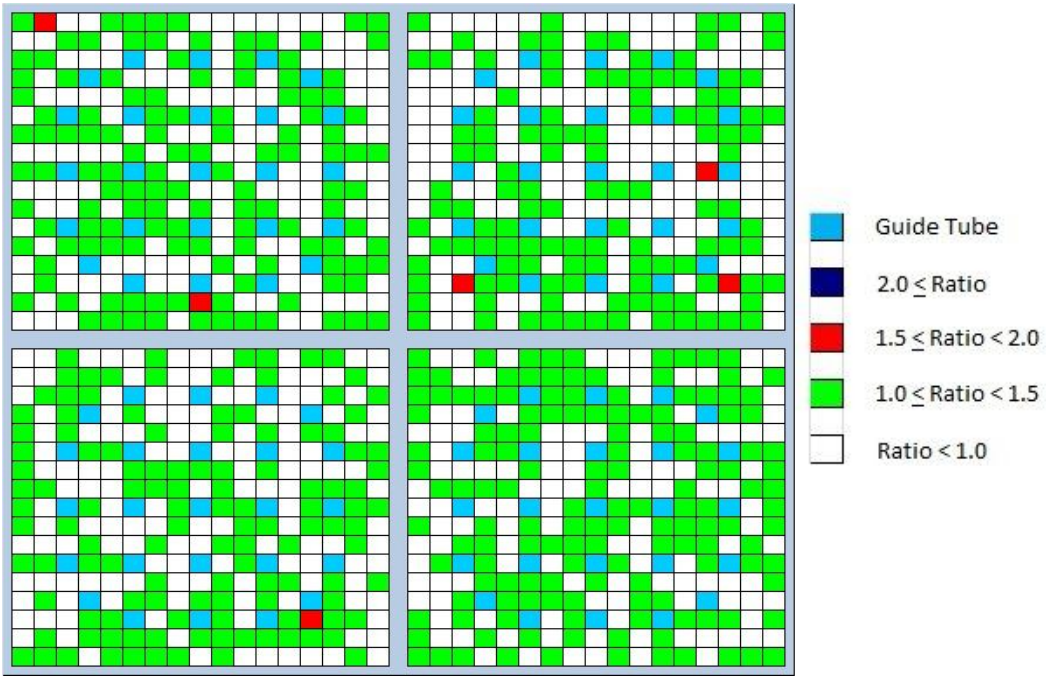

Figure C.1: Uncertainty Ratio Startup

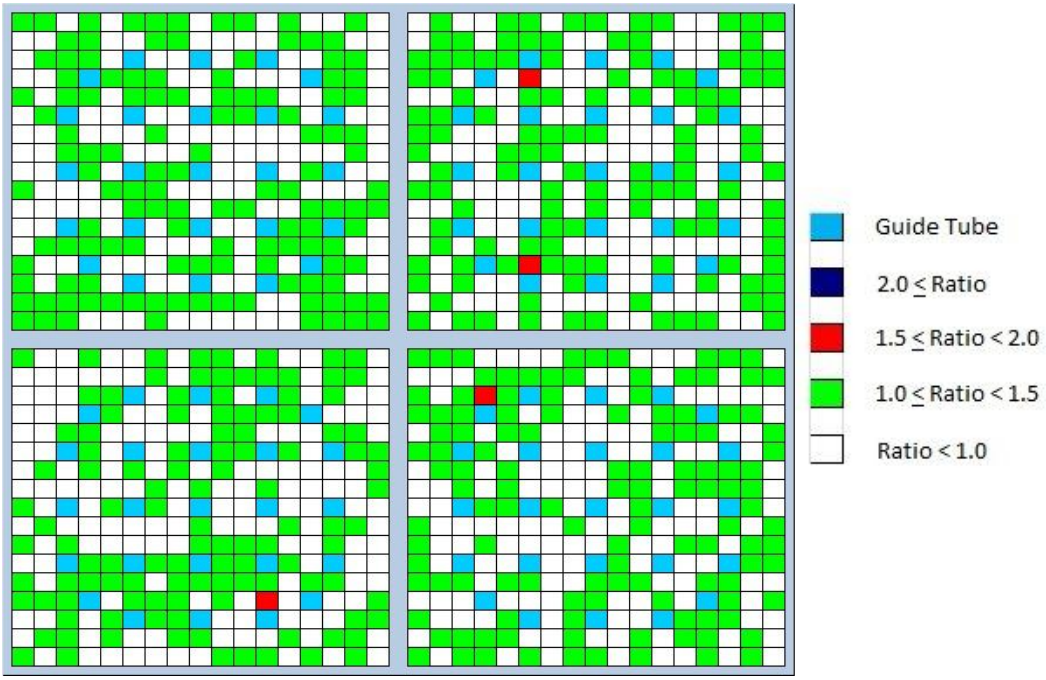

Figure C.2: Uncertainty Ratio 50 Days

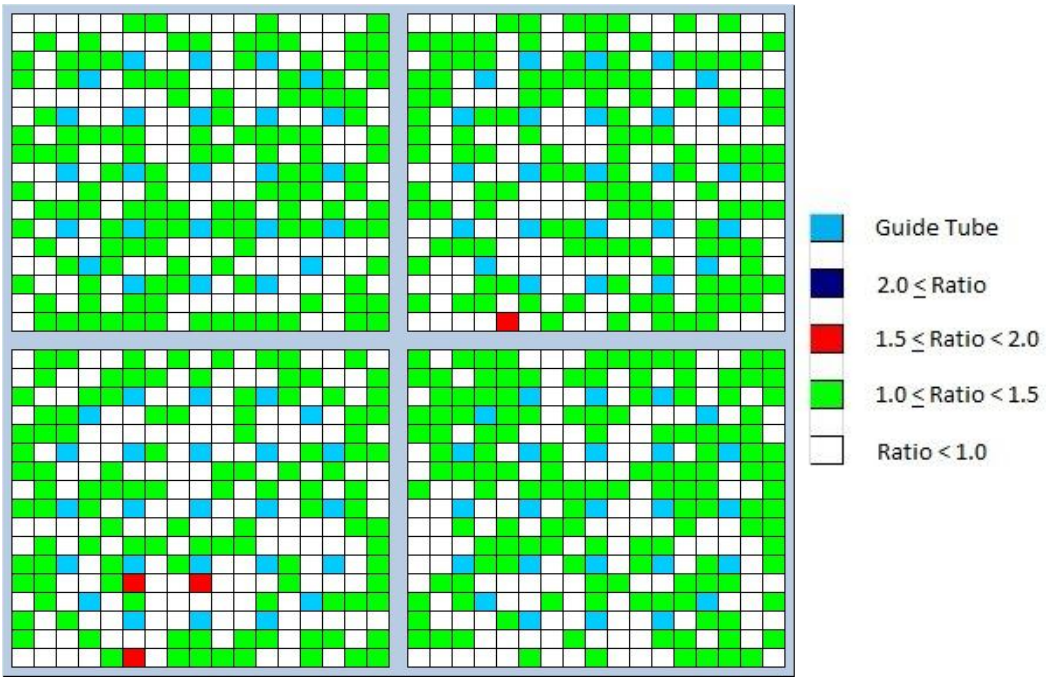

Figure C.3: Uncertainty Ratio 100 Days

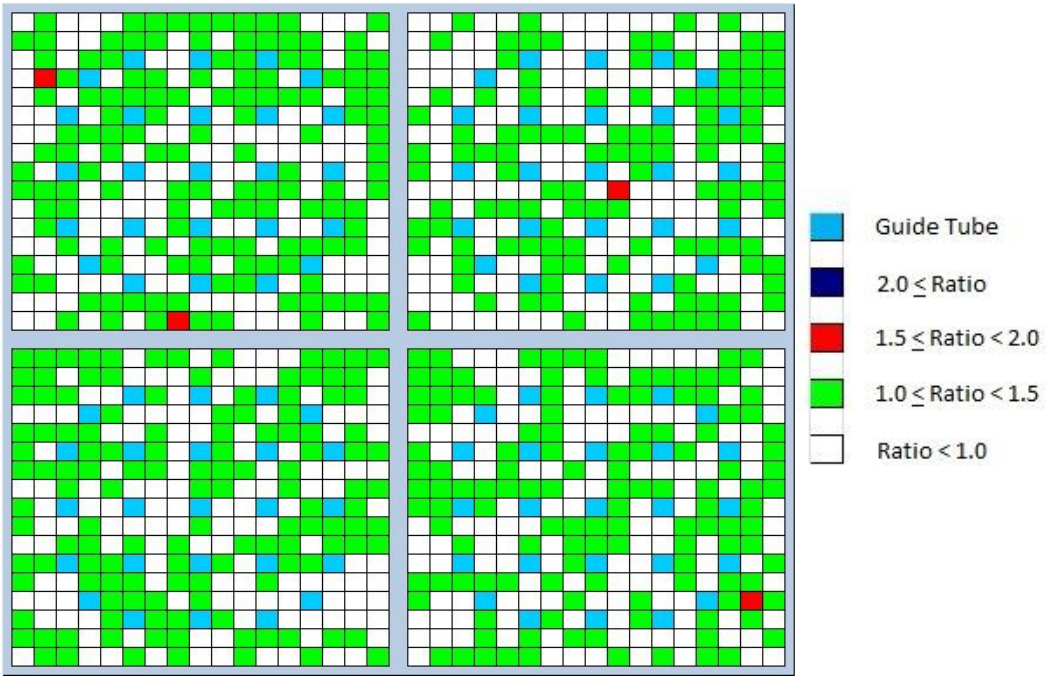

Figure C.4: Uncertainty Ratio 200 Days

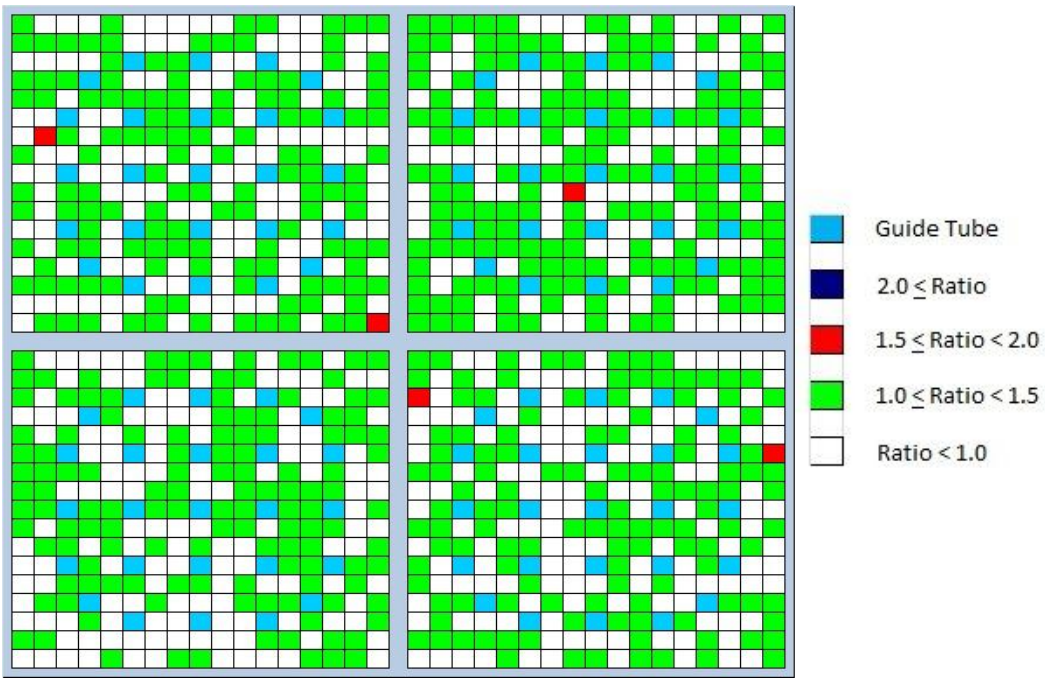

Figure C.5: Uncertainty Ratio 300 Days

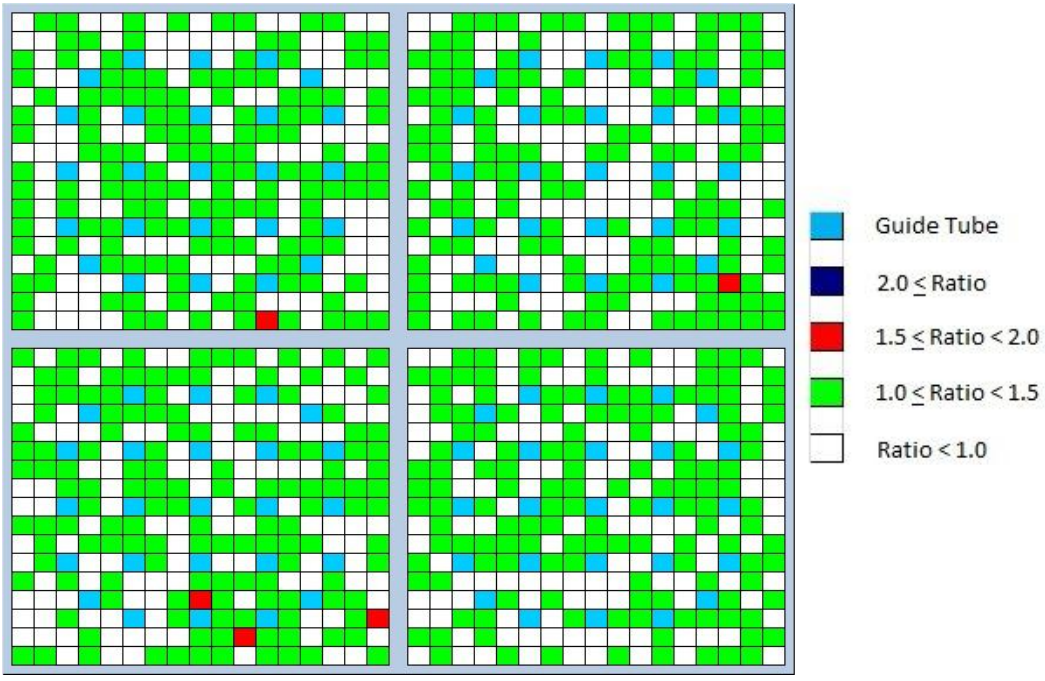

Figure C.6: Uncertainty Ratio 400 Days

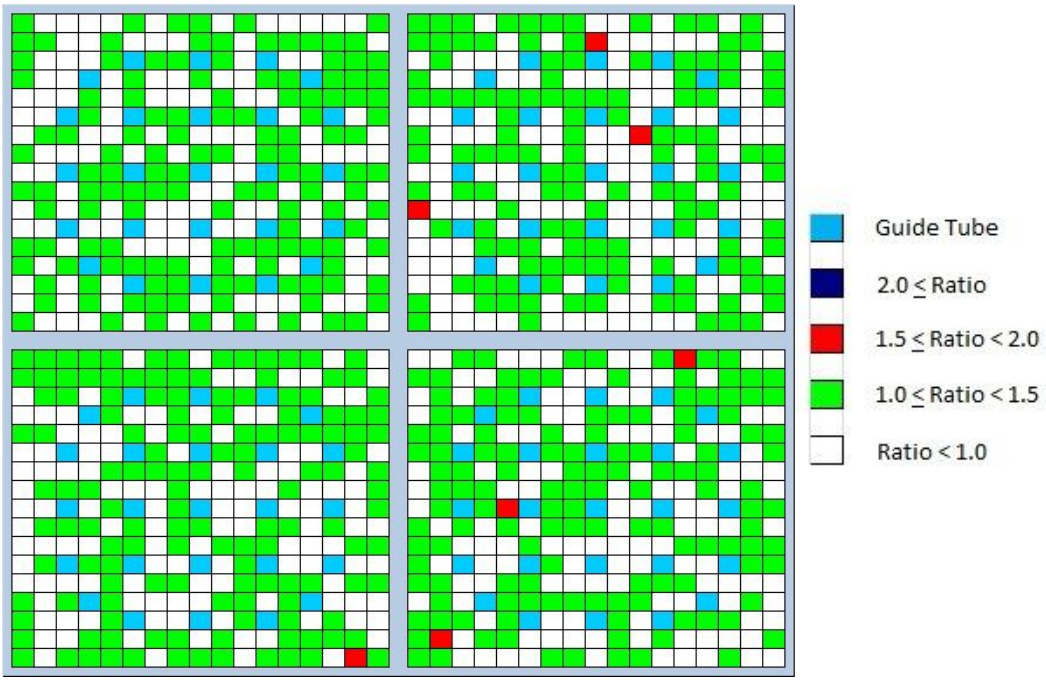

Figure C.7: Uncertainty Ratio 500 Days

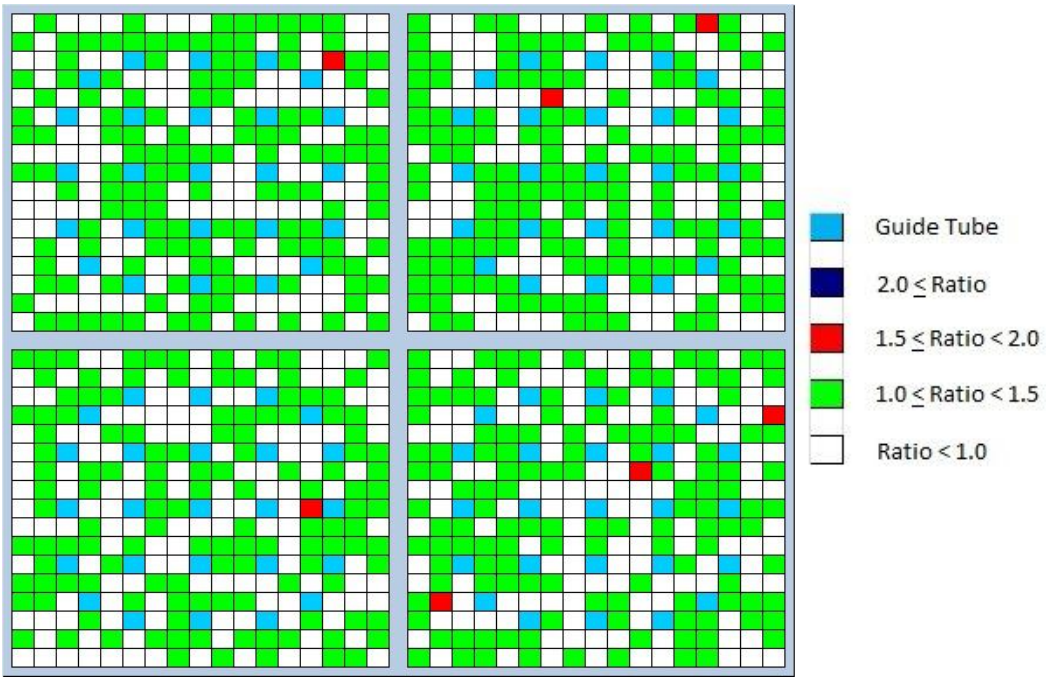

Figure C.8: Uncertainty Ratio 600 Days

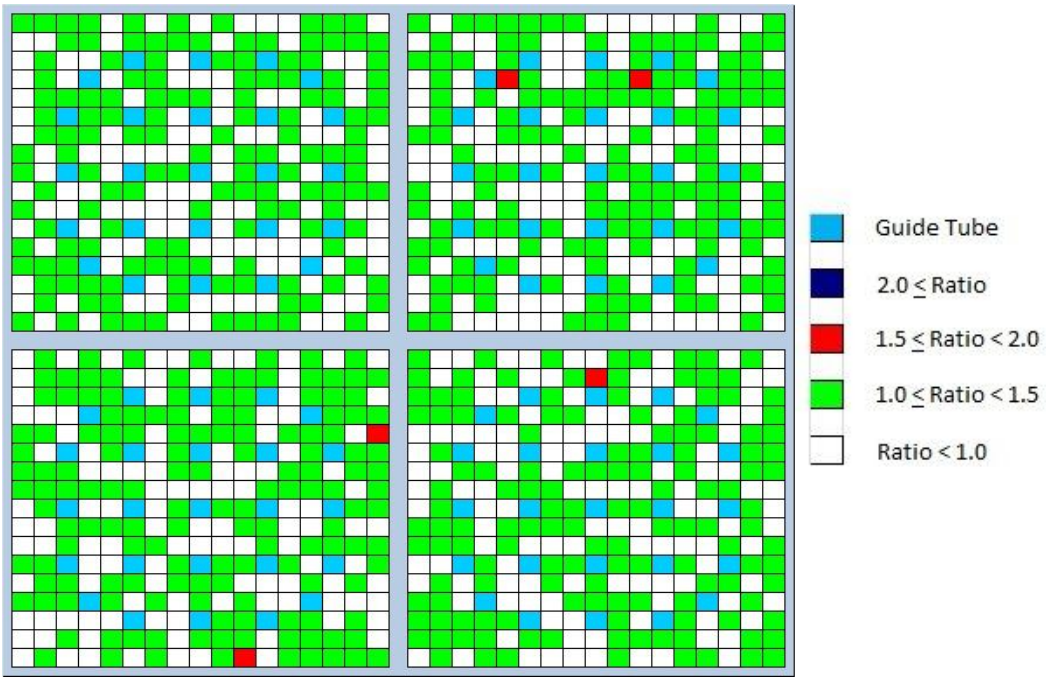

Figure C.9: Uncertainty Ratio 700 Days

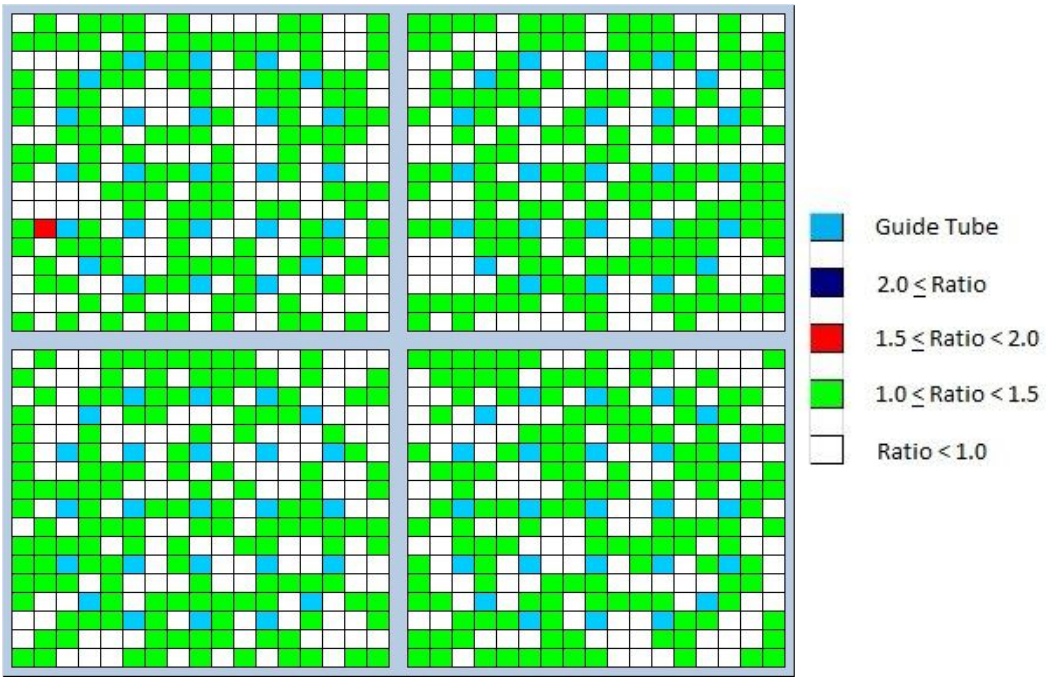

Figure C.10: Uncertainty Ratio 800 Days

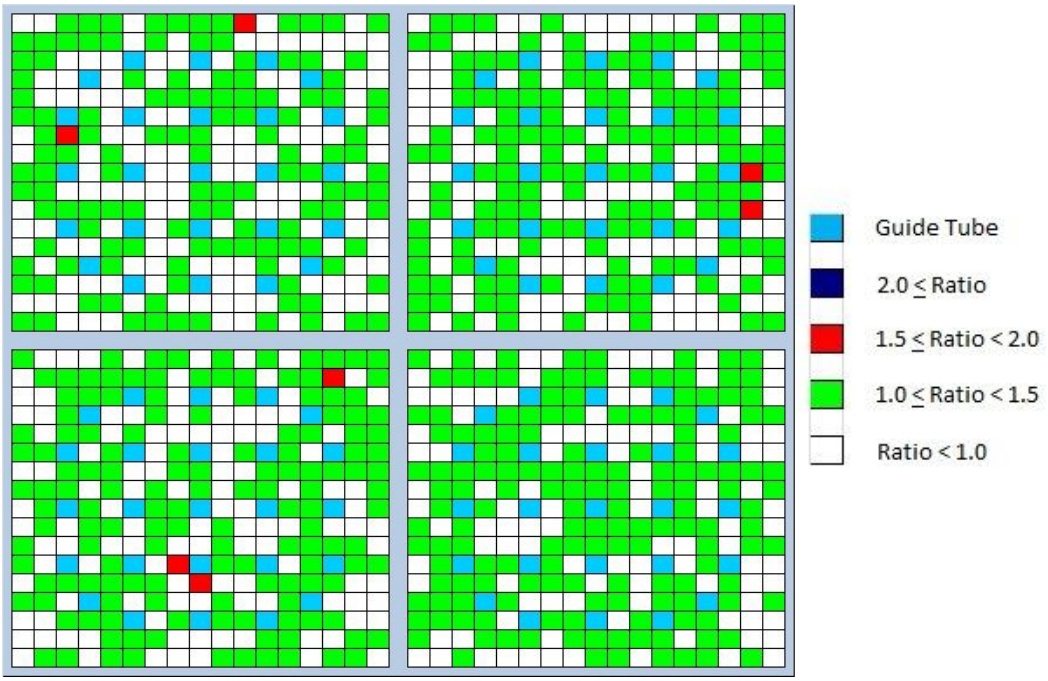

Figure C.11: Uncertainty Ratio 900 Days

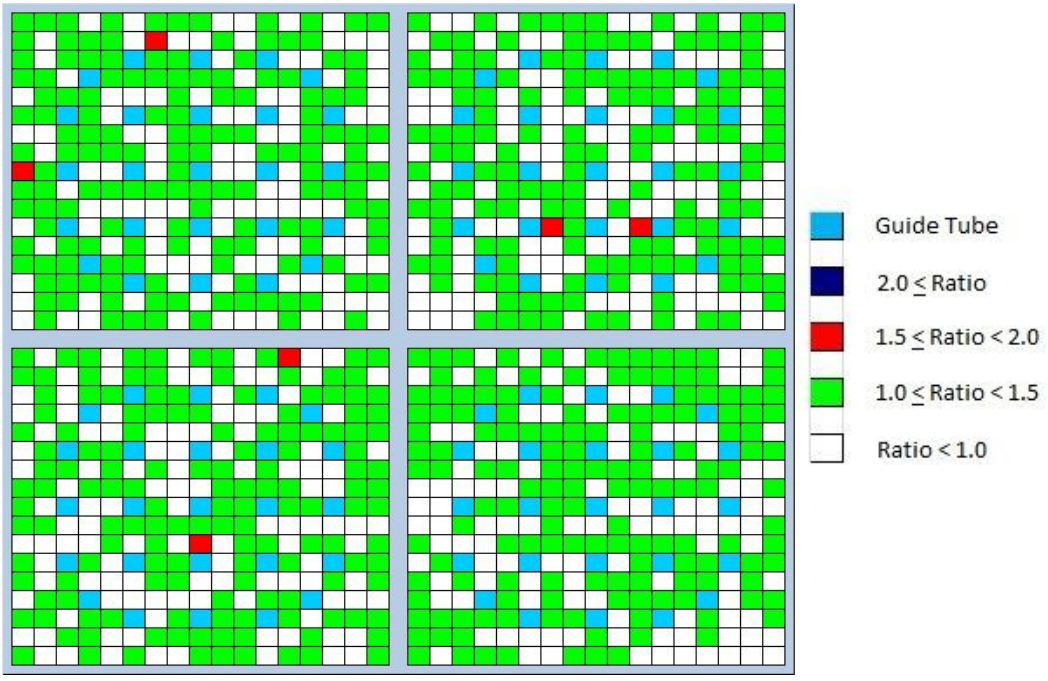

Figure C.12: Uncertainty Ratio 1000 Days

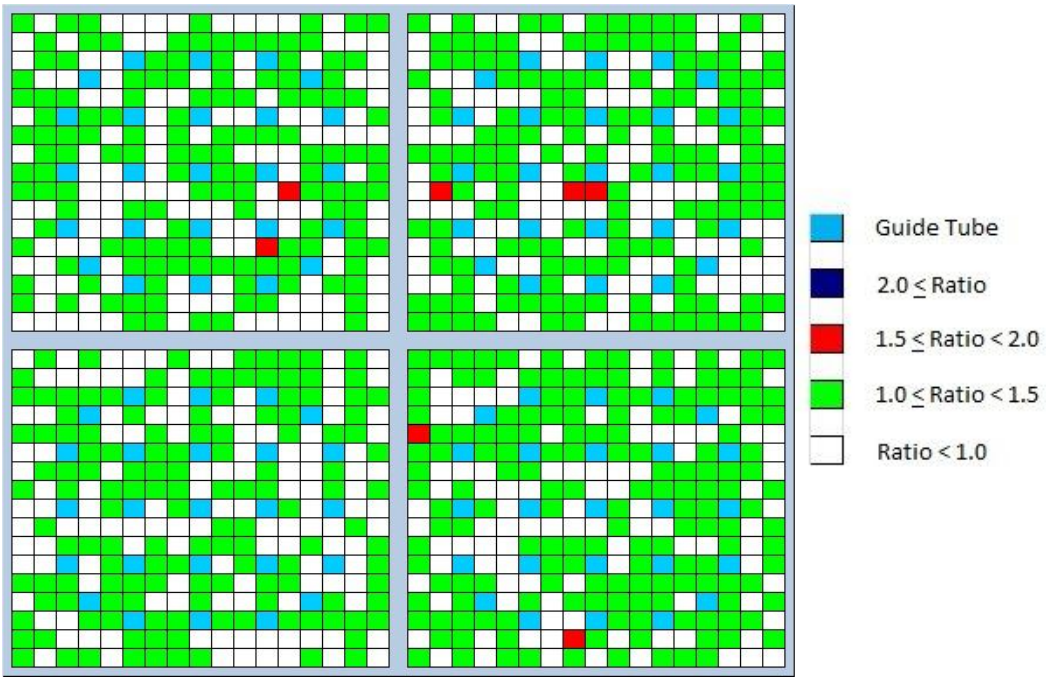

Figure C.13: Uncertainty Ratio 1100 Days

APPENDIX D

PIN POWER EDITS FOR TEST PROBLEM THREE

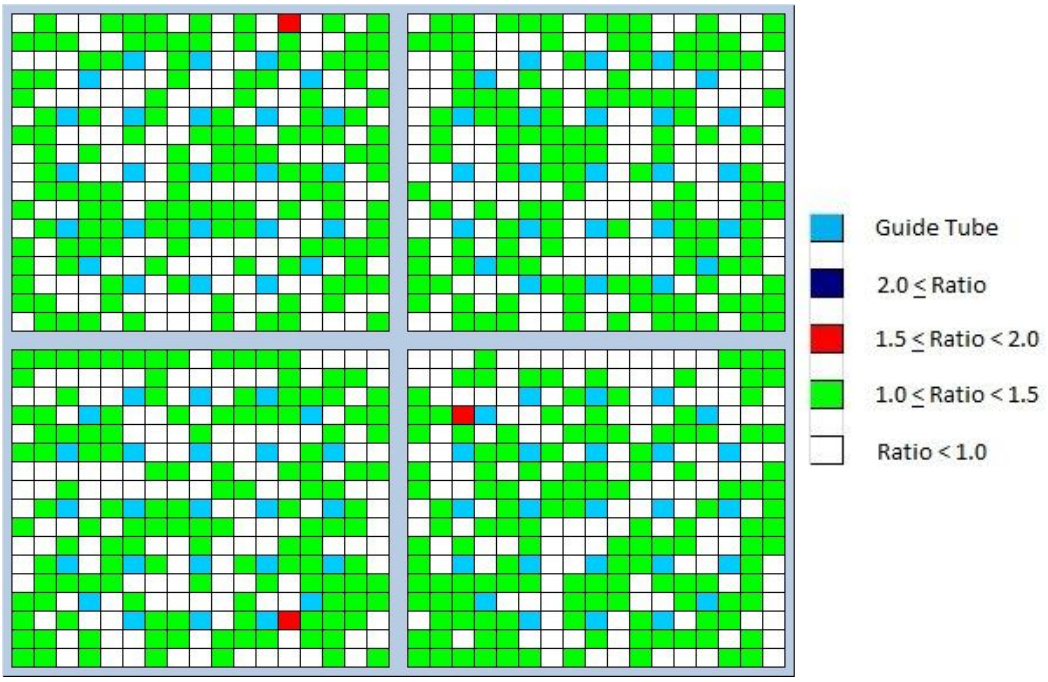

Figure C.1: Uncertainty Ratio Startup

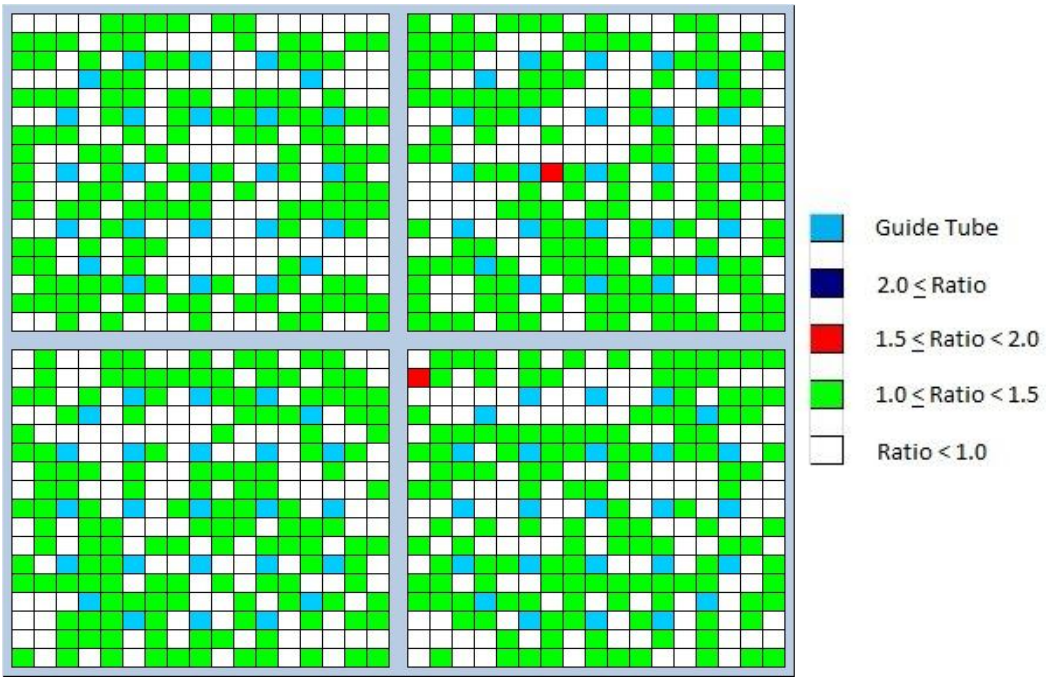

Figure C.2: Uncertainty Ratio 50 Days

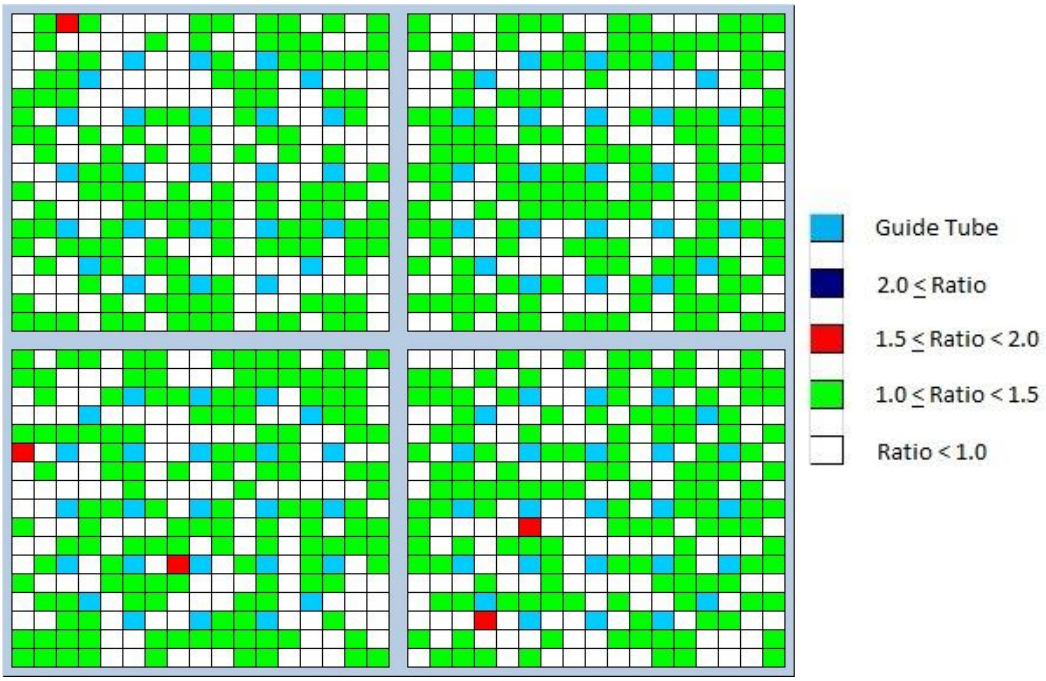

Figure D.3: Uncertainty Ratio 100 Days

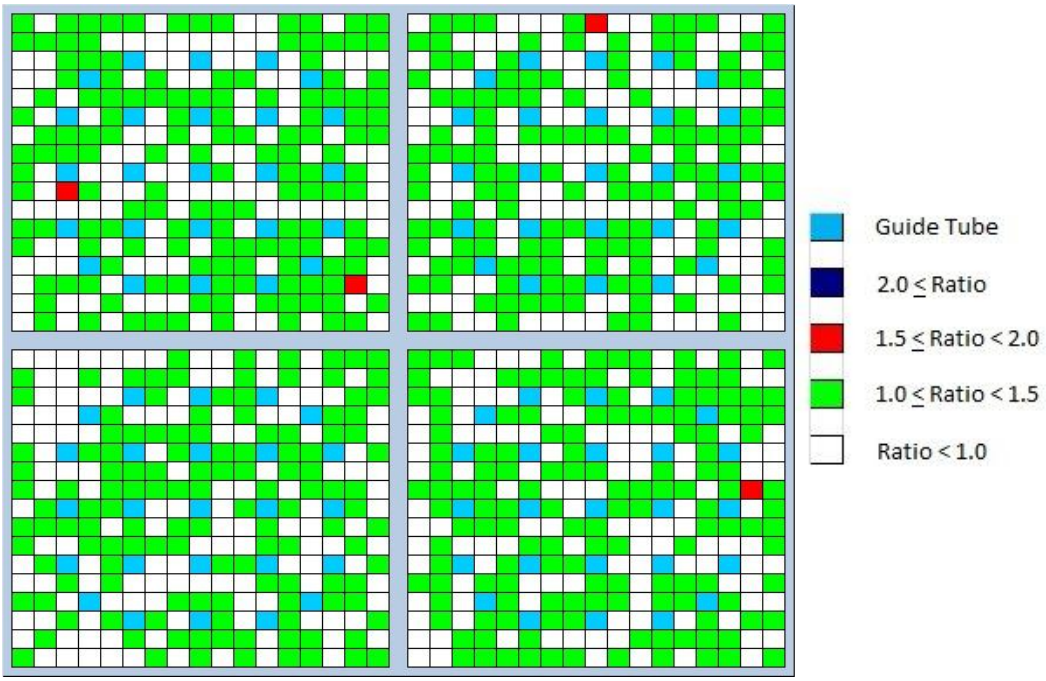

Figure D.4: Uncertainty Ratio 200 Days

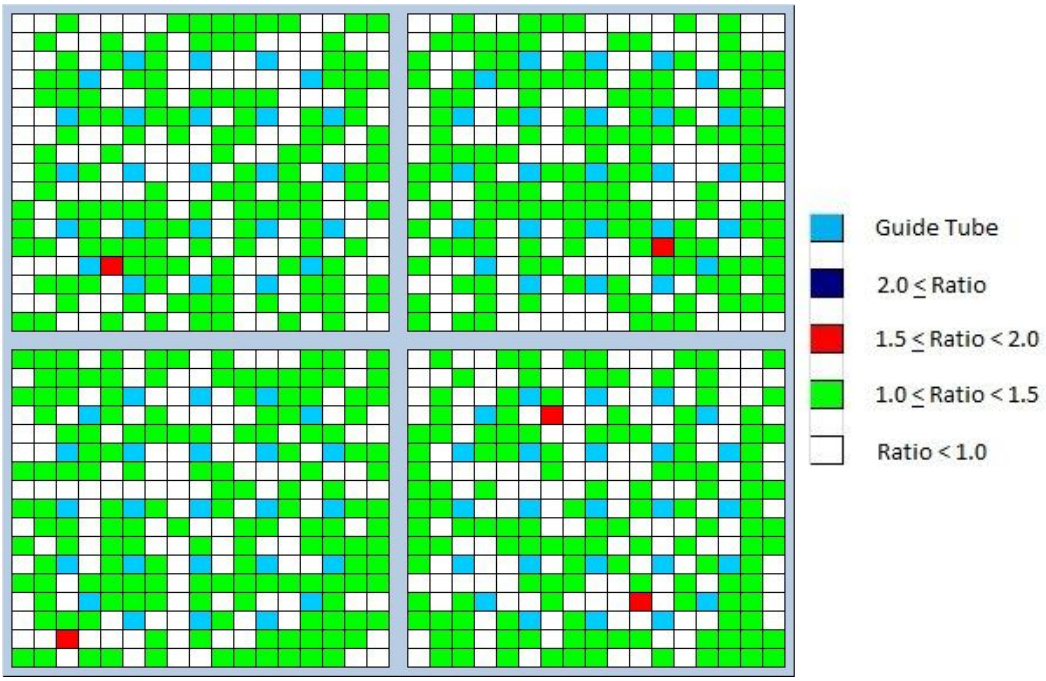

Figure D.5: Uncertainty Ratio 300 Days

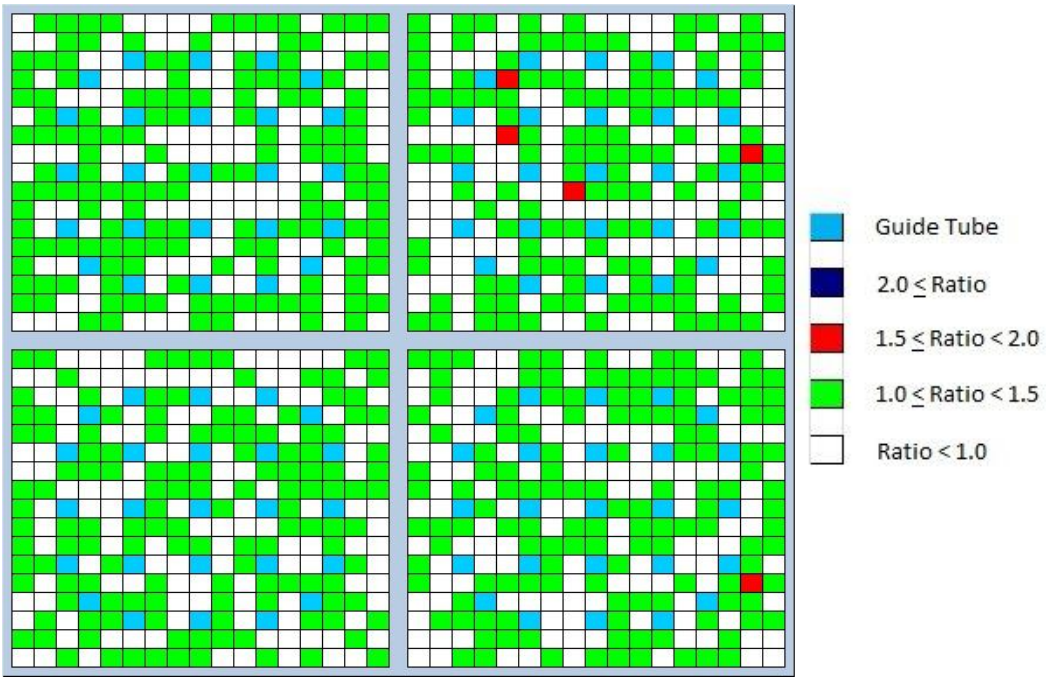

Figure D.6: Uncertainty Ratio 400 Days

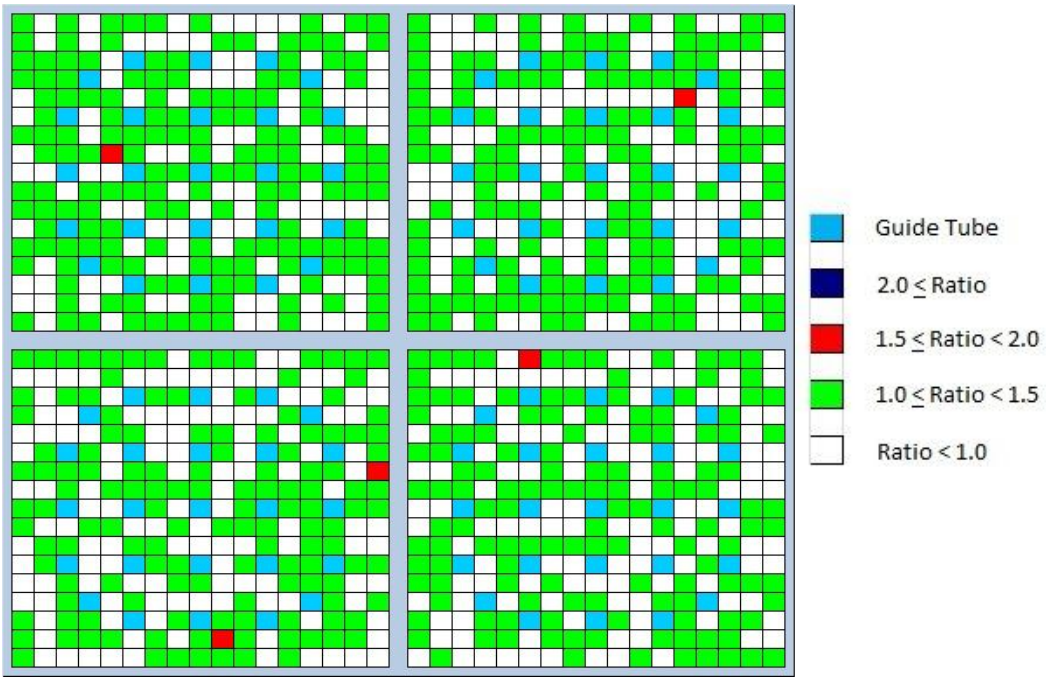

Figure D.7: Uncertainty Ratio 500 Days

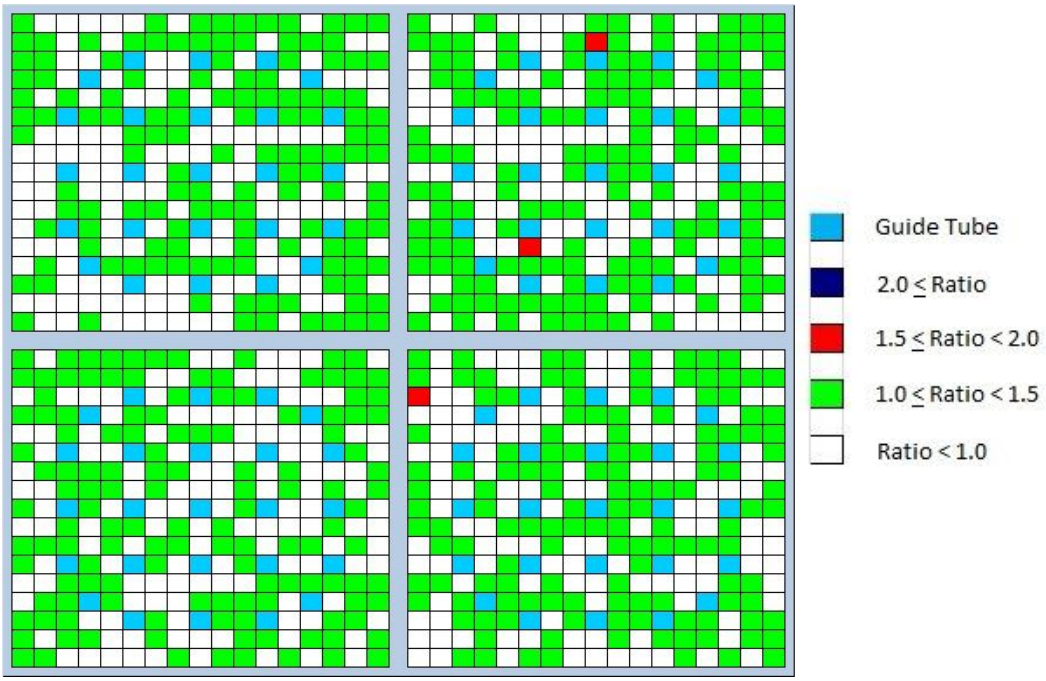

Figure D.8: Uncertainty Ratio 600 Days

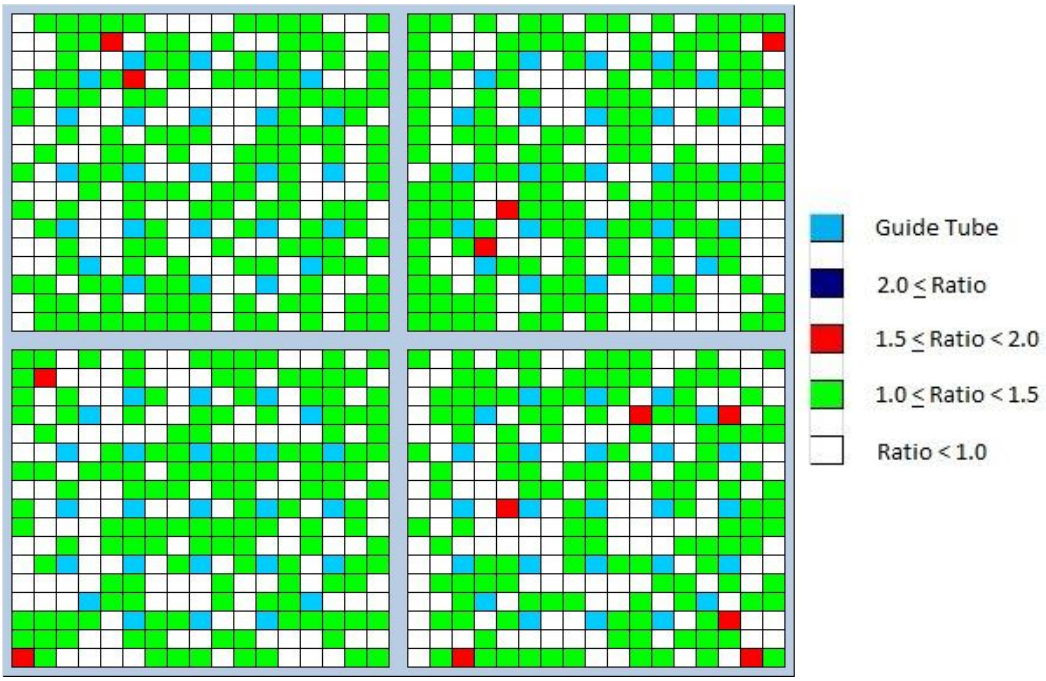

Figure D.9: Uncertainty Ratio 700 Days

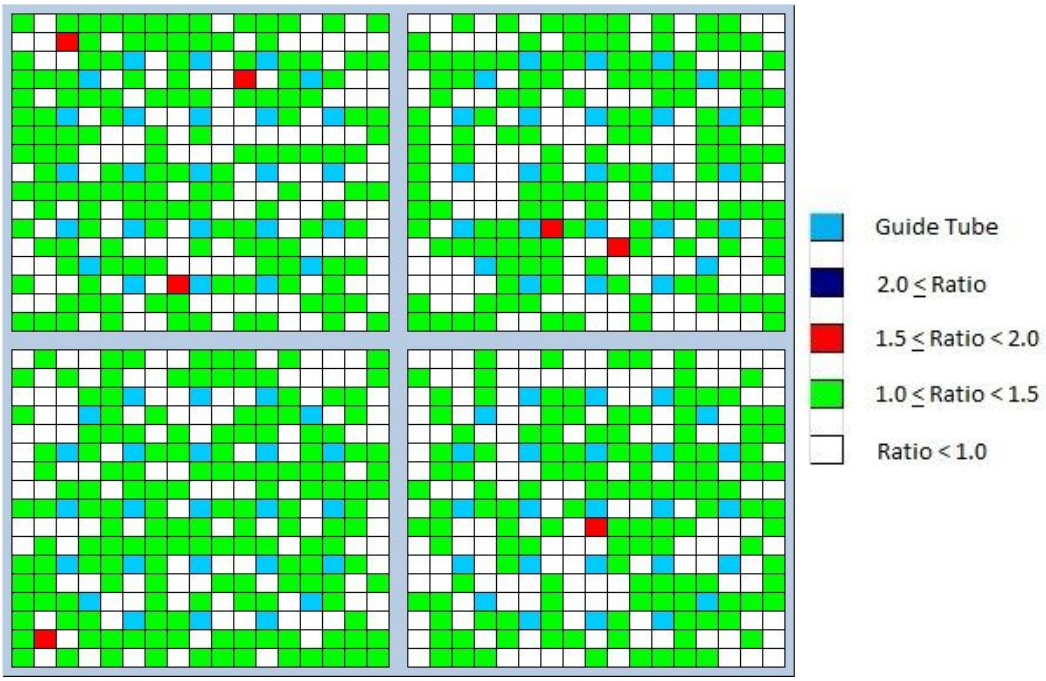

Figure D.10: Uncertainty Ratio 800 Days

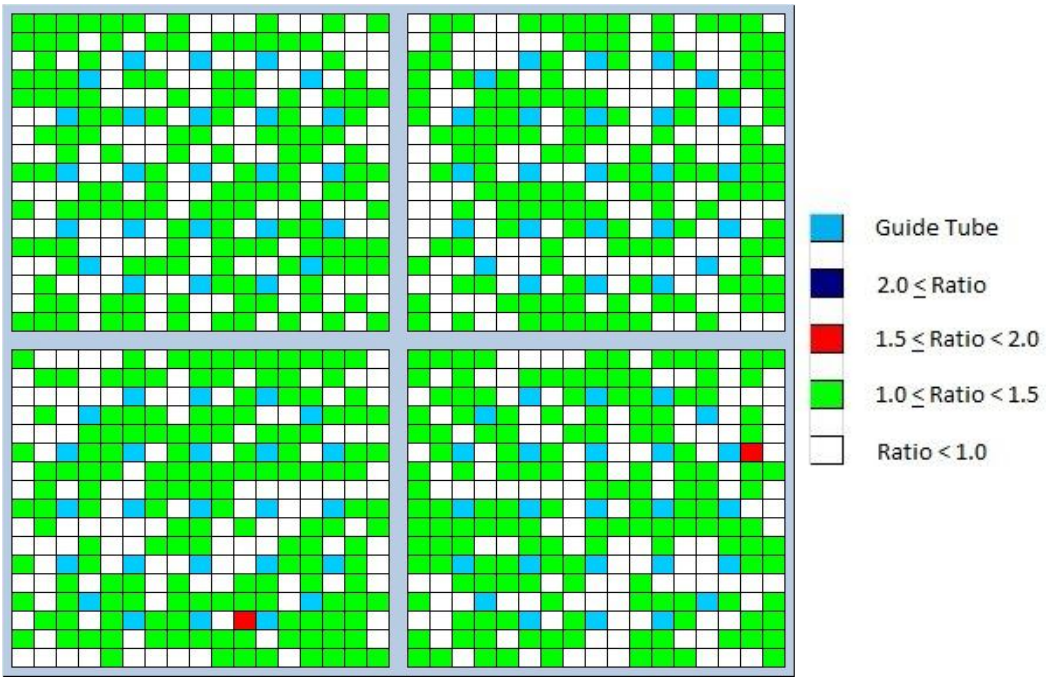

Figure D.11: Uncertainty Ratio 900 Days

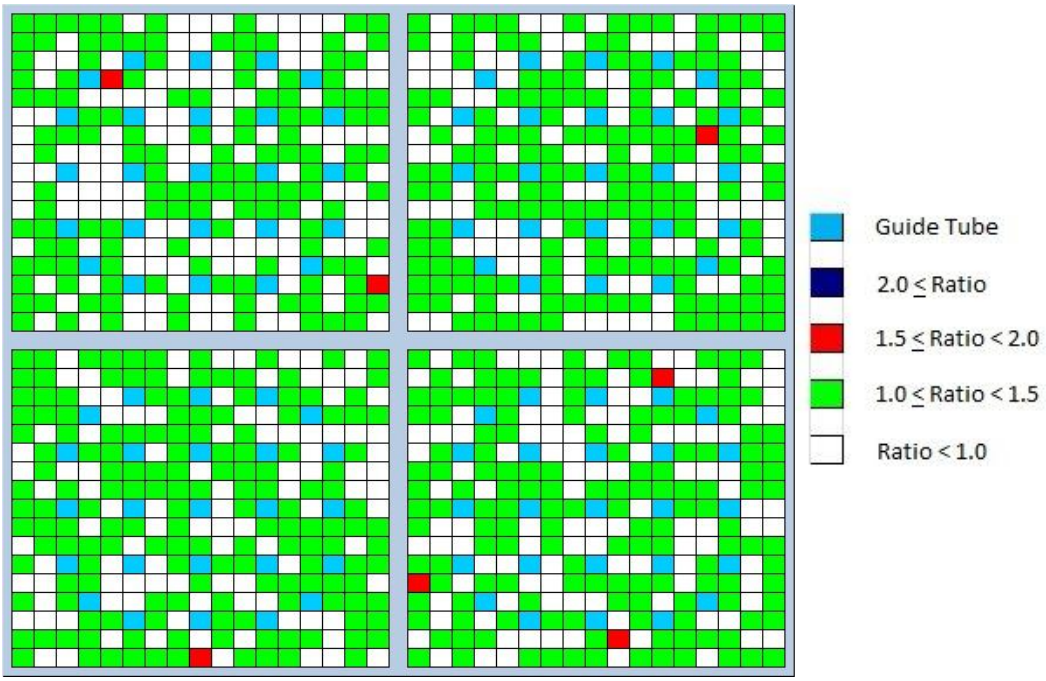

Figure D.12: Uncertainty Ratio 1000 Days

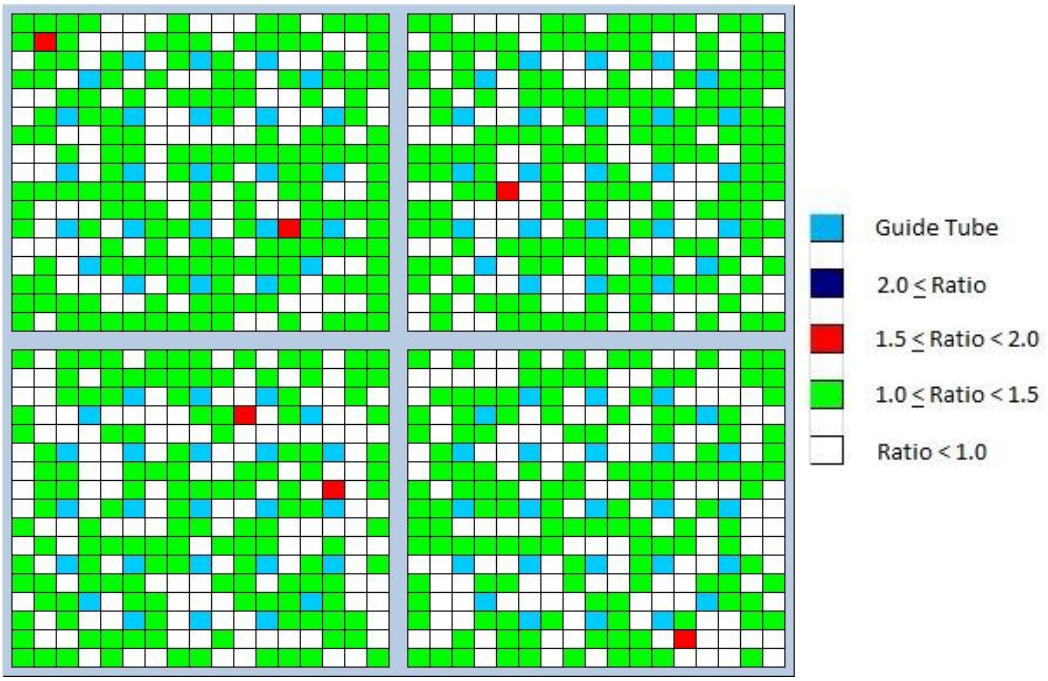

Figure D.13: Uncertainty Ratio 1100 Days

APPENDIX E

PIN POWER EDITS FOR TEST PROBLEM FOUR

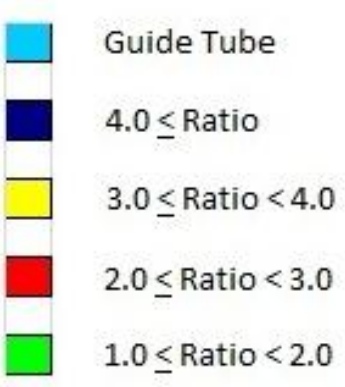

Figure E.1: Uncertainty Ratio Scale

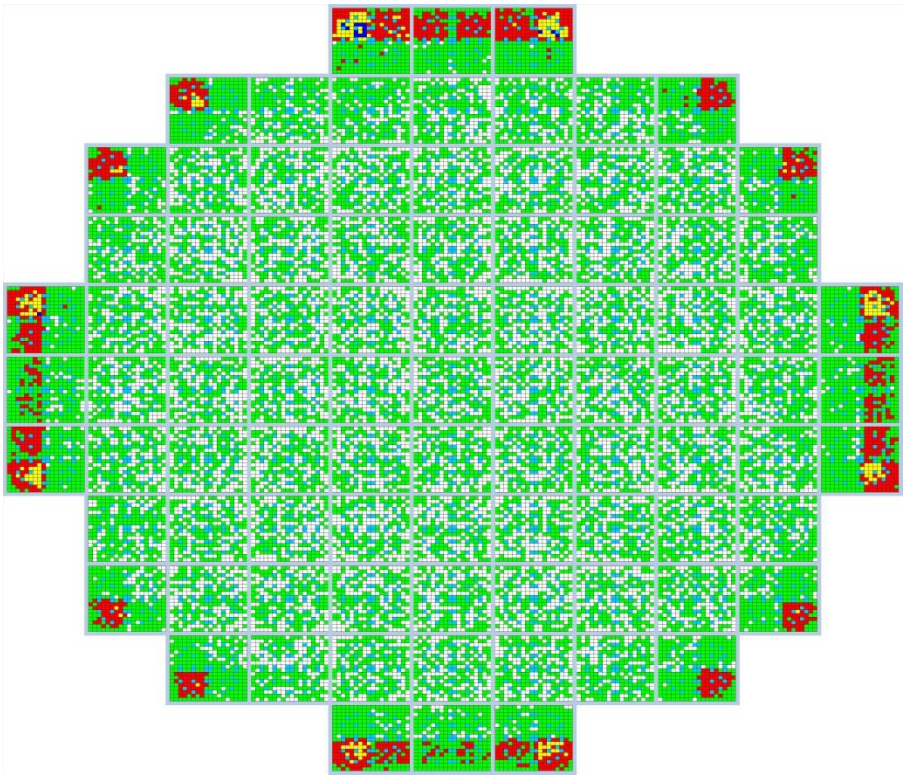

Figure E.2: Uncertainty Ratio startup

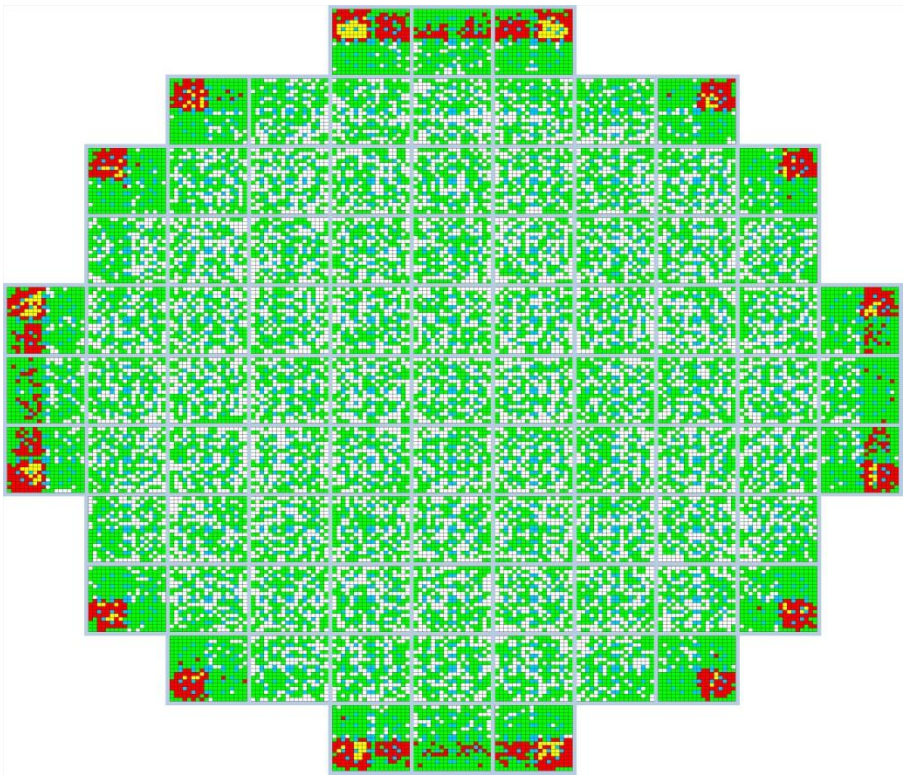

Figure E.3: Uncertainty Ratio 100 Days

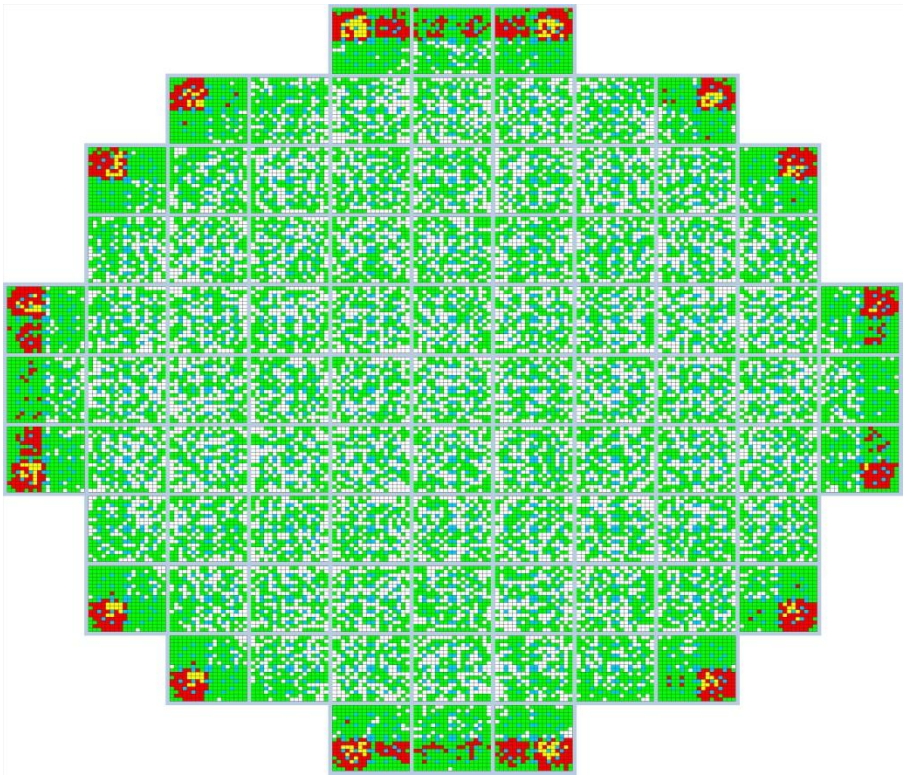

Figure E.4: Uncertainty Ratio 200

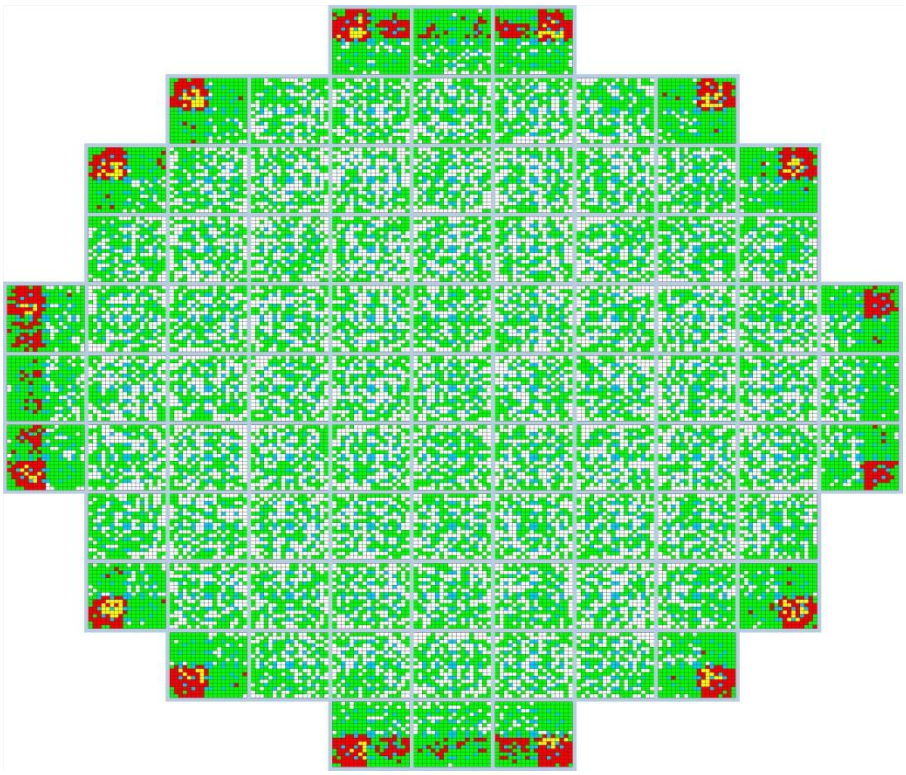

Figure E.5: Uncertainty Ratio 300 Days

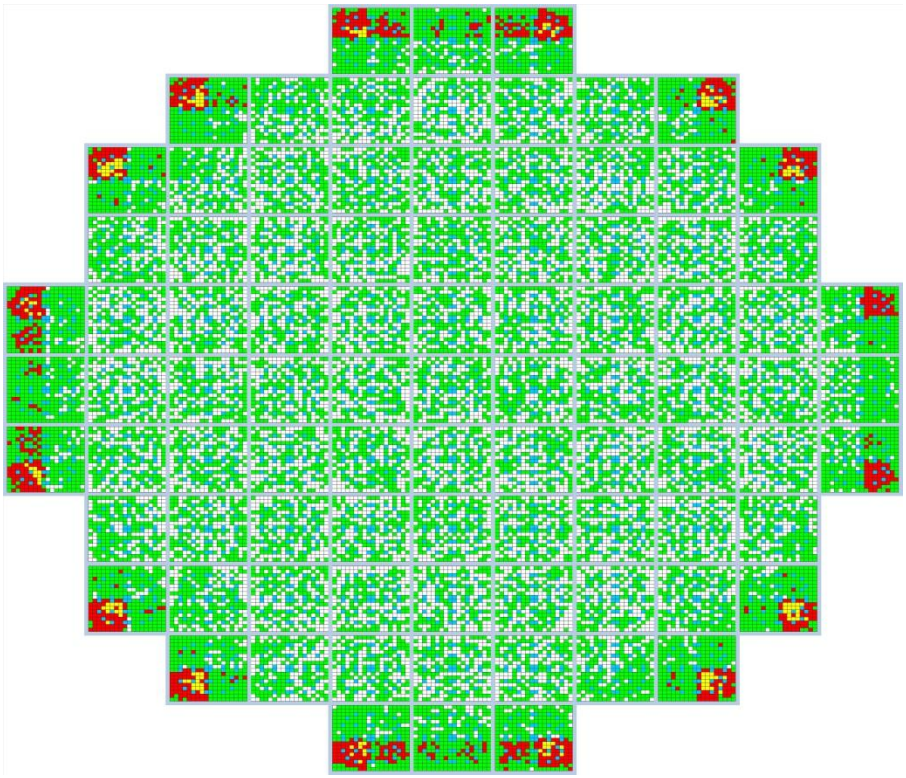

Figure E.6: Uncertainty Ratio 400 Days

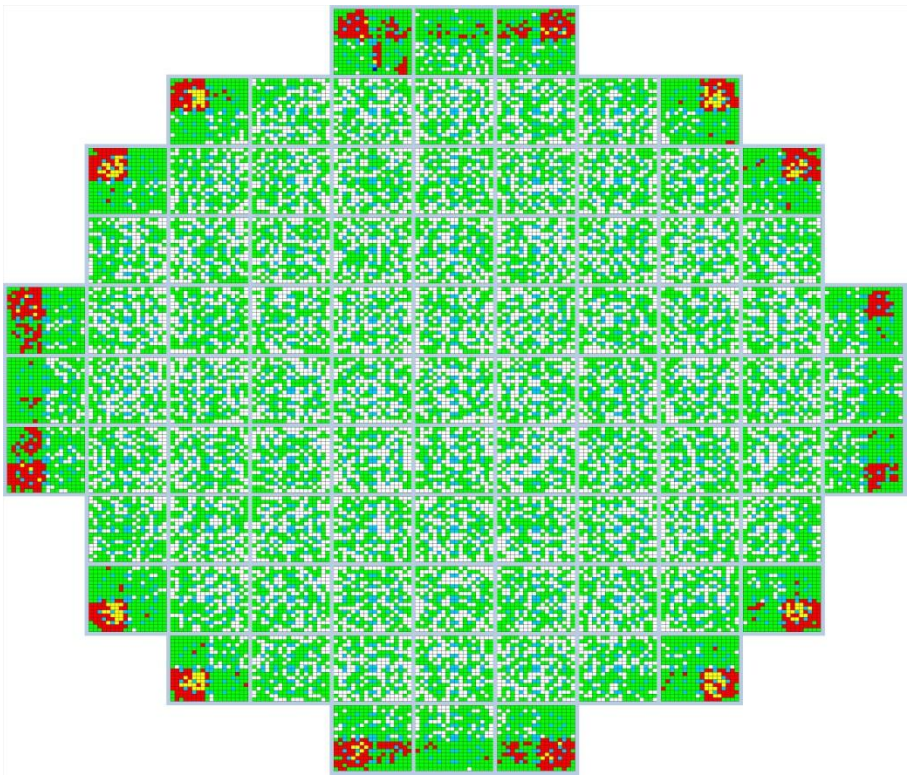

Figure E.7: Uncertainty Ratio 500 Days

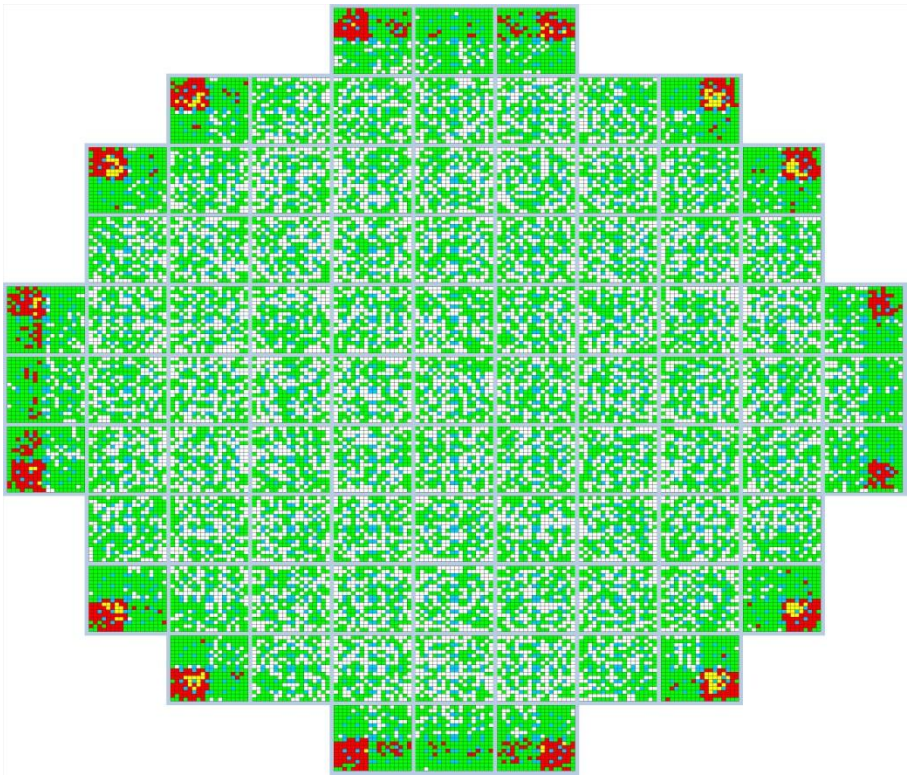

Figure E.8: Uncertainty Ratio 600 Days

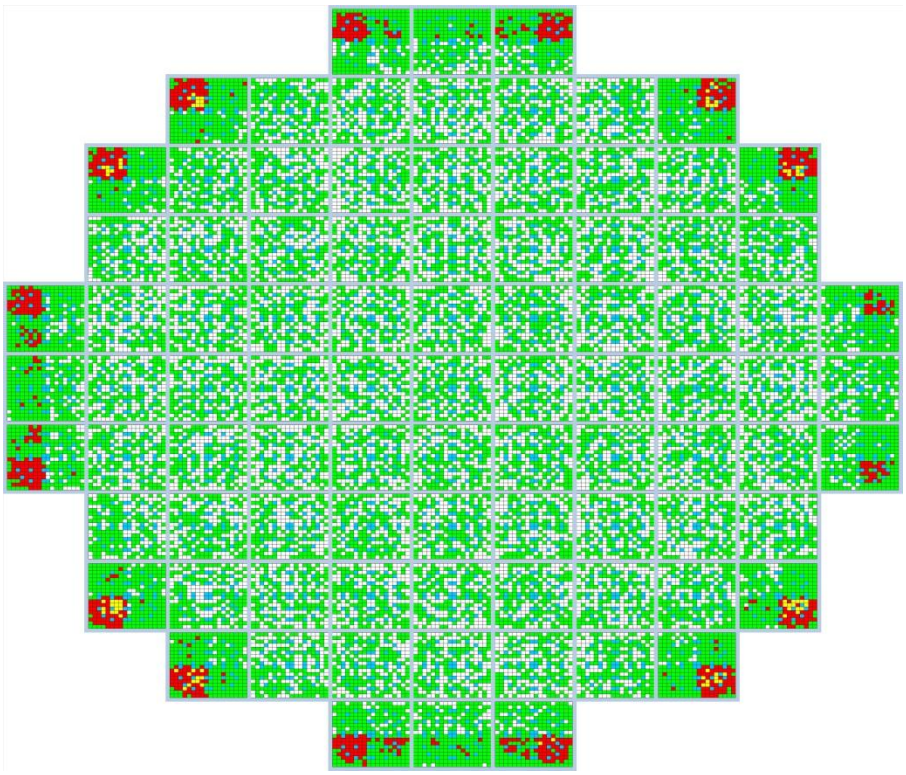

Figure E.9: Uncertainty Ratio 700 Days

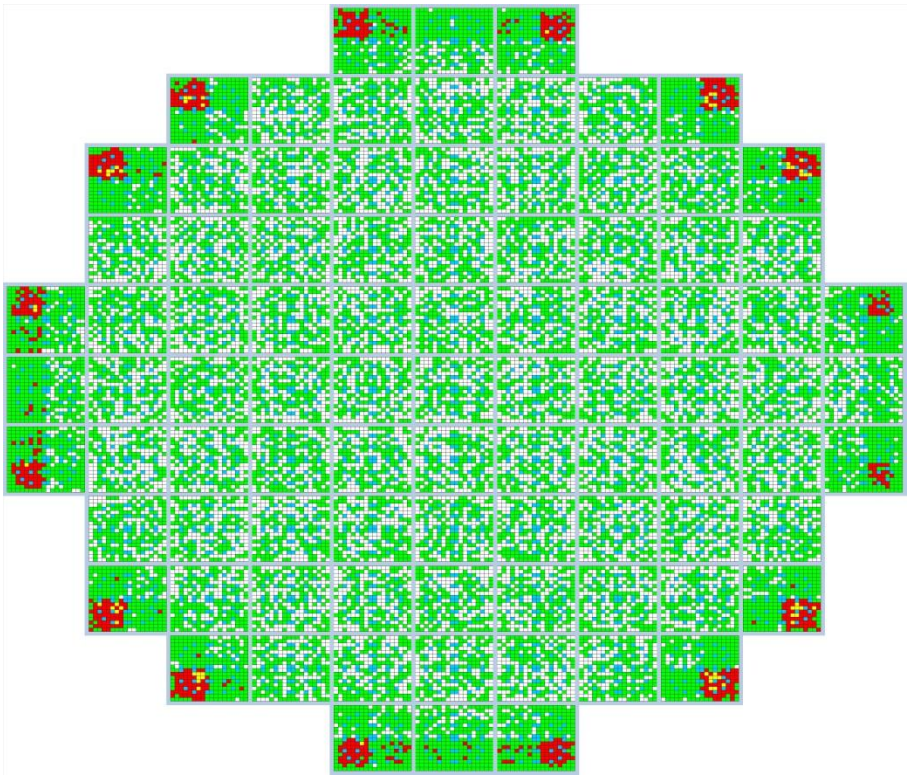

Figure D.10: Uncertainty Ratio 800 Days

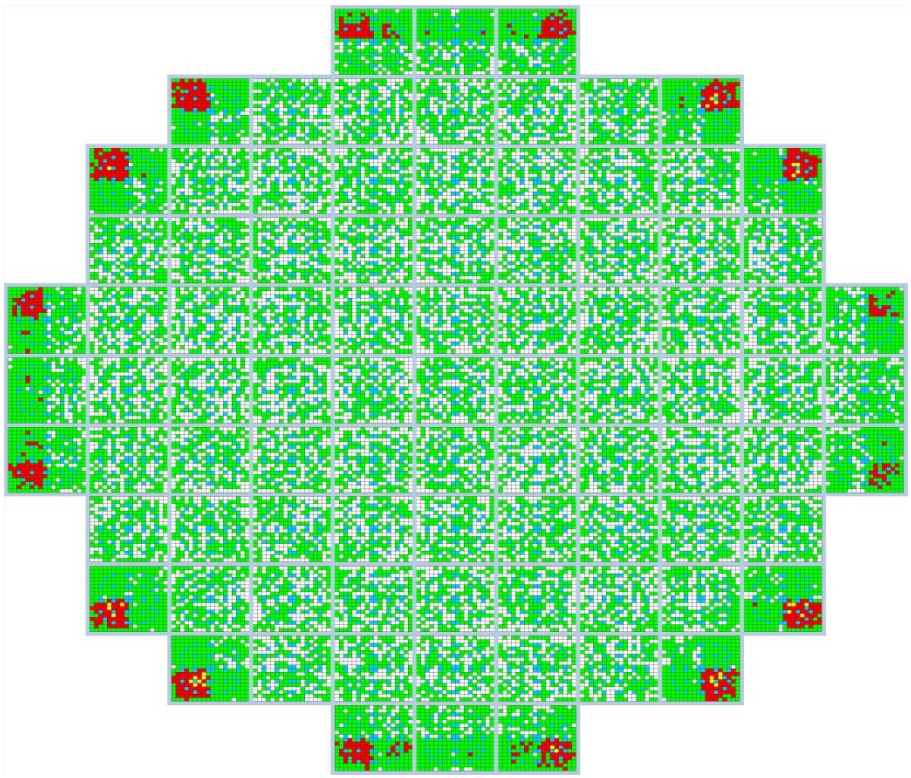

Figure E.11: Uncertainty Ratio 900 Days

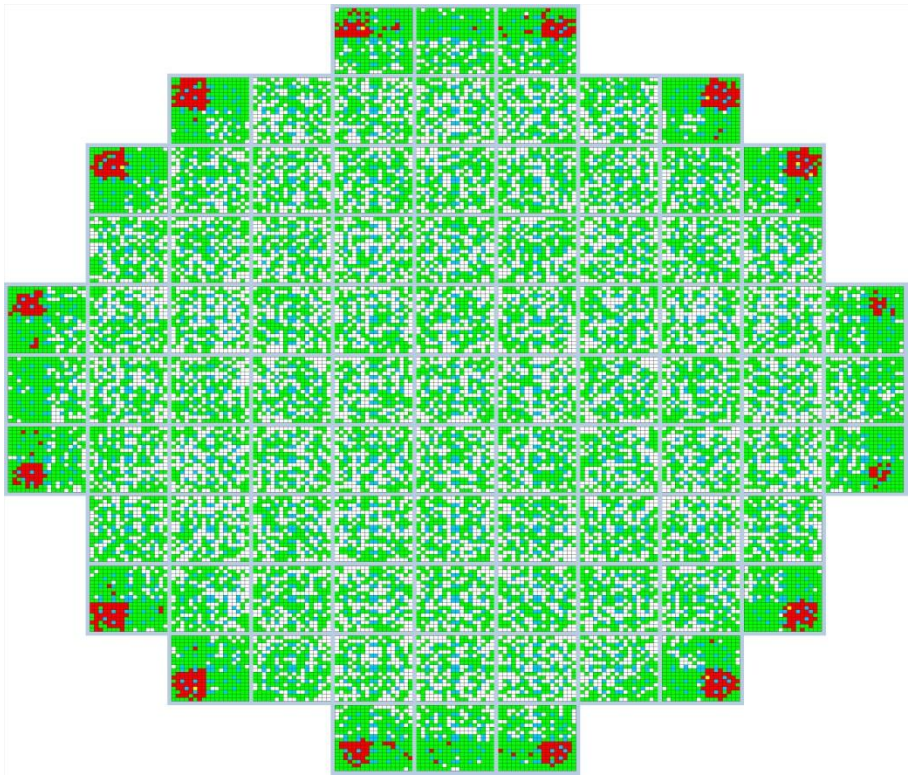

Figure E.12: Uncertainty Ratio 1000 Days

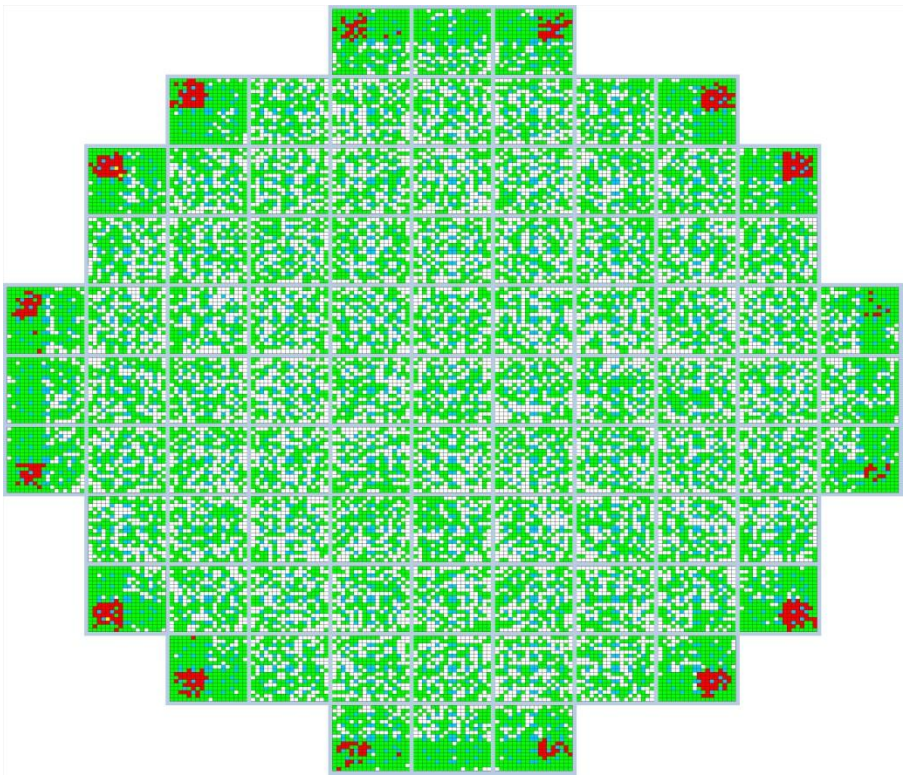

Figure E.13: Uncertainty Ratio 1200 Days

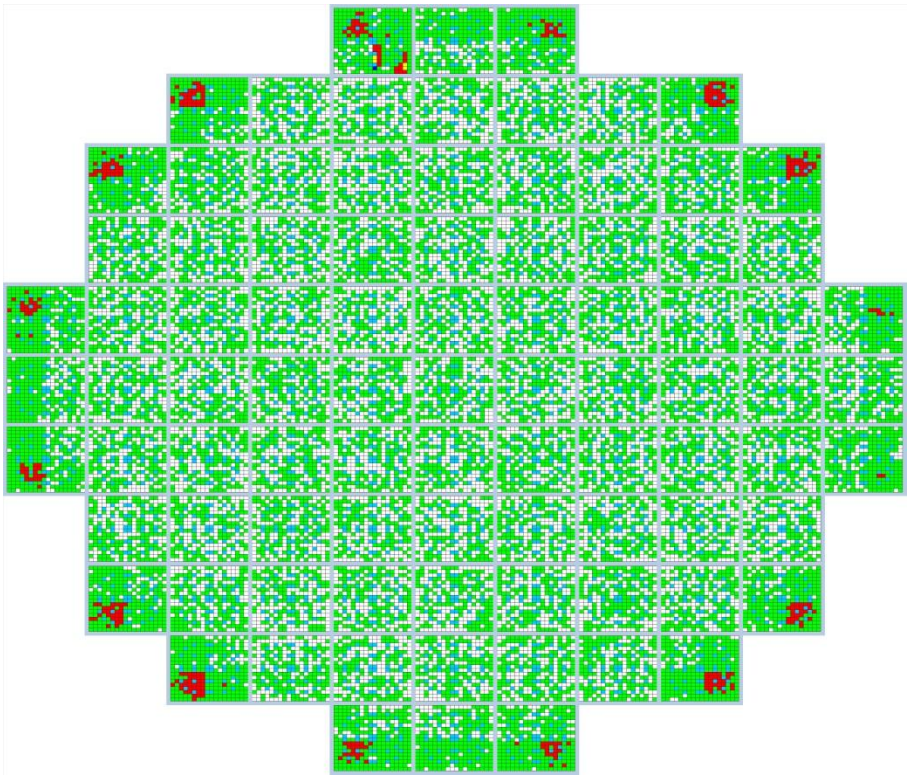

Figure E.14: Uncertainty Ratio 1400 Days

APPENDIX F

RELATIVE UNCERTAINTIES OF NUCLIDE DENSITIES

Table F.1: Relative Uncertainty of NND, Pin 1, TP1

Day	Pin One									
	^{235}U		^{239}Pu		^{241}Pu		^{237}Np		^{243}Am	
	mean	1σ (%)	mean	1σ (%)	mean	1σ (%)	mean	1σ (%)	mean	1σ (%)
0	9.642E-04	0.00%	0.000E+00	0.00%	0.000E+00	0.00%	0.000E+00	0.00%	0.000E+00	0.00%
1	9.629E-04	0.00%	6.092E-08	0.55%	1.819E-13	3.39%	1.235E-10	3.82%	2.222E-21	5.27%
2	9.617E-04	0.00%	2.280E-07	0.39%	1.891E-12	2.67%	4.838E-10	3.05%	1.465E-19	4.55%
3	9.604E-04	0.00%	4.745E-07	0.30%	7.484E-12	2.77%	1.065E-09	2.62%	1.587E-18	3.76%
5	9.578E-04	0.00%	1.129E-06	0.23%	4.208E-11	2.86%	2.826E-09	2.26%	2.894E-17	3.87%
10	9.515E-04	0.00%	3.208E-06	0.24%	4.327E-10	1.65%	1.016E-08	2.28%	1.399E-15	3.57%
20	9.388E-04	0.01%	7.747E-06	0.37%	4.145E-09	2.48%	3.361E-08	2.06%	6.129E-14	4.03%
30	9.264E-04	0.01%	1.219E-05	0.40%	1.489E-08	2.42%	6.477E-08	1.72%	5.203E-13	3.36%
50	9.019E-04	0.02%	2.057E-05	0.33%	6.963E-08	3.11%	1.428E-07	1.55%	7.133E-12	5.29%
75	8.722E-04	0.03%	3.017E-05	0.22%	2.230E-07	1.96%	2.658E-07	1.70%	5.553E-11	3.72%
100	8.433E-04	0.03%	3.887E-05	0.23%	4.893E-07	1.67%	4.135E-07	1.56%	2.300E-10	4.10%
125	8.153E-04	0.03%	4.677E-05	0.23%	8.811E-07	1.06%	5.828E-07	1.31%	6.788E-10	3.29%
150	7.880E-04	0.03%	5.400E-05	0.20%	1.389E-06	0.85%	7.743E-07	1.17%	1.624E-09	3.63%
175	7.614E-04	0.04%	6.058E-05	0.21%	2.019E-06	0.80%	9.861E-07	0.96%	3.290E-09	2.95%
200	7.355E-04	0.04%	6.659E-05	0.19%	2.754E-06	1.07%	1.215E-06	0.96%	6.055E-09	3.50%
225	7.103E-04	0.04%	7.209E-05	0.20%	3.575E-06	0.79%	1.460E-06	0.97%	1.032E-08	2.92%
250	6.858E-04	0.04%	7.712E-05	0.20%	4.482E-06	1.13%	1.722E-06	0.77%	1.663E-08	2.29%
275	6.618E-04	0.05%	8.171E-05	0.17%	5.457E-06	1.00%	1.997E-06	0.83%	2.539E-08	2.04%
300	6.385E-04	0.05%	8.590E-05	0.15%	6.481E-06	0.84%	2.290E-06	0.91%	3.719E-08	1.64%
325	6.157E-04	0.05%	8.973E-05	0.14%	7.554E-06	0.87%	2.597E-06	0.84%	5.246E-08	2.14%
350	5.936E-04	0.05%	9.320E-05	0.16%	8.655E-06	0.63%	2.913E-06	0.80%	7.179E-08	1.98%
375	5.720E-04	0.05%	9.636E-05	0.18%	9.785E-06	0.55%	3.238E-06	0.81%	9.557E-08	2.00%
400	5.509E-04	0.04%	9.926E-05	0.18%	1.094E-05	0.37%	3.572E-06	0.84%	1.246E-07	1.76%
450	5.103E-04	0.06%	1.042E-04	0.15%	1.327E-05	0.64%	4.277E-06	0.93%	2.001E-07	2.14%
500	4.718E-04	0.07%	1.082E-04	0.32%	1.562E-05	0.63%	5.008E-06	0.89%	3.057E-07	2.04%
550	4.354E-04	0.08%	1.116E-04	0.34%	1.792E-05	0.67%	5.759E-06	0.83%	4.446E-07	1.65%
600	4.009E-04	0.11%	1.142E-04	0.28%	2.016E-05	0.68%	6.536E-06	0.75%	6.142E-07	1.86%
650	3.682E-04	0.13%	1.162E-04	0.20%	2.228E-05	0.59%	7.323E-06	0.62%	8.282E-07	1.47%
700	3.373E-04	0.14%	1.176E-04	0.26%	2.424E-05	0.47%	8.119E-06	0.62%	1.079E-06	1.67%
750	3.083E-04	0.13%	1.187E-04	0.25%	2.610E-05	0.50%	8.923E-06	0.71%	1.373E-06	1.01%
800	2.810E-04	0.14%	1.194E-04	0.35%	2.786E-05	0.39%	9.717E-06	0.73%	1.715E-06	1.31%
850	2.555E-04	0.15%	1.198E-04	0.36%	2.948E-05	0.43%	1.052E-05	0.73%	2.108E-06	1.59%
900	2.317E-04	0.15%	1.200E-04	0.35%	3.091E-05	0.39%	1.132E-05	0.86%	2.548E-06	1.44%
950	2.094E-04	0.16%	1.201E-04	0.28%	3.223E-05	0.38%	1.209E-05	0.78%	3.026E-06	1.51%
1000	1.888E-04	0.18%	1.200E-04	0.26%	3.337E-05	0.56%	1.286E-05	0.82%	3.554E-06	1.55%
1050	1.696E-04	0.19%	1.197E-04	0.26%	3.442E-05	0.48%	1.360E-05	0.75%	4.132E-06	1.54%
1100	1.520E-04	0.21%	1.193E-04	0.28%	3.538E-05	0.36%	1.432E-05	0.66%	4.757E-06	1.73%

Table F.2: Relative Uncertainty of NND, Pin 2, TP1

Day	Pin Two									
	^{235}U		^{239}Pu		^{241}Pu		^{237}Np		^{243}Am	
	mean	1σ (%)	mean	1σ (%)	mean	1σ (%)	mean	1σ (%)	mean	1σ (%)
0	9.642E-04	0.00%	0.000E+00	0.00%	0.000E+00	0.00%	0.000E+00	0.00%	0.000E+00	0.00%
1	9.631E-04	0.00%	5.655E-08	0.53%	1.495E-13	4.03%	1.214E-10	4.11%	1.573E-21	9.46%
2	9.620E-04	0.00%	2.118E-07	0.38%	1.560E-12	2.35%	4.787E-10	3.15%	1.040E-19	5.75%
3	9.609E-04	0.00%	4.412E-07	0.33%	6.025E-12	2.20%	1.056E-09	2.47%	1.100E-18	3.94%
5	9.586E-04	0.00%	1.051E-06	0.29%	3.360E-11	1.86%	2.798E-09	1.76%	2.025E-17	4.97%
10	9.531E-04	0.00%	2.990E-06	0.31%	3.457E-10	2.32%	9.975E-09	1.83%	9.452E-16	4.66%
20	9.421E-04	0.01%	7.230E-06	0.27%	3.309E-09	1.79%	3.265E-08	2.41%	4.000E-14	4.98%
30	9.312E-04	0.01%	1.141E-05	0.24%	1.191E-08	2.03%	6.231E-08	2.08%	3.461E-13	4.44%
50	9.098E-04	0.01%	1.935E-05	0.21%	5.582E-08	1.88%	1.360E-07	2.12%	4.918E-12	4.21%
75	8.837E-04	0.02%	2.852E-05	0.30%	1.813E-07	1.43%	2.493E-07	1.82%	3.806E-11	3.49%
100	8.583E-04	0.02%	3.699E-05	0.26%	4.019E-07	1.55%	3.848E-07	1.60%	1.564E-10	3.23%
125	8.335E-04	0.03%	4.480E-05	0.24%	7.267E-07	1.63%	5.422E-07	1.44%	4.553E-10	3.59%
150	8.094E-04	0.03%	5.201E-05	0.26%	1.157E-06	1.17%	7.164E-07	1.33%	1.099E-09	3.69%
175	7.858E-04	0.04%	5.868E-05	0.24%	1.687E-06	0.57%	9.093E-07	1.15%	2.283E-09	2.34%
200	7.628E-04	0.04%	6.488E-05	0.26%	2.310E-06	0.79%	1.119E-06	0.96%	4.237E-09	2.74%
225	7.403E-04	0.05%	7.060E-05	0.26%	3.024E-06	1.00%	1.343E-06	0.86%	7.309E-09	2.11%
250	7.182E-04	0.05%	7.588E-05	0.24%	3.796E-06	0.74%	1.581E-06	0.76%	1.173E-08	2.56%
275	6.967E-04	0.05%	8.081E-05	0.26%	4.656E-06	0.55%	1.832E-06	0.69%	1.786E-08	2.49%
300	6.757E-04	0.06%	8.541E-05	0.25%	5.564E-06	0.66%	2.095E-06	0.77%	2.599E-08	2.39%
325	6.551E-04	0.05%	8.965E-05	0.26%	6.520E-06	0.57%	2.369E-06	0.67%	3.695E-08	2.16%
350	6.349E-04	0.06%	9.359E-05	0.24%	7.516E-06	0.40%	2.657E-06	0.67%	5.054E-08	1.77%
375	6.152E-04	0.06%	9.720E-05	0.27%	8.562E-06	0.45%	2.956E-06	0.70%	6.795E-08	1.52%
400	5.959E-04	0.06%	1.006E-04	0.28%	9.632E-06	0.47%	3.260E-06	0.71%	8.879E-08	1.92%
450	5.585E-04	0.06%	1.065E-04	0.29%	1.184E-05	0.47%	3.900E-06	0.79%	1.447E-07	2.12%
500	5.227E-04	0.07%	1.116E-04	0.29%	1.408E-05	0.58%	4.567E-06	0.57%	2.208E-07	2.17%
550	4.885E-04	0.08%	1.160E-04	0.29%	1.629E-05	0.63%	5.269E-06	0.73%	3.213E-07	1.93%
600	4.558E-04	0.07%	1.196E-04	0.30%	1.851E-05	0.59%	5.994E-06	0.79%	4.500E-07	2.41%
650	4.245E-04	0.09%	1.226E-04	0.33%	2.066E-05	0.46%	6.741E-06	0.80%	6.078E-07	2.31%
700	3.945E-04	0.10%	1.251E-04	0.36%	2.277E-05	0.58%	7.503E-06	0.75%	7.993E-07	1.91%
750	3.659E-04	0.11%	1.270E-04	0.35%	2.477E-05	0.58%	8.266E-06	0.77%	1.025E-06	1.74%
800	3.389E-04	0.10%	1.287E-04	0.27%	2.665E-05	0.49%	9.029E-06	0.74%	1.297E-06	1.92%
850	3.130E-04	0.11%	1.298E-04	0.29%	2.851E-05	0.53%	9.796E-06	0.75%	1.601E-06	2.00%
900	2.886E-04	0.11%	1.307E-04	0.30%	3.021E-05	0.44%	1.057E-05	0.76%	1.936E-06	1.55%
950	2.654E-04	0.12%	1.314E-04	0.31%	3.179E-05	0.35%	1.134E-05	0.64%	2.325E-06	1.41%
1000	2.436E-04	0.12%	1.319E-04	0.34%	3.324E-05	0.41%	1.210E-05	0.66%	2.748E-06	1.23%
1050	2.229E-04	0.12%	1.320E-04	0.30%	3.454E-05	0.32%	1.285E-05	0.53%	3.201E-06	0.91%
1100	2.036E-04	0.13%	1.321E-04	0.29%	3.575E-05	0.35%	1.358E-05	0.54%	3.685E-06	1.28%

Table F.3: Relative Uncertainty of NND, Pin 3, TP1

Day	Pin Three									
	^{235}U		^{239}Pu		^{241}Pu		^{237}Np		^{243}Am	
	mean	1σ (%)	mean	1σ (%)	mean	1σ (%)	mean	1σ (%)	mean	1σ (%)
0	9.642E-04	0.00%	0.000E+00	0.00%	0.000E+00	0.00%	0.000E+00	0.00%	0.000E+00	0.00%
1	9.631E-04	0.00%	5.666E-08	0.48%	1.465E-13	2.56%	1.238E-10	4.80%	1.573E-21	5.13%
2	9.620E-04	0.00%	2.122E-07	0.35%	1.544E-12	2.91%	4.839E-10	3.74%	1.040E-19	3.64%
3	9.609E-04	0.00%	4.420E-07	0.27%	6.075E-12	2.58%	1.064E-09	3.11%	1.080E-18	4.22%
5	9.586E-04	0.00%	1.052E-06	0.29%	3.408E-11	2.35%	2.809E-09	2.41%	1.980E-17	5.91%
10	9.531E-04	0.00%	2.991E-06	0.32%	3.422E-10	2.42%	1.003E-08	2.36%	9.413E-16	5.95%
20	9.421E-04	0.01%	7.236E-06	0.27%	3.352E-09	2.58%	3.286E-08	2.08%	4.061E-14	4.47%
30	9.312E-04	0.01%	1.141E-05	0.22%	1.199E-08	2.30%	6.273E-08	1.63%	3.516E-13	4.76%
50	9.097E-04	0.02%	1.935E-05	0.25%	5.695E-08	2.28%	1.364E-07	1.69%	5.033E-12	5.69%
75	8.836E-04	0.02%	2.851E-05	0.30%	1.828E-07	2.36%	2.501E-07	1.77%	3.883E-11	4.81%
100	8.582E-04	0.02%	3.697E-05	0.26%	4.020E-07	1.86%	3.848E-07	1.75%	1.604E-10	2.10%
125	8.335E-04	0.03%	4.476E-05	0.21%	7.263E-07	1.18%	5.387E-07	1.71%	4.672E-10	4.66%
150	8.094E-04	0.03%	5.196E-05	0.23%	1.150E-06	1.20%	7.118E-07	1.59%	1.100E-09	3.37%
175	7.858E-04	0.04%	5.860E-05	0.21%	1.678E-06	1.11%	9.036E-07	1.53%	2.262E-09	3.00%
200	7.628E-04	0.04%	6.478E-05	0.23%	2.303E-06	1.01%	1.111E-06	1.38%	4.224E-09	2.54%
225	7.403E-04	0.04%	7.050E-05	0.24%	3.007E-06	0.76%	1.335E-06	1.22%	7.203E-09	2.22%
250	7.183E-04	0.04%	7.583E-05	0.25%	3.796E-06	0.39%	1.573E-06	1.14%	1.155E-08	2.28%
275	6.967E-04	0.05%	8.076E-05	0.24%	4.640E-06	0.40%	1.824E-06	1.12%	1.768E-08	2.95%
300	6.757E-04	0.05%	8.535E-05	0.25%	5.553E-06	0.44%	2.087E-06	1.11%	2.601E-08	2.83%
325	6.551E-04	0.05%	8.959E-05	0.24%	6.519E-06	0.55%	2.363E-06	1.01%	3.675E-08	2.21%
350	6.349E-04	0.05%	9.352E-05	0.23%	7.529E-06	0.66%	2.651E-06	0.93%	5.063E-08	1.76%
375	6.152E-04	0.06%	9.714E-05	0.21%	8.556E-06	0.67%	2.949E-06	0.94%	6.776E-08	1.84%
400	5.959E-04	0.06%	1.005E-04	0.20%	9.631E-06	0.64%	3.258E-06	0.99%	8.864E-08	1.98%
450	5.585E-04	0.05%	1.065E-04	0.23%	1.184E-05	0.37%	3.898E-06	0.96%	1.445E-07	3.01%
500	5.227E-04	0.05%	1.116E-04	0.16%	1.410E-05	0.47%	4.569E-06	0.89%	2.201E-07	2.54%
550	4.885E-04	0.06%	1.159E-04	0.18%	1.632E-05	0.62%	5.271E-06	0.71%	3.204E-07	2.08%
600	4.558E-04	0.06%	1.196E-04	0.24%	1.852E-05	0.55%	5.995E-06	0.73%	4.472E-07	1.70%
650	4.245E-04	0.07%	1.225E-04	0.27%	2.066E-05	0.45%	6.735E-06	0.79%	6.032E-07	1.43%
700	3.946E-04	0.08%	1.251E-04	0.30%	2.272E-05	0.46%	7.493E-06	0.85%	7.960E-07	1.91%
750	3.661E-04	0.10%	1.270E-04	0.34%	2.471E-05	0.38%	8.253E-06	0.79%	1.024E-06	1.57%
800	3.389E-04	0.10%	1.286E-04	0.31%	2.665E-05	0.53%	9.017E-06	0.71%	1.287E-06	1.17%
850	3.131E-04	0.10%	1.298E-04	0.30%	2.849E-05	0.61%	9.778E-06	0.69%	1.592E-06	0.99%
900	2.887E-04	0.09%	1.307E-04	0.31%	3.014E-05	0.59%	1.054E-05	0.61%	1.933E-06	1.08%
950	2.655E-04	0.11%	1.313E-04	0.25%	3.172E-05	0.45%	1.132E-05	0.59%	2.311E-06	1.30%
1000	2.436E-04	0.12%	1.316E-04	0.31%	3.321E-05	0.39%	1.208E-05	0.52%	2.732E-06	1.29%
1050	2.230E-04	0.13%	1.319E-04	0.31%	3.458E-05	0.36%	1.284E-05	0.52%	3.196E-06	1.44%
1100	2.037E-04	0.13%	1.319E-04	0.32%	3.580E-05	0.38%	1.358E-05	0.61%	3.689E-06	1.24%

Table F.4: Relative Uncertainty of NND, Pin 4, TP1

Day	Pin Four									
	^{235}U		^{239}Pu		^{241}Pu		^{237}Np		^{243}Am	
	mean	1σ (%)	mean	1σ (%)	mean	1σ (%)	mean	1σ (%)	mean	1σ (%)
0	9.642E-04	0.00%	0.000E+00	0.00%	0.000E+00	0.00%	0.000E+00	0.00%	0.000E+00	0.00%
1	9.630E-04	0.00%	5.849E-08	0.49%	1.662E-13	3.19%	1.264E-10	2.98%	1.900E-21	5.30%
2	9.618E-04	0.00%	2.191E-07	0.38%	1.721E-12	2.66%	4.939E-10	2.63%	1.279E-19	4.53%
3	9.606E-04	0.00%	4.563E-07	0.29%	6.793E-12	1.69%	1.083E-09	2.72%	1.358E-18	4.52%
5	9.582E-04	0.00%	1.085E-06	0.18%	3.846E-11	2.24%	2.859E-09	2.64%	2.529E-17	2.83%
10	9.521E-04	0.00%	3.088E-06	0.24%	3.914E-10	2.84%	1.015E-08	2.53%	1.190E-15	6.59%
20	9.402E-04	0.01%	7.461E-06	0.32%	3.799E-09	3.34%	3.328E-08	2.31%	5.007E-14	5.29%
30	9.284E-04	0.01%	1.175E-05	0.25%	1.360E-08	2.89%	6.400E-08	2.27%	4.474E-13	4.13%
50	9.051E-04	0.02%	1.984E-05	0.24%	6.385E-08	2.04%	1.405E-07	2.08%	6.145E-12	4.87%
75	8.769E-04	0.02%	2.914E-05	0.25%	2.045E-07	1.72%	2.595E-07	2.02%	4.792E-11	3.95%
100	8.494E-04	0.02%	3.766E-05	0.27%	4.527E-07	1.66%	4.010E-07	1.86%	1.994E-10	3.46%
125	8.227E-04	0.03%	4.547E-05	0.25%	8.112E-07	1.05%	5.639E-07	1.79%	5.865E-10	2.85%
150	7.966E-04	0.04%	5.259E-05	0.28%	1.279E-06	0.93%	7.477E-07	1.48%	1.383E-09	2.05%
175	7.712E-04	0.05%	5.919E-05	0.24%	1.853E-06	0.78%	9.493E-07	1.27%	2.841E-09	2.87%
200	7.464E-04	0.05%	6.519E-05	0.26%	2.530E-06	0.77%	1.169E-06	1.02%	5.246E-09	2.63%
225	7.222E-04	0.05%	7.070E-05	0.24%	3.300E-06	0.53%	1.405E-06	1.02%	8.967E-09	2.64%
250	6.986E-04	0.04%	7.578E-05	0.26%	4.152E-06	0.59%	1.656E-06	1.04%	1.429E-08	1.86%
275	6.755E-04	0.04%	8.043E-05	0.23%	5.068E-06	0.51%	1.923E-06	0.95%	2.179E-08	2.11%
300	6.530E-04	0.05%	8.471E-05	0.22%	6.040E-06	0.57%	2.202E-06	0.81%	3.188E-08	2.28%
325	6.310E-04	0.06%	8.861E-05	0.21%	7.058E-06	0.65%	2.491E-06	0.77%	4.503E-08	2.33%
350	6.095E-04	0.05%	9.219E-05	0.20%	8.107E-06	0.79%	2.793E-06	0.68%	6.209E-08	2.18%
375	5.886E-04	0.06%	9.546E-05	0.17%	9.193E-06	0.52%	3.106E-06	0.67%	8.308E-08	1.67%
400	5.680E-04	0.06%	9.843E-05	0.18%	1.031E-05	0.51%	3.426E-06	0.70%	1.085E-07	1.55%
450	5.284E-04	0.07%	1.036E-04	0.19%	1.258E-05	0.70%	4.108E-06	0.79%	1.747E-07	2.13%
500	4.907E-04	0.09%	1.080E-04	0.17%	1.485E-05	0.50%	4.814E-06	0.97%	2.676E-07	2.16%
550	4.547E-04	0.09%	1.115E-04	0.27%	1.708E-05	0.49%	5.548E-06	1.03%	3.878E-07	1.70%
600	4.205E-04	0.10%	1.144E-04	0.36%	1.924E-05	0.52%	6.299E-06	1.05%	5.409E-07	1.80%
650	3.880E-04	0.10%	1.165E-04	0.36%	2.133E-05	0.66%	7.063E-06	0.95%	7.243E-07	1.95%
700	3.572E-04	0.10%	1.183E-04	0.36%	2.329E-05	0.68%	7.833E-06	0.96%	9.502E-07	1.57%
750	3.280E-04	0.11%	1.195E-04	0.37%	2.515E-05	0.43%	8.609E-06	0.83%	1.219E-06	1.54%
800	3.005E-04	0.11%	1.205E-04	0.39%	2.692E-05	0.41%	9.382E-06	0.65%	1.528E-06	1.65%
850	2.744E-04	0.09%	1.210E-04	0.33%	2.855E-05	0.50%	1.016E-05	0.53%	1.884E-06	1.85%
900	2.500E-04	0.11%	1.212E-04	0.36%	3.007E-05	0.45%	1.092E-05	0.53%	2.280E-06	1.64%
950	2.271E-04	0.12%	1.214E-04	0.37%	3.145E-05	0.39%	1.168E-05	0.57%	2.718E-06	1.64%
1000	2.057E-04	0.16%	1.213E-04	0.41%	3.269E-05	0.42%	1.244E-05	0.60%	3.197E-06	1.47%
1050	1.858E-04	0.17%	1.209E-04	0.32%	3.374E-05	0.44%	1.316E-05	0.56%	3.730E-06	1.35%
1100	1.672E-04	0.17%	1.205E-04	0.38%	3.471E-05	0.47%	1.385E-05	0.54%	4.309E-06	1.08%

Table F.5: Relative Uncertainty of NND, Pin 1, TP2

Day	Pin One									
	^{235}U		^{239}Pu		^{241}Pu		^{237}Np		^{243}Am	
	mean	1σ (%)	mean	1σ (%)	mean	1σ (%)	mean	1σ (%)	mean	1σ (%)
0	9.642E-04	0.00%	0.000E+00	0.00%	0.000E+00	0.00%	0.000E+00	0.00%	0.000E+00	0.00%
1	9.630E-04	0.00%	7.034E-08	0.75%	2.627E-13	3.77%	1.549E-10	3.22%	3.657E-21	5.23%
2	9.619E-04	0.00%	2.636E-07	0.56%	2.680E-12	2.78%	6.074E-10	2.61%	2.363E-19	5.12%
3	9.607E-04	0.00%	5.488E-07	0.50%	1.044E-11	2.62%	1.339E-09	2.39%	2.532E-18	4.44%
5	9.583E-04	0.00%	1.305E-06	0.36%	5.691E-11	2.43%	3.567E-09	2.06%	4.541E-17	4.54%
10	9.524E-04	0.00%	3.698E-06	0.31%	5.759E-10	2.95%	1.271E-08	1.74%	2.081E-15	4.49%
20	9.406E-04	0.01%	8.891E-06	0.26%	5.355E-09	2.06%	4.127E-08	1.92%	8.835E-14	4.52%
30	9.291E-04	0.01%	1.393E-05	0.28%	1.897E-08	2.16%	7.867E-08	1.81%	7.304E-13	3.25%
50	9.063E-04	0.01%	2.332E-05	0.34%	8.683E-08	3.39%	1.707E-07	1.98%	9.892E-12	5.10%
75	8.784E-04	0.02%	3.391E-05	0.32%	2.699E-07	1.87%	3.104E-07	2.25%	7.499E-11	3.57%
100	8.512E-04	0.02%	4.335E-05	0.28%	5.811E-07	1.24%	4.750E-07	2.06%	2.962E-10	3.63%
125	8.245E-04	0.03%	5.181E-05	0.29%	1.027E-06	1.12%	6.631E-07	1.69%	8.355E-10	3.36%
150	7.985E-04	0.04%	5.938E-05	0.26%	1.596E-06	1.07%	8.684E-07	1.35%	1.947E-09	2.96%
175	7.731E-04	0.04%	6.619E-05	0.24%	2.279E-06	0.87%	1.092E-06	1.00%	3.890E-09	2.01%
200	7.483E-04	0.04%	7.233E-05	0.24%	3.068E-06	1.15%	1.333E-06	0.89%	7.048E-09	2.68%
225	7.240E-04	0.04%	7.784E-05	0.26%	3.945E-06	0.98%	1.589E-06	0.75%	1.187E-08	2.37%
250	7.002E-04	0.04%	8.284E-05	0.24%	4.889E-06	0.85%	1.858E-06	0.57%	1.873E-08	2.53%
275	6.768E-04	0.04%	8.733E-05	0.20%	5.895E-06	0.54%	2.139E-06	0.55%	2.806E-08	2.22%
300	6.540E-04	0.04%	9.138E-05	0.18%	6.945E-06	0.45%	2.429E-06	0.57%	4.051E-08	1.82%
325	6.317E-04	0.05%	9.502E-05	0.16%	8.040E-06	0.55%	2.733E-06	0.62%	5.636E-08	2.07%
350	6.099E-04	0.05%	9.831E-05	0.14%	9.167E-06	0.61%	3.050E-06	0.69%	7.655E-08	2.00%
375	5.886E-04	0.06%	1.012E-04	0.12%	1.032E-05	0.50%	3.374E-06	0.73%	1.012E-07	1.73%
400	5.678E-04	0.06%	1.039E-04	0.13%	1.149E-05	0.38%	3.706E-06	0.74%	1.312E-07	1.87%
450	5.276E-04	0.06%	1.085E-04	0.16%	1.384E-05	0.44%	4.393E-06	0.71%	2.091E-07	1.91%
500	4.892E-04	0.08%	1.121E-04	0.22%	1.617E-05	0.44%	5.107E-06	0.76%	3.130E-07	1.56%
550	4.528E-04	0.08%	1.150E-04	0.22%	1.847E-05	0.56%	5.846E-06	0.89%	4.472E-07	1.51%
600	4.180E-04	0.09%	1.171E-04	0.22%	2.069E-05	0.44%	6.603E-06	0.78%	6.194E-07	1.28%
650	3.850E-04	0.09%	1.188E-04	0.24%	2.277E-05	0.51%	7.371E-06	0.71%	8.342E-07	2.11%
700	3.538E-04	0.08%	1.200E-04	0.26%	2.473E-05	0.41%	8.153E-06	0.68%	1.085E-06	2.01%
750	3.243E-04	0.09%	1.208E-04	0.27%	2.660E-05	0.47%	8.956E-06	0.65%	1.378E-06	1.77%
800	2.965E-04	0.09%	1.213E-04	0.19%	2.830E-05	0.53%	9.754E-06	0.54%	1.718E-06	1.92%
850	2.703E-04	0.08%	1.216E-04	0.20%	2.987E-05	0.40%	1.054E-05	0.48%	2.101E-06	1.65%
900	2.457E-04	0.10%	1.216E-04	0.24%	3.124E-05	0.44%	1.131E-05	0.57%	2.523E-06	1.95%
950	2.227E-04	0.10%	1.215E-04	0.30%	3.252E-05	0.35%	1.208E-05	0.71%	2.999E-06	1.83%
1000	2.013E-04	0.07%	1.212E-04	0.38%	3.365E-05	0.56%	1.283E-05	0.76%	3.520E-06	1.81%
1050	1.814E-04	0.08%	1.208E-04	0.37%	3.467E-05	0.59%	1.356E-05	0.67%	4.078E-06	1.65%
1100	1.630E-04	0.10%	1.203E-04	0.25%	3.557E-05	0.54%	1.429E-05	0.58%	4.673E-06	1.42%

Table F.6: Relative Uncertainty of NND, Pin 2, TP2

Day	Pin Two									
	^{235}U		^{239}Pu		^{241}Pu		^{237}Np		^{243}Am	
	mean	1σ (%)	mean	1σ (%)	mean	1σ (%)	mean	1σ (%)	mean	1σ (%)
0	9.642E-04	0.00%	0.000E+00	0.00%	0.000E+00	0.00%	0.000E+00	0.00%	0.000E+00	0.00%
1	9.631E-04	0.00%	6.880E-08	0.61%	2.430E-13	3.32%	1.606E-10	4.78%	3.253E-21	5.52%
2	9.620E-04	0.00%	2.574E-07	0.49%	2.508E-12	3.06%	6.228E-10	4.05%	2.142E-19	5.42%
3	9.608E-04	0.00%	5.355E-07	0.38%	9.784E-12	2.98%	1.363E-09	3.68%	2.236E-18	4.99%
5	9.585E-04	0.00%	1.273E-06	0.28%	5.342E-11	2.17%	3.584E-09	3.10%	3.993E-17	5.74%
10	9.529E-04	0.00%	3.611E-06	0.42%	5.305E-10	2.73%	1.264E-08	3.18%	1.832E-15	6.20%
20	9.417E-04	0.01%	8.682E-06	0.40%	4.987E-09	2.62%	4.113E-08	2.23%	7.713E-14	4.19%
30	9.305E-04	0.01%	1.361E-05	0.29%	1.746E-08	2.92%	7.840E-08	1.94%	6.375E-13	3.62%
50	9.086E-04	0.02%	2.284E-05	0.36%	8.030E-08	2.77%	1.704E-07	1.86%	8.766E-12	3.42%
75	8.818E-04	0.03%	3.328E-05	0.43%	2.520E-07	2.62%	3.090E-07	1.86%	6.510E-11	4.42%
100	8.557E-04	0.03%	4.263E-05	0.40%	5.471E-07	1.55%	4.693E-07	1.46%	2.572E-10	4.14%
125	8.301E-04	0.03%	5.099E-05	0.34%	9.649E-07	1.51%	6.506E-07	1.36%	7.395E-10	4.63%
150	8.051E-04	0.04%	5.853E-05	0.35%	1.498E-06	1.32%	8.507E-07	1.37%	1.740E-09	3.68%
175	7.806E-04	0.05%	6.534E-05	0.29%	2.145E-06	0.86%	1.067E-06	1.29%	3.485E-09	3.66%
200	7.565E-04	0.05%	7.149E-05	0.32%	2.882E-06	0.84%	1.298E-06	1.24%	6.288E-09	2.96%
225	7.330E-04	0.05%	7.706E-05	0.29%	3.718E-06	0.93%	1.546E-06	1.26%	1.058E-08	1.93%
250	7.100E-04	0.05%	8.210E-05	0.28%	4.618E-06	0.89%	1.805E-06	1.13%	1.678E-08	1.93%
275	6.874E-04	0.05%	8.668E-05	0.25%	5.577E-06	1.05%	2.075E-06	1.07%	2.518E-08	2.11%
300	6.653E-04	0.05%	9.079E-05	0.24%	6.607E-06	0.89%	2.361E-06	0.94%	3.643E-08	1.98%
325	6.436E-04	0.05%	9.452E-05	0.21%	7.654E-06	0.88%	2.657E-06	0.86%	5.039E-08	2.36%
350	6.224E-04	0.05%	9.792E-05	0.19%	8.752E-06	0.72%	2.960E-06	0.80%	6.870E-08	2.31%
375	6.017E-04	0.05%	1.010E-04	0.20%	9.840E-06	0.74%	3.274E-06	0.70%	9.084E-08	1.96%
400	5.814E-04	0.05%	1.037E-04	0.21%	1.097E-05	0.64%	3.595E-06	0.59%	1.179E-07	2.58%
450	5.421E-04	0.07%	1.086E-04	0.26%	1.329E-05	0.67%	4.266E-06	0.65%	1.883E-07	2.00%
500	5.045E-04	0.09%	1.125E-04	0.24%	1.559E-05	0.55%	4.962E-06	0.84%	2.848E-07	1.88%
550	4.685E-04	0.09%	1.156E-04	0.24%	1.783E-05	0.57%	5.679E-06	0.72%	4.082E-07	1.98%
600	4.342E-04	0.10%	1.181E-04	0.25%	2.004E-05	0.58%	6.421E-06	0.57%	5.653E-07	1.80%
650	4.015E-04	0.12%	1.200E-04	0.25%	2.212E-05	0.54%	7.164E-06	0.69%	7.569E-07	1.77%
700	3.705E-04	0.13%	1.214E-04	0.22%	2.410E-05	0.49%	7.927E-06	0.74%	9.804E-07	1.73%
750	3.409E-04	0.12%	1.224E-04	0.24%	2.593E-05	0.47%	8.691E-06	0.78%	1.252E-06	1.63%
800	3.129E-04	0.13%	1.230E-04	0.29%	2.771E-05	0.46%	9.463E-06	0.79%	1.562E-06	1.34%
850	2.865E-04	0.15%	1.233E-04	0.28%	2.932E-05	0.51%	1.022E-05	0.80%	1.920E-06	1.20%
900	2.616E-04	0.14%	1.234E-04	0.31%	3.079E-05	0.41%	1.099E-05	0.71%	2.312E-06	1.31%
950	2.382E-04	0.15%	1.233E-04	0.27%	3.210E-05	0.36%	1.176E-05	0.63%	2.759E-06	1.05%
1000	2.163E-04	0.14%	1.231E-04	0.29%	3.331E-05	0.37%	1.251E-05	0.61%	3.261E-06	1.11%
1050	1.958E-04	0.15%	1.226E-04	0.22%	3.437E-05	0.50%	1.325E-05	0.55%	3.790E-06	1.16%
1100	1.767E-04	0.15%	1.221E-04	0.28%	3.531E-05	0.44%	1.397E-05	0.55%	4.337E-06	1.06%

Table F.7: Relative Uncertainty of NND, Pin 3, TP2

Day	Pin Three									
	^{235}U		^{239}Pu		^{241}Pu		^{237}Np		^{243}Am	
	mean	1σ (%)	mean	1σ (%)	mean	1σ (%)	mean	1σ (%)	mean	1σ (%)
0	9.642E-04	0.00%	0.000E+00	0.00%	0.000E+00	0.00%	0.000E+00	0.00%	0.000E+00	0.00%
1	9.630E-04	0.00%	6.997E-08	0.63%	2.686E-13	3.33%	1.609E-10	4.11%	3.917E-21	7.14%
2	9.618E-04	0.00%	2.617E-07	0.50%	2.747E-12	2.76%	6.310E-10	3.19%	2.530E-19	4.60%
3	9.605E-04	0.00%	5.445E-07	0.44%	1.057E-11	1.93%	1.390E-09	2.61%	2.652E-18	3.48%
5	9.581E-04	0.00%	1.295E-06	0.37%	5.850E-11	2.70%	3.674E-09	2.19%	4.714E-17	4.34%
10	9.520E-04	0.00%	3.671E-06	0.31%	5.768E-10	3.73%	1.303E-08	1.71%	2.195E-15	6.08%
20	9.401E-04	0.01%	8.813E-06	0.42%	5.406E-09	3.29%	4.225E-08	2.13%	8.965E-14	5.75%
30	9.284E-04	0.01%	1.379E-05	0.38%	1.896E-08	2.39%	8.046E-08	1.89%	7.461E-13	6.42%
50	9.056E-04	0.01%	2.305E-05	0.36%	8.474E-08	1.93%	1.750E-07	1.24%	9.904E-12	4.65%
75	8.782E-04	0.02%	3.344E-05	0.38%	2.647E-07	1.76%	3.177E-07	1.25%	7.146E-11	3.89%
100	8.519E-04	0.02%	4.273E-05	0.33%	5.613E-07	1.52%	4.827E-07	1.11%	2.751E-10	3.42%
125	8.265E-04	0.03%	5.108E-05	0.35%	9.821E-07	1.47%	6.678E-07	1.04%	7.693E-10	3.69%
150	8.019E-04	0.03%	5.863E-05	0.30%	1.519E-06	1.38%	8.713E-07	1.14%	1.741E-09	4.01%
175	7.781E-04	0.04%	6.547E-05	0.24%	2.153E-06	1.39%	1.090E-06	0.93%	3.477E-09	3.14%
200	7.549E-04	0.04%	7.170E-05	0.26%	2.875E-06	0.97%	1.318E-06	0.91%	6.291E-09	3.20%
225	7.324E-04	0.04%	7.738E-05	0.23%	3.682E-06	0.70%	1.561E-06	0.91%	1.037E-08	2.96%
250	7.105E-04	0.05%	8.257E-05	0.22%	4.554E-06	0.78%	1.816E-06	0.83%	1.625E-08	2.79%
275	6.890E-04	0.05%	8.724E-05	0.19%	5.490E-06	0.83%	2.082E-06	0.78%	2.402E-08	2.39%
300	6.682E-04	0.06%	9.156E-05	0.16%	6.480E-06	0.60%	2.360E-06	0.75%	3.430E-08	2.78%
325	6.478E-04	0.07%	9.551E-05	0.15%	7.505E-06	0.40%	2.648E-06	0.66%	4.785E-08	2.50%
350	6.279E-04	0.07%	9.914E-05	0.16%	8.564E-06	0.55%	2.943E-06	0.70%	6.502E-08	2.38%
375	6.084E-04	0.07%	1.024E-04	0.19%	9.653E-06	0.40%	3.247E-06	0.67%	8.496E-08	2.02%
400	5.894E-04	0.07%	1.055E-04	0.20%	1.074E-05	0.44%	3.563E-06	0.63%	1.094E-07	1.93%
450	5.526E-04	0.08%	1.109E-04	0.28%	1.298E-05	0.37%	4.217E-06	0.69%	1.720E-07	1.41%
500	5.173E-04	0.09%	1.155E-04	0.29%	1.525E-05	0.45%	4.900E-06	0.63%	2.572E-07	1.88%
550	4.836E-04	0.10%	1.192E-04	0.28%	1.746E-05	0.41%	5.601E-06	0.62%	3.664E-07	2.24%
600	4.512E-04	0.12%	1.223E-04	0.29%	1.965E-05	0.46%	6.320E-06	0.70%	5.036E-07	1.77%
650	4.203E-04	0.12%	1.249E-04	0.23%	2.178E-05	0.48%	7.054E-06	0.62%	6.727E-07	2.08%
700	3.908E-04	0.16%	1.270E-04	0.29%	2.383E-05	0.46%	7.810E-06	0.59%	8.789E-07	1.73%
750	3.626E-04	0.18%	1.286E-04	0.32%	2.580E-05	0.34%	8.571E-06	0.55%	1.117E-06	1.11%
800	3.358E-04	0.21%	1.298E-04	0.36%	2.766E-05	0.37%	9.332E-06	0.56%	1.392E-06	1.34%
850	3.103E-04	0.22%	1.308E-04	0.30%	2.940E-05	0.34%	1.009E-05	0.45%	1.713E-06	1.02%
900	2.861E-04	0.23%	1.314E-04	0.22%	3.100E-05	0.33%	1.084E-05	0.43%	2.067E-06	1.21%
950	2.632E-04	0.21%	1.317E-04	0.22%	3.250E-05	0.35%	1.159E-05	0.55%	2.453E-06	1.01%
1000	2.416E-04	0.22%	1.319E-04	0.30%	3.389E-05	0.37%	1.235E-05	0.62%	2.887E-06	1.30%
1050	2.211E-04	0.24%	1.318E-04	0.34%	3.511E-05	0.31%	1.310E-05	0.69%	3.357E-06	1.30%
1100	2.020E-04	0.23%	1.317E-04	0.33%	3.630E-05	0.44%	1.382E-05	0.70%	3.873E-06	1.10%

Table F.8: Relative Uncertainty of NND, Pin 4, TP2

Day	Pin Four									
	^{235}U		^{239}Pu		^{241}Pu		^{237}Np		^{243}Am	
	mean	1σ (%)	mean	1σ (%)	mean	1σ (%)	mean	1σ (%)	mean	1σ (%)
0	9.642E-04	0.00%	0.000E+00	0.00%	0.000E+00	0.00%	0.000E+00	0.00%	0.000E+00	0.00%
1	9.630E-04	0.00%	7.063E-08	0.78%	2.665E-13	3.51%	1.636E-10	4.07%	3.817E-21	4.83%
2	9.618E-04	0.00%	2.644E-07	0.55%	2.684E-12	1.82%	6.354E-10	3.34%	2.388E-19	4.75%
3	9.606E-04	0.00%	5.503E-07	0.39%	1.048E-11	2.31%	1.388E-09	2.75%	2.541E-18	4.86%
5	9.582E-04	0.00%	1.308E-06	0.31%	5.753E-11	2.24%	3.650E-09	2.06%	4.642E-17	3.90%
10	9.523E-04	0.00%	3.711E-06	0.26%	5.740E-10	1.92%	1.288E-08	1.55%	2.112E-15	3.73%
20	9.405E-04	0.01%	8.926E-06	0.37%	5.468E-09	2.79%	4.194E-08	1.26%	9.069E-14	5.46%
30	9.288E-04	0.01%	1.398E-05	0.37%	1.906E-08	2.41%	7.999E-08	1.47%	7.586E-13	4.87%
50	9.059E-04	0.02%	2.340E-05	0.28%	8.696E-08	1.78%	1.738E-07	1.34%	1.003E-11	4.63%
75	8.780E-04	0.02%	3.395E-05	0.23%	2.712E-07	1.95%	3.161E-07	0.85%	7.390E-11	3.99%
100	8.508E-04	0.03%	4.338E-05	0.24%	5.836E-07	2.27%	4.819E-07	0.94%	2.950E-10	4.15%
125	8.243E-04	0.03%	5.182E-05	0.21%	1.027E-06	1.35%	6.688E-07	0.85%	8.427E-10	3.54%
150	7.984E-04	0.03%	5.941E-05	0.23%	1.593E-06	1.43%	8.766E-07	0.89%	1.953E-09	3.44%
175	7.732E-04	0.03%	6.621E-05	0.26%	2.275E-06	1.21%	1.100E-06	1.00%	3.914E-09	2.20%
200	7.486E-04	0.03%	7.240E-05	0.24%	3.056E-06	1.13%	1.339E-06	1.11%	7.069E-09	2.95%
225	7.244E-04	0.04%	7.792E-05	0.17%	3.919E-06	1.08%	1.590E-06	1.06%	1.175E-08	2.49%
250	7.008E-04	0.04%	8.294E-05	0.19%	4.854E-06	0.89%	1.856E-06	1.05%	1.854E-08	2.61%
275	6.778E-04	0.04%	8.746E-05	0.22%	5.864E-06	0.64%	2.134E-06	1.07%	2.756E-08	2.46%
300	6.553E-04	0.05%	9.152E-05	0.17%	6.922E-06	0.51%	2.424E-06	1.00%	3.985E-08	2.14%
325	6.333E-04	0.05%	9.520E-05	0.16%	8.001E-06	0.62%	2.726E-06	1.04%	5.549E-08	2.16%
350	6.118E-04	0.06%	9.856E-05	0.17%	9.132E-06	0.67%	3.038E-06	0.95%	7.537E-08	2.37%
375	5.907E-04	0.06%	1.016E-04	0.18%	1.028E-05	0.72%	3.359E-06	0.86%	9.992E-08	1.78%
400	5.702E-04	0.06%	1.043E-04	0.18%	1.143E-05	0.56%	3.687E-06	0.81%	1.301E-07	1.93%
450	5.304E-04	0.07%	1.089E-04	0.27%	1.381E-05	0.55%	4.365E-06	0.79%	2.047E-07	1.35%
500	4.924E-04	0.08%	1.126E-04	0.26%	1.611E-05	0.44%	5.076E-06	0.74%	3.080E-07	1.69%
550	4.563E-04	0.09%	1.156E-04	0.25%	1.841E-05	0.28%	5.820E-06	0.70%	4.429E-07	1.69%
600	4.220E-04	0.09%	1.179E-04	0.27%	2.061E-05	0.43%	6.583E-06	0.66%	6.109E-07	1.79%
650	3.893E-04	0.09%	1.197E-04	0.25%	2.272E-05	0.56%	7.352E-06	0.72%	8.173E-07	1.95%
700	3.584E-04	0.12%	1.210E-04	0.30%	2.469E-05	0.53%	8.131E-06	0.70%	1.063E-06	1.66%
750	3.290E-04	0.14%	1.220E-04	0.27%	2.654E-05	0.45%	8.918E-06	0.68%	1.347E-06	1.12%
800	3.014E-04	0.14%	1.225E-04	0.28%	2.823E-05	0.33%	9.705E-06	0.62%	1.669E-06	1.02%
850	2.753E-04	0.14%	1.228E-04	0.29%	2.981E-05	0.35%	1.048E-05	0.58%	2.052E-06	1.25%
900	2.508E-04	0.15%	1.230E-04	0.31%	3.124E-05	0.64%	1.124E-05	0.67%	2.467E-06	1.36%
950	2.278E-04	0.17%	1.229E-04	0.31%	3.260E-05	0.56%	1.200E-05	0.58%	2.926E-06	1.10%
1000	2.064E-04	0.16%	1.227E-04	0.36%	3.380E-05	0.50%	1.277E-05	0.53%	3.435E-06	1.60%
1050	1.864E-04	0.18%	1.223E-04	0.32%	3.485E-05	0.45%	1.352E-05	0.54%	3.978E-06	1.34%
1100	1.678E-04	0.18%	1.219E-04	0.32%	3.576E-05	0.49%	1.424E-05	0.48%	4.566E-06	1.22%

Table F.9: Relative Uncertainty of NND, Pin 1, TP3

Day	Pin One									
	^{235}U		^{239}Pu		^{241}Pu		^{237}Np		^{243}Am	
	mean	1σ (%)	mean	1σ (%)	mean	1σ (%)	mean	1σ (%)	mean	1σ (%)
0	9.642E-04	0.00%	0.000E+00	0.00%	0.000E+00	0.00%	0.000E+00	0.00%	0.000E+00	0.00%
1	9.628E-04	0.00%	6.969E-08	0.43%	2.670E-13	3.73%	1.513E-10	3.78%	7.511E-27	4.67%
2	9.614E-04	0.00%	2.609E-07	0.35%	2.821E-12	2.57%	5.924E-10	2.55%	1.201E-24	3.99%
3	9.600E-04	0.00%	5.428E-07	0.26%	1.100E-11	2.50%	1.305E-09	2.15%	2.202E-23	3.06%
5	9.571E-04	0.00%	1.290E-06	0.19%	6.209E-11	2.81%	3.441E-09	1.70%	7.981E-22	3.12%
10	9.501E-04	0.00%	3.658E-06	0.32%	6.271E-10	2.61%	1.226E-08	1.68%	9.434E-20	2.89%
20	9.362E-04	0.01%	8.782E-06	0.40%	5.970E-09	2.06%	4.030E-08	1.54%	9.181E-18	2.96%
30	9.226E-04	0.01%	1.374E-05	0.34%	2.100E-08	1.74%	7.747E-08	1.63%	1.232E-16	2.50%
50	8.962E-04	0.02%	2.294E-05	0.38%	9.622E-08	1.94%	1.696E-07	1.32%	2.908E-15	2.13%
75	8.646E-04	0.02%	3.326E-05	0.22%	2.972E-07	1.55%	3.138E-07	1.04%	3.317E-14	3.05%
100	8.345E-04	0.02%	4.246E-05	0.19%	6.354E-07	1.76%	4.856E-07	0.98%	1.728E-13	3.23%
125	8.055E-04	0.03%	5.068E-05	0.21%	1.110E-06	1.58%	6.798E-07	0.86%	6.073E-13	2.41%
150	7.778E-04	0.03%	5.805E-05	0.18%	1.707E-06	1.08%	8.923E-07	0.93%	1.650E-12	2.07%
175	7.511E-04	0.03%	6.466E-05	0.20%	2.415E-06	1.14%	1.125E-06	0.97%	3.786E-12	2.18%
200	7.253E-04	0.04%	7.065E-05	0.21%	3.224E-06	0.95%	1.374E-06	1.03%	7.655E-12	1.35%
225	7.004E-04	0.04%	7.601E-05	0.20%	4.105E-06	0.88%	1.637E-06	1.02%	1.398E-11	1.39%
250	6.763E-04	0.05%	8.091E-05	0.18%	5.057E-06	0.80%	1.914E-06	1.02%	2.391E-11	1.85%
275	6.530E-04	0.05%	8.537E-05	0.19%	6.062E-06	0.74%	2.201E-06	1.05%	3.837E-11	1.52%
300	6.304E-04	0.06%	8.943E-05	0.20%	7.116E-06	0.62%	2.498E-06	0.96%	5.862E-11	1.69%
325	6.084E-04	0.06%	9.305E-05	0.21%	8.199E-06	0.47%	2.806E-06	0.77%	8.615E-11	1.51%
350	5.871E-04	0.06%	9.634E-05	0.21%	9.324E-06	0.50%	3.126E-06	0.60%	1.222E-10	1.29%
375	5.663E-04	0.05%	9.937E-05	0.22%	1.046E-05	0.45%	3.453E-06	0.57%	1.695E-10	1.38%
400	5.461E-04	0.05%	1.021E-04	0.17%	1.160E-05	0.48%	3.790E-06	0.53%	2.286E-10	1.11%
450	5.073E-04	0.07%	1.068E-04	0.17%	1.393E-05	0.43%	4.485E-06	0.60%	3.919E-10	1.57%
500	4.705E-04	0.07%	1.106E-04	0.22%	1.622E-05	0.53%	5.208E-06	0.73%	6.242E-10	1.29%
550	4.356E-04	0.10%	1.138E-04	0.22%	1.847E-05	0.46%	5.948E-06	0.78%	9.379E-10	1.30%
600	4.024E-04	0.11%	1.163E-04	0.26%	2.060E-05	0.40%	6.709E-06	0.77%	1.350E-09	1.33%
650	3.711E-04	0.12%	1.182E-04	0.32%	2.268E-05	0.37%	7.476E-06	0.74%	1.864E-09	1.29%
700	3.414E-04	0.13%	1.197E-04	0.35%	2.459E-05	0.46%	8.247E-06	0.74%	2.509E-09	1.40%
750	3.133E-04	0.15%	1.208E-04	0.33%	2.641E-05	0.40%	9.018E-06	0.79%	3.268E-09	1.15%
800	2.868E-04	0.15%	1.215E-04	0.35%	2.809E-05	0.44%	9.804E-06	0.74%	4.155E-09	1.01%
850	2.619E-04	0.16%	1.220E-04	0.37%	2.971E-05	0.40%	1.059E-05	0.59%	5.166E-09	0.79%
900	2.385E-04	0.17%	1.221E-04	0.36%	3.114E-05	0.40%	1.135E-05	0.54%	6.312E-09	0.99%
950	2.166E-04	0.19%	1.221E-04	0.32%	3.242E-05	0.43%	1.211E-05	0.55%	7.594E-09	0.94%
1000	1.961E-04	0.18%	1.220E-04	0.25%	3.360E-05	0.44%	1.286E-05	0.60%	8.978E-09	1.08%
1050	1.771E-04	0.19%	1.217E-04	0.23%	3.469E-05	0.41%	1.360E-05	0.58%	1.043E-08	1.01%
1100	1.595E-04	0.20%	1.214E-04	0.25%	3.560E-05	0.36%	1.432E-05	0.60%	1.199E-08	1.00%

Table F.10: Relative Uncertainty of NND, Pin 2, TP3

Day	Pin Two									
	^{235}U		^{239}Pu		^{241}Pu		^{237}Np		^{243}Am	
	mean	1σ (%)	mean	1σ (%)	mean	1σ (%)	mean	1σ (%)	mean	1σ (%)
0	9.642E-04	0.00%	0.000E+00	0.00%	0.000E+00	0.00%	0.000E+00	0.00%	0.000E+00	0.00%
1	9.632E-04	0.00%	5.770E-08	0.81%	1.457E-13	3.40%	1.234E-10	5.00%	2.528E-27	4.72%
2	9.622E-04	0.00%	2.161E-07	0.58%	1.510E-12	3.66%	4.841E-10	3.68%	4.050E-25	4.26%
3	9.612E-04	0.00%	4.501E-07	0.41%	5.877E-12	2.25%	1.067E-09	2.76%	7.435E-24	3.35%
5	9.592E-04	0.00%	1.072E-06	0.32%	3.234E-11	2.46%	2.829E-09	1.99%	2.671E-22	2.98%
10	9.542E-04	0.00%	3.053E-06	0.28%	3.299E-10	2.34%	1.009E-08	1.99%	3.098E-20	3.45%
20	9.441E-04	0.01%	7.416E-06	0.26%	3.185E-09	3.24%	3.304E-08	2.13%	3.115E-18	2.96%
30	9.341E-04	0.01%	1.172E-05	0.28%	1.151E-08	2.03%	6.306E-08	2.26%	4.304E-17	2.86%
50	9.140E-04	0.01%	1.996E-05	0.27%	5.519E-08	2.06%	1.368E-07	1.91%	1.080E-15	2.24%
75	8.889E-04	0.02%	2.956E-05	0.29%	1.811E-07	2.42%	2.515E-07	1.86%	1.328E-14	1.94%
100	8.641E-04	0.03%	3.844E-05	0.23%	4.077E-07	1.32%	3.888E-07	1.89%	7.495E-14	3.00%
125	8.393E-04	0.03%	4.665E-05	0.23%	7.456E-07	1.33%	5.468E-07	1.61%	2.830E-13	2.34%
150	8.147E-04	0.03%	5.418E-05	0.25%	1.200E-06	0.98%	7.266E-07	1.33%	8.212E-13	2.77%
175	7.904E-04	0.03%	6.108E-05	0.21%	1.766E-06	0.99%	9.259E-07	1.23%	1.995E-12	1.88%
200	7.663E-04	0.03%	6.742E-05	0.20%	2.445E-06	1.08%	1.142E-06	1.03%	4.240E-12	1.90%
225	7.426E-04	0.04%	7.323E-05	0.20%	3.212E-06	0.89%	1.374E-06	0.96%	8.138E-12	1.92%
250	7.193E-04	0.04%	7.853E-05	0.21%	4.063E-06	0.84%	1.622E-06	0.98%	1.452E-11	1.39%
275	6.963E-04	0.04%	8.337E-05	0.19%	4.997E-06	0.77%	1.887E-06	0.91%	2.428E-11	1.59%
300	6.736E-04	0.05%	8.778E-05	0.21%	5.990E-06	0.70%	2.167E-06	0.96%	3.861E-11	1.48%
325	6.514E-04	0.05%	9.180E-05	0.20%	7.057E-06	0.66%	2.458E-06	1.01%	5.873E-11	1.54%
350	6.296E-04	0.05%	9.546E-05	0.21%	8.148E-06	0.63%	2.763E-06	1.02%	8.606E-11	1.39%
375	6.082E-04	0.05%	9.876E-05	0.19%	9.260E-06	0.60%	3.075E-06	1.02%	1.215E-10	1.34%
400	5.873E-04	0.05%	1.017E-04	0.17%	1.041E-05	0.51%	3.396E-06	0.99%	1.679E-10	1.21%
450	5.466E-04	0.07%	1.069E-04	0.21%	1.276E-05	0.63%	4.065E-06	1.03%	2.977E-10	1.83%
500	5.078E-04	0.09%	1.111E-04	0.23%	1.515E-05	0.45%	4.765E-06	0.83%	4.949E-10	1.64%
550	4.707E-04	0.10%	1.145E-04	0.25%	1.747E-05	0.44%	5.505E-06	0.89%	7.679E-10	1.53%
600	4.354E-04	0.11%	1.173E-04	0.30%	1.970E-05	0.62%	6.256E-06	0.90%	1.131E-09	1.06%
650	4.018E-04	0.12%	1.193E-04	0.26%	2.186E-05	0.53%	7.023E-06	0.85%	1.603E-09	1.66%
700	3.699E-04	0.14%	1.209E-04	0.29%	2.393E-05	0.49%	7.794E-06	0.78%	2.189E-09	1.66%
750	3.397E-04	0.14%	1.220E-04	0.31%	2.583E-05	0.49%	8.577E-06	0.68%	2.901E-09	1.51%
800	3.112E-04	0.14%	1.228E-04	0.31%	2.764E-05	0.46%	9.368E-06	0.64%	3.754E-09	1.25%
850	2.843E-04	0.15%	1.233E-04	0.39%	2.930E-05	0.53%	1.017E-05	0.64%	4.733E-09	1.46%
900	2.591E-04	0.17%	1.235E-04	0.28%	3.083E-05	0.49%	1.096E-05	0.62%	5.857E-09	1.15%
950	2.354E-04	0.19%	1.236E-04	0.27%	3.220E-05	0.34%	1.175E-05	0.51%	7.080E-09	1.13%
1000	2.133E-04	0.19%	1.234E-04	0.33%	3.345E-05	0.48%	1.251E-05	0.47%	8.408E-09	1.06%
1050	1.927E-04	0.19%	1.231E-04	0.34%	3.458E-05	0.48%	1.327E-05	0.52%	9.853E-09	1.06%
1100	1.736E-04	0.20%	1.227E-04	0.38%	3.560E-05	0.36%	1.403E-05	0.55%	1.139E-08	0.83%

Table F.11: Relative Uncertainty of NND, Pin 3, TP3

Day	Pin Three									
	^{235}U		^{239}Pu		^{241}Pu		^{237}Np		^{243}Am	
	mean	1σ (%)	mean	1σ (%)	mean	1σ (%)	mean	1σ (%)	mean	1σ (%)
0	9.642E-04	0.00%	0.000E+00	0.00%	0.000E+00	0.00%	0.000E+00	0.00%	0.000E+00	0.00%
1	9.633E-04	0.00%	5.286E-08	0.67%	1.134E-13	3.20%	1.141E-10	6.36%	1.619E-27	4.51%
2	9.625E-04	0.00%	1.983E-07	0.48%	1.152E-12	3.36%	4.465E-10	4.99%	2.641E-25	4.33%
3	9.616E-04	0.00%	4.137E-07	0.41%	4.491E-12	2.84%	9.812E-10	3.83%	4.768E-24	3.76%
5	9.598E-04	0.00%	9.872E-07	0.34%	2.497E-11	3.39%	2.592E-09	2.73%	1.703E-22	3.29%
10	9.553E-04	0.00%	2.821E-06	0.35%	2.561E-10	3.35%	9.224E-09	2.55%	2.011E-20	4.05%
20	9.462E-04	0.00%	6.885E-06	0.42%	2.457E-09	3.21%	3.004E-08	2.47%	2.052E-18	4.20%
30	9.372E-04	0.01%	1.092E-05	0.36%	9.131E-09	2.88%	5.735E-08	1.82%	2.846E-17	3.90%
50	9.188E-04	0.01%	1.872E-05	0.45%	4.377E-08	2.52%	1.253E-07	1.50%	7.386E-16	3.90%
75	8.957E-04	0.02%	2.796E-05	0.44%	1.502E-07	1.53%	2.304E-07	1.39%	9.256E-15	3.26%
100	8.722E-04	0.02%	3.659E-05	0.40%	3.440E-07	2.08%	3.566E-07	1.38%	5.464E-14	2.50%
125	8.486E-04	0.03%	4.464E-05	0.37%	6.399E-07	1.85%	5.037E-07	1.36%	2.129E-13	3.23%
150	8.250E-04	0.03%	5.211E-05	0.37%	1.045E-06	1.67%	6.724E-07	1.21%	6.291E-13	2.52%
175	8.013E-04	0.03%	5.907E-05	0.28%	1.561E-06	1.59%	8.616E-07	1.29%	1.549E-12	2.11%
200	7.777E-04	0.03%	6.546E-05	0.26%	2.184E-06	1.00%	1.067E-06	1.25%	3.378E-12	1.85%
225	7.542E-04	0.04%	7.132E-05	0.23%	2.910E-06	0.80%	1.289E-06	1.07%	6.635E-12	2.08%
250	7.308E-04	0.04%	7.671E-05	0.20%	3.722E-06	0.96%	1.530E-06	1.07%	1.201E-11	2.09%
275	7.077E-04	0.04%	8.165E-05	0.19%	4.616E-06	0.70%	1.787E-06	1.14%	2.043E-11	1.73%
300	6.849E-04	0.04%	8.616E-05	0.20%	5.579E-06	0.77%	2.058E-06	1.06%	3.302E-11	1.43%
325	6.624E-04	0.05%	9.028E-05	0.21%	6.607E-06	0.92%	2.344E-06	0.98%	5.092E-11	1.59%
350	6.403E-04	0.05%	9.404E-05	0.18%	7.676E-06	0.83%	2.643E-06	0.87%	7.571E-11	1.75%
375	6.185E-04	0.06%	9.739E-05	0.15%	8.791E-06	0.74%	2.952E-06	0.89%	1.085E-10	1.21%
400	5.971E-04	0.05%	1.004E-04	0.16%	9.937E-06	0.71%	3.271E-06	0.90%	1.513E-10	1.32%
450	5.555E-04	0.07%	1.058E-04	0.26%	1.231E-05	0.69%	3.944E-06	0.86%	2.759E-10	1.41%
500	5.157E-04	0.08%	1.101E-04	0.23%	1.470E-05	0.74%	4.649E-06	0.78%	4.613E-10	1.59%
550	4.776E-04	0.10%	1.135E-04	0.31%	1.704E-05	0.60%	5.380E-06	0.75%	7.252E-10	1.45%
600	4.412E-04	0.11%	1.163E-04	0.31%	1.932E-05	0.60%	6.135E-06	0.76%	1.078E-09	1.55%
650	4.067E-04	0.10%	1.183E-04	0.27%	2.150E-05	0.62%	6.921E-06	0.77%	1.544E-09	1.37%
700	3.740E-04	0.11%	1.198E-04	0.22%	2.359E-05	0.49%	7.711E-06	0.96%	2.111E-09	1.29%
750	3.429E-04	0.13%	1.209E-04	0.19%	2.553E-05	0.58%	8.504E-06	0.90%	2.816E-09	1.38%
800	3.137E-04	0.15%	1.217E-04	0.20%	2.735E-05	0.52%	9.311E-06	0.95%	3.656E-09	1.11%
850	2.861E-04	0.17%	1.221E-04	0.30%	2.906E-05	0.60%	1.011E-05	0.82%	4.639E-09	1.14%
900	2.603E-04	0.17%	1.222E-04	0.29%	3.058E-05	0.46%	1.091E-05	0.66%	5.741E-09	0.96%
950	2.361E-04	0.17%	1.221E-04	0.32%	3.190E-05	0.39%	1.170E-05	0.71%	6.968E-09	0.90%
1000	2.135E-04	0.18%	1.219E-04	0.30%	3.318E-05	0.40%	1.248E-05	0.75%	8.296E-09	0.91%
1050	1.925E-04	0.19%	1.215E-04	0.30%	3.433E-05	0.35%	1.325E-05	0.70%	9.746E-09	0.97%
1100	1.731E-04	0.20%	1.211E-04	0.33%	3.528E-05	0.45%	1.399E-05	0.69%	1.129E-08	1.26%

Table F.12: Relative Uncertainty of NND, Pin 4, TP3

Day	Pin Four									
	^{235}U		^{239}Pu		^{241}Pu		^{237}Np		^{243}Am	
	mean	1σ (%)	mean	1σ (%)	mean	1σ (%)	mean	1σ (%)	mean	1σ (%)
0	9.642E-04	0.00%	0.000E+00	0.00%	0.000E+00	0.00%	0.000E+00	0.00%	0.000E+00	0.00%
1	9.629E-04	0.00%	6.790E-08	0.67%	2.476E-13	3.18%	1.480E-10	3.81%	6.526E-27	3.50%
2	9.615E-04	0.00%	2.542E-07	0.53%	2.610E-12	2.32%	5.786E-10	3.08%	1.051E-24	2.55%
3	9.601E-04	0.00%	5.293E-07	0.40%	1.022E-11	2.24%	1.268E-09	2.55%	1.925E-23	4.05%
5	9.574E-04	0.00%	1.259E-06	0.27%	5.697E-11	1.56%	3.343E-09	1.75%	6.988E-22	2.88%
10	9.507E-04	0.00%	3.575E-06	0.24%	5.764E-10	2.68%	1.192E-08	1.26%	8.000E-20	2.76%
20	9.373E-04	0.01%	8.600E-06	0.32%	5.454E-09	2.77%	3.894E-08	1.23%	7.929E-18	2.95%
30	9.242E-04	0.01%	1.347E-05	0.32%	1.929E-08	1.69%	7.468E-08	1.53%	1.069E-16	2.94%
50	8.988E-04	0.01%	2.256E-05	0.28%	8.880E-08	2.69%	1.653E-07	2.26%	2.538E-15	3.15%
75	8.682E-04	0.02%	3.283E-05	0.25%	2.785E-07	1.54%	3.051E-07	2.37%	2.875E-14	2.88%
100	8.389E-04	0.02%	4.201E-05	0.24%	5.966E-07	1.77%	4.692E-07	2.15%	1.535E-13	3.17%
125	8.107E-04	0.03%	5.024E-05	0.25%	1.046E-06	1.81%	6.582E-07	2.02%	5.471E-13	2.33%
150	7.836E-04	0.03%	5.766E-05	0.23%	1.624E-06	1.38%	8.673E-07	1.77%	1.494E-12	2.34%
175	7.574E-04	0.04%	6.436E-05	0.20%	2.306E-06	0.94%	1.095E-06	1.61%	3.413E-12	2.54%
200	7.321E-04	0.04%	7.042E-05	0.18%	3.094E-06	0.88%	1.338E-06	1.37%	6.937E-12	2.26%
225	7.076E-04	0.04%	7.592E-05	0.16%	3.966E-06	0.72%	1.594E-06	1.14%	1.282E-11	2.31%
250	6.839E-04	0.05%	8.094E-05	0.16%	4.907E-06	0.70%	1.862E-06	1.10%	2.202E-11	2.26%
275	6.609E-04	0.05%	8.545E-05	0.15%	5.906E-06	0.72%	2.146E-06	1.04%	3.553E-11	1.65%
300	6.385E-04	0.04%	8.954E-05	0.13%	6.944E-06	0.77%	2.445E-06	0.90%	5.486E-11	1.71%
325	6.168E-04	0.05%	9.329E-05	0.13%	8.019E-06	0.77%	2.755E-06	0.73%	8.115E-11	1.64%
350	5.956E-04	0.06%	9.670E-05	0.15%	9.134E-06	0.58%	3.071E-06	0.65%	1.158E-10	1.66%
375	5.750E-04	0.06%	9.982E-05	0.17%	1.028E-05	0.46%	3.394E-06	0.64%	1.602E-10	1.38%
400	5.550E-04	0.06%	1.026E-04	0.17%	1.142E-05	0.44%	3.728E-06	0.66%	2.160E-10	1.20%
450	5.164E-04	0.08%	1.076E-04	0.20%	1.373E-05	0.44%	4.418E-06	0.56%	3.690E-10	1.42%
500	4.797E-04	0.10%	1.116E-04	0.15%	1.605E-05	0.42%	5.131E-06	0.57%	5.931E-10	1.41%
550	4.449E-04	0.09%	1.149E-04	0.20%	1.830E-05	0.52%	5.877E-06	0.67%	8.953E-10	1.57%
600	4.119E-04	0.10%	1.176E-04	0.24%	2.048E-05	0.57%	6.637E-06	0.75%	1.292E-09	1.34%
650	3.805E-04	0.11%	1.197E-04	0.26%	2.258E-05	0.68%	7.405E-06	0.74%	1.797E-09	1.10%
700	3.507E-04	0.11%	1.214E-04	0.32%	2.457E-05	0.46%	8.179E-06	0.68%	2.413E-09	1.40%
750	3.225E-04	0.09%	1.226E-04	0.32%	2.641E-05	0.51%	8.962E-06	0.61%	3.159E-09	1.62%
800	2.959E-04	0.10%	1.234E-04	0.23%	2.816E-05	0.53%	9.750E-06	0.58%	4.027E-09	1.21%
850	2.708E-04	0.10%	1.240E-04	0.29%	2.974E-05	0.55%	1.054E-05	0.51%	5.045E-09	0.99%
900	2.472E-04	0.12%	1.245E-04	0.26%	3.122E-05	0.49%	1.131E-05	0.49%	6.169E-09	1.21%
950	2.250E-04	0.12%	1.246E-04	0.30%	3.262E-05	0.31%	1.207E-05	0.55%	7.398E-09	1.08%
1000	2.043E-04	0.12%	1.245E-04	0.25%	3.382E-05	0.47%	1.283E-05	0.53%	8.765E-09	0.94%
1050	1.850E-04	0.15%	1.244E-04	0.24%	3.493E-05	0.53%	1.357E-05	0.44%	1.024E-08	1.25%
1100	1.670E-04	0.16%	1.241E-04	0.32%	3.595E-05	0.46%	1.430E-05	0.44%	1.180E-08	0.91%

Table F.13: Relative Uncertainty of NND, Fuel Region 1, TP4

Day	Fuel Region One									
	^{235}U		^{239}Pu		^{241}Pu		^{237}Np		^{243}Am	
	mean	1σ (%)	mean	1σ (%)	mean	1σ (%)	mean	1σ (%)	mean	1σ (%)
0	6.114E-04	0.00%	0.000E+00	0.00%	0.000E+00	0.00%	0.000E+00	0.00%	0.000E+00	0.00%
1	6.112E-04	0.00%	1.047E-08	0.86%	9.387E-16	2.36%	1.610E-11	2.99%	6.544E-31	3.39%
2	6.110E-04	0.00%	3.956E-08	0.56%	1.043E-14	1.69%	6.311E-11	1.85%	1.139E-28	1.82%
3	6.109E-04	0.00%	8.294E-08	0.39%	4.208E-14	1.32%	1.387E-10	1.47%	2.133E-27	2.09%
5	6.105E-04	0.00%	1.991E-07	0.24%	2.444E-13	1.88%	3.654E-10	1.52%	8.138E-26	2.23%
10	6.097E-04	0.00%	5.747E-07	0.31%	2.596E-12	2.13%	1.285E-09	1.33%	1.011E-23	2.35%
20	6.080E-04	0.00%	1.416E-06	0.44%	2.639E-11	1.78%	4.028E-09	1.38%	1.066E-21	2.73%
30	6.062E-04	0.00%	2.266E-06	0.38%	9.794E-11	1.44%	7.352E-09	1.20%	1.518E-20	2.29%
50	6.028E-04	0.01%	3.947E-06	0.37%	4.933E-10	1.44%	1.475E-08	0.96%	3.932E-19	2.51%
75	5.986E-04	0.01%	6.014E-06	0.35%	1.719E-09	1.75%	2.472E-08	1.20%	4.953E-18	2.31%
100	5.944E-04	0.01%	8.050E-06	0.28%	4.143E-09	1.22%	3.540E-08	1.06%	2.922E-17	2.09%
125	5.901E-04	0.01%	1.007E-05	0.26%	8.166E-09	1.11%	4.689E-08	0.84%	1.147E-16	2.25%
150	5.858E-04	0.01%	1.206E-05	0.26%	1.413E-08	0.79%	5.922E-08	0.89%	3.479E-16	1.61%
175	5.815E-04	0.01%	1.404E-05	0.22%	2.247E-08	0.84%	7.235E-08	0.91%	8.910E-16	1.52%
200	5.773E-04	0.01%	1.599E-05	0.23%	3.360E-08	0.86%	8.623E-08	0.89%	2.012E-15	1.54%
225	5.730E-04	0.02%	1.792E-05	0.21%	4.772E-08	0.83%	1.010E-07	0.80%	4.096E-15	1.35%
250	5.687E-04	0.02%	1.983E-05	0.23%	6.532E-08	0.90%	1.164E-07	0.75%	7.739E-15	1.52%
275	5.643E-04	0.02%	2.171E-05	0.21%	8.686E-08	0.91%	1.327E-07	0.71%	1.376E-14	1.30%
300	5.600E-04	0.02%	2.359E-05	0.20%	1.125E-07	0.81%	1.501E-07	0.65%	2.323E-14	1.35%
325	5.556E-04	0.02%	2.544E-05	0.18%	1.426E-07	0.64%	1.683E-07	0.59%	3.765E-14	1.24%
350	5.513E-04	0.02%	2.725E-05	0.16%	1.770E-07	0.59%	1.873E-07	0.55%	5.866E-14	1.16%
375	5.470E-04	0.02%	2.905E-05	0.16%	2.165E-07	0.70%	2.072E-07	0.52%	8.870E-14	1.28%
400	5.426E-04	0.02%	3.082E-05	0.14%	2.610E-07	0.68%	2.280E-07	0.51%	1.303E-13	1.04%
450	5.339E-04	0.02%	3.431E-05	0.15%	3.656E-07	0.62%	2.726E-07	0.48%	2.621E-13	1.13%
500	5.253E-04	0.03%	3.768E-05	0.14%	4.920E-07	0.66%	3.203E-07	0.44%	4.877E-13	1.18%
550	5.166E-04	0.03%	4.096E-05	0.12%	6.414E-07	0.45%	3.717E-07	0.50%	8.572E-13	1.08%
600	5.079E-04	0.03%	4.414E-05	0.08%	8.142E-07	0.59%	4.267E-07	0.57%	1.428E-12	1.08%
650	4.993E-04	0.03%	4.723E-05	0.09%	1.012E-06	0.68%	4.854E-07	0.43%	2.271E-12	0.90%
700	4.906E-04	0.03%	5.022E-05	0.11%	1.235E-06	0.64%	5.478E-07	0.38%	3.491E-12	0.83%
750	4.820E-04	0.03%	5.312E-05	0.11%	1.485E-06	0.59%	6.139E-07	0.36%	5.192E-12	0.85%
800	4.734E-04	0.03%	5.593E-05	0.11%	1.757E-06	0.52%	6.837E-07	0.36%	7.510E-12	0.78%
850	4.648E-04	0.03%	5.866E-05	0.12%	2.055E-06	0.40%	7.573E-07	0.37%	1.062E-11	0.72%
900	4.562E-04	0.03%	6.131E-05	0.11%	2.379E-06	0.38%	8.348E-07	0.41%	1.472E-11	0.83%
950	4.476E-04	0.04%	6.389E-05	0.11%	2.729E-06	0.31%	9.165E-07	0.38%	2.001E-11	0.80%
1000	4.390E-04	0.04%	6.638E-05	0.11%	3.102E-06	0.37%	1.003E-06	0.41%	2.677E-11	0.81%
1050	4.304E-04	0.04%	6.877E-05	0.10%	3.494E-06	0.41%	1.092E-06	0.39%	3.527E-11	0.89%
1100	4.218E-04	0.04%	7.109E-05	0.10%	3.914E-06	0.35%	1.187E-06	0.35%	4.587E-11	0.72%
1150	4.133E-04	0.04%	7.334E-05	0.10%	4.353E-06	0.31%	1.284E-06	0.32%	5.880E-11	0.69%
1200	4.048E-04	0.04%	7.551E-05	0.10%	4.813E-06	0.30%	1.386E-06	0.33%	7.452E-11	0.61%
1250	3.963E-04	0.04%	7.758E-05	0.10%	5.291E-06	0.24%	1.492E-06	0.30%	9.334E-11	0.45%
1300	3.879E-04	0.04%	7.958E-05	0.10%	5.790E-06	0.33%	1.604E-06	0.29%	1.159E-10	0.43%
1350	3.795E-04	0.05%	8.151E-05	0.10%	6.310E-06	0.31%	1.719E-06	0.30%	1.427E-10	0.44%
1400	3.710E-04	0.06%	8.337E-05	0.10%	6.845E-06	0.33%	1.839E-06	0.29%	1.742E-10	0.61%

Table F.14: Relative Uncertainty of NND, Fuel Region 2, TP4

Day	Fuel Region Two									
	^{235}U		^{239}Pu		^{241}Pu		^{237}Np		^{243}Am	
	mean	1σ (%)	mean	1σ (%)	mean	1σ (%)	mean	1σ (%)	mean	1σ (%)
0	1.164E-03	0.00%	0.000E+00	0.00%	0.000E+00	0.00%	0.000E+00	0.00%	0.000E+00	0.00%
1	1.163E-03	0.00%	3.896E-08	0.38%	4.654E-14	1.31%	9.263E-11	2.27%	3.913E-28	2.19%
2	1.162E-03	0.00%	1.453E-07	0.28%	4.727E-13	1.29%	3.589E-10	1.64%	6.041E-26	1.62%
3	1.161E-03	0.00%	3.014E-07	0.24%	1.821E-12	1.15%	7.839E-10	1.21%	1.084E-24	1.42%
5	1.160E-03	0.00%	7.149E-07	0.24%	1.009E-11	1.19%	2.061E-09	0.81%	3.862E-23	1.93%
10	1.155E-03	0.00%	2.031E-06	0.18%	1.021E-10	1.14%	7.236E-09	0.81%	4.426E-21	1.06%
20	1.147E-03	0.00%	4.926E-06	0.17%	9.850E-10	0.95%	2.321E-08	0.94%	4.395E-19	1.40%
30	1.138E-03	0.00%	7.802E-06	0.19%	3.575E-09	1.19%	4.364E-08	0.95%	6.069E-18	1.62%
50	1.121E-03	0.01%	1.337E-05	0.20%	1.730E-08	1.31%	9.284E-08	0.74%	1.521E-16	1.74%
75	1.100E-03	0.01%	1.997E-05	0.23%	5.755E-08	0.98%	1.663E-07	0.54%	1.831E-15	1.45%
100	1.080E-03	0.01%	2.617E-05	0.20%	1.316E-07	0.99%	2.515E-07	0.59%	1.030E-14	1.20%
125	1.059E-03	0.02%	3.198E-05	0.18%	2.441E-07	0.72%	3.473E-07	0.65%	3.804E-14	1.52%
150	1.040E-03	0.02%	3.743E-05	0.16%	3.983E-07	0.55%	4.528E-07	0.56%	1.092E-13	1.29%
175	1.020E-03	0.02%	4.253E-05	0.16%	5.953E-07	0.62%	5.670E-07	0.51%	2.620E-13	1.29%
200	1.001E-03	0.02%	4.733E-05	0.13%	8.334E-07	0.54%	6.894E-07	0.45%	5.515E-13	0.94%
225	9.824E-04	0.02%	5.182E-05	0.12%	1.113E-06	0.46%	8.193E-07	0.42%	1.058E-12	0.83%
250	9.640E-04	0.02%	5.604E-05	0.10%	1.433E-06	0.33%	9.569E-07	0.42%	1.876E-12	0.93%
275	9.460E-04	0.02%	6.002E-05	0.10%	1.788E-06	0.33%	1.101E-06	0.44%	3.132E-12	0.82%
300	9.284E-04	0.02%	6.376E-05	0.10%	2.177E-06	0.27%	1.251E-06	0.45%	4.953E-12	0.76%
325	9.110E-04	0.02%	6.728E-05	0.09%	2.598E-06	0.30%	1.407E-06	0.43%	7.515E-12	0.73%
350	8.938E-04	0.02%	7.058E-05	0.08%	3.048E-06	0.27%	1.569E-06	0.38%	1.104E-11	0.87%
375	8.769E-04	0.02%	7.370E-05	0.08%	3.525E-06	0.24%	1.735E-06	0.35%	1.570E-11	0.71%
400	8.604E-04	0.02%	7.664E-05	0.08%	4.023E-06	0.22%	1.906E-06	0.32%	2.171E-11	0.58%
450	8.280E-04	0.02%	8.199E-05	0.08%	5.084E-06	0.26%	2.263E-06	0.28%	3.894E-11	0.56%
500	7.966E-04	0.03%	8.675E-05	0.06%	6.210E-06	0.27%	2.636E-06	0.25%	6.490E-11	0.72%
550	7.661E-04	0.03%	9.096E-05	0.08%	7.377E-06	0.32%	3.023E-06	0.35%	1.020E-10	0.76%
600	7.366E-04	0.03%	9.469E-05	0.07%	8.573E-06	0.23%	3.423E-06	0.38%	1.529E-10	0.68%
650	7.080E-04	0.04%	9.796E-05	0.07%	9.786E-06	0.24%	3.835E-06	0.33%	2.200E-10	0.70%
700	6.801E-04	0.05%	1.009E-04	0.08%	1.102E-05	0.30%	4.258E-06	0.27%	3.064E-10	0.72%
750	6.532E-04	0.06%	1.034E-04	0.09%	1.225E-05	0.23%	4.688E-06	0.26%	4.144E-10	0.63%
800	6.271E-04	0.05%	1.056E-04	0.09%	1.348E-05	0.26%	5.125E-06	0.24%	5.460E-10	0.47%
850	6.018E-04	0.05%	1.075E-04	0.09%	1.468E-05	0.24%	5.569E-06	0.25%	7.028E-10	0.46%
900	5.772E-04	0.05%	1.092E-04	0.08%	1.587E-05	0.24%	6.018E-06	0.26%	8.884E-10	0.42%
950	5.534E-04	0.06%	1.106E-04	0.09%	1.702E-05	0.23%	6.471E-06	0.23%	1.103E-09	0.51%
1000	5.303E-04	0.06%	1.118E-04	0.09%	1.814E-05	0.22%	6.928E-06	0.25%	1.350E-09	0.54%
1050	5.080E-04	0.06%	1.129E-04	0.11%	1.923E-05	0.23%	7.387E-06	0.23%	1.629E-09	0.46%
1100	4.863E-04	0.05%	1.138E-04	0.12%	2.028E-05	0.20%	7.848E-06	0.21%	1.942E-09	0.40%
1150	4.653E-04	0.06%	1.144E-04	0.12%	2.130E-05	0.18%	8.310E-06	0.22%	2.289E-09	0.47%
1200	4.450E-04	0.07%	1.150E-04	0.12%	2.226E-05	0.14%	8.774E-06	0.24%	2.673E-09	0.45%
1250	4.253E-04	0.08%	1.154E-04	0.12%	2.319E-05	0.22%	9.236E-06	0.23%	3.093E-09	0.53%
1300	4.062E-04	0.09%	1.157E-04	0.10%	2.409E-05	0.17%	9.695E-06	0.25%	3.547E-09	0.52%
1350	3.877E-04	0.10%	1.159E-04	0.08%	2.495E-05	0.13%	1.015E-05	0.26%	4.036E-09	0.55%
1400	3.698E-04	0.10%	1.160E-04	0.08%	2.577E-05	0.17%	1.062E-05	0.24%	4.562E-09	0.54%

Table F.15: Relative Uncertainty of NND, Fuel Region 3, TP4

Day	Fuel Region Three									
	^{235}U		^{239}Pu		^{241}Pu		^{237}Np		^{243}Am	
	mean	1σ (%)	mean	1σ (%)	mean	1σ (%)	mean	1σ (%)	mean	1σ (%)
0	1.164E-03	0.00%	0.000E+00	0.00%	0.000E+00	0.00%	0.000E+00	0.00%	0.000E+00	0.00%
1	1.163E-03	0.00%	2.744E-08	0.74%	1.635E-14	2.15%	6.408E-11	1.34%	6.922E-29	3.84%
2	1.163E-03	0.00%	1.030E-07	0.60%	1.722E-13	1.76%	2.494E-10	1.03%	1.132E-26	3.01%
3	1.162E-03	0.00%	2.148E-07	0.52%	6.766E-13	1.80%	5.462E-10	0.87%	2.071E-25	3.03%
5	1.161E-03	0.00%	5.123E-07	0.40%	3.772E-12	1.19%	1.438E-09	0.64%	7.518E-24	2.03%
10	1.158E-03	0.00%	1.463E-06	0.36%	3.888E-11	1.85%	5.046E-09	0.68%	8.767E-22	2.30%
20	1.151E-03	0.00%	3.563E-06	0.40%	3.768E-10	1.55%	1.603E-08	0.86%	8.799E-20	2.42%
30	1.145E-03	0.01%	5.651E-06	0.32%	1.366E-09	1.05%	2.979E-08	0.83%	1.206E-18	1.70%
50	1.132E-03	0.01%	9.688E-06	0.32%	6.553E-09	1.22%	6.170E-08	0.76%	2.963E-17	1.79%
75	1.117E-03	0.01%	1.451E-05	0.29%	2.197E-08	1.17%	1.076E-07	0.77%	3.539E-16	1.79%
100	1.101E-03	0.02%	1.909E-05	0.26%	5.054E-08	0.89%	1.596E-07	0.60%	1.984E-15	1.91%
125	1.087E-03	0.02%	2.346E-05	0.27%	9.493E-08	1.07%	2.169E-07	0.50%	7.373E-15	1.54%
150	1.072E-03	0.02%	2.763E-05	0.21%	1.573E-07	1.00%	2.797E-07	0.49%	2.126E-14	1.33%
175	1.057E-03	0.02%	3.162E-05	0.15%	2.391E-07	0.84%	3.473E-07	0.51%	5.164E-14	0.98%
200	1.043E-03	0.02%	3.544E-05	0.13%	3.420E-07	0.75%	4.198E-07	0.52%	1.107E-13	0.91%
225	1.029E-03	0.02%	3.911E-05	0.14%	4.659E-07	0.60%	4.974E-07	0.51%	2.152E-13	1.01%
250	1.015E-03	0.02%	4.264E-05	0.14%	6.120E-07	0.56%	5.794E-07	0.50%	3.881E-13	1.05%
275	1.001E-03	0.02%	4.602E-05	0.13%	7.795E-07	0.52%	6.659E-07	0.47%	6.590E-13	0.92%
300	9.873E-04	0.03%	4.925E-05	0.12%	9.671E-07	0.51%	7.564E-07	0.41%	1.061E-12	1.00%
325	9.737E-04	0.03%	5.237E-05	0.11%	1.176E-06	0.45%	8.510E-07	0.34%	1.645E-12	0.91%
350	9.603E-04	0.03%	5.536E-05	0.10%	1.405E-06	0.41%	9.500E-07	0.30%	2.454E-12	0.88%
375	9.471E-04	0.03%	5.825E-05	0.11%	1.654E-06	0.39%	1.053E-06	0.31%	3.555E-12	0.72%
400	9.339E-04	0.03%	6.102E-05	0.11%	1.922E-06	0.38%	1.159E-06	0.28%	5.023E-12	0.57%
450	9.080E-04	0.03%	6.624E-05	0.13%	2.515E-06	0.37%	1.384E-06	0.29%	9.334E-12	0.64%
500	8.825E-04	0.04%	7.108E-05	0.12%	3.178E-06	0.43%	1.624E-06	0.29%	1.619E-11	0.60%
550	8.575E-04	0.03%	7.556E-05	0.09%	3.897E-06	0.40%	1.877E-06	0.30%	2.642E-11	0.57%
600	8.328E-04	0.03%	7.970E-05	0.09%	4.675E-06	0.30%	2.144E-06	0.30%	4.106E-11	0.51%
650	8.084E-04	0.03%	8.355E-05	0.09%	5.506E-06	0.28%	2.424E-06	0.30%	6.153E-11	0.58%
700	7.844E-04	0.04%	8.712E-05	0.09%	6.374E-06	0.25%	2.717E-06	0.31%	8.905E-11	0.68%
750	7.607E-04	0.04%	9.042E-05	0.09%	7.286E-06	0.26%	3.021E-06	0.31%	1.251E-10	0.52%
800	7.373E-04	0.04%	9.347E-05	0.07%	8.231E-06	0.25%	3.338E-06	0.34%	1.715E-10	0.40%
850	7.142E-04	0.05%	9.629E-05	0.07%	9.200E-06	0.25%	3.665E-06	0.37%	2.297E-10	0.48%
900	6.915E-04	0.05%	9.888E-05	0.07%	1.020E-05	0.24%	4.005E-06	0.34%	3.019E-10	0.52%
950	6.690E-04	0.05%	1.012E-04	0.08%	1.121E-05	0.24%	4.354E-06	0.32%	3.899E-10	0.56%
1000	6.470E-04	0.05%	1.034E-04	0.09%	1.223E-05	0.21%	4.713E-06	0.31%	4.950E-10	0.46%
1050	6.250E-04	0.06%	1.054E-04	0.09%	1.326E-05	0.19%	5.083E-06	0.30%	6.211E-10	0.37%
1100	6.035E-04	0.06%	1.072E-04	0.09%	1.429E-05	0.15%	5.463E-06	0.32%	7.690E-10	0.36%
1150	5.822E-04	0.06%	1.088E-04	0.08%	1.532E-05	0.16%	5.853E-06	0.27%	9.418E-10	0.37%
1200	5.612E-04	0.07%	1.103E-04	0.07%	1.634E-05	0.15%	6.250E-06	0.23%	1.141E-09	0.52%
1250	5.407E-04	0.06%	1.116E-04	0.06%	1.737E-05	0.18%	6.656E-06	0.24%	1.367E-09	0.42%
1300	5.203E-04	0.07%	1.128E-04	0.05%	1.839E-05	0.20%	7.070E-06	0.26%	1.626E-09	0.37%
1350	5.004E-04	0.07%	1.138E-04	0.06%	1.939E-05	0.19%	7.492E-06	0.26%	1.914E-09	0.35%
1400	4.809E-04	0.07%	1.147E-04	0.06%	2.036E-05	0.18%	7.918E-06	0.27%	2.235E-09	0.38%

Table F.16: Relative Uncertainty of NND, Fuel Region 4, TP4

Day	Fuel Region Four									
	^{235}U		^{239}Pu		^{241}Pu		^{237}Np		^{243}Am	
	mean	1σ (%)	mean	1σ (%)	mean	1σ (%)	mean	1σ (%)	mean	1σ (%)
0	6.114E-04	0.00%	0.000E+00	0.00%	0.000E+00	0.00%	0.000E+00	0.00%	0.000E+00	0.00%
1	6.109E-04	0.00%	2.782E-08	0.68%	1.842E-14	2.12%	5.238E-11	1.68%	9.732E-29	3.10%
2	6.104E-04	0.00%	1.042E-07	0.51%	1.979E-13	1.37%	2.036E-10	1.53%	1.605E-26	1.89%
3	6.099E-04	0.00%	2.169E-07	0.43%	7.887E-13	1.83%	4.453E-10	1.41%	2.957E-25	2.76%
5	6.089E-04	0.00%	5.158E-07	0.36%	4.479E-12	1.42%	1.167E-09	1.31%	1.085E-23	2.28%
10	6.065E-04	0.00%	1.467E-06	0.31%	4.675E-11	1.37%	4.056E-09	1.04%	1.281E-21	1.86%
20	6.018E-04	0.01%	3.542E-06	0.31%	4.593E-10	1.41%	1.273E-08	0.71%	1.295E-19	2.12%
30	5.972E-04	0.01%	5.582E-06	0.30%	1.659E-09	1.50%	2.338E-08	0.78%	1.763E-18	1.92%
50	5.882E-04	0.01%	9.458E-06	0.28%	7.822E-09	1.36%	4.757E-08	0.78%	4.252E-17	1.87%
75	5.773E-04	0.02%	1.398E-05	0.26%	2.549E-08	1.17%	8.107E-08	0.63%	4.893E-16	2.20%
100	5.669E-04	0.02%	1.817E-05	0.25%	5.708E-08	1.06%	1.175E-07	0.57%	2.627E-15	1.65%
125	5.569E-04	0.03%	2.206E-05	0.25%	1.045E-07	0.85%	1.566E-07	0.50%	9.418E-15	1.71%
150	5.472E-04	0.03%	2.570E-05	0.22%	1.691E-07	0.85%	1.979E-07	0.42%	2.620E-14	1.43%
175	5.378E-04	0.03%	2.912E-05	0.18%	2.516E-07	0.82%	2.415E-07	0.41%	6.144E-14	1.52%
200	5.287E-04	0.03%	3.234E-05	0.16%	3.524E-07	0.62%	2.874E-07	0.47%	1.273E-13	1.25%
225	5.198E-04	0.03%	3.537E-05	0.14%	4.708E-07	0.48%	3.354E-07	0.42%	2.403E-13	1.18%
250	5.111E-04	0.03%	3.824E-05	0.14%	6.064E-07	0.60%	3.853E-07	0.40%	4.210E-13	1.07%
275	5.027E-04	0.03%	4.094E-05	0.13%	7.582E-07	0.57%	4.369E-07	0.39%	6.947E-13	1.09%
300	4.944E-04	0.03%	4.350E-05	0.12%	9.266E-07	0.57%	4.899E-07	0.37%	1.090E-12	1.01%
325	4.863E-04	0.03%	4.594E-05	0.10%	1.111E-06	0.44%	5.449E-07	0.38%	1.646E-12	0.86%
350	4.784E-04	0.03%	4.825E-05	0.10%	1.309E-06	0.41%	6.016E-07	0.33%	2.403E-12	0.84%
375	4.706E-04	0.03%	5.046E-05	0.09%	1.521E-06	0.39%	6.599E-07	0.29%	3.406E-12	0.81%
400	4.630E-04	0.03%	5.256E-05	0.09%	1.747E-06	0.43%	7.196E-07	0.28%	4.708E-12	0.72%
450	4.481E-04	0.05%	5.648E-05	0.09%	2.232E-06	0.41%	8.436E-07	0.32%	8.440E-12	0.78%
500	4.337E-04	0.05%	6.006E-05	0.08%	2.768E-06	0.35%	9.738E-07	0.32%	1.414E-11	0.73%
550	4.197E-04	0.05%	6.332E-05	0.07%	3.338E-06	0.37%	1.109E-06	0.34%	2.240E-11	0.76%
600	4.061E-04	0.04%	6.634E-05	0.06%	3.945E-06	0.33%	1.251E-06	0.35%	3.395E-11	0.70%
650	3.928E-04	0.04%	6.911E-05	0.07%	4.587E-06	0.28%	1.399E-06	0.34%	4.950E-11	0.63%
700	3.797E-04	0.05%	7.166E-05	0.07%	5.254E-06	0.28%	1.553E-06	0.29%	7.007E-11	0.56%
750	3.670E-04	0.05%	7.401E-05	0.07%	5.944E-06	0.25%	1.712E-06	0.34%	9.654E-11	0.48%
800	3.545E-04	0.06%	7.618E-05	0.06%	6.658E-06	0.21%	1.878E-06	0.35%	1.302E-10	0.55%
850	3.422E-04	0.07%	7.819E-05	0.05%	7.387E-06	0.19%	2.050E-06	0.36%	1.720E-10	0.55%
900	3.302E-04	0.06%	8.003E-05	0.06%	8.132E-06	0.16%	2.227E-06	0.34%	2.235E-10	0.54%
950	3.184E-04	0.07%	8.172E-05	0.06%	8.888E-06	0.20%	2.409E-06	0.27%	2.854E-10	0.50%
1000	3.068E-04	0.06%	8.327E-05	0.06%	9.649E-06	0.19%	2.596E-06	0.26%	3.592E-10	0.44%
1050	2.954E-04	0.07%	8.470E-05	0.05%	1.043E-05	0.17%	2.789E-06	0.24%	4.463E-10	0.45%
1100	2.843E-04	0.08%	8.600E-05	0.06%	1.120E-05	0.17%	2.986E-06	0.21%	5.488E-10	0.57%
1150	2.733E-04	0.07%	8.718E-05	0.06%	1.198E-05	0.17%	3.189E-06	0.20%	6.671E-10	0.44%
1200	2.626E-04	0.08%	8.828E-05	0.06%	1.275E-05	0.16%	3.398E-06	0.22%	8.034E-10	0.29%
1250	2.520E-04	0.07%	8.926E-05	0.06%	1.352E-05	0.19%	3.612E-06	0.24%	9.586E-10	0.31%
1300	2.417E-04	0.09%	9.016E-05	0.05%	1.429E-05	0.18%	3.830E-06	0.23%	1.135E-09	0.32%
1350	2.316E-04	0.06%	9.097E-05	0.05%	1.505E-05	0.14%	4.051E-06	0.20%	1.331E-09	0.29%
1400	2.218E-04	0.07%	9.168E-05	0.06%	1.579E-05	0.16%	4.276E-06	0.20%	1.550E-09	0.36%

REFERENCES

[1]MARTIN, W. R., "Challenges and Prospects for Whole-Core Monte Carlo Analysis" Nuclear Engineering and Technology, Vol 44 No. 2 pp. 151-160, 2012.

[2] LEWIS, E.E. and MILLER, W. F., "Computational Methods of Neutron Transport," American Nuclear Society, La Grange Park, IL, pp. 296 (1993).

[3]JESSEE, M. A. and DEHART, M. D. "Scale: A Comprehensive Modeling and Simulation Suite for Nuclear Safety Analysis and Design," ORNL/TM-2005/39, Version 6.1., pp. 1-6 and F21.iii, 2011.

[4]SHREIDER, YU. A., "The Monte Carlo Method," Pergamon Press, Oxford, England pp.1 (1966).

[5]BROWN, F. B., "Fundamentals of Monte Carlo Particle Transport," LA-UR-05-4983, pp. 1-10.

[6]BROWN, F. B., "Advances in Monte Carlo Criticality Methods," LA-UR-09-02442, pp. 5

[7]SUTTON T.M. et al, "The MC21 Monte Carlo Transport Code," Proc. Joint International Topical Meeting on Mathematics & Computation and Supercomputing in Nuclear Applications, Monterey, CA, 2007.

[8]ALDER, H. L, and ROESSLER, E. B., "Introduction to Probability and Statistics," W. H. Freeman and Company, San Francisco, CA pp. 42-110, 1968.

[9]DUMONTEIL, E. AND COURAU, T., "Dominance Ratio Assessment and Monte Carlo Criticality Simulations: Dealing with High Dominance Ratio Systems," Nuclear Technology, Vol 172 Iss. 2 pp. 120-131, 2010.

[10]HOOGENBOOM, J., MARTIN, W., PETROVIC, B., "The Monte Carlo Performance Benchmark Tesy- Aims, Specifications, and First Results," Proc. International Conference on Mathematics and Computational Methods Applied to Nuclear Science and Engineering, Rio de Janeiro, Brazil, 2011.

[11]The most up-to-date description of the SERPENT code, along with a copy of the user's manual featuring complete input and output descriptions, can be found at the developers website: http://montecarlo.vtt.fi/

[12]LEPPANEN, J., PUSA, M., "Burnup Calculation Capability in the PSG2/SERPENT Monte Carlo Reactor Physics Code," Proc. International Conference on Mathematics, Computational Methods and Reactor Physics, LaGrange Park, IL, 2009.

[13]LEPPANEN, J. "PSG2/Serpent – a Continuous-energy Monte Carlo Reactor Physics Burnup Calculation Code," User's Manual, pp.36-36, 5 MAR 2012.

[14]STACEY, W. M., "Nuclear Reactor Physics," Wiley-VCH Weinheim, Germany, pp. 198-200, 2007.

[15]ROQUE, B., MARIMBEAU, P., GROUILLER, J.P., "Specification for the Phase 1 of a Depletion Calculation Benchmark devoted to Fuel Cycles," NEA/NSC/DOC(2004)11, pp. 1-7

[16]"Nuclear Fuel: Zirconium Diboride Integral Fuel Burnable Absorbers," http:www.westinghousenuclear.com/Products_&_Services/docs/flysheets/NF-FE-0028.pdf (2012)

[17]SANDERS, C. and WAGNER, J., "Study of the Effect of Integral Burnable Absorbers for PWR Burnup Credit." NUREG/CR-6760, ORNL/TM-2000/321, pp.15 (2002)

[18]Jaakko Leppanen, "Discussion Forum for SERPENT Users", http://ttuki.vtt.fi/serpent/viewtopic.php?f=15&t=47&sid=0a1cb91512f0c9aea815b67f554c1784 (Accessed May 24,2012).

[19]LEPPANEN, J., "Use of the Serpent Monte Carlo Reactor Physics Code for Full-Core Calculations," Proc. Joint International Conference on Supercomputing in Nuclear Applications and Monte Carlo 2010, Tokyo, Japan, 2010

[20]CARELLI, M., "IRIS International Reactor Innovative and Secure: Final Technical Progress Report," Report Number: STD-ES-03-40, November 3, 2003

[21]PETROVIC, B., RICOTTI, M., MONTI, S., CAVLINA, N., and NINOKATA, H., "The Pioneering Role of IRIS in Resurgence of Small Modural Reactors (SMR's), Nuclear Technology, 178. Pp.126-152. 2012.

[22]FRANCESCHINI, F., “Advanced Fuel Cycles for Light Water Reactors,” Thesis for the award of Ph.D., Corco di Dottorato in Sicurezza Nucleare ed Industriale, University fo Pisa, 2006. pp 58.

[23]PLATTE, J., “Implementation of Erbia with ZrB_2 in 17x17 Assemblies for a 4-Loop Core with a 24-Month Cycle,” Proc. 10^{th} International Conference on Nuclear Engineering, Arlington, VA, USA, 2002.

[24]PETRIE, L, LEFEBVRE, R., and WIARDI, D., ”Standard Composition Library,” ORNL/TM-2005/39 Version 6.1, pp.M8.2.77

[25]SHIM, H. et al., “Uncertainty Propagation in Monte Carlo Depletion Analysis,” Nuclear Science and Engineering, Vol 82 Issue 42 pp. 196-208, 2008.

[26]TOHJOH, M. et al., “Effect of Error Propagation of Nuclide Number Densities on Monte Carlo Burn-up Calculations,” Annals of Nuclear Energy vol. 33 pp. 1424-1436, 2006.